NASA CR-134941
VOLUME IX

ENERGY CONVERSION ALTERNATIVES STUDY
-ECAS-
WESTINGHOUSE PHASE I FINAL REPORT
Volume IX —CLOSED-CYCLE MHD

by
T.C. Tsu, et al

WESTINGHOUSE ELECTRIC CORPORATION RESEARCH LABORATORIES

Prepared for

NATIONAL AERONAUTICS AND SPACE ADMINISTRATION
ENERGY RESEARCH AND DEVELOPMENT ADMINISTRATION
NATIONAL SCIENCE FOUNDATION

NASA Lewis Research Center
Contract NAS 3-19407

1. Report No. NASA CR-134941 Volume IX	2. Government Accession No.	3. Recipient's Catalog No.
4. Title and Subtitle ENERGY CONVERSION ALTERNATIVES STUDY (ECAS), WESTINGHOUSE PHASE I FINAL REPORT VOLUME IX - CLOSED-CYCLE MHD		5. Report Date February 12, 1976 6. Performing Organization Code
7. Author(s) T. C. Tsu, et al		8. Performing Organization Report No. Westinghouse Report No. 76-9E9-ECAS-R1v.9
9. Performing Organization Name and Address Westinghouse Electric Corporation Research Laboratories Pittsburgh, PA 15235		10. Work Unit No. 11. Contract or Grant No. NAS 3-19407
12. Sponsoring Agency Name and Address Energy Research and Development Administration National Aeronautics and Space Administration National Science Foundation Washington, D.C.		13. Type of Report and Period Covered Contractor Report 14. Sponsoring Agency Code

15. Supplementary Notes

Project Managers:
W. J. Brown, NASA Lewis Research Center, Cleveland, OH 44135
D. T. Beecher, Westinghouse Research Laboratories, Pittsburgh, PA 15235

16. Abstract

The closed-cycle MHD system consists of 3 interlocking loops, the external heating loop, the closed-cycle cesium seeded argon nonequilibrium ionization MHD loop, and the steam bottomer. With MHD duct maximum temperature of 2366°K (3800°F), a pressure of 0.939 MPa (9.27 atm) and a Mach Number of 0.9 were found to give a topping cycle efficiency of 59.3% but when combined with an integrated gasifier and optimistic steam bottomer the coal to bus bar efficiency was only 45.5%. The 1978°K (3100°F) cycle had an efficiency of 55.1% and a power plant efficiency of 42.2%. The high cost of the external heating loop components resulted in a cost of electricity of 21.41 mills/MJ (77.07 mills/kWh) for the high temperature system and 19.0 mills/MJ (68.5 mills/kWh) for the lower temperature system. It is, therefore, thought that this cycle may be more applicable to internally heated systems such as some futuristic high temperature gas cooled reactor.

17. Key Words (Suggested by Author(s))			18. Distribution Statement
MHD	nonequilibrium	efficiency	Unclassified - Unlimited
argon	coal	cost	
steam	cesium		
turbine	plant		

19. Security Classif. (of this report)	20. Security Classif. (of this page)	21. No. of Pages	22. Price*
Unclassified	Unclassified	213	

* For sale by the National Technical Information Service, Springfield, Virginia 22161

ACKNOWLEDGMENTS

Section 10 entitled "Closed-Cycle MHD" was centered in the Westinghouse Research Laboratories under the direction of T. C. Tsu.

Those making significant contributions were:

- R. Draper, who described the requirements of the heat recovery steam generator.
- P. W. Eckels, who developed a design for the preheaters and stoves.
- L. S. Frost, who assisted in the assessment of existing data and in the development of the plasma properties used.
- S. Huo, who described the performance of sub- and supersonic diffusers.
- R. W. Liebermann, who wrote the computational routine for the plasma properties, MHD generator design and overall heat balance.
- J. H. Murphy, who developed the superconducting magnet field design and costs.
- R. E. Voshall, who contributed to the plasma properties development and did the power conditioning system design.
- R. J. Wright, who was heavily involved in developing the heat balance and in making the cycle optimization.

- J. L. Steinberg and G. J. Silvestri of the Westinghouse Steam Turbine Division who calculated the performance and price of certain steam turbines.
- C. T. McCreedy and S. M. Scherer of Chas. T. Main, Inc. of Boston, who prepared the balance of plant description and costing, site drawings, and provided consultation on plant island arrangements and plant constructability.

TABLE OF CONTENTS

EXPANDED TABLE OF CONTENTS

Volume IX

EXPANDED TABLE OF CONTENTS (Continued)

EXPANDED TABLE OF CONTENTS (Continued)

EXPANDED TABLE OF CONTENTS (Continued)

SUMMARY

The combined power plant under study here consists of three interlocking loops: the external heating loop, the closed-cycle MHD power system, and the bottoming steam power plant. Except for one parametric variation in which high Btu gas is used, the external heating system gasifies coal to make low Btu gas, which is burned and the heat is transferred to the MHD working fluid through periodic-flow, refractory stoves. There are also air preheaters, argon preheaters, and other auxiliary equipment to assure the best possible heat utilization in the heating system. The heated argon gas (helium is used in one parametric variation, however) enters the MHD loop where it is accelerated and cesium seed is added. The seeded gas then enters the MHD generator where some of its enthalpy is extracted in the form of dc electricity (which is converted into ac through a suitable power conditioning system) plus minor losses. The MHD generator operates on the principle of non-equilibrium ionization except in one parametric variation where thermal ionization is assumed. The necessary magnetic induction is provided by a specially designed superconducting magnet. Leaving the MHD generator, the hot gas is decelerated in a diffuser and then gives up its heat to the steam generator of the bottoming plant. The cooled gas, with its cesium seed condensed out, is then recompressed in a two-stage compressor (with intercooler) and returned to the periodic heat exchanger to start the cycle anew.

The bottoming plant is essentially conventional except that the steam generator therein is really an unfired boiler without the usual furnace losses, stack losses, and draft fan losses. It also receives hot pressurized water which is used for intercooling between the two stages of the argon compressor, for cooling the MHD generator duct, and for cooling the dc/ac inverter. Most of the turbine power

produced in the bottoming plant is used to drive the argon compressors. The remainder is used to drive an alternator. The combined ac output from the MHD generator and from the bottoming plant is 1000 MWe.

A very large number of geometric, thermodynamic, and electrical parameters can be varied to optimize the plant. Our objective is to seek out, by means of a logical sequence of parametric variations, that plant configuration which is not only feasible but efficient, and also results in a competitive cost of electricity, if possible. To aid in this search, we developed a special computer program which is capable of calculating plasma properties (with either thermal ionization or non-equilibrium ionization), designing the MHD generator, and making the overall heat balance. After completing more than 900 computer runs, we found that for an inlet stagnation temperature of 1978°K (3100°F), the best system employs argon gas seeded with 0.0005 mole fraction of cesium, an inlet stagnation pressure of 1.096 MPa (10.82 atm), a generator coefficient of 0.70, a Mach number varying from 0.90 at generator inlet to 0.85 at exit, and a magnetic flux density varying from 6.0 T at generator inlet to 4.2 T at exit. The MHD duct is 12.2 m (40 ft) long with an inlet area of 2.15 m^2 (23.13 ft^2) and an exit area of 11.4 m^2 (122.66 ft^2). The cycle thermodynamic efficiency (plant ac output divided by heat input to argon gas) is 55.1%. When losses in the external heating system are taken into account, the thermodynamic efficiency is reduced to the power plant efficiency of 43.9%. After the necessary auxiliary power is deducted from the plant output, this efficiency is reduced further to the net plant efficiency of 42.2%.

Capital cost is estimated at $1,912/kwe, and cost of electricity, 19.0 mills/MJ (68.5 mills/kWh). These costs are distressingly high. However, it should be pointed out that 88% of the cost of electricity is due to capital investment, and 72% of the total major component cost is due to the external heating system.

In conclusion, we found that the non-equilibrium MHD generator operating on cesium seeded argon is capable of high power density, large enthalpy extraction, and good isentropic efficiency without requiring excessively high temperatures or very strong magnetic fields. However, the external heating system assumed in this study detracts significantly from the cycle thermodynamic efficiency and imposes an unbearable cost burden. It is, therefore, recommended that the external heating system be replaced with an internal one, namely, a high-temperature, gas-cooled, nuclear reactor, and the entire power plant be reevaluated. Separately, it is recommended that non-equilibrium plasma research be continued upon the hope that a viable power plant might emerge at significantly lower temperatures than herein assumed (but higher than that acceptable by gas turbines).

10. CLOSED-CYCLE MHD

10.1 State of the Art

In 1961 Kerrebrock (Reference 10.1) pointed out that the phenomenon of electron-temperature elevation can be induced by joule heating to enhance plasma conductivity. Ever since that time the nonequilibrium MHD generator has aroused widespread interest. The initial enthusiasm was reflected in a prolific outpouring of theoretical and experimental papers, a few of which are cited in Reference 10.2. Although the early experiments confirmed the existence of the so-called "Kerrebrock effect," the degree of conductivity enhancement was much less than had been theoretically predicted (Reference 10.3). There followed a sustained period of basic research, with important contributions made by such investigators as Velikhov and Dykhne (Reference 10.4), Zampaglione (References 10.5 to 10.8), Solbes (Reference 10.9), Kerrebrock et al. (Reference 10.10), Kruger and Evans (Reference 10.11), Brederlow and Witte (Reference 10.12), and others. As a result, the nature of plasma turbulence induced by ionization instability became better understood, and the theory of nonequilibrium ionization was much improved. Experimentally, Zauderer and his colleagues have, since 1961, persistently and methodically carried out a series of shock-tube tests with gradually improving results. Most recently, they have paid considerable attention to electrode studies (Reference 10.13) and have demonstrated an impressive 20% enthalpy extraction (Reference 10.14). Also, using shock-tunnel MHD generators, investigators at Eindhoven University of Technology (Reference 10.15) have independently achieved an enthalpy extraction of 24% and a power density of 140 MWe/m^3 (3.96 MWe/ft^3).

The research effort has been strongly motivated by the hope that some day the nonequilibrium MHD generator may find application in large-scale power generation. The MHD generator, whose only function is

Fig. 10.1— Closed-cycle, inert gas, MHD generator combined power plant

to convert heat into electricity, must then be integrated into a complete power generation system including, as a minimum, a heat source, a means to circulate the MHD fluid in a closed circuit, and a heat sink. For base-load power generation, efficiency and economy considerations dictate that the MHD generator be combined with a bottoming plant which produces additional power and rejects heat to the environment. The technical and economic feasibility of such a combined power plant cannot be taken for granted. Although the possibility of combining a nuclear heat source with a nonequilibrium MHD generator has been investigated (References 10.16 and 10.17), feasibility has not been established, principally because of the lack of a suitable high-temperature, gas-cooled, reactor. The purpose of the present work is to study the feasibility of using a fossil-fuel heat source where heat is generated by the combustion of coal or coal-derived fuels.

10.2 Description of Parametric Points to Be Investigated

10.2.1 Cycle and Component Description

The combined power plant to be evaluated is shown schematically in Figure 10.1. It consists of three interlocking loops serving three distinct and necessary functions. On the left is the external heating loop, where coal is gasified to produce a low-Btu gas. The gasifier is described in more detail in Subsection 4.4. The gas so produced, with an HHV of about 5.35 MJ/kg (2300 Btu/lb) at a temperature of 794°K (970°F), is burned in combustors which are made integral with the high-temperature section of the main heat exchanger, HX_1. The high-temperature section actually consists of multiple units of refractory "stoves" of the periodic flow type. The stoves are designed not only to heat the required flow of MHD gas to the desired temperature, but also to impart no more than 300 ppm of impurity to it. This is necessary because excessive impurity would be detrimental to the mechanism of nonequilibrium ionization (Reference 10.18). The checker work of the stove is divided into several sections with appropriate materials being selected for their respective temperature ranges. Before entering the stoves, the noble gas (which is

the MHD working fluid) is preheated in the low-temperature section of HX_1, which is actually a separate heat exchanger of shell and tube design. The air preheater is also a shell-and-tube type with hot combustion products on the shell side. Detailed design and costing information on HX_1 (including combustors) and air preheater is given in Appendix A 10.1. After passing through the air preheater, the combustion products are discharged to a stack at a temperature of 400°K (260°F). The effluent is treated to meet emission standards.

The loop in the middle of Figure 10.1 is the MHD loop where the working fluid is argon gas seeded with cesium. (Helium is used instead of argon in one parametric variation.) The argon gas acquires a high velocity through an expansion nozzle where a predetermined amount of cesium is injected. The gas then flows through the MHD generator which is of the segmented Faraday type. Where nonequilibrium ionization is desired, the electrodes are assumed to be tungsten wires lined up in the direction of the magnetic field slightly above the duct wall. Otherwise, flush segmented electrodes are assumed. The MHD generator is surrounded with a superconducting magnet capable of producing a magnetic flux density of 5 or 6 T at the generator duct (see Appendix A 10.2). The dc output of the generator is converted into ac through suitably designed inversion equipment described in Appendix A 10.3. The gas leaving the MHD generator immediately enters a diffuser where the gas is slowed down to a low subsonic speed. A discussion of diffuser geometry and performance is given in Appendix A 10.4. After the diffuser, the gas flows through the heat exchanger, HX_2, which is really an unfired steam generator. HX_2 also receives heat in the form of hot pressurized water which is used for intercooling between the two stages of the argon compressor, for cooling the MHD generator duct, and for cooling the dc/ac inverter. Details of the steam generator are described in Appendix A 10.5. Cesium is condensed into liquid form in the coldest section of the steam generator. The liquid is removed and reinjected into the gas stream at the nozzle. A two-stage compressor with intercooler circulates the argon gas around the closed loop.

On the right side of Figure 10.1 is the steam loop. The steam generated in HX_2 is used to run a 24.13 MPa/811°K/811°K (3500 psia/1000°F/1000°F) turbine plant which produces substantial power. Some of this power is used to drive the argon compressors. The remainder is converted to electricity. This power, when added to the inverted ac from the MHD generator, makes up the total plant output of 1000 MWe. Since the steam generator, HX_2, is required to utilize low-grade heat from pressurized cooling water streams, conventional turbine bleeding and water heating must be rearranged carefully in order to achieve the most beneficial heat balance.

To get a better idea of the components involved and their relative size, a plant island layout of the base case is given in Figure 10.2. This is a 1000 MWe plant burning Montana subbituminous coal. The MHD fluid (argon + 0.001 cesium) is heated to a stagnation temperature of 2367°K (3800°F) before entering the MHD generator at a stagnation pressure of 0.939 MPa (9.27 atm) and a Mach number of 0.9. The MHD generator, operating on nonequilibrium ionization, is 18 m (59 ft) long. The superconducting magnet, omitted from Figure 10.2 for the sake of clarity, produces a magnetic flux density of 5 T at the entrance of the MHD generator which decreases linearly along the duct length to 2.3 T at its exit. The diffuser, with an efficiency of 90%, is 44.8 m (147 ft) long. The steam generator receives most of its heat (898 MWt) from the argon gas, which enters it at 1319°K (1914°F). It also receives 269 MWt from pressurized water which comes from the intercooler at 670°K (746°F), plus smaller amounts from other cooling water streams. Of the heat received by the steam generator 99.5% is assumed to be absorbed by the steam, the other 0.5% being lost by radiation. The two compressors require 269 MW each or 538 MW total, which is supplied by steam turbine drives. The turbogenerator in the bottoming plant supplies only 14 MWe out of a total plant output of 1000 MWe.

The dc/ac inversion equipment occupies a large area, but the external heating system takes up the most space. Because of design limitations on size, it is necessary to use four gasifiers (Figure 10.2),

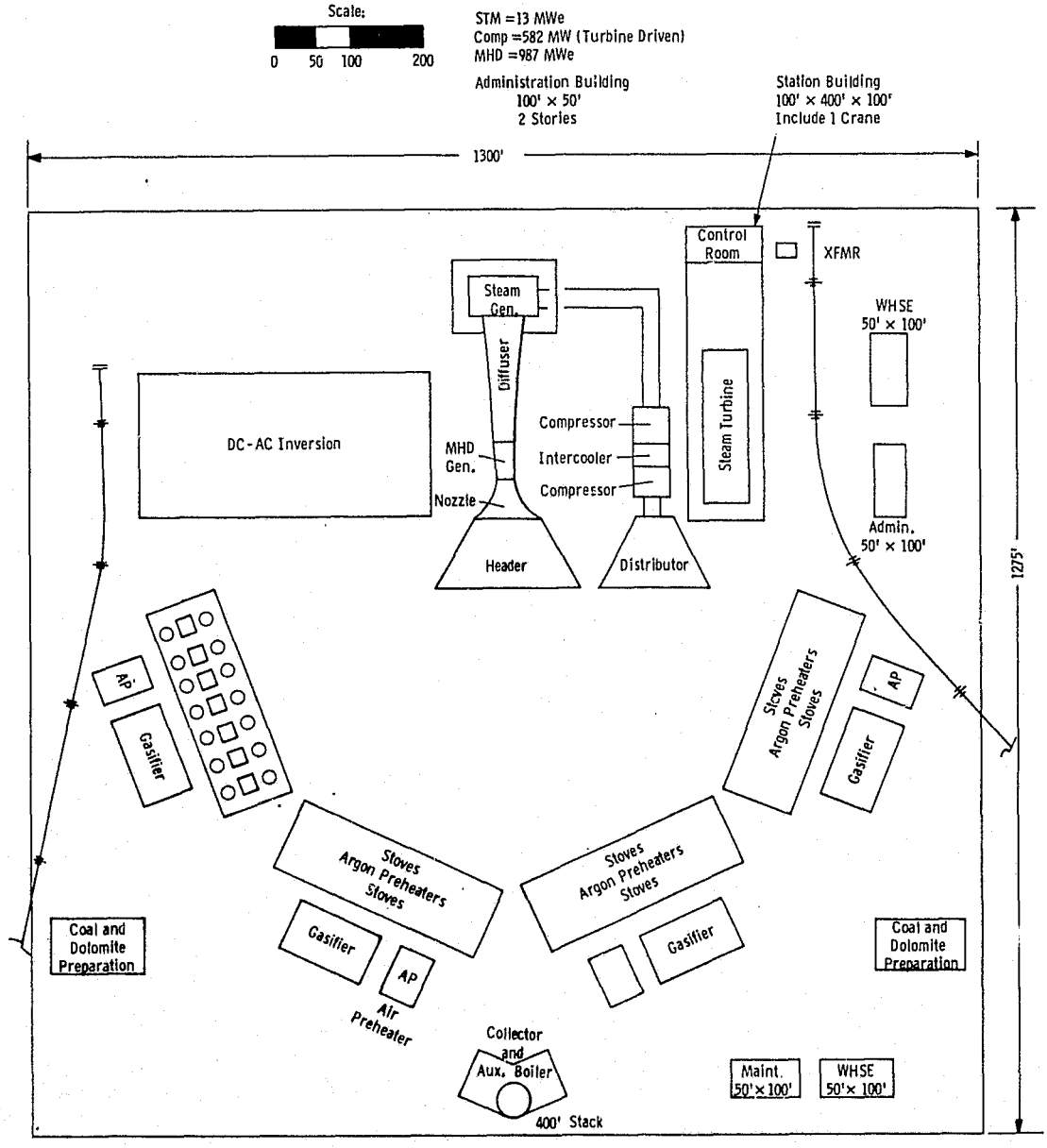

Fig. 10.2—Closed cycle MHD - Base Case 1 plant island layout

each of which is fed more than 20 kg/s (80 tons/hr) of coal. Grouped around each gasifier are 1 air preheater, 7 argon preheaters, and 14 refractory stoves which heat the argon gas to its final temperature. The hottest section of the checker in the stoves is made of yttria-stabilized zirconia, which is unfortunately very expensive. The heated argon is then piped to the MHD loop. The hot pipes and valves (not shown in Figure 10.2) are also very expensive. After Figure 10.2 was completed, the heating system was rearranged in order to shorten the pipes, but the final cost was still very high. Another cost reduction idea utilized was to use a large concrete duct (instead of steel pipes) to convey the argon gas from the steam generator to the compressor.

10.2.2 Parametric Point Selection

It is evident from the preceding description that the combined power plant under investigation will be very complex and, probably, very expensive. The objective of this study is, therefore, to seek out, by means of a logical sequence of parametric variations, that power plant configuration which is not only feasible but also efficient, and whose capital costs result in a competitive cost of electricity, if possible. There are, however, three basic constraints:

- The power plant must include a closed-cycle, inert-gas, MHD generator
- The source of heat must come from the combustion of coal or a coal-derived fuel
- The design of unconventional components must be based on state-of-the-art technology or a reasonable (i.e., justifiable) extrapolation thereof.

The last condition applies especially to the design of the MHD generator, the main heat exchanger, HX_1, the superconducting magnet, and the dc/ac power conditioning equipment.

The parameters to be studied and their range of variation were, for the most part, specified by the contracting agency and are cited in Table 10.1.

Table 10.1 - Specified Parameters

- Fuel/Furnace Type
    1. Illinois No. 6 bituminous coal → integrated fluidized bed gasifier → combustor
    2. Montana subbituminous coal → integrated fluidized bed gasifier → combustor
    3. North Dakota lignite coal → integrated fluidized bed gasifier → combustor
    4. High-Btu gas → combustor
- MHD Working Gas
    1. Argon
    2. Helium
- Stagnation Temperature at Inlet to MHD Generator
    1. 2367°K (3800°F)
    2. 1978°K (3100°F)
- Ionization Mechanism for MHD Generator
    1. Nonequilibrium ionization (elevation of electron temperature)
    2. Thermal equilibrium ionization
- Assumptions Regarding Nonequilibrium Plasma Properties
    1. A turbulence factor of 1.0 and an interaction parameter limited to 0.5 (state-of-the-art)
    2. A turbulence factor of 0.5 and no limit on interaction parameter (extrapolated technology)

It is not necessary to permute all the parameters listed; some of the combinations would be impossible or meaningless anyway. We chose to study eight sets of parametric combinations, as listed in Table 10.2.

The first four sets involve the same basic MHD cycle. The only difference is the fuel used. Thus, the eight sets involve five different MHD cycles. Set 5 is based on a plasma turbulence factor of 1.0, while the interaction parameter is limited to 0.5. For Set 6 the inlet stagnation temperature is lowered to 1978°K (3100°F). Set 7 is based on thermal equilibrium ionization at an inlet temperature of 2367°K (3800°F). Set 8 uses helium instead of argon as the MHD gas. For reasons which will become apparent later, cost information will not be generated for Set 8. It remains to find the optimum cycle (optimum combination of all operating parameters) for each set.

10.3 Approach

Before proceeding to search for the optimum cycle, we of course must define what is meant by the optimum cycle. Unfortunately, the best cycle cannot be defined by a single figure of merit, either numerically or functionally. Although one might define the best cycle as that which results in the lowest power cost, to evaluate power cost is a laborious, lengthy, and uncertain procedure. At this stage of our study even the design features and materials of construction of several unconventional components are not clearly defined, let alone their cost. It is not possible, therefore, to computerize cost calculations. On the other hand, we can calculate with reasonable accuracy such quantities as cycle efficiency, size of MHD generator, and the amount of superconducting wire required.

There is relatively little we can do to influence the cost of equipment in the combustor loop, which is virtually fixed once the fuel type, the combustor type, and the plant size are fixed. The cost of the main heat exchanger, HX_1, depends almost entirely on the top temperature, the gas flow rate, and the impurity carry-over requirement. The costs of

Table 10.2 - Parametric Combinations

Set	1	2	3	4	5	6	7	8
Fuel								
Bituminous coal	X				X	X	X	
Subbituminous coal		X						
Lignite coal			X					
High-Btu gas				X				
Fluid Bed Gasifier	X	X	X		X	X	X	
MHD Gas	A	A	A	A	A	A	A	He
MHD Inlet Temp., °F	3800	3800	3800	3800	3800	3100	3800	3800
Ionization Mechanism	NE	NE	NE	NE	NE	NE	TE	NE
Turbulence Factor	0.5	0.5	0.5	0.5	1.0	0.5	N.A.	1.0
Interaction Parameter	N.L.	N.L.	N.L.	N.L.	$\leq$ 0.5	N.L.	N.A.	$\leq$ 0.5

Notes: NE = nonequilibrium
TE = thermal equilibrium
N.A. = not applicable
N.L. = not limited.

the bottoming plant and the dc/ac inverter are relatively insensitive to our parametric variations. On the other hand, such variations do have considerable influence on a number of thermodynamic and geometric quantities. Accordingly, our optimum cycle may be defined as that cycle which best satisfies the following criteria:

a. A cycle efficiency as high as possible

b. An MHD generator (hence superconducting magnet) as small as possible, specifically less than 25 m in length for a total plant output of 1000 MW

c. A reasonable generator aspect ratio, specifically falling between 5 and 10.

A separate investigation has demonstrated that two-stage compression with intercooling is definitely better than single-stage compression. Three-stage compression with intercooling is too complicated; the slight gain in efficiency will almost certainly be offset by the increased equipment cost.

Our strategy is, therefore, to search for the cycle with the highest efficiency, at the same time taking care to make sure that conditions (b) and (c) are satisfied. Thus defined, finding the best cycle might be regarded as an extremum problem in applied mathematics. Unfortunately, because of the nature of the problem and its complexity, standard mathematical techniques for optimization, such as the calculus of variations, the method of steepest descent, geometric programming, and so forth, provide little help. The method we adopted may be described as one of selective, systematic search, but not one of indiscriminate, morphological probing. A physical understanding of the problem and mathematical intuition were used to eliminate a great deal of fruitless exploration. Even so, the performance of a large number of cycles still had to be calculated and examined. For this purpose we developed a very versatile computer program (see Appendix A 10.6 for details). In the "plasma properties" portion of the program, it can handle either thermal-equilibrium ionization or nonequilibrium ionization. The working fluid

can be either argon or helium seeded with various amounts of cesium. The loss factor δ (to allow for inelastic collision and radiation losses) and the turbulence factor ξ (to allow for the effect of plasma turbulence in the relation between scalar conductivity and effective conductivity) are adjustable. In the "generator design" portion, the flow can be either subsonic or supersonic. The velocity along the duct can be either constant or decreasing at an adjustable rate. The magnetic flux density can be either constant or tapering down at an adjustable gradient. The generator coefficient can be varied. Allowances are made for friction loss, heat loss, and electrode voltage drop. The design calculation terminates when:

- The interaction parameter becomes too high (this stopping criterion can be removed, however)
- The Hall parameter becomes too high
- The generated voltage becomes too low
- The generator duct becomes too long
- A prescribed amount of power has been generated.

The "heat balance" portion of the program is also flexible. State properties at MHD generator inlet can of course be varied over a wide range. The diffuser exit Mach number is adjustable. Compression can be either single stage or multistage with intercooling. Component efficiencies and pressure-drop coefficients are all adjustable. The program also includes various numerical techniques to hasten convergence and to perform accurate integration in the fastest way.

A number of the constants used in the computer program will be mentioned and the values selected for them justified. The plasma loss factor, δ, and the electrode voltage drop are discussed in Appendix A 10.6. The friction factor, f, for flow through the MHD generator duct was taken to be 0.008 after consulting References 10.19 and 10.20. The heat loss factor λ_2 was taken to be 0.05. This was modified from the value used in Reference 10.19 because of the different

temperature and flow conditions and, hence, the different heat transfer characteristics pertinent to this study. By making use of our computer program, we made a sensitivity study for the friction factor (Figure 10.3), the heat loss factor (Figure 10.4), and the electrode voltage drop (Figure 10.5). It can be seen from these figures that even if our selected values were somewhat inaccurate, the effect on overall cycle efficiency, η, is negligibly small. The effects on enthalpy extraction and on isentropic efficiency of the MHD generator are larger in most cases. For the purposes of the present study, we can proceed by using the selected values.

Other performance parameters of major components which were chosen and held constant are:

Compressor efficiency = 90%

Nozzle efficiency = 99%

Diffuser efficiency = 90% (subsonic) or 87% (supersonic)

Inverter (dc/ac) efficiency = 98.5%

Bottoming plant efficiency = 45%

Alternator efficiency in bottoming plant = 98.5%

Pressure drops in heat exchangers HX_1 and HX_2 = 3% of inlet pressure in each case.

A compressor efficiency of 90% might appear to be high by current industry standards, but it should be realized that the compressors involved would be very large and their pressure ratio low. The assumed efficiency should be achievable if special designs were made to meet the specific flow conditions. The assumed bottoming plant efficiency (45%) is higher than conventional steam plant efficiency because, in this case, there are no combustion losses, no stack losses, and no draft fan losses. It is also assumed that there are no restrictions on machine availability to compromise efficiency. Today's steam turbine compressor drives and steam turbine generators would be expected to have efficiencies of $\sim$ 43% Since the closed-cycle MHD plant is not expected to go on line before 1995 a hoped for higher efficiency of 45% was chosen.

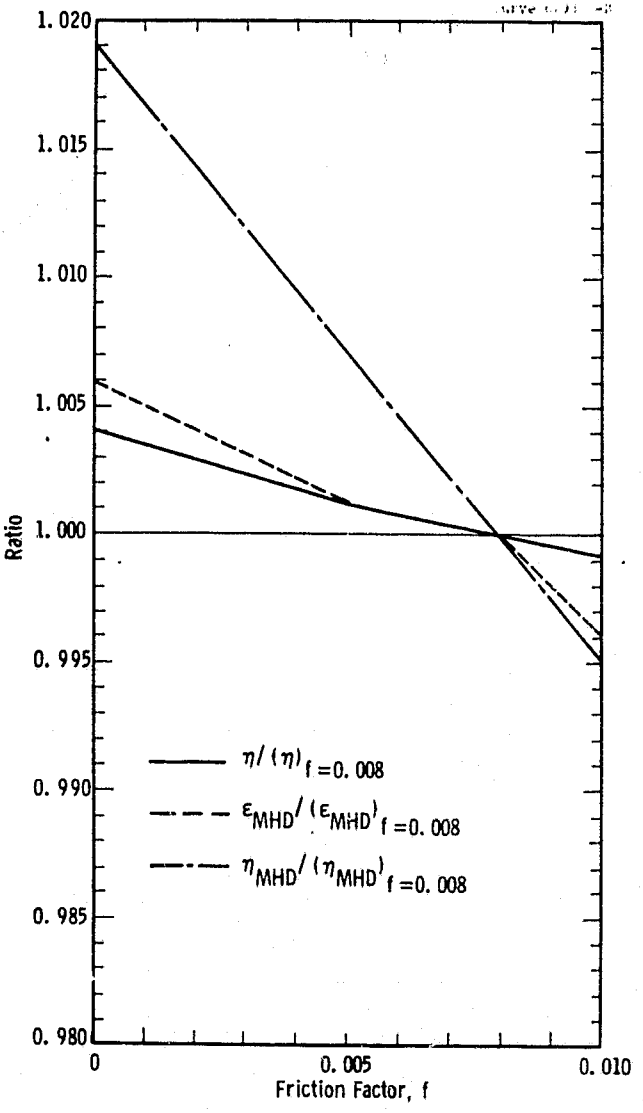

Fig. 10.3 –Sensivity of η, ϵ_{MHD} and η_{MHD} to friction factor, f

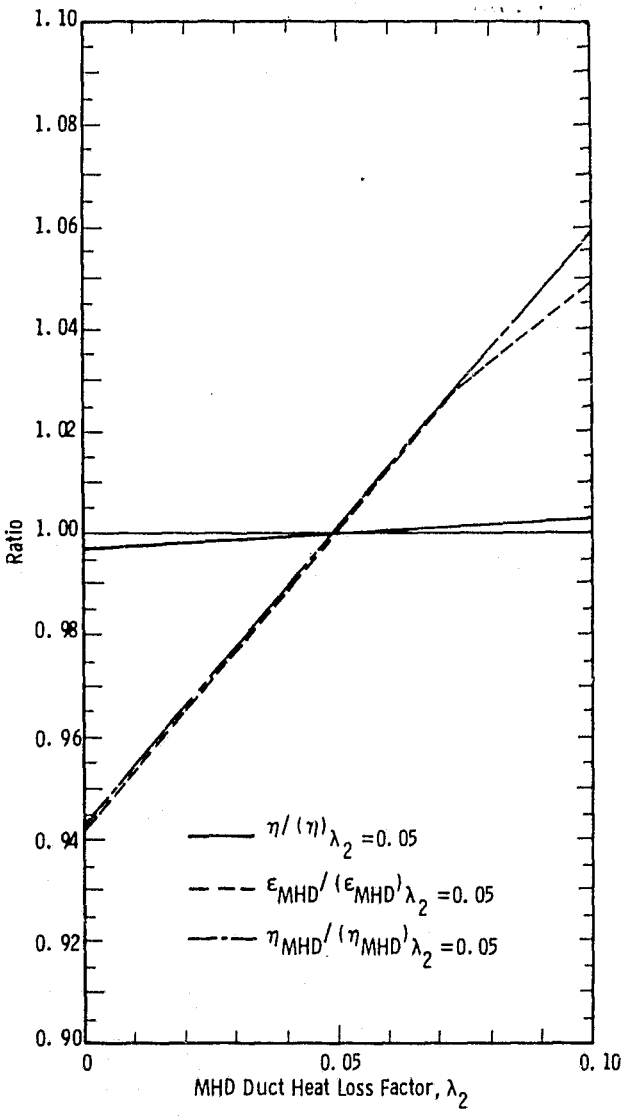

Fig. 10.4 —Sensivity of η, ϵ_{MHD} and η_{MHD} to heat loss factor, λ_2

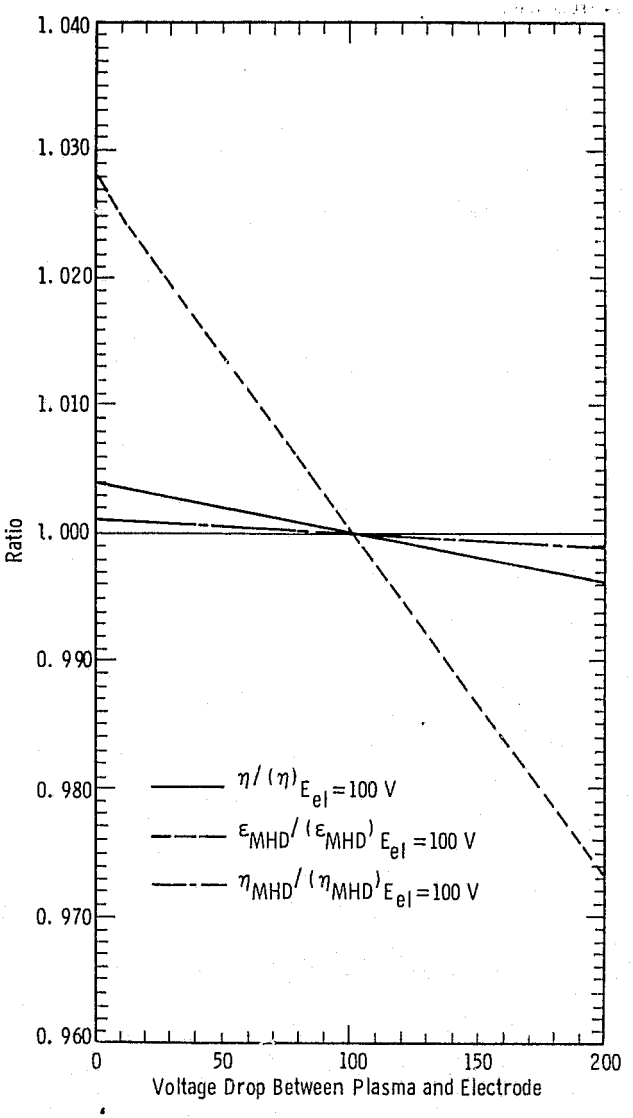

Fig. 10.5 –Sensivity of η, ε_{MHD} and η_{MHD} to voltage drop between plasma and electrode

Thermodynamic calculations for the conventional components (the nozzle, diffuser, compressor, intercooler, main heat exchanger, and steam generator) are straightforward. The generator design section of the computer program calculates electron temperature, electron density, plasma conductivity, effective conductivity, gas velocity, other gas properties, and duct area as the gas flows downstream in incremental steps. Electrical current, load voltage, and accumulated power output are also calculated. The step-by-step calculation continues until it is terminated by one of the stopping criteria mentioned earlier. At this point the enthalpy extraction and isentropic efficiency of the generator are calculated, as is the total dc power output. This power, when multiplied by the inverter efficiency, gives the MHD ac output. Inverter losses, in the form of heat, are removed by cooling water and fed into the steam generator, HX_2. The steam generator receives its main heat from the MHD exhaust, but also receives lesser amounts from the compressor intercooler and from cooling water used to cool the MHD generator duct. It is assumed that 99.5% of the heat received by the steam generator is absorbed by the steam. The enthalpy rise of the steam is converted at bottoming plant efficiency into turbine power, some of which is used to drive the argon compressors. The remainder, when multiplied by the alternator efficiency, becomes the ac output of the bottoming plant. The combined ac output of the bottoming plant and the MHD generator is the total plant output. The ratio of the total plant output to the heat added to the MHD gas by the main heat exchanger HX_1 is called the thermodynamic efficiency.

The method of selective-systematic search discussed previously has been used successfully to optimize the thermodynamic efficiency. After making some 950 computer runs, we have found the maximum thermodynamic efficiency for each of the eight sets of combined MHD steam cycles described in Subsection 10.2.

Dwg 2570199

TABLE 10.3 – CLOSED CYCLE MHD PERFORMANCE AND COSTS FOR OPTIMUM CASES

Parametric Point	1	2	3	4	5	6	7
Electric Power Output, MWe	1000	1000	1000	1000	1000	1000	1000
MHD, MWe	986	986	986	986	810	989	559
Turbo-generator, MWe	14.2	14.2	14.2	14.2	190	11.5	441
Steam Turbine Output, MW	552	552	552	552	678	660	655
Compressor, MW	538	538	538	538	485	648	207
Generator, MW	14.4	14.4	14.4	14.4	193	11.7	448
Fuel							
Bituminous Coal	X				X	X	X
Subbituminous Coal		X					
Lignite Coal			X				
High-Btu Gas				X			
Furnace Type-Fluid Bed	X	X	X		X	X	X
Oxidant-Preheated Air	X	X	X	X	X	X	X
Main Heat Exchanger (3)	X	X	X	X	X	X	X
MHD Gas	A	A	A	A	A	A	A
Seed Material	Cs	Cs	Cs	Cs	Cs	Cs	Cs
Flow Rate (Seeded Gas), kg/s	1933	1933	1933	1933	2068	2645	1927
Ionization Mechanism	N.E.	N.E.	N.E.	N.E.	N.E.	N.E.	T.E.
MHD Generator Inlet Conditions							
Stagnation Temp.,	2367	2367	2367	2367	2367	1978	2367
Stagnation Press., Atm	9.27	9.27	9.27	9.27	10.26	10.82	7.33
Mach Number	0.9	0.9	0.9	0.9	1.2	0.9	0.5
Magnetic Flux Density, T	5	5	5	5	5	6	6
MHD Generator Parameters							
Seed Fraction	0.0010	0.0010	0.0010	0.0010	0.0015	0.0005	0.0050
Generator Coeff.	0.75	0.75	0.75	0.75	0.80	0.70	0.80
Velocity Gradient Coeff.	0.20	0.20	0.20	0.20	0.20	0.20	0.25
Magnetic Flux Gradient Coeff., m^{-1}	0.03	0.03	0.03	0.03	0.03	0.025	0.004
Turbulence Factor	0.5	0.5	0.5	0.5	1.0	0.5	N.A.
Interaction Parameter	N.L.	N.L.	N.L.	N.L.	≤0.5	N.L.	N.A.
MHD Generator Results							
Length, m	18.0	18.0	18.0	18.0	19.2	12.2	25.0
Mean Width, m	2.48	2.48	2.48	2.48	2.23	2.42	2.71
Length/Mean Width	7.25	7.25	7.25	7.25	8.60	5.02	9.25
Enthalpy Extraction, %	62.5	62.5	62.5	62.5	47.0	58.1	32.8
Isentropic Eff., %	77.3	77.3	77.3	77.3	68.2	72.7	83.3
Bottoming Plant Eff., %	45.0	45.0	45.0	45.0	45.0	45.0	45.0
Thermodynamic Eff., (MHD/Steam)% (1)	59.3	59.3	59.3	59.3	54.1	55.1	54.2
Powerplant Eff., %	45.5	46.1	46.1	50.0	41.4	42.2	41.3
Overall Efficiency, %	45.5	46.1	46.1	33.6	41.4	42.2	41.3
Total Capital Cost $\times 10^{-6}$, $	2206.8	2178.4	2202.3	1666.7	2336.6	1839.4	2057.2
Capital Cost ($/kWe)	2287.5	2228.3	2256.4	1686.6	2434.4	1912.5	2146.7
Cost of Elect., Mills/kWh							
Capital	72.312	70.442	71.329	53.316	76.956	60.459	67.861
Fuel (2)	6.370	6.287	6.297	17.745	7.012	6.870	7.023
Oper. & Maint.	1.081	0.345	0.363	0.048	1.196	1.171	1.198
Total	79.763	77.074	77 988	71.109	85.164	68 501	76 082
Est. Time of Construction	8.0	8.0	8.0	8.0	8.0	8.0	8.0

Notes:

(1) Where Applicable
(2) Use Base Delivered Fuel Cost
(3) Low Temp. - Shell & Tube Recuperative;
High Temp. - Periodic Refractory Stove

10.4 Results of the Parametric Study

Results for the optimum cases are summarized in Table 10.3. The seven parametric points correspond to the first seven sets of Table 10.2.* The six lines at the top of Table 10.3 give electrical and turbine output results. The next 21 lines specify heating system parameters, MHD generator inlet conditions, and operating parameters. The remainder of the table gives MHD generator results, plant efficiencies, capital cost information, and cost of electricity.

The term "thermodynamic efficiency" has been defined previously. It is (total ac output of plant)/(heat added to argon gas). "Power plant efficiency" is the product of thermodynamic efficiency and heating system efficiency, which is defined as

$$\frac{\text{Heat added to argon gas}}{\text{Heat input from primary fuel}} .$$

The heating system efficiency is 85.3% for Point 4, for which the primary fuel is high-Btu gas. For all other parametric points the primary fuel is coal, and the heating system efficiency is 79.6%. In other words, to get 1 Btu into the argon gas, we must burn the equivalent of 1-1/4 Btu of coal. This extra 1/4 Btu is needed because of gasifier, losses, and other minor but unavoidable losses.

When the necessary auxiliary power** is deducted from the gross electrical output of 1000 MWe, the power plant efficiency is lowered and becomes the "net plant efficiency." Details of auxiliary power calculation are given in Section 2. Tabulations of capital costs and calculations for cost of electricity are given elsewhere.

---

*Results for Set 8 (with helium as the MHD gas) are presented in Table 10.7. Since the helium set was not costed, it is not represented in Table 10.3.

**Auxiliary power is needed for fuel handling and waste processing, for the gasifiers, for the cooling tower, and for other miscellaneous electrical equipment.

Dwg. 1675B34

TABLE 10.4— CLOSED CYCLE MHD PARAMETRIC INVESTIGATION OF SERIES I, ARGON AT 2367°K (3800°F)

Parametric Point	1	2	3	4	5	6	7	8	9	10	11	12	13	14	15	16	17	18
Electric Power Output, MWe	1000	992	994	993	886	1008	990	1013	961	1017	1014	983	962	997	942	910	893	1018
MHD, MWe	986	888	985	947	288	904	779	844	612	827	872	794	644	923	459	292	330	785
Turbo-generator, MWe	14.2	104	8.37	45.6	598	104	211	169	350	190	142	189	318	74.0	483	618	563	233
Steam Turbine Output, MW	552	584	553	565	783	573	614	589	669	592	580	611	660	571	718	775	770	604
Compressor, MW	538	479	544	519	176	467	400	417	314	400	436	420	338	496	228	148	198	367
Generator, MW	14.4	105	8.49	46.3	607	106	214	172	355	192	144	191	322	75.2	490	627	572	237
MHD Gas	A	A	A	A	A	A	A	A	A	A	A	A	A	A	A	A	A	A
Seed Material	Cs	Cs	Cs	Cs	Cs	Cs	Cs	Cs	Cs	Cs	Cs	Cs	Cs	Cs	Cs	Cs	Cs	Cs
Flow Rate (Seeded Gas), kg/s	1933	1933	1933	1933	1933	1933	1933	1933	1933	1933	1933	1933	1933	1933	1933	1933	1933	1933
Ionization Mechanism	N.E.	N.E.	N.E.	N.E.	N.E.	N.E.	N.E.	N.E.	N.E.	N.E.	N.E.	N.E.	N.E.	N.E.	N.E.	N.E.	N.E.	N.E.
MHD Generator Inlet Conditions																		
Stagnation Temp., °K	2367	2367	2367	2367	2367	2367	2367	2367	2367	2367	2367	2367	2367	2367	2367	2367	2367	2367
Stagnation Press., Atm	9.27	9.27	9.27	9.27	9.27	9.27	9.27	9.27	9.27	8.25	8.75	9.75	10.25	9.27	9.27	9.27	9.27	9.27
Mach Number	0.9	0.9	0.9	0.9	0.9	0.9	0.9	0.9	0.9	0.9	0.9	0.9	0.9	1.1	0.8	0.7	0.9	0.9
Magnetic Flux Density, T	5	5	5	5	5	5	5	5	5	5	5	5	5	5	5	5	4	6
MHD Generator Parameters																		
Seed Fraction	0.0010	0.0005	0.0015	0.0010	0.0010	0.0010	0.0010	0.0010	0.0010	0.0010	0.0010	0.0010	0.0010	0.0010	0.0010	0.0010	0.0010	0.0010
Generator Coeff.	0.75	0.75	0.75	0.70	0.80	0.75	0.75	0.75	0.75	0.75	0.75	0.75	0.75	0.75	0.75	0.75	0.75	0.75
Velocity Gradient Coeff.	0.20	0.20	0.20	0.20	0.20	0.15	0.25	0.20	0.20	0.20	0.20	0.20	0.20	0.20	0.20	0.20	0.20	0.20
Magnetic Flux Gradient Coeff., m^{-1}	0.03	0.03	0.03	0.03	0.03	0.03	0.03	0.02	0.04	0.03	0.03	0.03	0.03	0.03	0.03	0.03	0.03	0.03
Turbulence Factor	0.5	0.5	0.5	0.5	0.5	0.5	0.5	0.5	0.5	0.5	0.5	0.5	0.5	0.5	0.5	0.5	0.5	0.5
Interaction Parameter	N.L.	N.L.	N.L.	N.L.	N.L.	N.L.	N.L.	N.L.	N.L.	N.L.	N.L.	N.L.	N.L.	N.L.	N.L.	N.L.	N.L.	N.L.
MHD Generator Results																		
Length, m	18.0	25.0	20.9	4.2	25.0	10.1	25.0	9.1	23.7	7.2	9.8	25.0	25.0	3.1	25.0	25.0	25.0	4.5
Mean Width, m	2.48	2.34	2.50	2.44	1.69	2.29	2.17	2.18	1.97	2.26	2.29	1.92	1.92	2.34	1.83	1.73	1.74	2.06
Length/Mean Width	7.25	10.69	8.37	1.72	14.78	4.42	11.53	4.18	12.05	3.20	4.26	13.05	13.03	1.32	13.70	14.52	14.42	2.16
Enthalpy Extraction, %	62.5	55.3	62.7	59.8	16.5	56.2	47.5	51.7	36.4	50.4	53.7	48.7	38.6	57.8	26.7	16.6	19.0	47.4
Isentropic Eff., %	77.3	74.3	77.0	75.8	51.3	77.1	72.6	76.9	67.4	77.4	77.3	72.0	67.4	77.4	64.3	59.4	52.8	77.8
Bottoming Plant Eff., %	45.0	45.0	45.0	45.0	45.0	45.0	45.0	45.0	45.0	45.0	45.0	45.0	45.0	45.0	45.0	45.0	45.0	45.0
Thermodynamic Eff. (MHD/Steam), %	59.3	57.8	59.0	58.6*	47.5	58.6*	56.4	58.0*	53.5	57.9*	58.4*	56.3	53.8	58.4*	51.2	48.4	48.1	57.5*

* These solutions are not acceptable because the aspect ratio is less than 5

As mentioned previously, the first four parametric points involve the same basic MHD cycle with different primary fuels being used to heat the argon gas. Parametric variations of that cycle are shown in Table 10.4. The MHD cycle represented in the first column of Table 10.4 is the same as that represented in the first four columns of Table 10.3. That this is the optimum cycle can be seen by looking at the other 17 columns of Table 10.4. If any one parameter is allowed to deviate from its optimum value, either upward or downward, the thermodynamic efficiency drops. This effect can be seen more clearly from the graphical representation in Figures 10.6, 10.7, and 10.8. In these figures the double circle represents the optimum point where the efficiency is 59.3%. Any deviation of any independent variable causes the efficiency to drop. In Figure 10.6 the top curve shows the effect of varying the cesium fraction; the middle curve, the inlet stagnation pressure; and the bottom curve, the generator coefficient. In Figure 10.7 the top curve shows the effect of varying the inlet Mach number; and the bottom curve, the velocity gradient coefficient.* In Figure 10.8 the top curve shows the effect of varying the initial magnetic flux density B_o; and the bottom curve, the magnetic flux gradient coefficient b.**

Point 5 of Table 10.3 represents the optimum cycle, in which the plasma turbulence factor is assumed to be 1.0 and the interaction parameter is limited to a value of 0.5. Variations of this cycle are shown in Table 10.5. Column 1 of Table 10.5 is the same as column 5 of Table 10.3. Other columns of data in Table 10.5 indicate that if any independent variable is allowed to deviate from the value shown in column 1, the efficiency drops.

---

*The velocity gradient coefficient, c, describes the variation of gas velocity along the MHD generator duct. The coefficient c is given in the expression:

$$\frac{d}{dx}\left(\frac{u^2}{2}\right) = \frac{c}{\rho}\frac{dp}{dx}$$

**The magnetic flux density is varied along the MHD generator duct according to $B = B_o (1 - bx)$, where B_o is the initial flux density and b is the flux gradient coefficient.

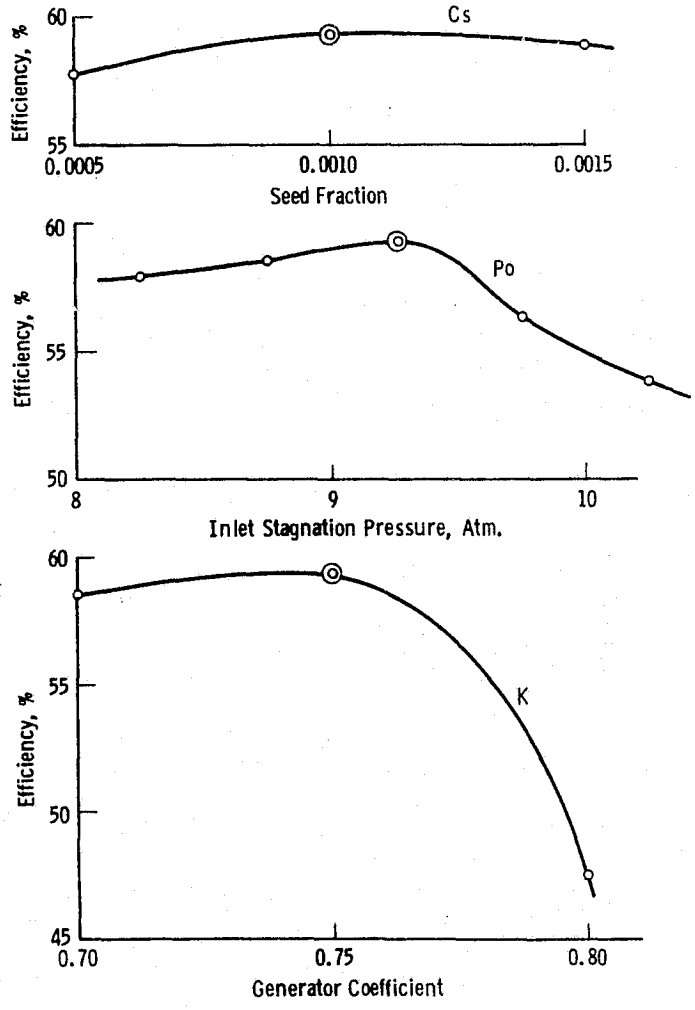

Fig. 10.6—Parametric Point 1 deviations from optimum

Curve 680351-A

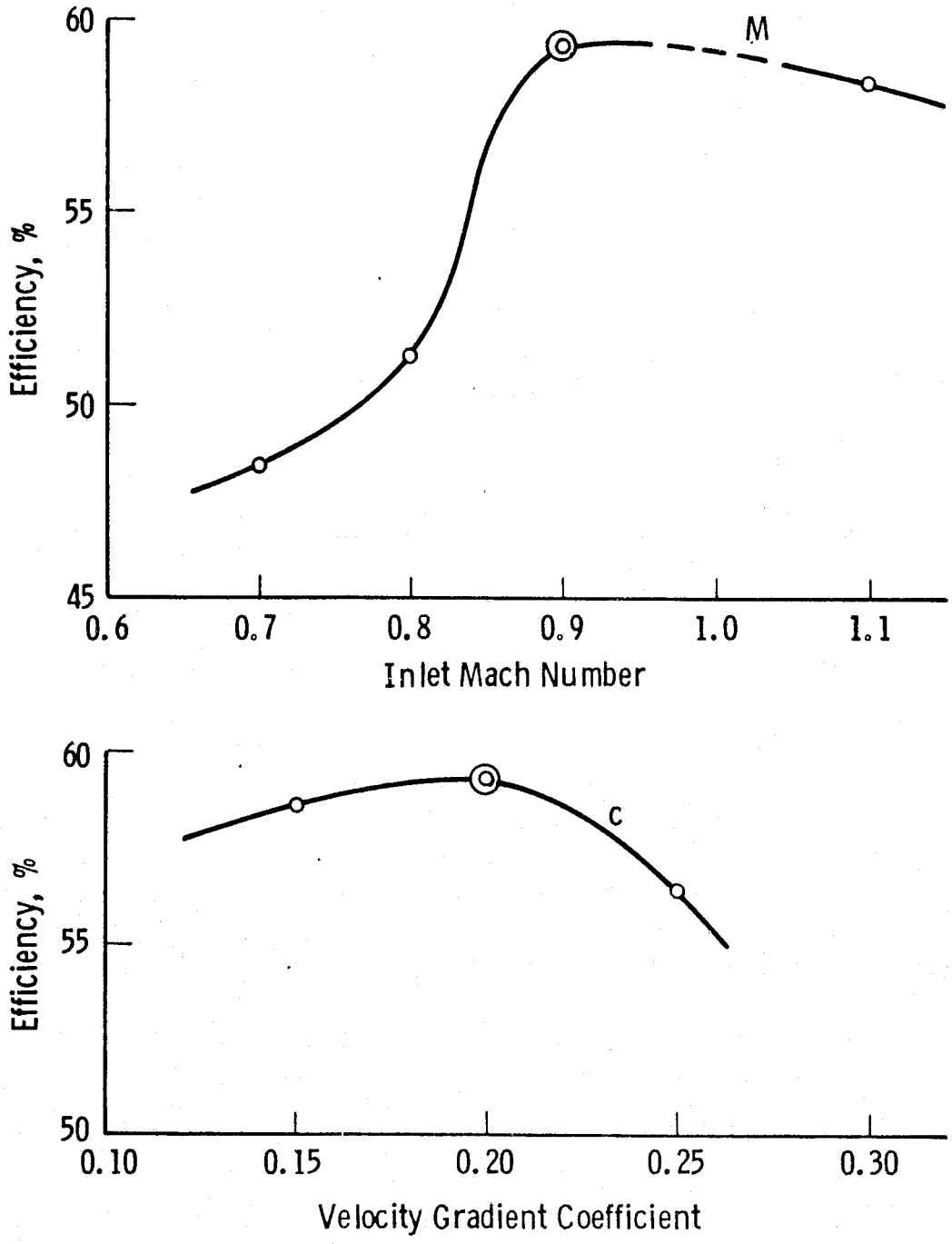

Fig. 10.7 – Parametric Point 1 deviations form optimum

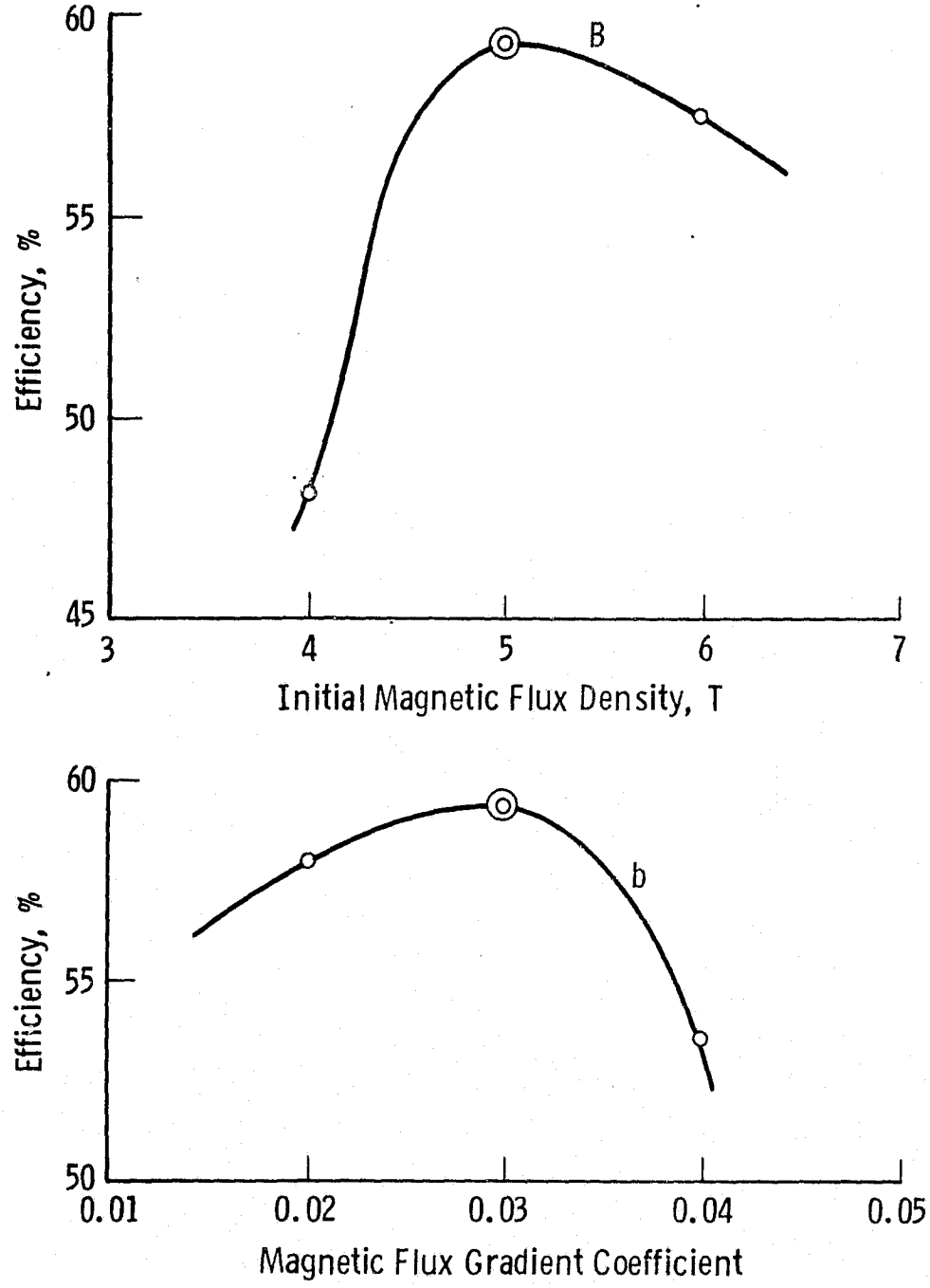

Fig. 10.8—Parametric Point 1 deviations from optimum

TABLE 10.5—CLOSED CYCLE MHD PARAMETRIC INVESTIGATION OF SERIES III, ARGON AT 2367°K (3800°F)

LIMITED INTERACTION PARAMETER

Parametric Point	1	2	3	4	5	6	7	8	9
Electric Power Output, MWe	1000	1002	998	1000	981	988	992	987	1004
MHD, MWe	810	792	825	573	669	413	523	454	466
Turbo-generator, MWe	190	210	173	427	312	575	469	533	538
Steam Turbine Output, MW	678	683	675	748	358	794	760	783	774
Compressor, MW	485	470	499	314	41	210	285	242	228
Generator, MW	193	213	176	434	317	584	475	541	546
MHD Gas	A	A	A	A	A	A	A	A	A
Seed Material	Cs	Cs	Cs	Cs	Cs	Cs	Cs	Cs	Cs
Flow Rate (Seeded Gas), kg/s	2068	2068	2068	2068	2068	2068	2068	2068	2068
Ionization Mechanism	N.E.	N.E.	N.E.	N.E.	N.E.	N.E.	N.E.	N.E.	N.E.
MHD Generator Inlet Conditions									
Stagnation Temp., °K	2367	2367	2367	2367	2367	2367	2367	2367	2367
Stagnation Press., Atm.	10.26	10.26	10.26	10.26	10.26	10.26	10.26	10.26	10.26
Mach Number	1.2	1.2	1.2	1.2	1.2	1.2	1.2	1.2	1.2
Magnet Flux Density, T	5	5	5	5	5	5	5	5	6*
MHD Generator Parameters									
Seed Fraction	0.0015	0.0015	0.0015	0.0010*	0.0020*	0.0015	0.0015	0.0015	0.0015
Generator Coeff.	0.80	0.80	0.80	0.80	0.80	0.75*	0.80	0.80	0.80
Velocity Gradient Coeff.	0.20	0.20	0.20	0.20	0.20	0.20	0.15*	0.20	0.20
Magnetic Flux Gradient Coeff., m^{-1}	0.03	0.03	0.03	0.03	0.03	0.03	0.03	0.02*	0.03
Turbulence Factor	1.0	1.0	1.0	1.0	1.0	1.0	1.0	1.0	1.0
Interaction Parameter	≤0.5	≤0.5	≤0.5	≤0.5	≤0.5	≤0.5	≤0.5	≤0.5	≤0.5
MHD Generator Results									
Length, m	19.2	18.2	20.2	10.7	19.2	2.2	9.2	7.1	3.8
Mean Width, m	2.23	2.20	2.26	1.87	2.06	1.67	1.82	1.73	1.70
Length/Mean Width	8.60	8.29	8.92	5.71	9.35	1.32	5.06	4.11	2.20
Enthalpy Extraction, %	47.0	45.7	47.0	31.7	38.0	22.3	28.8	24.7	25.3
Isentropic Eff., %	68.2	68.2	68.2	66.3	63.7	69.0	65.7	66.2	72.1
Bottoming Plant Eff., %	45.0	45.0	45.0	45.0	45.0	45.0	45.0	45.0	45.0
Thermodynamic Eff. (MHD/Steam), %	54.1	54.0	54.1	51.7	51.9	49.7*	50.9	50.1*	50.8*

* These solutions are not acceptable because the aspect ratio is less than 5

Dwg. 1675875

TABLE 10.6–CLOSED CYCLE MHD PARAMETRIC INVESTIGATION OF SERIES III, ARGON AT 1978°K (3100°F)

Parametric Point	1	2	3	4	5	6	7	8	9	10	11	12	13	14	15	16	17	18
Electric Power Output, MWe	1000	973	1000	975	931	998	994	1005	985	1017	1008	990	980	924	965	934	980	937
MHD, MWe	939	605	989	996	302	995	985	986	985	957	990	985	857	1009	411	195	700	366
Turbo-generator, MWe	11.5	368	11.6	(21.0)	629	3.46	9.10	19.6	0	59.7	18.0	5.05	123	(8.52)	554	739	280	571
Steam Turbine Output, MW	660	778	658	666	874	659	662	659	665	663	657	663	703	754	833	904	747	855
Compressor, MW	648	404	646	678	235	655	653	639	665	603	639	658	578	763	270	153	463	275
Generator, MW	11.7	374	11.8	(21.3)	639	3.52	9.24	19.8	0	60.6	18.3	5.13	125	(8.65)	563	751	284	580
MHD Gas	A	A	A	A	A	A	A	A	A	A	A	A	A	A	A	A	A	A
Seed Material	Cs	Cs	Cs	Cs	Cs	Cs	Cs	Cs	Cs	Cs	Cs	Cs	Cs	Cs	Cs	Cs	Cs	Cs
Flow Rate (Seeded Gas), kg/s	2645	2645	2645	2645	2645	2645	2645	2645	2645	2645	2645	2645	2645	2645	2645	2645	2645	2645
Ionization Mechanism	N.E.	N.E.	N.E.	N.E.	N.E.	N.E.	N.E.	N.E.	N.E.	N.E.	N.E.	N.E.	N.E.	N.E.	N.E.	N.E.	N.E.	N.E.
MHD Generator Inlet Conditions																		
Stagnation Temp., °K	1978	1978	1978	1978	1978	1978	1978	1978	1978	1978	1978	1978	1978	1978	1978	1978	1978	1978
Stagnation Press., Atm.	10.82	10.82	10.82	10.82	10.82	10.82	10.82	10.82	10.82	9.75*	10.25*	11.25*	11.75*	1978	1978	1978	1978	1978
Mach Number	0.9	0.9	0.9	0.9	0.9	0.9	0.9	0.9	0.9	0.9	0.9	0.9	0.9	1.1*	0.8*	0.7*	0.9	0.9
Magnet Flux Density, T	6	6	6	6	6	6	6	6	6	6	6	6	6	6	6	6	5.5*	5*
MHD Generator Parameters																		
Seed Fraction	0.0005	0.0001*	0.0010*	0.0005	0.0005	0.0005	0.0005	0.0005	0.0005	0.0005	0.0005	0.0005	0.0005	0.0005	0.0005	0.0005	0.0005	0.0005
Generator Coeff.	0.70	0.70	0.70	0.65	0.75*	0.70	0.70	0.70	0.70	0.70	0.70	0.70	0.70	0.70	0.70	0.70	0.70	0.70
Velocity Gradient Coeff.	0.20	0.20	0.20	0.20	0.20	0.15*	0.25*	0.20	0.20	0.20	0.20	0.20	0.20	0.20	0.20	0.20	0.20	0.20
Magnetic Flux Gradient Coeff., m^{-1}	0.025	0.025	0.025	0.025	0.025	0.025	0.025	0.020*	0.030*	0.025	0.025	0.025	0.025	0.025	0.025	0.025	0.025	0.025
Turbulence Factor	0.5	0.5	0.5	0.5	0.5	0.5	0.5	0.5	0.5	0.5	0.5	0.5	0.5	0.5	0.5	0.5	0.5	0.5
Interaction Parameter	N.L.	N.L.	N.L.	N.L.	N.L.	N.L.	N.L.	N.L.	N.L.	N.L.	N.L.	N.L.	N.L.	N.L.	N.L.	N.L.	N.L.	N.L.
MHD Generator Results																		
Length, m	12.2	25.0	11.0	4.4	25.0	9.4	20.0	10.2	19.8	7.4	9.2	16.0	25.0	10.0	25.0	25.0	25.0	25.0
Mean Width, m	2.42	2.01	2.41	2.51	1.75	2.41	2.47	2.40	2.46	2.45	2.46	2.40	2.21	2.14	1.84	1.71	2.11	1.81
Length/Mean Width	5.02	12.47	4.54	1.73	14.31	3.89	8.10	4.22	8.04	3.00	3.75	6.69	11.31	4.68	13.64	14.62	11.89	13.84
Enthalpy Extraction, %	58.1	33.3	58.2	59.2	15.9	58.6	58.0	57.8	58.2	55.6	58.1	58.1	49.4	61.3	21.9	10.1	39.2	19.5
Isentropic Eff., %	72.7	60.9	73.0	70.8	47.9	73.0	71.9	73.1	71.4	73.6	73.5	71.8	67.5	69.5	56.8	46.2	63.84	50.4
Bottoming Plant Eff., %	45.0	45.0	45.0	45.0	45.0	45.0	45.0	45.0	45.0	45.0	45.0	45.0	45.0	45.0	45.0	45.0	45.0	45.0
Thermodynamic Eff. (MHD/Steam), %	55.1	50.2	55.1*	54.3*	46.1	55.1*	54.8	55.2*	54.5	55.3*	55.4*	54.7	53.0	52.5*	48.2	45.3	51.4	46.8

* These solutions are not acceptable because the aspect ratio is less than 5

Variations of the optimum cycles represented by Points 6 and 7 of Table 10.3 are given in Tables 10.6 and 10.8, respectively. It should be noted that in Table 10.6, the efficiencies listed in columns 8, 10, and 11 are higher than that listed in column 1, but in those three cases the MHD generator is rather short and fat, its aspect ratio being less than 5. They do not satisfy criterion (c) of an optimum cycle (see p. 10-11). According to our definition, therefore, column 1 of Table 10.6 represents the optimum cycle for argon at 1978°K (3100°F) with nonequilibrium ionization. The comparison displayed by Table 10.8 is more clear-cut. Column 1 of that table represents the optimum cycle for argon at 2367°K (3800°F) with thermal-equilibrium ionization.

Table 10.7 presents cycle information with helium as the MHD gas. The inlet stagnation temperature is 2367°K (3800°F) and the interaction parameter is limited to a value of 0.5. A comparison between Table 10.5 and Table 10.7 will reveal the difference between argon and helium. The best argon cycle is 54.1% efficient and the best helium cycle only 50.1% efficient. The MHD generators are about equal in length, but the argon cycle requires a magnetic flux density of only 5 T compared to 6 T for the helium cycle. Argon is clearly the better choice. It was not, therefore, deemed necessary to generate cost information for the helium cycle.

State properties at various points of each of the five optimum cycles are given in Tables 10.9 through 10.13. The station numbers used in those tables correspond to the circled numbers shown in Figure 10.9:

Station 1 = Inlet to first-stage compressor

Station 2 = Exit from first-stage compressor or inlet to intercooler

Station 3 = Exit from intercooler or inlet to second-stage compressor

Station 4 = Exit from second-stage compressor or inlet to heat exchanger HX_1

TABLE 10.7 — CLOSED CYCLE MHD PARAMETRIC INVESTIGATION OF SERIES IV, HELIUM AT 2367°K (3800°F) WITH LIMITED INTERACTION PARAMETER

Parametric Point	1	2	3	4	5	6	7	8	9
Electric Power Output, MWe	1000	1000	988	960	970	990	978	1000	1000
MHD, MWe	457	394	467	274	326	394	335	454	454
Turbo-generator, MWe	543	606	521	686	644	596	643	546	546
Steam Turbine Output, MW	747	784	729	811	793	768	788	748	749
Compressor, MW	196	169	200	115	139	163	135	194	195
Generator, MW	551	615	529	696	654	605	653	554	554
MHD Gas	He	He	He	He	He	He	He	He	He
Seed Material	Cs	Cs	Cs	Cs	Cs	Cs	Cs	Cs	Cs
Flow Rate (Seeded Gas), kg/s	207.5	207.5	207.5	207.5	207.5	207.5	207.5	207.5	207.5
Ionization Mechanism	N.E.	N.E.	N.E.	N.E.	N.E.	N.E.	N.E.	N.E.	N.E.
MHD Generator Inlet Conditions									
Stagnation Temp., °K	2367	2367	2367	2367	2367	2367	2367	2367	2367
Stagnation Press., Atm.	2.65	2.65	2.65	2.65	2.65	2.65	2.65	2.65	2.65
Mach Number	0.6	0.6	0.6	0.6	0.6	0.6	0.6	0.6	0.6
Magnet Flux Density, T	6	6	6	6	6	6	6	6	6
MHD Generator Parameters									
Seed Fraction	0.0010	0.0005	0.0015	0.0010	0.0010	0.0010	0.0010	0.0010	0.0010
Generator Coeff.	0.80	0.80	0.80	0.75 *	0.85 *	0.80	0.80	0.80	0.80
Velocity Gradient Coeff.	0.00	0.00	0.00	0.00	0.00	0.05 *	0.10 *	0.00	0.00
Magnetic Flux Gradient Coeff., m^{-1}	0.0065	0.0065	0.0065	0.0065	0.0065	0.0065	0.0065	0.0060 *	0.0070 *
Turbulence Factor	1.0	1.0	1.0	1.0	1.0	1.0	1.0	1.0	1.0
Interaction Parameter	≤ 0.5	≤0.5	≤ 0.5	≤0.5	≤0.5	≤0.5	≤0.5	≤0.5	≤ 0.5
MHD Generator Results									
Length, m	19.4	19.4	17.4	4.0	19.4	14.6	10.8	18.8	19.4
Mean Width, m	1.94	1.90	1.94	1.80	1.84	1.90	1.86	1.94	1.94
Length/Mean Width	9.97	10.17	8.97	2.22	10.50	7.72	5.82	9.70	9.98
Enthalpy Extraction, %	25.2	21.3	26.2	14.8	17.7	21.6	18.2	25.0	25.0
Isentropic Eff., %	73.8	71.6	75.1	74.3	72.3	75.0	75.9	73.9	73.7
Bottoming Plant Eff., %	45.0	45.0	45.0	45.0	45.0	45.0	45.0	45.0	45.0
Thermodynamic Eff. (MHD/Steam), %	50.1	49.8	49.5	47.1 *	47.9	49.2	48.3	50.1	50.0

* These solutions are not acceptable because the aspect ratio is less than 5

Dwg. 1675877

TABLE 10.8—CLOSED CYCLE MHD PARAMETRIC INVESTIGATION OF SERIES V, ARGON AT 2367°K (3800°F) WITH EQUILIBRIUM IONIZATION

Parametric Point	1	2	3	4	5	6	7	8	9	10	11	12	13	14	15	16	17	18
Electric Power Output, MWe	1000	996	983	979	997	993	999	998	999	956	977	997	993	980	968	936	904	985
MHD, MWe	559	512	548	504	518	536	546	548	555	382	463	547	533	460	454	356	262	502
Turbo-generator, MWe	441	484	435	475	479	457	453	450	444	574	514	450	460	520	514	580	642	483
Steam Turbine Output, MW	655	678	645	677	667	663	659	659	656	717	688	659	294	688	694	731	767	675
Compressor, MW	207	187	204	194	181	199	199	202	205	135	166	202	197	160	172	142	115	185
Generator, MW	448	491	441	483	486	464	460	457	451	582	522	457	467	528	522	589	652	490
MHD Gas	A	A	A	A	A	A	A	A	A	A	A	A	A	A	A	A	A	A
Seed Material	Cs	Cs	Cs	Cs	Cs	Cs	Cs	Cs	Cs	Cs	Cs	Cs	Cs	Cs	Cs	Cs	Cs	Cs
Flow Rate (Seeded Gas), kg/s	1927	1927	1927	1927	1927	1927	1927	1927	1927	1927	1927	1927	1927	1927	1927	1927	1927	1927
Ionization Mechanism	T.E.	T.E.	T.E.	T.E.	T.E.	T.E.	T.E.	T.E.	T.E.	T.E.	T.E.	T.E.	T.E.	T.E.	T.E.	T.E.	T.E.	T.E.
MHD Generator Inlet Conditions																		
Stagnation Temp., °K	2367	2367	2367	2367	2367	2367	2367	2367	2367	2367	2367	2367	2367	2367	2367	2367	2367	2367
Stagnation Press., Atm.	7.33	7.33	7.33	7.33	7.33	7.33	7.33	7.33	7.33	6.25	6.75*	7.75*	8.25*	7.33	7.33	7.33	7.33	7.33
Mach Number	0.5	0.5	0.5	0.5	0.5	0.5	0.5	0.5	0.5	0.5	0.5	0.5	0.5	0.4*	0.6*	0.7*	0.8*	0.5
Magnet Flux Density, T	6	6	6	6	6	6	6	6	6	6	6	6	6	6	6	6	6	5*
MHD Generator Parameters																		
Seed Fraction	0.0050	0.0025*	0.0100*	0.0050	0.0050	0.0050	0.0050	0.0050	0.0050	0.0050	0.0050	0.0050	0.0050	0.0050	0.0050	0.0050	0.0050	0.0050
Generator Coeff.	0.80	0.80	0.80	0.75*	0.85*	0.80	0.80	0.80	0.80	0.80	0.80	0.80	0.80	0.80	0.80	0.80	0.80	0.80
Velocity Gradient Coeff.	0.25	0.25	0.25	0.25	0.25	0.20*	0.30*	0.25	0.25	0.25	0.25	0.25	0.25	0.25	0.25	0.25	0.25	0.25
Magnetic Flux Gradient Coeff., m^{-1}	0.004	0.004	0.004	0.004	0.004	0.004	0.004	0.003*	0.005*	0.004	0.004	0.004	0.004	0.004	0.004	0.004	0.004	0.004
Turbulence Factor	N.A.	N.A.	N.A.	N.A	N.A.	N.A.	N.A.	N.A.	N.A.	N.A.	N.A.	N.A.	N.A.	N.A.	N.A.	N.A.	N.A.	N.A.
Interaction Parameter	N.L.	N.L.	N.L.	N.L.	N.L.	N.L.	N.L.	N.L.	N.L.	N.L.	N.L.	N.L.	N.L.	N.L.	N.L.	N.L.	N.L.	N.L.
MHD Generator Results																		
Length, m	25.0	25.0	17.3	13.9	25.0	20.7	25.0	22.6	25.0	6.4	11.7	25.0	25.0	24.2	13.5	9.6	7.4	25.0
Mean Width, m	2.71	2.54	2.66	2.61	2.47	2.45	3.04	2.66	2.69	2.40	2.49	2.59	2.47	3.56	2.12	1.91	1.79	2.52
Length/Mean Width	9.25	9.86	6.49	5.31	10.15	8.43	8.24	8.48	9.31	2.68	4.71	9.67	10.16	6.79	6.33	5.03	4.14	9.94
Enthalpy Extraction, %	32.8	29.7	32.7	29.5	30.2	31.4	32.0	32.1	32.6	22.0	26.9	32.1	31.2	26.7	26.4	20.5	15.0	29.3
Isentropic Eff., %	83.3	82.2	83.9	79.1	86.5	82.6	83.8	83.3	83.3	83.1	83.2	83.0	82.6	84.6	80.2	76.4	71.4	82.1
Bottoming Plant Eff., %	45.0	45.0	45.0	45.0	45.0	45.0	45.0	45.0	45.0	45.0	45.0	45.0	45.0	45.0	45.0	45.0	45.0	45.0
Thermodynamic Eff. (MHD/Steam), %	54.2	53.7	53.2	52.9	53.7	53.7	54.0	54.0	54.1	50.8*	52.4*	54.0	53.7	52.5	52.0	49.9	47.8*	53.1

* These solutions are not acceptable because the aspect ratio is less than 5

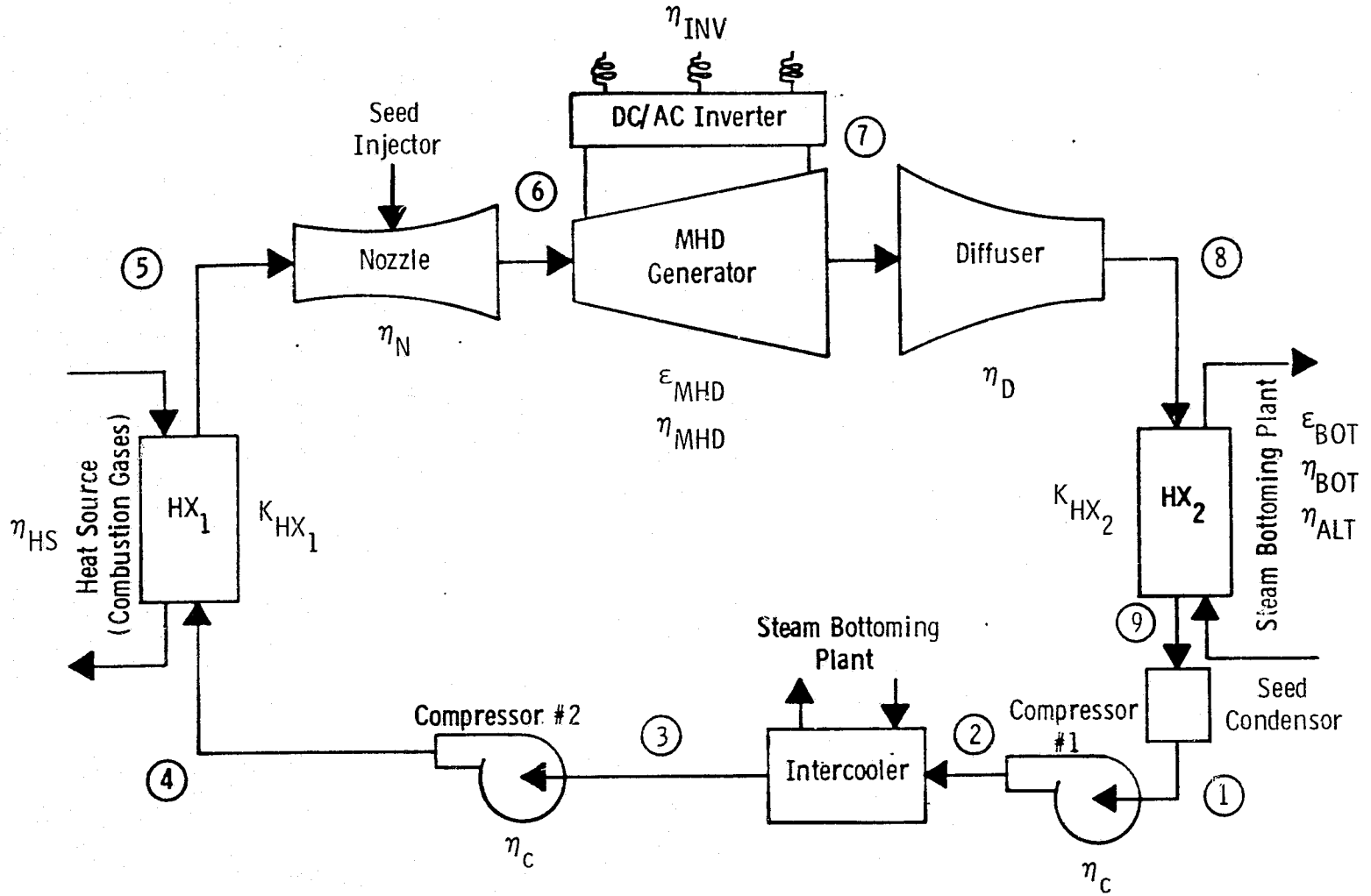

Fig. 10.9 —Schematic of MHD closed cycle

Station 5 = Exit from heat exchanger HX_1 or inlet to nozzle

Station 6 = Exit from nozzle or inlet to MHD generator

Station 7 = Exit from MHD generator or inlet to diffuser

Station 8 = Exit from diffuser or inlet to steam generator HX_2

Station 9 = Exit from steam generator HX_2.

The symbols used in Tables 10.7 to 10.11 are as follows:

T = static temperature, °K

TS = stagnation temperature, °K

P = static pressure, Pa

PS = stagnation pressure, Pa

RHO = density, kg/m^3

U = velocity, m/s

M = Mach number

Q = heat added, watts

W = power generated, watts

ξ = turbulence factor

S = interaction parameter.

Returning now to Table 10.3, we can draw certain conclusions by examining the seven optimized cycles. Comparing Points 1, 2, and 3, we see that there is not much difference among the three coals, with Montana subbituminous being slightly better than the other two. Montana subbituminous is better than Illinois No. 6 bituminous because of its lower sulfur content and is better than North Dakota lignite because of its lower moisture content and greater heating value. The high-Btu gas (Point 4) results in higher fuel cost and higher power cost. It is not a

Table 10.9 – State Properties for Best Argon Cycle at 3800°F,
$\xi = 0.5$, S unlimited

STATION	T	TS	P	PS	RHO	U	M	Q	W
1	.4230+03	.4230+03	.1026+06	.1026+06	.1165+01	.0000	.0000	.0000	-.2690+09
2	.6904+03	.6904+03	.3162+05	.3162+06	.2201+01	.0000	.0000	-.2690+09	.0000
3	.4230+03	.4230+03	.3162+06	.3162+06	.3592+01	.0000	.0000	.0000	-.2690+09
4	.6904+03	.6904+03	.9750+06	.9750+06	.6785+01	.0000	.0000	.1586+10	.0000
5	.2367+04	.2367+04	.9457+06	.9457+06	.1920+01	.0000	.0000	.0000	.0000
6	.1864+04	.2367+04	.5163+06	.9393+06	.1337+01	-.7224+03	-.9000+00	-.5003+08	-.1001+10
7	.1053+04	.1319+04	.6395+05	.1122+06	.2927+00	.5247+03	.8695+00	.0000	.0000
8	.1314+04	.1319+04	.1057+06	.1066+06	.3878+00	.6741+02	.1000+00	-.8978+09	.0000
9	.4230+03	.4230+03	.1026+06	.1026+06	.1169+01	.0000	.0000	.0000	.0000

MHD .9856+09 STEAM PLANT .1415+08 TOTAL .9998+09 EFFICIENCY .5930+00

ETA-MHD .7734+00 EFF-MHD .6253+00

Table 10.10 - State Properties for Best Argon Cycle at 3800°F
$\xi = 1.0, \quad S \leq 0.5$

STATION	T	TS	P	PS	RHO	U	M	Q	W
1	.4230+03	.4230+03	.1461+06	.1461+06	.1659+01	.0000	.0000	.0000	-.2495+09
2	.6549+03	.6549+03	.3981+06	.3981+06	.2920+01	.0000	.0000	-.2495+09	.0000
3	.4230+03	.4230+03	.3981+06	.3981+06	.4521+01	.0000	.0000	.0000	-.2495+09
4	.6549+03	.6549+03	.1085+07	.1085+07	.7959+01	.0000	.0000	.1842+10	.0000
5	.2367+04	.2367+04	.1052+07	.1052+07	.2136+01	.0000	.0000	.0000	.0000
6	.1599+04	.2367+04	.3901+06	.1040+07	.1178+01	.8915+03	.1200+01	-.4183+08	.8367+09
7	.9754+03	.1546+04	.5564+05	.1760+06	.2754+00	.7688+03	.1325+01	.0000	.0000
8	.1526+04	.1546+04	.1506+06	.1557+06	.4765+00	.1451+03	.2000+00	-.1203+10	.0000
9	.4230+03	.4230+03	.1461+06	.1461+06	.1667+01	.0000	.0000	.0000	.0000

MHD .8241+09 STEAM PLANT .1736+09 TOTAL .9977+09 EFFICIENCY .5416+00
ETA-MHD .6817+00 EFF-MHD .4793+00

Table 10.11 – State Properties for Best Argon Cycle at 3100°F, $\xi = 0.5$, S unlimited

STATION	T	TS	P	PS	RHO	U	M	Q	W
1	.4230+03	.4230+03	.1493+06	.1493+06	.1696+01	.0000	.0000	.0000	-.3240+09
2	.6584+03	.6584+03	.4122+06	.4122+06	.3008+01	.0000	.0000	-.3240+09	.0000
3	.4230+03	.4230+03	.4122+06	.4122+06	.4682+01	.0000	.0000	.0000	-.3240+09
4	.6584+03	.6584+03	.1137+07	.1137+07	.8300+01	.0000	.0000	.1816+10	.0000
5	.1978+04	.1978+04	.1103+07	.1103+07	.2681+01	.0000	.0000	.0000	.0000
6	.1557+04	.1978+04	.6029+06	.1096+07	.1863+01	.6609+03	.9000+00	-.5018+08	.1004+10
7	.9750+03	.1211+04	.9493+05	.1631+06	.4686+00	.4947+03	.8514+00	.0000	.0000
8	.1207+04	.1211+04	.1540+06	.1553+06	.6141+00	.6464+02	.1000+00	-.1082+10	.0000
9	.4230+03	.4230+03	.1493+06	.1493+06	.1699+01	.0000	.0000	.0000	.0000

MHD .9886+09 STEAM PLANT .1153+08 TOTAL .1000+10 EFFICIENCY .5509+00
ETA-MHD .7273+00 EFF-MHD .5814+00

Table 10.12 – State Properties for Best Argon Cycle at 3800°F with Thermal Ionization

STATION	T	TS	P	PS	RHO	U	M	Q	W
1	.4230+03	.4230+03	.2848+06	.2848+06	.3235+01	.0000	.0000	.0000	-.1033+09
2	.5260+03	.5260+03	.4675+06	.4675+06	.4270+01	.0000	.0000	-.1033+09	.0000
3	.4230+03	.4230+03	.4675+06	.4675+06	.5810+01	.0000	.0000	.0000	-.1033+09
4	.5260+03	.5260+03	.7672+06	.7672+06	.7008+01	.0000	.0000	.1846+10	.0000
5	.2367+04	.2367+04	.7442+06	.7442+06	.1511+01	.0000	.0000	.0000	.0000
6	.2165+04	.2367+04	.6079+06	.7426+06	.1359+01	.4317+03	.5000+00	-.2838+08	.5675+09
7	.1729+04	.1763+04	.2835+06	.2975+06	.8010+00	.1853+03	.2413+00	.0000	.0000
8	.1757+04	.1763+04	.2936+06	.2961+06	.8165+00	.7742+02	.1000+00	-.1321+10	.0000
9	.4230+03	.4230+03	.2848+06	.2848+06	.3289+01	.0000	.0000	.0000	.0000

MHD .5590+09 STEAM PLANT .4413+09 TOTAL .1000+10 EFFICIENCY .5420+00
ETA-MHD .8331+00 FFF-MHD .3282+00

Table 10.13 – State Properties for Best Helium Cycle at 3800°F,
$\xi = 1.0$, $S \leq 0.5$

STATION	T	TS	P	PS	RHO	U	M	Q	W
1	.4230+03	.4230+03	.1150+06	.1150+06	.1308+00	.0000	.0000	.0000	-.9790+08
2	.5139+03	.5139+03	.1788+06	.1788+06	.1675+00	.0000	.0000	-.9790+08	.0000
3	.4230+03	.4230+03	.1788+06	.1788+06	.2035+00	.0000	.0000	.0000	-.9790+08
4	.5139+03	.5139+03	.2782+06	.2782+06	.2406+00	.0000	.0000	.1997+10	.0000
5	.2367+04	.2367+04	.2698+06	.2698+06	.5489-01	.0000	.0000	.0000	.0000
6	.2116+04	.2367+04	.2026+06	.2690+06	.4770-01	.1597+04	.6000+00	-.2318+08	.4637+09
7	.1646+04	.1900+04	.8639+05	.1236+06	.2610-01	.1597+04	.6798+00	.0000	.0000
8	.1894+04	.1900+04	.1185+06	.1195+06	.3113-01	.2519+03	.1000+00	-.1540+10	.0000
9	.4230+03	.4230+03	.1150+06	.1150+06	.1352+00	.0000	.0000	.0000	.0000

MHD .4567+09 STEAM PLANT .5432+09 TOTAL .9999+09 EFFICIENCY .5008+00
ETA-MHD .7377+00 EFF-MHD .2519+00

suitable fuel for this application. Point 5 differs from the first four in that a different value was assumed for the plasma turbulence factor, and a limit was placed upon the interaction parameter. Point 5 is based on our current knowledge of nonequilibrium plasma properties, and an MHD generator designed on that basis can be expected to perform satisfactorily in the near future. The first four points are based on a technological extrapolation. Their realization must depend on continued progress in plasma research. It is interesting to compare Points 1 and 5. The former is 5 points better in thermodynamic efficiency and 1.50 mills/MJ (5.4 mills/kWh) lower in power cost. For Point 6 the inlet stagnation temperature is lowered to 1978°K (3100°F). The thermodynamic efficiency is 4 points lower, and the capital cost is 16.6% lower. Power cost is about 3.13 mills/MJ (11.26 mills kWh) lower than Point 1. Point 7 is based on thermal ionization at an inlet temperature of 2367°K (3800°F). The thermodynamic efficiency is 5 points lower, and a higher magnetic flux density is required. However, capital cost is 6.8% lower and power cost is 1.02 mills/MJ (3.68 mills/kWh) lower than Point 1.

To summarize, Point 6 appears to be the best system. It can convert 55% of every Btu added to the argon gas into electrical energy. But to get 1 Btu into the argon gas, it is necessary to burn 1-1/4 Btu worth of coal. This extra 1/4 Btu, needed because of gasifier losses, stack losses, station auxiliary power and other minor losses, cuts down the power plant efficiency from 55 to 42%. The cost of electricity, estimated at 19.0 mills/MJ (68.5 mills/kWh), is very high. The major culprit is the very high capital cost of the external heating system.

10.5 Capital and Installation Costs of Plant Components

By far the most expensive component in the closed-cycle MHD plant is the main heat exchanger, HX_1. For Point 6, the material and installation cost of the refractory stoves (including piping and valves) was estimated at $366.7 million. (See Appendix A 10.1 for details.) There is

considerable margin for error in this figure for two reasons. First, time did not permit us to look at alternative designs; and second, again for lack of time, there was no opportunity to cost-optimize the design selected. The time period of the heating/cooling cycle, the number of stoves, and the checker size was selected arbitrarily. The question of impurity carry-over, which has a profound influence upon the design, is rather poorly understood. There is a dearth of design data. For all these reasons, we are unable to establish by what margin the estimated cost could be reduced.

After the main heat exchanger, the next most expensive components are gasifiers ($97.6 million), dc/ac power conditioning system ($56 million), superconducting magnet ($36 million), and steam generator for bottoming plant ($47 million). Gasifiers are discussed in Section 4.4 of this report.

Westinghouse has made several design studies of dc/ac conversion systems. The information in Appendix A 10.3 is based on a recent study which was conducted with great technical sophistication, but Westinghouse has yet to market such a system in very large power ratings. The installation cost is particularly uncertain. The estimated total direct cost could be off by ± 25%.

The superconducting magnet (Appendix A 10.2) was designed to a lesser degree of sophistication than the dc/ac inverter. The dewar and the supporting structure were not designed in great detail in the time available. The estimated cost could be in error by ± 100%.

The estimated cost of the steam generator is probably too high but by a smaller margin, proportionately, than the main heat exchanger, HX_1.

A detailed account listing of material and installation costs for Parametric Point 6 [with the 1978°K (3100°F) stoves] is given in Tables 10.14, 10.15, and 10.16. Similar data is given in Appendix A 10.7, Tables A 10.7.1, A 10.7.2 and A 10.7.3 for Parametric Point 2. Point 2 is similar to Point 6 except for the use of a higher argon temperature 2367°K (3800°F).

Table 10.14 CLOSED CYCLE MHD SYSTEM ACCOUNT LISTING
PARAMETRIC POINT NO. 6

ACCOUNT NO. & NAME	UNIT	AMOUNT	MAT $/UNIT	INS $/UNIT	MAT COST,$	INS COST,$
SITE DEVELOPMENT						
1. 1 LAND COST	ACRE	231.0	1000.00	.00	231000.00	.00
1. 2 CLEARING LAND	ACRE	77.0	.00	600.00	.00	46195.38
1. 3 GRADING LAND	ACRE	231.0	.00	3000.00	.00	693000.00
1. 4 ACCESS RAILROAD	MILE	5.0	115000.00	110000.00	575000.00	550000.00
1. 5 LOOP RAILROAD TRACK	MILE	3.0	120000.00	70000.00	360000.00	210000.00
1. 6 SIDING R R TRACK	MILE	.0	125000.00	80000.00	.00	.00
1. 7 OTHER SITE COSTS	ACRE	.0	.00	.00	477275.38	477275.38
PERCENT TOTAL DIRECT COST IN ACCOUNT 1 =			.473	ACCOUNT TOTAL,$	1643275.37	1976470.75
EXCAVATION & PILING						
2. 1 COMMON EXCAVATION	YDT	2538000.0	.00	3.00	.00	805500.00
2. 2 PILING	FT	716000.0	8.50	8.00	4854000.00	6086000.00
PERCENT TOTAL DIRECT COST IN ACCOUNT 2 =			1.446	ACCOUNT TOTAL,$	4854000.00	6891500.00
PLANT ISLAND CONCRETE						
3. 1 PLANT IS. CONCRETE	YDT	88500.0	70.00	80.00	6265000.00	7160000.00
3. 2 SPECIAL STRUCTURES	YDT	2340.0	.00	.00	.00	.00
PERCENT TOTAL DIRECT COST IN ACCOUNT 3 =			1.891	ACCOUNT TOTAL,$	6265000.00	7160000.00
HEAT REJECTION SYSTEM						
4. 1 COOLING TOWERS	EACH	14.0	.00	.00	2149000.00	1071000.00
4. 2 CIRCULATING H2O SYS	EACH	1.0	.00	.00	933062.77	1251119.23
4. 3 SURFACE CONDENSER	FT2	370483.0	.00	.00	1650104.03	245342.27
PERCENT TOTAL DIRECT COST IN ACCOUNT 4 =			.914	ACCOUNT TOTAL,$	4732156.75	2567461.47
STRUCTURAL FEATURES						
5. 1 STAT. STRUCTURAL ST.	TON	2600.0	670.00	175.00	1722500.00	467750.00
5. 2 SILOS & BUNKERS	TPH	.0	1800.00	750.00	.00	.00
5. 3 CHIMNEY	FT	400.0	.00	.00	435070.92	652606.38
5. 4 STRUCTURAL FEATURES	EACH	1.0	966000.00	231000.00	966000.00	231000.00
PERCENT TOTAL DIRECT COST IN ACCOUNT 5 =			.580	ACCOUNT TOTAL,$	3123570.91	1347356.37
BUILDINGS						
6. 1 STATION BUILDINGS	FT2	430000.0	.16	.16	688000.00	688000.00
6. 2 ADMINSTRATION	FT2	10000.0	16.00	14.00	150000.00	140000.00
6. 3 WAREHOUSE & SHOP	FT2	20000.0	12.00	8.00	240000.00	160000.00
PERCENT TOTAL DIRECT COST IN ACCOUNT 6 =			.256	ACCOUNT TOTAL,$	1088000.00	988000.00
FUEL HANDLING & STORAGE						
7. 1 COAL HANDLING SYS	TPH	358.3	.00	.00	5071350.31	2204299.03
7. 2 DOLOMITE HAND. SYS	TPH	133.8	.00	.00	1423623.05	673776.48
7. 3 FUEL OIL HAND. SYS	CAL	110000.0	.00	.00	22370.43	18100.14
PERCENT TOTAL DIRECT COST IN ACCOUNT 7 =			1.179	ACCOUNT TOTAL,$	6522343.69	2896175.62
FUEL PROCESSING						
8. 1 COAL DRYER & CRUSHER	TPH	.0	.00	.00	.00	.00
8. 2 CARBONIZERS	TPH	.0	.00	.00	.00	.00
8. 3 GASIFIERS	TPH	358.3	.00	.00	52469861.00	35150546.50
PERCENT TOTAL DIRECT COST IN ACCOUNT 8 =			12.236	ACCOUNT TOTAL,$	52469861.00	35150546.50

Table 10.14 Continued — CLOSED CYCLE MHD SYSTEM ACCOUNT LISTING
PARAMETRIC POINT NO. 6

ACCOUNT NO. & NAME	UNIT	AMOUNT	MAT $/UNIT	INS $/UNIT	MAT COST,$	INS COST,$
FIRING SYSTEM						
9. 1		.0	.00	.00	.00	.00
PERCENT TOTAL DIRECT COST IN ACCOUNT 9 = .000 ACCOUNT TOTAL,$					.00	.00
VAPOR GENERATOR (FIRED)						
10. 1		.0	.00	.00	.00	.00
PERCENT TOTAL DIRECT COST IN ACCOUNT 10 = .000 ACCOUNT TOTAL,$					.00	.00
ENERGY CONVERTER						
11. 1 AIR PREHEATER	EA	1.0	351000.00	597000.00	851000.00	597000.00
11. 2 ARGON PREHEATER	EA	1.0	30300000.00	19400000.00	30900000.00	19400000.00
11. 3 REFRACTORY STOVES		1.0	1195400000.00	30500000.00	1195240000.00	30500000.00
11. 4 PIPING,VALVES,ETC		1.0	13548000.00	5420000.00	13548000.00	5420000.00
11. 5 HEADER & NOZZLE	EA	1.0	194382.00	194382.00	194382.00	194382.00
11. 6 MHD GENERATOR DUCT	EA	1.0	397828.00	462402.00	397828.00	462402.00
11. 7 SUPERCONDUCTING MAGNET	EA	1.0	76000000.00	.00	76000000.00	.00
11. 8 DIFFUSER	EA	1.0	129588.00	129588.00	129588.00	129588.00
11. 9 COMPRESSORS		1.0	3629000.00	.00	3629000.00	.00
11.10 INTERCOOLERS		1.0	2407000.00	.00	2407000.00	.00
11.11 COMPRESSED ARGON DISTRIB		1.0	129588.00	129588.00	129588.00	129588.00
11.12 CESIUM COLLECTOR/INJECT		1.0	100000.00	50000.00	100000.00	50000.00
11.13 A & CS INVENTORY		1.0	200000.00	.00	200000.00	.00
PERCENT TOTAL DIRECT COST IN ACCOUNT 11 = 73.682 ACCOUNT TOTAL,$					411853482.00	56982960.00
COUPLING HEAT EXCHANGER						
12. 1 STEAM GENERATOR	EA	1.0	47046000.00	.00	47046000.00	.00
12. 2 COMP DRIVE TURBINE	EA	1.0	19297000.00	1265041.23	19297000.00	1265041.23
12. 3 STEAM TURB-GEN	EA	1.0	459000.00	88795.31	459000.00	88795.31
12. 4 FEED WATER HEATER PIPING		1.0	310000.00	.00	310000.00	.00
PERCENT TOTAL DIRECT COST IN ACCOUNT 12 = 3.573 ACCOUNT TOTAL,$					67112000.00	1353837.14
HEAT RECOVERY HEAT EXCH.						
13. 1		.0	.00	.00	.00	.00
PERCENT TOTAL DIRECT COST IN ACCOUNT 13 = .000 ACCOUNT TOTAL,$					.00	.00
WATER TREATMENT						
14. 1 DEMINERALIZER	GPM	797.5	2000.00	560.00	1587979.52	444382.27
14. 2 CONDENSATE POLISHING	KWE	397600.0	1.25	.30	824624.98	197910.00
PERCENT TOTAL DIRECT COST IN ACCOUNT 14 = .392 ACCOUNT TOTAL,$					2411704.50	642292.26
POWER CONDITIONING						
15. 1 INVERTER SETS		1.0	39630000.00	3705600.00	39630000.00	3705600.00
15. 2 INVERTER TRANSFORMER		1.0	8328000.00	999360.00	8328000.00	999360.00
15. 3 DC INTERRUPTERS		1.0	5935000.00	712320.00	5935000.00	712320.00
15. 4 AC CIRCUIT BREAKERS		1.0	614000.00	73680.00	614000.00	73680.00
15. 5 POWER TRANSFORMERS		1.0	4592000.00	551040.00	4592000.00	551040.00
15. 6 STD TRANSFORMER		14300.0	.00	.00	545962.99	10919.26
PERCENT TOTAL DIRECT COST IN ACCOUNT 15 = 7.131 ACCOUNT TOTAL,$					79895962.50	6052919.25

Table 10.14 Continued

CLOSED CYCLE MHD SYSTEM ACCOUNT LISTING
PARAMETRIC POINT NO. 9

ACCOUNT NO. & NAME	UNIT	AMOUNT	MAT $/UNIT	INS $/UNIT	MAT COST,$	INS COST,$
AUXILIARY MECH EQUIPMENT						
16. 1 BOILER FEED PUMP &DR.	KWE	573813.9	1.87	.10	1058489.25	63991.39
16. 2 OTHER PUMPS	KWE	531913.6	.89	.12	512083.91	66829.62
16. 3 MISC SERVICE SYS	KWE	1059855.9	1.17	.73	1134731.39	707334.80
16. 4 AUXILIARY BOILER	PPH	300000.0	4.00	.80	1200000.00	240000.00
PERCENT TOTAL DIRECT COST IN ACCOUNT 16 = .526			ACCOUNT TOTAL,$		3915304.53	1081805.90
PIPE & FITTINGS						
17. 1 CONVENTIONAL PIPING	TON	1777.0	7000.00	1800.00	5925000.00	3555000.00
17. 2 HIGH TEMP AIR PIPING	TON	.0	.00	.00	.00	.00
17. 3 LOW TEMP AIR PIPING	TON	.0	.00	.00	.00	.00
17. 4 RECIR PRODUCT PIPING	TON	.0	.00	.00	.00	.00
PERCENT TOTAL DIRECT COST IN ACCOUNT 17 = 1.197			ACCOUNT TOTAL,$		5925000.00	3555000.00
AUXILIARY ELEC EQUIPMENT						
18. 1 MISC MOTORS,TIE		578813.1	1.40	.17	350458.77	115412.85
18. 2 SWITCHGEAR & MCC PAN	KWE	879800.1	1.95	.45	1323853.28	395504.51
18. 3 CONDUIT,CABLES,TRAYS	FT	3450000.0	1.32	1.35	7133999.94	7411999.94
18. 4 ISOLATED PHASE BUS	FT	250.0	510.00	450.00	127500.00	112500.00
18. 5 LIGHTING & COMMUN	KWE	979855.9	.35	.43	339449.56	417038.04
PERCENT TOTAL DIRECT COST IN ACCOUNT 18 = 2.291			ACCOUNT TOTAL,$		9935261.37	8362455.37
CONTROL, INSTRUMENTATION						
19. 1 COMPUTER	EACH	1.0	650000.00	15000.00	650000.00	15000.00
19. 2 OTHER CONTROLS	EACH	1.0	951000.00	571000.00	951000.00	571000.00
PERCENT TOTAL DIRECT COST IN ACCOUNT 19 = .275			ACCOUNT TOTAL,$		1511000.00	586000.00
PROCESS WASTE SYSTEMS						
20. 1 BOTTOM ASH	TPH	.0	.00	.00	.00	.00
20. 2 DRY ASH	TPH	24.4	2030357.78	522714.45	2030357.78	522714.45
20. 3 WET SLURRY	TPH	189.8	4812269.44	1263067.36	4812269.44	1263067.36
20. 4 ONSITE DISPOSAL	ACRE	602.5	8527.75	8425.53	3330265.94	5075098.19
20. 5 SEED TREATMENT	EACH	.0	.00	.00	.00	.00
PERCENT TOTAL DIRECT COST IN ACCOUNT 20 = 2.173			ACCOUNT TOTAL,$		10233393.12	6901879.94
STACK GAS CLEANING						
21. 1 PRECIPITATOR	EACH	.0	.00	.00	.00	.00
21. 2 SCRUBBER	KWE	.0	22.54	10.38	.00	.00
21. 3 MISC STEEL & DUCTS		.0	.00	.00	.00	.00
PERCENT TOTAL DIRECT COST IN ACCOUNT 21 = .000			ACCOUNT TOTAL,$		.00	.00
TOTAL DIRECT COSTS,$					654211230.00	144396556.00

Table 10.15

CLOSED CYCLE MHD SYSTEM COST OF ELECTRICITY, MILLS/KW.HR
PARAMETRIC POINT NO. [illegible]

ACCOUNT	RATE, PERCENT	LABOR RATE, $/HR 6.00	8.00	10.50	15.00	21.50
TOTAL DIRECT COSTS,$	.0	737943232.	770801648.	798607928.	858545168.	947091288.
INDIRECT COST,$	51.0	41624717.	59052792.	73642293.	104210792.	149368802.
PROF & OWNER COSTS,$	8.0	50875518.	51500833.	63838634.	58583693.	75757703.
CONTINGENCY COST,$	11.0	80553275.	84700114.	87846871.	94440077.	104180041.
SUB TOTAL,$	.0	917450123.	973354016.	1023985712.	1125380720.	1276407408.
ESCALATION COST,$	6.5	321235832.	341705940.	358534668.	394211820.	446916632.
INTREST DURING CONST,$	10.0	403380728.	435220498.	456920804.	502388184.	569555836.
TOTAL CAPITALIZATION,$	.0	1642031680.	1772081408.	1839441168.	2022480704.	2292879968.
COST OF ELEC-CAPITAL	18.0	54.16355	57.58835	60.45932	65.47552	75.36309
COST OF ELEC-FUEL	.0	6.87039	6.87039	6.87039	6.87039	6.87039
COST OF ELEC-OP & MAIN	.0	1.17103	1.17103	1.17103	1.17103	1.17103
TOTAL COST OF ELEC	.0	62.21108	65.62977	68.50074	74.51694	83.40451

ACCOUNT	RATE, PERCENT	CONTINGENCY, PERCENT -5.00	.00	11.00	5.00	20.00
TOTAL DIRECT COSTS,$	.0	798607928.	798607928.	798607928.	798607928.	798607928.
INDIRECT COST,$	51.0	73642293.	73642293.	73642293.	73642293.	73642293.
PROF & OWNER COSTS,$	8.0	63888634.	63888634.	63888634.	63888634.	63888634.
CONTINGENCY COST,$	20.0	-39930396.	0.	87846871.	39930396.	159721584.
SUB TOTAL,$	.0	896208456.	936138848.	1023985712.	976069240.	1095860432.
ESCALATION COST,$	6.5	313795200.	327776294.	358534668.	341757368.	383700624.
INTREST DURING CONST,$	10.0	399504300.	417721956.	456920804.	435537612.	488932592.
TOTAL CAPITALIZATION,$	.0	1609507935.	1681637072.	1839441168.	1753366208.	1968553648.
COST OF ELEC-CAPITAL	18.0	52.95495	55.27257	60.45932	57.63018	64.70303
COST OF ELEC-FUEL	.0	6.87039	6.87039	6.87039	6.87039	6.87039
COST OF ELEC-OP & MAIN	.0	1.17103	1.17103	1.17103	1.17103	1.17103
TOTAL COST OF ELEC	.0	60.99637	63.31399	68.50074	65.67160	72.74445

ACCOUNT	RATE, PERCENT	ESCALATION RATE, PERCENT 5.00	6.50	8.00	10.00	.00
TOTAL DIRECT COSTS,$	.0	798607928.	798607928.	798607928.	798607928.	798607928.
INDIRECT COST,$	51.0	73642293.	73642293.	73642293.	73642293.	73642293.
PROF & OWNER COSTS,$	8.0	63888634.	63888634.	63838634.	63888634.	63888634.
CONTINGENCY COST,$	11.0	87846871.	87846871.	87846871.	87846871.	87846871.
SUB TOTAL,$	.0	1023985712.	1023985712.	1023985712.	1023985712.	1023985712.
ESCALATION COST,$	.0	276056080.	358534668.	455770064.	594907648.	0.
INTREST DURING CONST,$	10.0	431621034.	456920804.	483521763.	521110784.	355004248.
TOTAL CAPITALIZATION,$	.0	1722662849.	1839441168.	1963277535.	2140004144.	1378989952.
COST OF ELEC-CAPITAL	18.0	56.62102	60.45932	64.52962	70.33832	45.35794
COST OF ELEC-FUEL	.0	6.87039	6.87039	6.87039	6.87039	6.87039
COST OF ELEC-OP & MAIN	.0	1.17103	1.17103	1.17103	1.17103	1.17103
TOTAL COST OF ELEC	.0	64.66243	68.50074	72.57103	78.37974	53.39935

ACCOUNT	RATE, PERCENT	INT DURING CONST, PERCENT 6.00	8.00	10.00	12.00	15.00
TOTAL DIRECT COSTS,$	.0	798607928.	798607928.	798607928.	798607928.	798607928.
INDIRECT COST,$	51.0	73642293.	73642293.	73642293.	73642293.	73642293.
PROF & OWNER COSTS,$	8.0	63888634.	63888634.	63838634.	63888634.	63888634.
CONTINGENCY COST,$	11.0	87846871.	87846871.	87846871.	87846871.	87846871.
SUB TOTAL,$	.0	1023985712.	1023985712.	1023985712.	1023985712.	1023985712.
ESCALATION COST,$	6.5	358534668.	358534668.	358534668.	358534668.	358534668.
INTREST DURING CONST,$	15.0	259619412.	355689906.	456920804.	591102872.	734263064.
TOTAL CAPITALIZATION,$	.0	1642139776.	1738210352.	1839441168.	1973623252.	2116783424.
COST OF ELEC-CAPITAL	18.0	53.97436	57.13204	60.45932	64.86966	69.57510
COST OF ELEC-FUEL	.0	6.87039	6.87039	6.87039	6.87039	6.87039
COST OF ELEC-OP & MAIN	.0	1.17103	1.17103	1.17103	1.17103	1.17103
TOTAL COST OF ELEC	.0	62.01577	65.17345	68.50074	72.91108	77.61651

Table 10.15 Continued CLOSED CYCLE MHD SYSTEM COST OF ELECTRICITY, MILLS/KW.HR
PARAMETRIC POINT NO. 8

ACCOUNT	RATE, PERCENT	FIXED CHARGE RATE, PCT 10.00	14.40	18.00	21.60	25.00
TOTAL DIRECT COSTS,$	.0	799607928.	799607928.	799607928.	799607928.	799607928.
INDIRECT COST,$	11.0	73642293.	73642293.	73642293.	73642293.	73642293.
PROF & OWNER COSTS,$	8.0	63888634.	63888634.	63888634.	63888634.	63888634.
CONTINGENCY COST,$	11.0	87846871.	87846871.	87846871.	87846871.	87846871.
SUB TOTAL,$	.0	1023985712.	1023985712.	1023985712.	1023985712.	1023985712.
ESCALATION COST,$	8.5	358534668.	358534668.	358534668.	358534668.	358534668.
INTREST DURING CONST,$	10.0	456920804.	456920804.	456920804.	456920804.	456920804.
TOTAL CAPITALIZATION,$	.0	1839441168.	1839441168.	1839441168.	1839441168.	1839441168.
COST OF ELEC-CAPITAL	20.0	33.58871	48.36746	60.45932	72.55118	83.97128
COST OF ELEC-FUEL	.0	6.87039	6.87039	6.87039	6.87039	6.87039
COST OF ELEC-OP & MAIN	.0	1.17103	1.17103	1.17103	1.17103	1.17103
TOTAL COST OF ELEC	.0	41.62943	56.40887	68.50074	80.59260	92.01270

ACCOUNT	RATE, PERCENT	FUEL COST, $/10**6 BTU .50	.95	1.50	2.50	1.02
TOTAL DIRECT COSTS,$	.0	799607928.	799607928.	799607928.	799607928.	799607928.
INDIRECT COST,$	11.0	73642293.	73642293.	73642293.	73642293.	73642293.
PROF & OWNER COSTS,$	8.0	63888634.	63888634.	63888634.	63888634.	63888634.
CONTINGENCY COST,$	11.0	87846871.	87846871.	87846871.	87846871.	87846871.
SUB TOTAL,$	.0	1023985712.	1023985712.	1023985712.	1023985712.	1023985712.
ESCALATION COST,$	8.5	358534668.	358534668.	358534668.	358534668.	358534668.
INTREST DURING CONST,$	10.0	456920804.	456920804.	456920804.	456920804.	456920804.
TOTAL CAPITALIZATION,$	.0	1839441168.	1839441168.	1839441168.	1839441168.	1839441168.
COST OF ELEC-CAPITAL	18.0	60.45932	60.45932	60.45932	60.45932	60.45932
COST OF ELEC-FUEL	.0	4.74140	5.87039	12.12421	20.20702	8.24446
COST OF ELEC-OP & MAIN	.0	1.17103	1.17103	1.17103	1.17103	1.17103
TOTAL COST OF ELEC	.0	66.37176	68.50074	73.75456	81.83737	69.87482

ACCOUNT	RATE, PERCENT	CAPACITY FACTOR, PERCENT 10.00	45.00	50.00	65.00	80.00
TOTAL DIRECT COSTS,$	.0	799607928.	799607928.	799607928.	799607928.	799607928.
INDIRECT COST,$	11.0	73642293.	73642293.	73642293.	73642293.	73642293.
PROF & OWNER COSTS,$	8.0	63888634.	63888634.	63888634.	63888634.	63888634.
CONTINGENCY COST,$	11.0	87846871.	87846871.	87846871.	87846871.	87846871.
SUB TOTAL,$	.0	1023985712.	1023985712.	1023985712.	1023985712.	1023985712.
ESCALATION COST,$	8.5	358534668.	358534668.	358534668.	358534668.	358534668.
INTREST DURING CONST,$	10.0	456920804.	456920804.	456920804.	456920804.	456920804.
TOTAL CAPITALIZATION,$	.0	1839441168.	1839441168.	1839441168.	1839441168.	1839441168.
COST OF ELEC-CAPITAL	18.0	327.43300	87.33014	78.53712	60.45932	49.12320
COST OF ELEC-FUEL	.0	6.87039	6.87039	6.87039	6.87039	6.87039
COST OF ELEC-OP & MAIN	.0	1.17104	1.17103	1.17103	1.17103	1.17103
TOTAL COST OF ELEC	.0	335.47442	95.37155	86.63854	68.50074	57.16462

Table 10.16 CLOSED CYCLE MHD SYSTEM

ACCOUNT NO	AUX POWER,MWE	PERC PLANT POW	OPERATION COST	MAINTENANCE COST
4	7.31283	.82273	45.40893	12.49936
7	5.27012	.54379	1014.31078	.00000
8	10.89731	1.11224	3.30234	.00000
14	.00000	.00000	63.25142	.00000
18	5.07020	.52717	.00000	.00000
20	19.99909	2.07625	.00000	.00000
TOTALS	38.21575	3.97342	1126.27351	12.49936

CLOSED CYCLE MHD SYSTEM BASE CASE INPUT

NOMINAL POWER, MWE	1000.0000	NET POWER, MWE	961.7842
NOM HEAT RATE, BTU/KW-HR	7773.9178	NET HEAT RATE, BTU/KW-HR	8082.8085
OFF DESIGN HEAT RATE	1.0200		
CONDENSER			
DESIGN PRESSURE, IN HG A	2.0100	NUMBER OF SHELLS	3.0000
NUMBER OF TUBES/SHELL	5782.1128	TUBE LENGTH, FT	77.4467
U, BTU/HR-FT2-F	691.4077	TERMINAL TEMP DIFF, F	5.0000
HEAT REJECTION			
DESIGN TEMP, F	51.4000	APPROACH, F	21.6744
RANGE, F	27.0000	OFF DESIGN TEMP, F	77.0000
OFF DESIGN PRES, IN HG A	3.0031	LP TURBINE BLADE LEN, IN	29.5000

1	1000.000	2	.951	3	.439	4	.000	5	8.000
6	11.700	7	3.000	8	813.000	9	3.000	10	2.000
11	1.000	12	648.000	13	1.000	14	4.000	15	1.000
16	2.000	17	231.000	18	3.000	19	5.000	20	3.000
21	.000	22	39500.000	23	2340.000	24	2650.000	25	400.000
26	4300000.000	27	10000.000	28	20000.000	29	110000.000	30	.600
31	1.000	32	1975.000	33	.000	34	.700	35	.700
36	5450000.000	37	250.000	38	1.000	39	1.000	40	966000.000
41	231000.000	42	660000.000	43	15000.000	44	951000.000	45	571000.000
46	1.000	47	.000	48	3.000	49	1.000	50	.000
51	.500	52	5.350						
1	1.000	2	1.000	3	1.000	4	1.000	5	1.000
6	1.000	7	1.000	8	1.000	9	1.000	10	1.000
11	1.000	12	1.000	13	1.000	14	851000.000	15	597000.000
16	30900000.000	17	17400000.000	18	125240000.000	19	30600000.000	20	135480000.000
21	5420000.000	22	194382.000	23	194382.000	24	393898.000	25	462402.000
26	35000000.000	27	.000	28	129588.000	29	129588.000	30	9628000.000
31	.000	32	2407000.000	33	.000	34	129588.000	35	129588.000
36	100000.000	37	50000.000	38	200000.000	39	.000	40	1.000
41	1.000	42	1.000	43	1.000	44	4704000.000	45	.000
46	19297000.000	47	.000	48	459000.000	49	.000	50	310000.000
51	.000	52	1.000	53	1.000	54	1.000	55	1.000
56	1.000	57	1.000	58	70980000.000	59	3705600.000	60	8328000.000
61	989360.000	62	5936000.000	63	712320.000	64	614000.000	65	73680.000
66	4592000.000	67	551040.000	68	300000.000	69	.000	70	.000
71	.000	72	.000	73	.000	74	.000	75	.000

10.6 Analysis of Overall Cost of Electricity

The method of calculation is described in Section II of this report. Results for Parametric Point 6 are given in Table 10.15. Sensitivity to changes in labor rate, contingency, escalation rate, and so forth, is displayed. Plant results, including the cost of electricity for Parametric Points 1 through 7 are summarized in Tables 10.17 and 10.18. Natural resources requirements (coal, water, land, etc.) are listed in Table 10.19.

As can be seen from Table 10.3, 10.17, or 10.18, the lowest cost of electricity is 19.0 mills/MJ (68.5 mills/kWh) for Parametric Point 6. This figure is unacceptably high. It should be noted that 88.2% of the cost of electricity is due to capital investment, and 72% of the total major component cost is due to the external heating system.

10.7 Conclusions and Recommendations

1. Taken by itself, the nonequilibrium MHD generator is a very attractive energy converter. It is capable of high power density, large enthalpy extraction, and good isentropic efficiency without requiring excessively high temperatures or very strong magnetic fields. Its working fluid, an inert gas seeded with a very low concentration of cesium, is much less corrosive than combustion products seeded with cesium or potassium. Its continued development is recommended.

2. When combined with a 24.13 MPa/811°K/811°K (3500 psia/1000°F/1000°F) steam plant, it is capable of a thermodynamic efficiency as high as 59.3%. This efficiency drops to 45.5%, however, if the argon gas has to be heated externally [to 2367°K (3800°F)] with gasified coal through a periodic heat exchanger of the refractory-stove type, which is exceedingly expensive. A similar system which heats the argon to 1978°K (3100°F) shows a thermodynamic efficiency of 55.1% and a power plant efficiency of 42.2%.

3. The combined power plant being evaluated, although efficient, is very capital intensive. The 1978°K (3100°F) external heating system accounts for 72% of the total major component cost. The cost of electricity [$\sim$ 19.0 mills/MJ ($\sim$ 68.5 mills/kWh)] is distressingly high, and 88% of this cost is due to capital investment.

Table 10.17 CLOSED CYCLE MHD SYSTEM SUMMARY PLANT RESULTS

PARAMETRIC POINT	1	2	3	4	5	6	7	8
THERMODYNAMIC EFF	.593	.593	.593	.593	.541	.551	.542	.000
POWER PLANT EFF	.455	.461	.461	.500	.414	.422	.413	.000
OVERALL ENERGY EFF	.455	.461	.461	.336	.414	.422	.413	.000
CAP COST MILLION $	2200.827	2178.449	2202.289	1666.694	2378.639	1839.441	2057.212	.000
CAPITAL COST,$/KWE	2287.464	2223.309	2256.367	1335.553	2434.354	1912.530	2145.665	.000
COE CAPITAL	72.312	70.442	71.329	53.316	76.956	60.459	67.861	.000
COE FUEL	5.370	6.237	6.237	17.745	7.012	8.870	7.023	.000
COE OP & MAIN	1.081	.345	.363	.048	1.196	1.171	1.198	.000
COST OF ELECTRIC	73.753	77.074	77.933	71.109	85.154	68.501	76.092	.000
EST TIME OF CONST	8.000	8.000	8.000	8.000	8.000	8.000	8.000	.000

Table 10.18 CLOSED CYCLE MHD SYSTEM SUMMARY PLANT RESULTS

PARAMETRIC POINT		1	2	3	4	5	6	7	8
TOTAL CAPITAL COST	,M$	2206.83	2178.45	2202.29	1666.69	2336.64	1839.44	2057.21	.00
PLANT HX1 SYSTEM-STOVES & PIPING	,M$	572.272	572.272	572.272	443.607	612.218	361.620	440.240	.000
SUPER CONDUCTING MAGNET	,M$	41.300	41.300	41.300	41.300	33.400	36.000	99.900	.000
GASIFIER & AIR PREHEATER	,M$	65.931	64.311	66.070	18.100	72.005	63.341	71.460	.000
DC POWER CONDITIONING	,M$	50.197	50.197	50.197	50.197	41.238	50.350	28.457	.000
STM TURB-GEN & FEED STRING	,M$	.841	.841	.841	.841	7.892	.769	17.892	.000
COMP-DRIVE TURB-INTERCOOLER	,M$	25.512	25.512	25.512	25.512	24.308	31.332	15.634	.000
HEAT RECOV STEAM GENERATOR	,M$	39.037	39.037	39.037	38.037	52.916	47.046	52.438	.000
MHD GENERATOR ASSEMBLY	,M$	1.663	1.663	1.663	1.613	1.532	1.147	2.628	.000
TOT MAJOR COMPONENT COST	,M$	796.753	795.133	796.892	620.207	845.509	591.605	728.648	.000
TOT MAJOR COMPONENT COST	,$/KWE	825.866	813.332	816.460	627.601	880.871	615.112	760.332	.000
BALANCE OF PLANT COST	,$/KWE	62.695	56.535	61.659	43.166	66.115	65.094	66.594	.000
SITE LABOR	,$/KWE	127.068	120.777	124.188	82.748	134.268	150.134	124.135	.000
TOTAL DIRECT COST	,$/KWE	1015.620	990.644	1002.307	753.513	1081.254	830.340	951.012	.000
INDIRECT COSTS	,$/KWE	64.805	61.596	63.336	42.201	68.477	76.568	63.309	.000
PROF & OWNER COSTS	,$/KWE	81.250	79.251	80.185	60.231	86.500	65.427	76.091	.000
CONTINGENCY COST	,$/KWE	111.719	108.971	110.254	82.886	118.938	91.337	104.611	.000
ESCALATION COST	,$/KWE	445.861	434.331	439.800	328.736	474.494	372.781	418.417	.000
INT DURING CONSTRUCTION	,$/KWE	568.210	553.516	560.486	418.945	604.701	475.076	533.236	.000
TOTAL CAPITALIZATION	,$/KWE	2287.464	2228.309	2256.367	1686.563	2434.364	1912.530	2146.666	.000
COST OF ELEC-CAPITAL	,MILLS/KWE	72.312	70.442	71.329	53.316	76.958	60.459	67.861	.000
COST OF ELEC-FUEL	,MILLS/KWE	6.370	6.287	6.297	17.745	7.012	6.870	7.023	.000
COST OF ELEC-OP&MAIN	,MILLS/KWE	1.081	.345	.363	.048	1.196	1.171	1.198	.000
TOTAL COST OF ELEC	,MILLS/KWE	79.763	77.074	77.988	71.109	85.164	68.501	76.082	.000
COE 0.5 CAP. FACTOR	,MILLS/KWE	101.456	98.206	99.387	87.104	108.251	86.639	96.440	.000
COE 0.8 CAP. FACTOR	,MILLS/KWE	56.204	53.866	54.614	61.113	70.735	57.165	63.358	.000
COE 1.2XCAP. COST	,MILLS/KWE	94.225	91.162	92.254	81.772	100.555	80.593	89.654	.000
COE 1.2XFUEL COST	,MILLS/KWE	81.037	78.331	79.248	74.658	96.566	69.875	77.486	.000
COE (CONTINGENCY=0)	,MILLS/KWE	73.419	70.886	71.727	66.402	78.410	63.314	70.141	.000
COE (ESCALATION=0)	,MILLS/KWE	61.701	59.479	60.172	57.792	65.942	53.399	59.132	.000

Table 10.19 CLOSED CYCLE MHD SYSTEM NATURAL RESOURCE REQUIREMENTS

PARAMETRIC POINT	1	2	3	4	5	6	7	8
COAL, LB/KW-HR	.69090	.79883	1.00792	.93995	.76048	.74513	.76170	.00000
SORBANT OR SEED,LB/KW-HR	.36556	.09053	.07804	.00000	.40237	.39425	.40301	.00000
TOTAL WATER, GAL/KW-HR	.541	.535	.534	.489	.666	.640	.665	.000
COOLING WATER	.495	.489	.490	.483	.615	.590	.614	.000
GASIFIER PROCESS HZO	.03980	.04084	.03851	.00000	.04380	.04292	.04387	.00000
CONDENSATE MAKE UP	.00549	.00542	.00543	.00536	.00675	.00658	.00656	.00000
WASTE HANDLING SLURRY	.0000	.0000	.0000	.0000	.0000	.0000	.0000	.0000
SCRUBBER WASTE WATER	.00000	.00000	.00000	.00000	.00000	.00000	.00000	.00000
NOX SUPPRESSION	.00000	.00000	.00000	.00000	.00000	.00000	.00000	.00000
TOTAL LAND ACRES/100MWE	104.54	98.24	98.98	37.66	116.41	113.12	116.50	.00
MAIN PLANT	23.94	23.63	27.67	15.58	24.07	24.02	24.10	.00
DISPOSAL LAND	58.08	52.29	47.96	.00	63.93	62.64	64.03	.00
LAND FOR ACCESS RR	22.52	22.32	23.35	22.08	28.41	26.47	28.46	.00

@@RKPT PRINT$

4. Looking to the future, we see several possibilities which will drastically reduce the capital cost:

- Further advances in nonequilibrium plasma research, particularly in the understanding and control of turbulence induced by ionization instability, may enable the MHD generator to operate at a temperature lower than 1978°K (3100°F) without loss of performance
- A suitable nuclear heat source may be developed to replace the external heating system herein assumed, thus increasing the efficiency toward 59.3%, in addition to reducing the capital cost
- New materials and/or new heat exchanger technology may be discovered to make a fossil-fuel fired heating system less costly.

5. It is recommended that the closed-cycle MHD system be re-evaluated in five or ten years without any restriction being placed on the heat source.

10.8 References

10.1 J. L. Kerrebrock, "Conduction in Gases with Elevated Electron Temperature," Second Symposium on the Engineering Aspects of MHD, Philadelphia, PA, March 9-10, 1961.

10.2 T. C. Tsu and L. S. Frost, "MHD Power Generation: Promises and Problems," Advanced Propulsion Concepts, Volume 1, (1963) Gordon and Breach Science Publishers, pp. 261-268.

10.3 T. C. Tsu and W. S. Emmerich, "A Reexamination of the Kerrebrock Effect as a Means for Enhancing Conductivity of MHD Fluids," Westinghouse Research Memo No. 63-118-266-M4, October 4, 1963.

10.4 E. P. Velikhov and A. M. Dykhne, "Plasma Turbulence Due to Ionization Instability in a Strong Magnetic Field," 6th International Conference on Ionization Phenomena in Gases, Paris, 1963.

10.5 V. Zampaglione, "Effective Conductivity of an MHD Plasma in a Turbulent State," Electricity from MHD, Volume I, International Atomic Energy Agency, Vienna, 1968, pp. 593-604.

10.6 V. Zampaglione, "Influence of Ionization Turbulence on the Performance of Nonequilibrium Plasma MHD Generators," 12th Symposium on Engineering Aspects of MHD, Argonne, Illinois, March 27-29, 1972.

10.7 P. Gay and V. Zampaglione, "Investigation of the MHD Interaction in a Subsonic Generator with Turbulent Non-Equilibrium Plasma," 13th Symposium, Engineering Apsects of MHD, Stanford University, March 26-28, 1973.

10.8 M. Gasparotto, et al., "Recent Results of Nonequilibrium MHD Generator Experiments in the C.N.E.N. Blow-Down Loop Facility," 6th International Conference on MHD Electrical Power Generation, Washington, D. C., June 9-13, 1975; Vol. III, pp. 47-62.

10.9 A. Solbes, "Quasi Linear Plane Wave Study of Electrothermal Instabilities," Electricity from MHD, International Atomic Energy Agency, Vienna, 1968; Vol. I, pp. 499-518.

10.10 R. Decher, M. A. Hoffman, and J. L. Kerrebrock, "Behavior of a Large Nonequilibrium MHD Generator," AIAA Journal, Vol. 9, No. 3, March 1971, pp. 357-364.

10.11 R. M. Evans and C. H. Kruger, "Effects of Channel Size on the Ionization Instability in MHD Generators," AIAA Journal, Vol. II, No. 7, July 1973, pp. 1006-1012.

10.12 G. Brederlow and K. J. Witte, "Effective Electrical Conductivity and Related Properties of a Nonequilibrium High Pressure MHD Plasma," AIAA Journal, Vol. 12, No. 1, January 1974, pp. 83-90.

10.13 B. Zauderer, E. Tate, and C. H. Marston, "Electrode Studies and Recent Results of Nonequilibrium MHD Generator Experiments," 14th Symposium Engineering Aspects of MHD, Tullahoma, Tenn., April 8-10, 1974.

10.14 C. Marston, E. Tate, and B. Zauderer, "Large Enthalpy Extraction Results in a Nonequilibrium MHD Generator," 6th International Conference on MHD Electrical Power Generation, Washington, D. C., June 9-13, 1975; Vol. III, pp. 89-104.

10.15 J. Blom, A. Veefkind, J. Houben, and L. Rietjens, "High Power Density Experiments in the Eindhoven Shocktunnel MHD Generator," 6th International Conference on MHD Electrical Power Generation, Washington, D. C., June 9-13, 1975; Vol. III, pp. 73-88.

10.16 W. E. Gunson, E. E. Smith, T. C. Tsu, and J. H. Wright, "MHD Power Conversion," Nucleonics, Vol. 21, No. 7, July 1963, pp. 43-47.

10.17 T. C. Tsu, "MHD Power Generators in Central Stations," IEEE Spectrum, Vol. 4, No. 6, June 1967, pp. 59-65.

10.18 A. R. Bishop and L. D. Nichols, "Conductivity of an Impure, Non-equilibrium Plasma with Electrothermal Instabilities," AIAA Journal, Vol. 8, No. 4, February 1970, pp. 829-831.

10.19 "Feasibility Study of Coal-Burning MHD Generation," Report in Three Volumes from Westinghouse Electric Corporation to Office of Coal Research, Contract No. 14-01-0001-476, Feb. 4, 1965 to Feb. 3, 1966.

10.20 B. Zauderer and E. Tate, "High Enthaply Extraction Experiments in a Large Non-Equilibrium MHD Generator," 13th Symposium, Engineering Aspects of MHD, March 26-28, 1973.

10.21 F. A. Hals, et al, "High Temperature Air Preheaters for Open Cycle MHD Energy Conversion Systems," AIChE Paper No. 16, 15th National Heat Transfer Conf., Aug. 1975.

10.22 Properties of Refractory Materials: Collected Data and References, LMSD-2466, Lockheed Aircraft Corp., Sunnyvale, CA, 15 Jan. 1959.

10.23 J. R. Hamm, Personal Communication, Oct. 18, 1966.

10.24 P. J. Schneider, "Conduction Heat Transfer," Addison Wesley, 1957, pg. 258.

10.25 W. H. McAdams, "Heat Transmission," McGraw-Hill, Third Edition, 1954, pg. 295,8.

10.26 P. Razelos and V. Paschkis, "The Thermal Design of Blast Furnace Stove Regenerators," Iron and Steel Engineer, Aug. 1968, pg. 81.

10.27 K. Rummel, J. Inst. Fuel, 4, 1931, p. 160-73.

10.28 F. Kreith, "Principles of Heat Transfer," International Textbook Co., 1960, Figure 9-18.

10.29 E. P. Neumann and F. Lustwerk, "Supersonic Diffusers for Wind Tunnels," Journal of Applied Mechanics, Vol. 71, 1949 pp. 195-202.

10.30 H. W. Emmons, Editor. "Fundamental of Gas Dynamics," Princeton University Press, 1958.

10.31 H. W. Liepmann and A. Roshko, "Elements of Gas Dynamics," J. Wiley, 1957.

10.32 "Compressed Gas Handbook," NASA SP-3045, 1970.

10.33 E. P. Neumann and F. Lustwerk, "High-Efficiency Supersonic Diffusers," Journal of Aeronautical Sciences, Vol. 51, No. 6, June 1951, pp. 369-374.

10.34 S. Huo, "Optimization Based on Boundary Layer Concept for Compressible Flows," Journal of Engineering for Power, Trans. ASME, April, 1975, pp. 195-206.

10.35 P. W. Runstadler, Jr. and R. C. Dean, Jr., "Straight Channel Diffuser Performance at High Inlet Mach Numbers," Journal of Basic Engineering, Trans. ASME, Vol. 91, September 1969, pp. 397-422.

10.36 F. X. Dolan and P. W. Runstadler, Jr., "Pressure Recovery Performance of Conical Diffusers at High Subsonic Mach Numbers," NASA CR-2299, 1973.

10.37 P. C. Chang, "Separation of Flow," 1st Edition, Pergamon Press, 1970.

10.38 T. C. Tsu, W. E. Young, and S. Way, "Optimization Studies of MHD Steam Plants," Electricity from MHD, Vol. III, International Atomic Energy Agency, Vienna, 1966.

10.39 L. S. Frost, "Conductivity of Seeded Atmospheric Pressure Plasmas," Journal of Applied Physics, Vol. 32, No. 10, 2029-2036, Oct. 1961.

10.40 E. Tate, C. H. Marston, B. Zauderer, "Large Enthalphy Extraction Experiments in a Non-equilibrium Magnetohydrodynamic Generator," Applied Physics Letters, Vol. 25, No. 10, 15 Nov. 1974, pp. 551-553.

10.41 E. Bertolini, M. Gasparotto, P. Gay, L. Panaccione, A. Tamburrano, "Closed-Cycle MHD Subsonic Power Generation Experiments at Frascati," 13th MHD Symposium, Stanford University, March 26-28, 1973, pp. I.1.1 - I.1.11.

10.42 R. Decher, M. A. Hoffman, J. L. Kerrebrock, "Behavior of a Large Non-equilibrium MHD Generator," AIAA Journal, Vol. 9, No. 3, 357-364, March 1971.

10.43 B. Zauderer, E. Tate, "Performance of a Large Scale, Non-equilibrium MHD Generator with Rare Gases," AIAA Journal, Vol. 9, No. 6, 1136-1143, June 1971.

10.44 Yu. M. Volkov, "Nonisothermal Pulse Discharge in Mixtures of Inert Gases with Cesium," High Temperature, Vol. 3, No. 1, 1-11, Jan-Feb. 1965.

10.45 I. P. Shkarofsky, M. P. Bachynski, T. W. Johnston, RCA Research Report 7-801, December 5, 1959.

10.46 A. J. Robertson, Private communication.

10.47 W. L. Nighan, A. J. Postma, "Electron Momentum Transfer Cross Section in Cesium," Phys. Rev. A., Vol. 6, No. 6, 2109-2117, December 1972.

10.48 R. S. Devoto, "Transport Coefficients of Partially Ionized Argon," Phys. of Fluids, Vol. 10, No. 2, 354-364, Feb. 1967.

10.49 B. Zauderer, E. Tate, "Electrode and Gasdynamic Effects in a Large Non-equilibrium MHD Generator," AIAA Journal, Vol. 11, No. 2, 149-155, February 1973.

10.50 L. A. Booth, "MHD Cycle Thermodynamics and 1000-MW_e Plant Studies," Nuclear Reactor Magnetohydrodynamic Power Generation, Los Alamos Scientific Laboratory of the University of California, LA-3368, 1966.

10.51 F. B. Hildebrand, Introduction to Numerical Analysis, McGraw-Hill New York, 1956.

10.52 R. W. Hamming, "Stable Predictor-Corrector Methods for Ordinary Differential Equations," Journal of the Assoc. for Comput.. Mach., January 1959, Vol. 6, No. 1, pp. 37-49.

10.53 R. W. Hamming, Numerical Methods for Scientists and Engineers, McGraw Hill, New York, 1962.

Appendix A 10.1

CLOSED-CYCLE MHD EXTERNAL COMBUSTION AND HEAT EXCHANGE SYSTEM DESIGN AND COSTING

A 10.1.1 Introduction

The purpose of the closed-cycle MHD combustion and heat exchange system is to provide for the external combustion of fuels and the transfer of the heat of combustion to a power plant topping cycle working fluid. The system consists of a combined combustion chamber and refractory periodic heat exchanger of the hot blast stove type, a combustion air preheater and various high-temperature valves. Figure A 10.1.1 shows the system schematic, and Figure 10.2 of the text shows the integration of this system into a plant layout. Figure A 10.1.2 details the heat exchange interconnecting piping of Figure 10.2 of the text. Several operational requirements are imposed on the heat exchange system:

- Noble gas must be supplied to the preionizer with a maximum of 300 ppm impurity.
- The apparatus must have a reasonable life expectancy.
- Noble gas must be supplied to meet cycle requirements for pressure level, pressure drop, mass flow, and temperature.

A 10.1.1.1 Stoves

A general discussion of stoves for MHD air preheating appears in Appendices A 9.2.1 and A 9.2.5. For a broader background, a publication unavailable during this study but currently available is Reference 10.21. The closed-cycle, nonequilibrium MHD system assumes the use of a fixed core regenerator which alternately is heated by combustion products at 101.3 kPa (1 atm) and cooled by releasing this heat to a

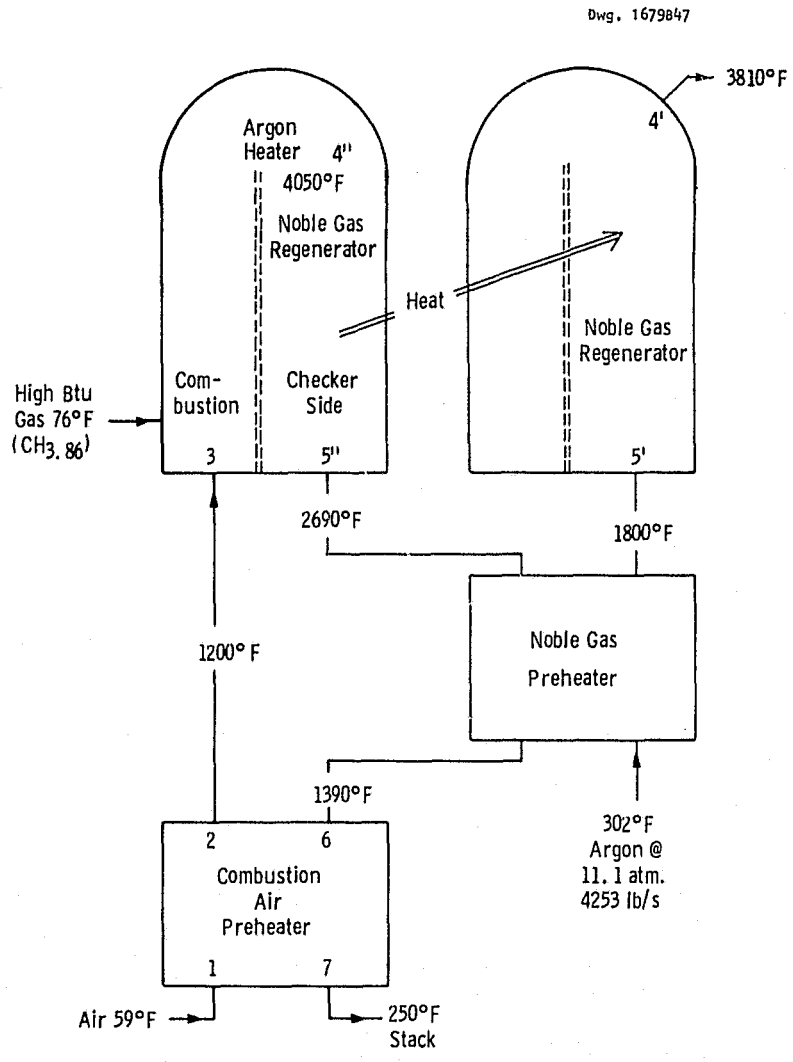

Fig. A 10.1.1 — Closed cycle MHD external combustion and heat exchange system schematic

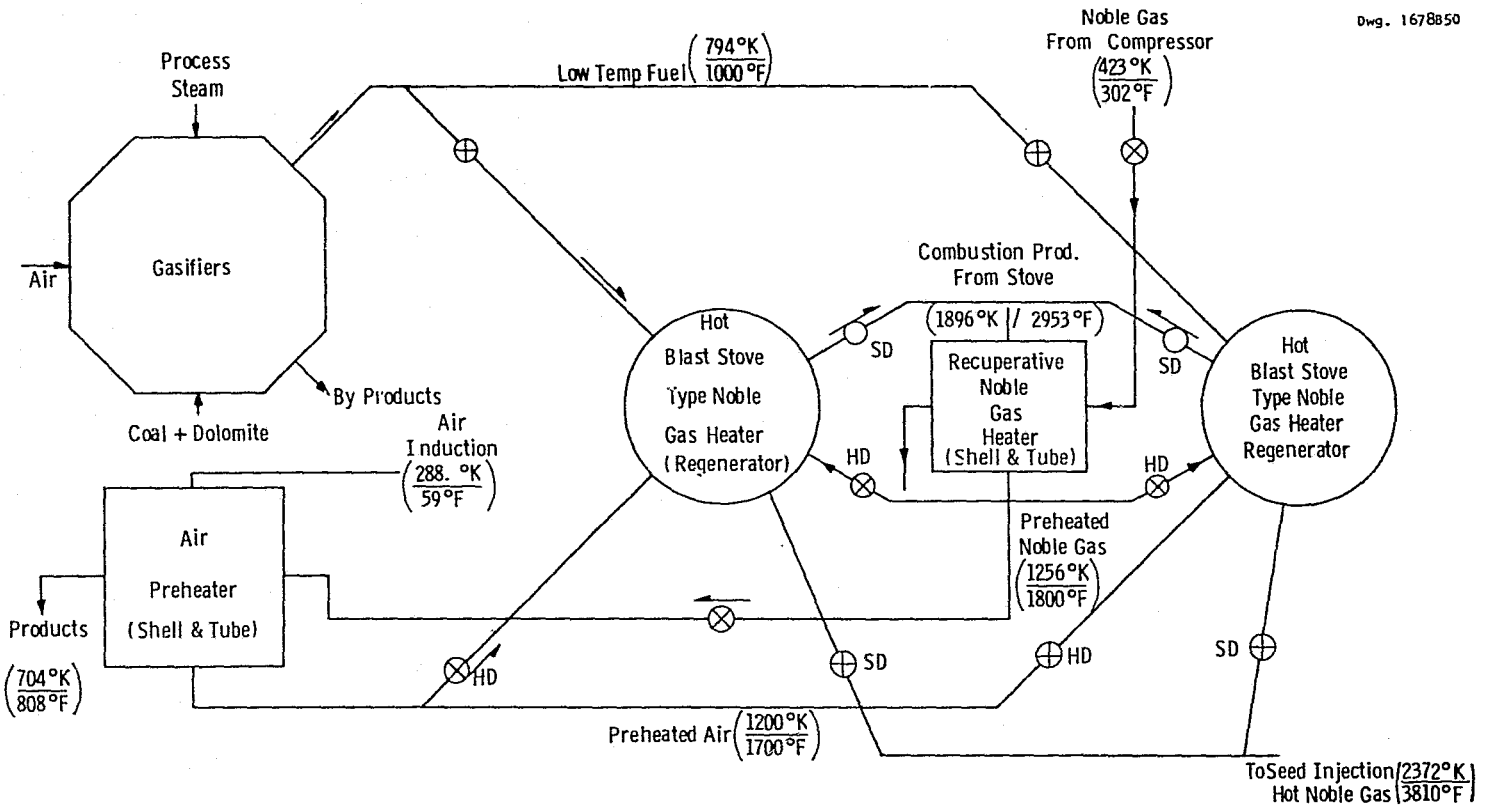

Symbols ⊗ H D Heavy duty water cooled gate valve with separate recessed, purge protected, water cooled goggle type automated seal.

⊗ S D Two heavy duty water cooled gate valves either side of the above goggle seal valve.

Fig. A 10.1.2-Combustion / heat exchange system plant interface schematic

noble gas at 1.114 MPa (11 atm). After firing fuel and preheated air in the stove to the proper checker temperature, the combustion products must be purged and the stove pressurized with noble gas. Following a checker cooling period the pressurized stove must be blown down to atmospheric pressure and refilled with combustion products. It is unlikely that the noble gas left in the stove after blowdown can be vented and lost so it is assumed to be purged into the low-temperature purifiers.

The purity of noble gas required significantly influences the stove design. Impurities in the noble gas circuit originate from three sources:

- Erosion from refractory surfaces and dust deposits
- Contaminants retained within the swept volume of the regenerator on purge cycle
- Out-gassing of absorbed impurities during the stove cool cycle.

All mechanisms of contamination are essentially proportional to the regenerator (stove) surface and heating-cooling time interval length. For long time intervals higher checker mass-to-surface area ratios are required.

Neglecting the first and third sources of contamination, swept volume considerations indicate that 3600 s (60 min) heat/cool cycles yield satisfactory contaminant levels.

Guidelines of Appendix A 9.2 concerning flue size are for dust loadings as follows: dust loadings of $\leq$ 0.114 g/m^3 (0.05 gr/ft^3) require 2.54 cm (1 in) diameter flues, and for dust loadings $\leq$ 0.343 g/m^3 (0.15 gr/ft^3) 5.08 cm (2 in) flues may be used. The increase in required flue diameter with dust loading is due to higher deposition and slump rates.

Refractory materials included for heat storage capacity are alumina-based superduty fireclay used to 1533°K (2300°F) checker temperature, mullite from 1533 to 1755°K (2300 to 2700°F), superduty high-density

alumina between 1755 and 1978°K (2700 and 3100°F), and calcium oxide stabilized zirconium oxide (ZrO_2) or chromium oxide (CrO_2) bonded alumina oxide (Al_2O_3) between 1978 and 2200°K (3100 and 3500°F), and yttrium oxide (Y_2O_3) stabilized zirconium oxide from 2200 to 2533°K (3500 to 4100°F). Unfortunately, the effects of various slags on zirconia are unknown and must be investigated before a workable design is claimed. Nonstandard checker bricks are used, best pricing is based on standard shapes because of the large number required. The price of yttria stabilized zirconia upon which the design is costed is about one-third of the present market price and is based on a large yttria consumption. The present market in yttria is extremely volatile.

The heat exchanger required for the closed-cycle MHD plant must operate through large temperature difference thermal cycles. Stress build-up during thermal cycling is greater for the thick wall checker of a long time period stove. Since refractories are more tolerant of thermal cycling above 1366°K (2000°F), a recuperative (shell and tube) noble gas preheater is used. The preheater increases hot valving problems while decreasing the amount of contaminants entering the noble gas stream.

A 10.1.1.2 Noble Gas Preheater

The noble gas preheater is a shell-and-tube, rectangular heat exchanger with low-pressure combustion products on the shell side arranged with one counterflow gas pass and several tube passes. In the cycle analyzed, the working fluid, argon flows inside 5.08 (2 in) schedule 80 pipes. Where required, the pipe material is RA 333, a high-nickel alloy with a small percentage of aluminum. At lower temperatures [1140°K (1600°F)] Type 347 stainless steel is specified. Still lower,[922°K (1200°F] Croloy 9M or an equivalent is indicated. Gunned insulation is applied to the 1.27 cm (0.5 in) steel shell.

A 10.1.1.3 Combustion Air Preheater

Because of the high flame temperatures required by external combustion and subsequent heat exchange to the working fluid, a high-

temperature combustion air preheat is required. The combustion air preheater is also a shell and tube exchanger with combustion products on the shell side. Neither the tube shell side is under significant pressure so thin-walled tubing is used.

A 10.1.1.4 Valving

Hot valving capable of separating 1.114 MPa (11 atm) noble gas from 101.3 kPa (1 atm) combustion products represents a very difficult design condition. Tolerable maximum leak rates are much less than any hot valving has yet achieved. Conceptually, the problems of valve seat erosion and corrosion may be negated by using two superduty water-cooled gate valves to thermally isolate a pipe zone. Between the two gate valves an automated goggle valve with recessed protected seats may be used as a positive seal. The seats must be protected by cooling and a clean gas purge protective environment. The very complicated valve system also indicates very long stove periods. Cost estimates are based on the above concepts.

A 10.1.1.5 Piping

Hot gas piping presents no insurmountable technical problems but is a major factor in plant cost because the refractory lining is, of necessity, a very high-cost material.

A 10.1.1.6 Costing

The general philosophy of this design was to strike a balance between cycle efficiency and initial capital cost, emphasizing higher cycle efficiency with perhaps a high but less than optimum capital cost. In all cases the designs — and in some cases the concepts — are not cost optimized.

A good example is the stove. Current industrial art for increasing heat exchange capacity for a given capital investment includes the technique of heating a stove to more nearly constant temperature than is usually used with a high-efficiency regenerator. With this technique there is more loss of availability, but the capacity of a stove is

increased. By "pushing the heat down the bricks" it is possible to vary the brick corrosion environment and reduce noble gas contamination, two very desirable side effects.

In any case, it is doubtful that the costs are an accurate reflection of an optimized power plant and cycle.

Component cost is obtained by determining the quantity of each material in the component and ascribing the best available cost per unit material and unit labor cost. The simple sum over all materials yields the basic component cost transmitted forward for application of other factors of pricing policy.

A 10.1.2 Combustion System Mass Flow and Temperature Estimates

Figure A 10.1.1 indicates that, for this system, efficiency is maximized by achieving the maximum permissible flame temperature. Flame temperatures are limited to 2506°K (4051°F) for combustion products on zirconia brick (Reference 10.22). For this flame temperature and 20% excess air, high-Btu gas ($CH_{3.85}$ equivalent) requires 922°K (1200°F) combustion air preheat (Reference 10.23). A preheater of 85% effectiveness indicates the products should enter the air preheater at 1028°K (1390°F).

The mass flow rate of products is determined by a First Law of Thermodynamics energy balance across the noble gas heaters, both recuperative and regenerative. Table A 10.1.1 is a summary of parameters used in Equation A 10.1.1.

$$\dot{m}_p = \frac{\dot{Q}_A}{C_{pp}\,(T_{4''} - T_{5''})} \qquad \text{(A 10.1.1)}$$

$$\dot{m}_p = \frac{1.600 \times 10^6}{0.303\ (4510 - 1850)} = 1.983 \times 10^3 \text{ lb/s}$$

The heat exchange split between the argon preheater and periodic exchanger is determined by the maximum acceptable metal temperature in the preheater, taken as 1366°K (2000°F). Thus, the argon temperature is fixed at about

Table A 10.1.1

Design Parameters

Parameter	Value
Argon Heat Rate, $\dot{Q}_A$	1.600×10^6 Btu/s*
Products Specific Heat, C_{p_p} (considered as air)	0.303 Btu/lb°F
Temperatures from Figure A 10.1.1	
Products in (flame temperature)	4510°R
Products to Air Preheater	1850°R
Argon Flow Rate, in	4.25×10^3 lb/s
Average Argon Density, ρ_a	0.1806 lb/ft^3
Average Combustion Product Density, ρ_p	0.0104 lb/ft^3

* 1.686 GJ/s from closed-cycle computer program output dated 5-2-75 (T. C. Tsu, personal communication).

1255°K (1800°F). First Law considerations then determine the temperature of products out of the periodic exchangers as 1750°K (2690°F). With the overall system temperatures determined, the individual elements may be sized through transport and material considerations.

A 10.1.3 Periodic Exchanger and Combustor

Although the variables which influence the performance of a stove-type periodic heat exchanger are manifold, the fundamental principles allowing their performance to be estimated are very simple. In a well-designed stove the center-line temperature of a checker wall is nearly constant. This enables the designer to consider the stove as a steady-flow device with heat flow from a hot to cold stream through a refractory wall. This concept is useful in obtaining initial estimates of checker height. The thickness of refractory wall may be estimated through recourse to the Heisler Transient Heating and Cooling Charts (Reference 10.24) and maintaining the center-line temperature drop less than 15%. These concepts, with the prescribed pressure drop and heat transfer correlations and conservation laws of mass and energy, yield an initial design. This initial design should be refined using methods outlined in McAdams (Reference 10.25) or Razelos and Paschkis (Reference 10.26) which approximately account for time-dependent thermal storage and internal thermal resistance of the checkerwork.

A sample computation follows. To minimize capital investment, it is desirable to operate the stoves in symmetrical one-on-one heat/cool cycles. Continuity considerations and tabular data of Table A 10.1.1 yield the flow velocity relation shown in Equation A 10.1.2.

$$\overline{V}_A = \left(\frac{\dot{m}_A}{\rho_A}\right) \left(\frac{\rho_p}{\dot{m}_p}\right) \overline{V}_p \qquad \text{(A 10.1.2)}$$

$$\overline{V}_A = \left(\frac{4.25 \times 10^3}{0.1806}\right) \left(\frac{0.0104}{1.985 \times 10^3}\right) V_p = 0.123\, V_p$$

Thus, the products velocity is approximately eight times the argon velocity.

Since the stove is a true counterflow device, the log mean temperature difference is applicable

$$LMTD = \frac{(T_{5''} - T_{5'}) - (T_{4''} - T_{4'})}{\ell n \left(\frac{T_{5''} - T_{5'}}{T_{4''} - T_{4'}} \right)} \qquad \text{(A 10.1.3)}$$

$$LMTD = \frac{890 - 240}{\ell n \left(\frac{890}{240} \right)} = 496°F$$

The stove heat rate is computed as the difference of the total argon and preheater heat rates given by Equation A 10.1.4.

$$\dot{Q}_{stove} = \dot{Q}_A - \dot{m}_A \left(i_{\substack{11.1 \text{ atm} \\ 2260°R}} - i_{\substack{11.1 \text{ atm} \\ 762°R}} \right) \qquad \text{(A 10.1.4)}$$

$$\dot{Q}_{stove} = 1.6 \times 10^6 - 4250 \left[\frac{(3866)(491.7)}{778} (11.4-3.85) \right]$$

$$= 815.5 \times 10^3 \text{ Btu/s}$$

The overall thermal conductance per foot of flue in the regenerator between the argon and products in the analogous steady-flow model is

$$(UA)' = \frac{1.0}{\frac{1}{h_A A'} + \frac{2r_B}{k_s A'} + \frac{1}{h_p A'} + \frac{2}{h_{fl} A'}} \qquad \text{(A 10.1.5)}$$

For pipeline quality gas and high temperature, the fouling conductance is neglected. Also considered neglible in this initial sizing of the stoves is the thermal capacity impedance term of Rummel (Reference 10.27), $\theta/(2.5\ C_p \rho_s r_B A')$. For the special checker having 2.54 cm (1.0 in) square holes on 5.08 cm (2.0 in) in-line centers and laid with flues straight and smooth, the equivalent checker thickness is given by Equation A 10.1.6.

$$r_B = \frac{\forall_s}{\forall} = \frac{2^2 - 1^2}{2^2(12)} = 0.063 \text{ ft} \qquad \text{(A 10.1.6)}$$

The average property of the checker is determined from Table A 10.1.2.

The heat exchanger coefficient within the flue is estimated by the Dittus-Boelter relation (Equation A 10.1.7) for smooth flues neglecting radiation effects; a decidedly conservative approach.

$$h_A = 0.023 \frac{k}{d_i} \, Re_A^{0.8} \, Pr_A^{0.33} \qquad \text{(A 10.1.7)}$$

The parameters of Equation A 10.1.7 are given in Table A 10.1.3 with those of the products. Substitution of parameters from Table A 10.1.3 into Equation A 10.1.7 yield the heating and cooling cycle heat transfer coefficients of 56.32 W/m^2-°K (9.92 Btu/hr-ft^2-°F) and 46.84 W/m^2-°K (8.25 Btu/hr-ft^2-°F), respectively. Substituting these values for h_p and h_A, 1/3 for A' and the value of k_s given in Table A 10.1.1 in Equation A 10.1.5 gives the overall conductance.

$$(UA)' = \frac{1.0}{\left(\frac{3}{8.25}\right) + \left(\frac{3(0.126)}{1.3}\right) + \left(\frac{3}{9.92}\right)\left(\frac{120}{160}\right)^{0.8}} \qquad \text{(A 10.1.8)}$$

$$= 1.12 \text{ Btu/hr-ft}^2_{\text{flue}}\text{-°F}$$

The initial checker height is estimated by Equation A 10.1.9.

$$L = \frac{\dot{Q}_A/\text{flue}}{(UA)' \text{ LMTD}} = \frac{Q_A \left(\frac{\rho_A A_{\text{flue}} \bar{V}_A}{\dot{m}_A} \right)}{(UA)' \text{ LMTD}} \qquad \text{(A 10.1.9)}$$

Table A 10.1.2

Checker Properties

Stove Height %	Checker	$\bar{\rho}_s$, lb/ft^3	$\bar{C}_s$ Btu/lb-°F	$\bar{k}_s$ Btu/hr-ft-°F	Temperature from °F	to:
5.3	X.H.D. fireclay	145	0.264	0.83		2300
21.1	Mullite	155	0.252	1.0	2300	2700
21.1	High alumina	185	0.278	1.58	2700	3100
26.3	Chromia-bonded alumina or $CaO - ZrO_3$	185	0.278	1.7	3100	3500
26.2	$Y_2O_3 - ZrO_3$	322	0.17	1.0	3500	4100
100%	Average checker	212	0.243	1.3		

Table A 10.1.3

Stove Parameters

Parameter	
$\bar{V}_A$	20 ft/s
$\bar{V}_p$	120 ft/s
d_i	1/12 ft
$\bar{\rho}_A$	0.181 lb/ft^3
$\bar{\rho}_p \approx \bar{\rho}_{air}$	0.123 lb/ft^3
μ_A	0.2 lb/hr-ft
$\mu_p \approx \mu_{air}$	3.92 x 10^{-5} lb/ft-s
$Re_A = \rho\bar{V}d/\mu$	5423
Re_p	3140
$Pr_A^{1/3}$	0.878
$Pr^{1/3}$	$\approx$1.0
k_A	0.0366 Btu/hr-ft^2-°F
$k_p \approx k_{air}$	0.057 Btu/hr-ft^2-°F

$$L = \frac{815.5 \times 10^3 \; \frac{0.181 \; (1/44)20}{4.25 \times 10^3} \; 3600}{(1.12)\; 496} \qquad \text{(A 10.1.10)}$$

$$L = 31.0 \text{ ft}$$

Substituting into the more exact equations given by McAdams, (Reference 10.25), we have:

checker void fraction,

$$\varepsilon = \frac{1}{2^2} = 0.25 \qquad \text{(A 10.1.11)}$$

the dimensionless stove height

$$\lambda_A = \frac{h}{C_p G_o}\Big|_A \left(\frac{1-\varepsilon}{r_B}\right)L \qquad \text{(A 10.1.12)}$$

$$\lambda_A = \frac{8.25}{\left(\frac{38.66}{778}\; 2.5\right)[0.181\; \left(\frac{20}{4}\right)\; 3600]} \left(\frac{1-0.25}{0.0625}\right) \quad (31)$$

$$\lambda_A = 7.6$$

$$\lambda_p = \frac{h}{C_p G_o}\Big|_p \left(\frac{1-\varepsilon}{r_B}\right)L = 14.0 \qquad \text{(A 10.1.13)}$$

the average nondimensional stove height is defined accordingly to Equation A 10.1.14.

$$\lambda_s = \frac{2.0}{\lambda_A^{-1} + \lambda_p^{-1}} = 10.0 \qquad \text{(A 10.1.14)}$$

The dimensionless time interval

$$\tau_A = \frac{h_A \theta}{C_s \rho_s r_B} = 2.54\ \theta \qquad \text{(A 10.1.15)}$$

$$\tau_p = \frac{h_p \theta}{C_s \rho_s r_B} = 3.05\ \theta \qquad \text{(A 10.1.16)}$$

$$\tau_s = (\tau_A + \tau_p)/2 = 2.8 \qquad \text{(A 10.1.17)}$$

From Figure 11.11, McAdams (Reference 10.25), for a one-hour stove cycle the effectiveness ϕ is 0.82. The average temperature rise (Reference 10.25) of the argon is

$$\Delta T = \frac{(\tau_A/\tau_A)\ (\text{LMTD})}{\frac{1}{\tau_p} + \frac{1}{\tau_A} + \frac{2}{\tau_A+\tau_p}\left[\lambda_s\left(\frac{1}{\phi_s} - 1\right) - 2\right]} \qquad \text{(A 10.1.18)}$$

$$\Delta T = 1882\,^\circ F$$

This gives an average argon output temperature of 2301°K (3682°F) which is less than the required 2372°K (3810°F). Since the term in brackets is negligible in its variation with height, an increase in height to 10 m (33 ft) is required. The underestimate of height by Equation A 10.1.10 is probably due to neglecting the heat storage thermal resistance. The thermal droop in the argon is (Reference 10.25)

$$\delta T_A = \frac{\tau_A (T_{p4''} - T_{A4'})}{\left(\frac{1}{\phi_s} - 1\right)(\lambda_A + 1)} \qquad \text{(A 10.1.19)}$$

$$= 335\,^\circ F$$

Although 8% thermal drop is too high, the phased operation of the stoves will attenuate this figure.

The stove combustion chamber geometry is similar to the open-cycle stoves (see Appendix A 9.2.5). Total superficial flow area is given by Equation A 10.1.20.

$$A_f = \frac{\dot{m}_A}{\rho_A \bar{\bar{V}}_A \varepsilon} \qquad \text{(A 10.1.20)}$$

$$= \frac{4.25 \times 10^3}{0.1806\ (20)\ (0.25)} = 4707 \quad ft^2$$

The number of stoves, each having 176.7 ft^2 of flow area, in the cool cycle at a given instant is given by Equation A 10.1.21.

$$n = \frac{4707}{176.7} = 27. \qquad \text{(A 10.1.21)}$$

If each bank of three stoves could be cycled from cool to heat in six minutes, only one extra stove would be required. Thus the total number of stoves is given as 56 for the high-Btu, clean, pipeline gas.

A 10.1.3.1 Regenerator Material Quantities

Techniques for computation of the regenerator materials and methods of scaling are detailed in the open-cycle MHD Appendix A 9.2. Table A 10.1.4 gives a summary of the various material accounts. The cost of material and labor is given in Tables A10.1.5 and A 10.1.6. An example of the scaling technique is given below for the number of stoves and mass of the active checker bricks. Constant argon velocity is a reasonable choice for flue velocity because dust entrainment must be controlled. From Equation A 9.2.78, the number of stoves is given as the next higher even multiple of four

$$n_{3100} = \frac{\dot{m}_{A_{3100}}}{\dot{m}_{A_{3800}}} \; n_{3800} = \frac{5819}{4253}\,(56) \approx 80$$

The argon flow rates are given in Figures A 10.1.3 and A 10.1.4.

The mass of active checker bricks, given as 1645 and 1900 k-lb for the 3800 and 3100°F low Btu gas cases in Table A 10.1.4, is determined by a three dimensional form of Equation A 9.2.77 for constant stove diameters

$$\text{Mass} \propto \bar{\rho}\ n\ L = \bar{\rho}\ n\ \frac{\Delta T_A}{\Delta T_{em} U}$$

Note that specific heat is assumed constant and radiation is not considered. For 3100°F service the average brick mass is (173.6 lb/ft^3) as compared to 212.0 for 3800°F service. The average U changes by one-half the products mass flow rate to the 0.8 power, or 3% approximately using the data from Figures A 10.1.3 and .4. The mass of the 3100°F low Btu gas checkers may then be written as

$$\text{Mass}_{3100} = 1645\left(\frac{173.6}{212.0}\right)\left(\frac{80}{56}\right)\frac{(3100-1800)}{(3810-1800)}\left(\frac{\left(\frac{913}{\ell n(\frac{1153}{240})}\right)}{\left(\frac{193}{\ell n(\frac{493}{300})}\right)}\right)\left(\frac{1.03}{1.0}\right)$$

$$= 1900 \text{ k-lb}$$

It should be noted that stoves for the gasified coal case were not scaled, but were redesigned using a checker with 6.35 cm (2.5 in) square flues on 12.7 cm (5 in) centers which is consistent with the higher dust loading of the low Btu gas.

A 10.1.3.2 Noble Gas Contamination

From the noble gas flow rate, volume of stove, and period of operation, noble gas contamination can be expected to be well below 300 ppm in normal operation. Blowdown and purge to th low-temperature purifier will further reduce the impurity level in the MHD channel and preionizer.

Table A 10.1.4 Material Quantity for Closed-Cycle H.X. Apparatus

Combustion and Heat Exchange System	High-Btu Gas (3800°F) Noble Gas Heaters No. Units	Amt.* per Unit	Air Preheater No. Units	Amt.* per Unit	Low-Btu Gas (3800°F) Noble Gas Heaters No. Units	Amt.* per Unit	Air Preheater No. Units	Amt.* per Unit	Low-Btu Gas (3100°F) Noble Gas Heaters No. Units	Amt.* per Unit	Air Preheater No. Units	Amt.* per Unit
Concrete, Stoves	56	42 yd^3			56	42 yd^3			80	48.5 yd^3		
Concrete, Preheater	28	90 yd^3	4	153 yd^3	28	90 yd^3	4	66 yd^3	40	134 yd^3	4	7.2 yd^3
RA 333 Metal Tubes	28	35,500 ft			28	25,900 ft			40	52,700 ft		
Stainless St. Tubes	28	35,500 ft	4	1,962,000 ft	28	25,900 ft	4	847,000 ft	40	52,700 ft	4	92,200 ft
Alloy Tubes												
Insulation, Recup.	28	106	4	279	28	77	4	120	40	157.3	4	13.1
Structural Steel, Recup.	28	24	4	60	28	17.5	4	26	40	35.6	4	2.8
Containment Steel, Recup.	28	93.1	4	684	28	68	4	295	40	138.1	4	32.1
Checker Bricks, Stove	56	1087			56	1645			80	1900.0		
Insulation, Stove	56	276			56	418			80	483.0		
Containment Steel, Stove	56	89.1			56	135			80	156		
Structural Steel, Stove	56	18.8			56	28			80	32.3		
Burners, Stove, each**	56	ea.			56	ea.			80	ea.		
High-Temp. Valves, each***	140	ea.			196	ea.			280	ea.		
Refractory Baffles	28	203			28	148			40	324		

* Weight x 10^{-3}/unit in lb except as noted.

** Costs summed with stove costs.

*** Costs summed with piping costs.

Table A 10.1.5 Material Cost for Closed-Cycle H.X. Apparatus

Combustion and Heat Exchange System	High-Btu Gas (3800°F) Noble Gas Heaters $/lb*	High-Btu Gas (3800°F) Air Preheaters $/lb*	Low-Btu Gas (3800°F) Noble Gas Heaters $/lb*	Low-Btu Gas (3800°F) Air Preheater $/lb*	Low-Btu Gas (3100°F) Noble Gas Heaters $/lb*	Low-Btu Gas (3100°F) Air Preheater $/lb*
Concrete, Stoves	$77.78/yd^3	$75/yd^3				
Concrete, Preheater						
RA-333 Metal Tubes	$9.430/ft					
Stainless St. Tubes	$2.194/ft	$2.194/ft				
Alloy Tubes						
Insulation, Recup.	0.291	0.250				
Structural Steel, Recup.	0.375	0.383				
Containment Steel, Recup.	0.204	0.177				
Checker Bricks, Stove	4.14		4.14		1.15	
Insulation, Stove	0.32					
Containment Steel, Stove	0.35					
Structural Steel, Stove	0.47					
Burners, Stove, $/each	$15,000/each		$28,000 each		$28,000 each	
High-Temp. Valves, $/each	120,000					
Refractory Baffles	0.192					

*$/lb except as noted.

Table A 10.1.6 Labor Cost for Closed-Cycle H.X. Apparatus

Combustion and Heat Exchange System	High-Btu Gas (3800°F) Noble Gas Heaters $/lb*	High-Btu Gas (3800°F) Air Preheater $/lb*	Gasified Coal (3800°F) Noble Gas Heaters $/lb	Gasified Coal (3800°F) Air Preheater $/lb	Gasified Coal (3100°F) Noble Gas Heaters $/lb	Gasified Coal (3100°F) Air Preheater $/lb
Concrete, Stoves	72.22	75.0				
Preheater						
RA-333 Metal Tubes	5.60					
Stainless St. Tubes	1.50					
Alloy Tubes						
Insulation, Recup.	0.214	0.401				
Structural Steel, Recup.	0.25	0.25				
Containment Steel, Recup.	0.0859	0.137				
Checker Bricks, Stove	0.15					
Insulation, Stove	0.15					
Containment Steel, Stove						
Structural Steel, Stove						
Burners, Stove						
High-Temp. Valves	$10,000 each					
Refractory Baffles	0.15					

*$/lb except as noted.

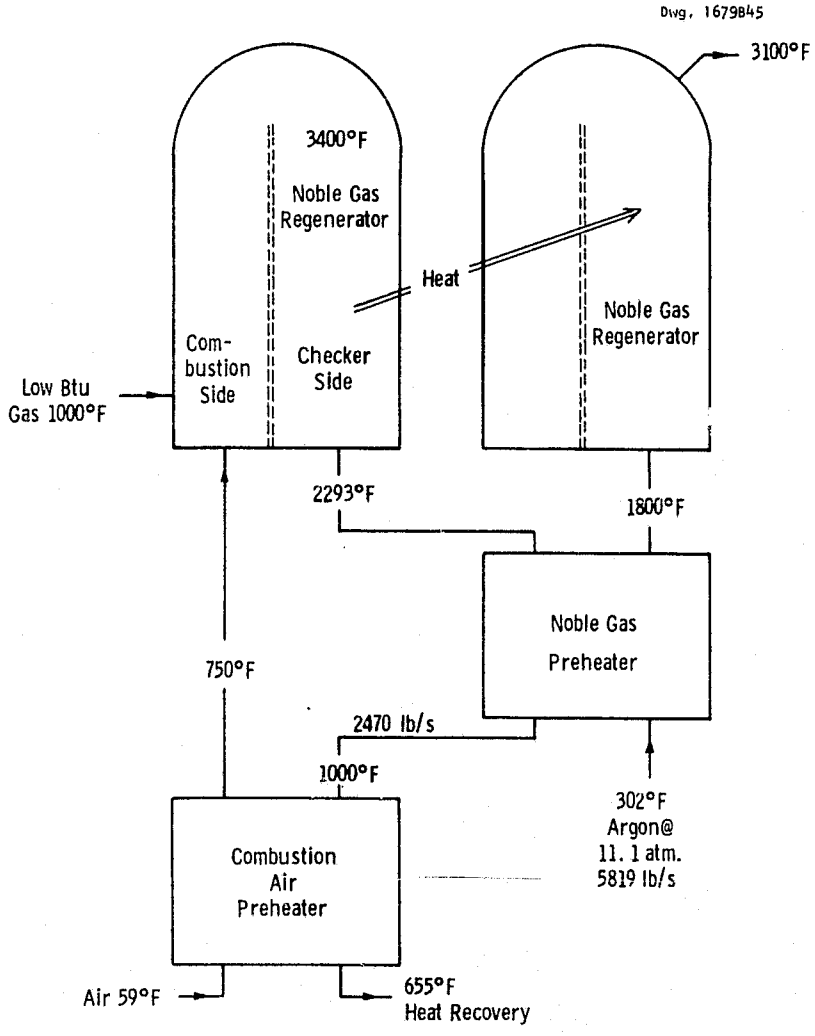

Fig. A 10.1.3—Closed cycle MHD external combustion and heat exchange system schematic for 2033°K (3100°F) low-Btu gas cycle. Similar to Point 6.

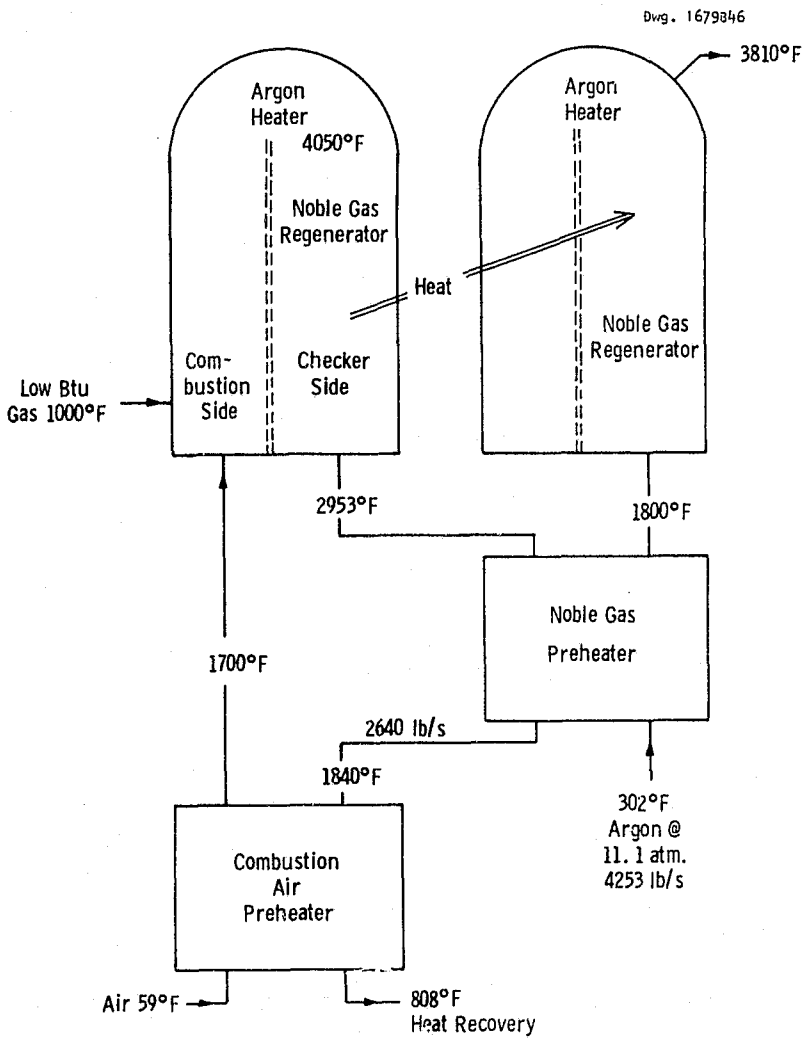

Fig. A 10.1.4—Closed cycle MHD external combustion and heat exchange system schematic for the 2367°K (3800°F) low-Btu gas cycle. Similar to Points 5 and 7.

As stated earlier, outgassing and erosive pickups of contaminants during the regenerator cool cycle are neglected because, to a great extent, they are functions of the quality of the refractory, density, manufacturing tolerances, and thermal stability. Erosion by the noble gas is minimal because the products are at a higher velocity than is the noble gas, density being a lesser effect in this case.

In a single-stove cycle one stove volume of products is introduced into the noble gas loop on the change-over from products to noble gas, and perhaps two on change from noble gas to product (noble gas recovery). The following computation was performed for conditions and dimensions given in Table A 10.1.7.

Table A 10.1.7 Stove Description

Active Checker Height	44 ft*
ε (void volume fraction)	0.25
Stove Cycle	1 hr
Argon Flow Rate	4.62×10^3 lb/s*
Number of Stoves	29.0*
Pump-Down Pressure	3 atm
Molecular Weight of Products	30.0
Superficial Flow Area	176.7 ft^2
Flow Area Ratio, Combustor/(Combustor & Insulation)	0.3

*Not a final design condition

The volume of a stove is the volume of checker flow area plus combustion chamber area

$$\text{Stove Volume} = 44[(\varepsilon)(176.7) + 0.3\ (240.5-176.7)] = 2786\ ft^3 \qquad \text{(A 10.1.22)}$$

The number of molecules of products per stove volume is given as Equation A 10.1.23.

$$\text{Molecules Product/Stove} = (6.023 \times 10^{23}) \left(\frac{P_p \Psi_p}{M_p R_p R_p}\right) \frac{1}{454} \qquad \text{(A 10.1.23)}$$

The number of molecules of argon per stove volume is given as Equation A 10.1.24.

$$\frac{\text{Molecules Argon}}{\text{Stove Volume}} = \frac{(6.023 \times 10^{23})(4.62)(3.6)\ 10^{6}}{M_A} \left(\frac{1}{454}\right) \qquad \text{(A 10.1.24)}$$

The parts per million of contaminants are given as Equation A 10.1.25 for three stove volumes.

$$PPM = \frac{M_A P_p \forall_p\ 10^6\ (29)}{M_p\ (4.62)(3.6)10^6\ R_p T_p}\ (3) \qquad \text{(A 10.1.25)}$$

$$= \frac{39.94\ P_p[\text{psf}]\ 2786\ (29)(3)}{30.0(4.62)(3.6)(53.34)(3700)}$$

$$= 14.16\ P_p[\text{psi}]$$

For blowdown to atmospheric pressure the total parts per million is 208 ppm. Therefore, neglecting any contamination of the bricks during heating, three volumes of products will give a concentration of no more than 208 ppm in the total argon flow over a one hour period.

A 10.1.4 Noble Gas Preheater (NGP)

The design of the noble gas preheater is subject to several somewhat flexible criteria. The purpose of the device is to ameliorate several regenerator problems (thermal shock fracture, noble gas contamination, excess capital cost of stoves) whose significance is not presently known. The cost of the preheater, then, is presumed to be less than the cost of the equivalent stove surface. A maximum metal temperature of 1366°K (2000°F) has been used without certainty of achieving a cost optimum.

The NGP is a shell-and-tube exchanger with 5.08 cm (2 in) schedule 80 tubes on 11.4 cm (4.5 in) equilateral pitch with several tube passes. Refractory baffles are used along with refractory lined walls. Cold wall temperatures are 361°K (190°F). As shown in Figure A 10.1.1 the combustion products enter at 101.3 kPa (1 atm) and 1750°K (2690°F) and leave at 1028°K (1390°F) while 1928.1 g/s (4250 lbm/s) of noble gas enter in counterflow at 1.125 MPa (11.1 atm) and 423°K (302°F) and exits at 1256°K (1800°F). Metal temperature is maintained by variable baffle spacing. The NGP heat rate is 828 MWt (785,000 Btu/s) from the difference of total heat rate (Table A 10.1.1) and stove heat rate (Equation A 10.1.4. The length of tube required is given by Equation A 10.1.26:

$$L = \frac{\dot{Q}}{(UA)'(F)(LMTD)} \qquad \text{(A 10.1.26)}$$

where F is 1.0 for true counterflow. The conductance per tube length is given by Equation A 10.1.27:

$$(UA)' = \frac{1.0}{\frac{1}{\pi h_A d_i} + \frac{\ell n(d_o/d_i)}{2\pi k} + \frac{1}{\pi h_o d_o} + \frac{1}{\pi h_{fl} d_o}} \qquad \text{(A 10.1.27)}$$

The density of the argon is given by the ideal gas approximation

$$\rho_A = \frac{P}{RT} = \frac{11.1\ (14.7)(144)}{38.66\ (1511)} = 0.402\ \text{lb/ft}^3 \qquad \text{(A 10.1.28)}$$

The argon heat transfer coefficient is given as

$$h_A = 0.023 \frac{k}{d} Re^{0.8} Pr^{0.33} \qquad \text{(A 10.1.29)}$$

$$= 27.2\ \text{Btu/hr-ft}^2\text{-°F}$$

and the products Colburn j factor is 0.017 using Reference 10.28 as a guide. The shell-side heat transfer coefficient is given by the j factor definition, Equation A 10.1.30.

Table A 10.1.8 Parameters for Determination of Tube Conductance

Parameter	Value
ρ_A	0.402 lb/ft^3
V_A	50 ft/s
d_i	2/12 ft
μ_A	3.24 x 10^{-5} lb/ft-s
k_A	0.0221 Btu/hr-ft-°F
$Pr_A^{1/3}$	0.871
$V_{P_{max}}$	21.5 ft/s
C_{P_p}	0.298 Btu/lb-°F
$Pr_p^{2/3}$	0.82
D_o	2.375/12 ft
μ_p	3.73 x 10^{-5} lb/ft-s
$Re_A = \left.\frac{\rho \bar{V} d_i}{\mu}\right\|_A$	10^5
$Re_{P_{max}} = \frac{\rho_p V_{P_{max}} d_o}{\mu_p}$	1.54 x 10^3
h_{fl}	66 Btu/hr-ft^2-°F

$$h_p = C_{p_p} \rho_p V_{p_{max}} j_h Pr^{-0.66} \qquad \text{(A.10.1.30)}$$

$$h_p = 6.4 \text{ Btu/hr-ft}^2\text{-°F}$$

Considering fouling, the effective heat exchange coefficient, h*, is given as Equation A 10.1.31.

$$h^* = \frac{1}{\frac{1}{h_{fl}} + \frac{1}{h_p}} = 5.75 \text{ Btu/hr-ft}^2\text{-°F} \qquad \text{(A 10.1.31)}$$

Note that the definition of an effective heat transfer coefficient consolidates the two right-hand demoninator terms of Equation A 10.1.27 into a single term. The maximum tube wall temperature in °F which should remain below 1366°K (2000°F) is approximated at the outlet by and the thermal impedance ratio times the temperature difference from Figure A 10.1.1.

$$\text{Maximum Tube Temperature} = 1800 + \{1/(h_A \pi d_i)/[1/(h_A \pi d_i) + 1/(h^* \pi d_o)]\}(3150 - 2260) \qquad \text{(A 10.1.32)}$$

$$= 1800 + \frac{0.0183\ (890)}{0.092} = 1981°F$$

Designing for a slightly high shell-side flow area is sufficient to avoid flow distribution-caused hot spots.

The overall conductance per unit length of tube is given by Equation A 10.1.27, with substitutions shown in Equation A 10.1.33.

$$(UA)' = \frac{1}{\frac{12}{2.82\pi(1.94)} + \frac{\ell n\left(\frac{2.375}{1.94}\right)}{2\pi(15)} + \frac{12}{5.75\pi(2.375)}} \qquad \text{(A 10.1.33)}$$

$$= 2.84 \text{ Btu/hr-ft}_{tube}\text{-°F}$$

The log mean temperature difference in counterflow from Figure A 10.1.1, is given by Equation A 10.1.34.

$$LMTD = \frac{890-1088}{\ell n \frac{890}{1088}} = 981.2°F \qquad \text{(A 10.1.34)}$$

The length of tube is

$$L = \frac{785 \times 10^3 \ (3600)}{2.84 \ (981.2)} = 1.014 \times 10^6 \text{ ft} \qquad \text{(A 10.1.35)}$$

The number of parallel passes is

$$n_{11} = \frac{\dot{m}_A}{\rho_A \bar{V}_A A_f} = \frac{4.25 \times 10^3}{0.402(50)(0.0205)} \approx 10,314 \qquad \text{(A 10.1.36)}$$

Tube length per pass is given

$$L_{pass} = \frac{L}{n_{11}} = \frac{1.014 \times 10^6}{10.3 \times 10^3} = 98 \text{ ft} \qquad \text{(A 10.1.37)}$$

The shell-side superficial flow area (face area) is given by Equation A 10.1.37.

$$A_{f_p} = \frac{1.985 \times 10^3}{0.0134 \ (10)} = 1.48 \times 10^4 \text{ft}^2 \qquad \text{(A 10.1.37)}$$

For 27 active noble gas preheaters, the tube nest is

$$\text{Tubes/Unit} = n_{11}/\text{unit} = \frac{10314}{27} \approx 382 \text{ tubes} \qquad \text{(A 10.1.38)}$$

(38 tubes wide and 10 deep)

The superficial shell-side flow area is

$$A_{f_p}/\text{unit} = \frac{14800}{27} = 548 \text{ ft}^2 \qquad \text{(A 10.1.39)}$$

or, for 38 tubes wide, 13.2 m (38.5 ft) along the tube axis dimension. The head exchanger is arranged in true counterflow with the tube axis vertical. As the average products and argon temperatures decrease downstream, the tube-side coefficient may be increased to reduce cost. After the first pass the shell-side pass area is halved and the conductance per tube length increases to 8.167 $W/m^{2\circ}K$ (4.72 $Btu/hr\text{-}ft_{tube}\text{-}^\circ F$). The total length of tube weighted for variable (UA)' is given by Equation A 10.1.69.

$$L = \frac{785 \times 10^3 \ (3600)}{[\frac{1}{3}(2.84) + \frac{2}{3}(4.72)]981.2} = 703 \times 10^3 \text{ ft} \qquad \text{(A 10.1.40)}$$

Note that the effect of radiation has not been included, so some protection (cold inlet argon tubes upstream of the first tube row) is probably necessary.

The argon pressure drop is given by the usual equation

$$\Delta p = (f \frac{\ell}{d} + C_L)\rho \frac{V_A^2}{290} \qquad \text{(A 10.1.41)}$$

Allowing two velocity heads loss for headers, the pressure drop is estimated as 151.7 kPa (2.2 psi).

A 10.1.4.1 Scaling and Material Estimates

The methods for estimating scaling and costing the material requirements of the NGP is similar to the method used in Appendix A 9.2 in estimating open-cycle MHD regenerators. A summary of material type and cost, and labor cost is given in Table A 10.1.4, A 10.1.5 and A 10.1.6.

A 10.1.5 Combustion Air Preheater

The purpose of the combustion air preheater is to raise the flame temperature of the combustion products to a sufficient level that heat may be supplied to the noble gas topping cycle working fluid through the regenerator thermal approach temperature difference at the required peak cycle temperature. High-Btu gas combustion air requires less preheat to reach a given temperature than does low- or medium-Btu gas. This is evidenced by the amount of preheater material in Table A 10.1.4. Low-Btu gas requires less preheater material because the gas is delivered at 811°K (1000°F) and the fuel-air ratio is higher for low- or medium-Btu gas. The preheater operates at essentially atmospheric pressure. Only the design for high-Btu gas is presented and the schematic of its relation to other combustion system components is shown in Figure A 10.1.1.

For the case of neglible internal pressure and 978°K (1300°F) maximum initial temperatures 10.16 cm (4 in) 3.81 cm (1.5 in) tube with 2.11 (0.083 in) wall thickness on 10.2 cm (4.0) equilateral pitch is adequate. The mass flow of combustion products is 1.06 times the air-side flow rate, and the specific heat is slightly larger in the products, making the heat rate higher on the products side. This reaction has been neglected in the heat exchanger sizing for convenience. The air preheater heat rate is established as per Equation A 10.1.42.

$$\dot{Q} = \dot{m} C_p \Delta T \qquad \text{(A 10.1.42)}$$

$$\dot{Q} = (1985.0)(0.252)(1660 - 519) = 0.571 \times 10^6 \text{ Btu/s}$$

The log mean temperature difference is approximately 105.6°K (190°F).

For inside and outside velocities of 30.5 m/s (100 ft/s) and 15.3 m/s (50 ft/s) the heat exchange coefficients are given as Equation A.10.1.29. Entries into this equation are given in Table 10.1.9.

Table A 10.1.9 Summary of Air Preheater Properties

Property	Value
Temperature of Inlet Air	519°R
Temperature of Outlet Air	1660°R
Temperature of Inlet Products	1850°R
Temperature of Outlet Products	710°R
μ_a	2.7×10^{-5} lb/ft-s
ρ_a	0.023 lb/ft^3
Re_a	8550
$Pr_a^{1/3}$	0.8875
k_a	0.0377 Btu/hr-ft-°F
μ_p	2.85×10^{-5} lb/ft-s
ρ_p	0.0214 lb/ft^3
Re_p	7510
$Pr_p^{1/3}$	0.889
k_p	0.039 Btu/hr-ft-°F
k_{tube}	25 Btu/hr-ft-°F
V_a	100 ft/s
V_p	50 ft/s

The air-side heat transfer coefficient is found to be 59.61 W/m^2-°K(10.5 Btu/hr-ft^2-°F). The shell-side coefficient is given by Equation A 10.1.43.

$$h_p = 0.33 \frac{k_p}{d_o} Re_{max}^{0.6} Pr^{0.33}$$
$$= 19.4 \text{ Btu/hr-ft}^2\text{°F} \qquad \text{(A 10.1.43)}$$

The conductance per foot of tube is given as

$$(UA)' = \frac{1.0}{\frac{1.0}{\pi h_a d_i} + \frac{\ell n\, d_o/d_i}{2\pi k} + \frac{1.0}{\pi h_p d_p} + \frac{1.0}{\pi h_{fl} d_o}} \qquad \text{(A 10.1.44)}$$

$$(UA)' = \frac{1.0}{\frac{12.0}{\pi(10.5)(1.31)} + \frac{0.136}{2(25)\pi} + \frac{12}{\pi(19.4)1.5} + \frac{12}{\pi(100)1.5}}$$

$$= 2.30 \text{ Btu/hr-ft}_{\text{tube}}\text{-°F}$$

The length of tube required is

$$L = \frac{Q}{(UA)'(LMTD)F} \qquad \text{(A 10.1.45)}$$

$$= \frac{0.571 \times 10^6 (3600)}{2.41(190)(1)} = 4.70 \times 10^6 \text{ ft}$$

The number of parallel passes is

$$n_{11} = \frac{\dot{m}_a}{\rho V A_f} = \frac{1985}{0.031(100)} \left(\frac{144}{1.35}\right) = 68300 \qquad \text{(A 10.1.46)}$$

The length of a single pass is found to be 20.97 m (68.8 ft).

The product-side superficial flow area is given by Equation A 10.1.47.

$$A_{\substack{\text{flow} \\ \text{prod.}}} = \frac{\dot{m}_p}{P_p V_p} = \frac{1985}{0.0214(50)} = 1855 \text{ ft}^2 \qquad \text{(A 10.1.47)}$$

If there are four air preheaters, a reasonable unit design consists of one tube pass 21.3 m (70 ft) long, 140 tubes in transverse pitch and 122 tubes in longitudinal pitch. A single gas pass would include a tube length of 3.03 m (9.94 ft). Eight passes are a conservative design.

The quantities of material shown in Table A 10.1.4, high-Btu gas air preheater are based on 140 tubes by 139 tubes in a unit bundle. This is adequate to cover a crossflow correction factor of 0.9, and any maldistribution problems. Note that the preheater was redesigned by similar techniques to use 5.1 cm (2.0 in) tubes on 9.53 cm (3.75 in) staggered centers for the low-Btu gasified coal case.

A 10.1.6 Nomenclature

A_f	Flow area, ft^2
A'	Area of checker tube per foot of length, ft
c	Circumference, ft.
C_L	Fluid loss coefficient
C_p	Constant pressure specific heat, Btu/lb-°F
C_s	Specific heat of solid, Btu/lb-°F
d_h	Hydraulic diameter, $4A_f/C$
f	Fluid friction factor
F	Crossflow correction factor to LMTD
g_c	Gravitation constant
G	Mass velocity, lb/ft^2-s
h	Heat transfer coefficient, Btu/hr-ft^2-°F
i	Specific enthalpy, Btu/lb
k	Thermal conductivity, Btu/hr-ft-°F
L	Length, ft
LMTD	Log mean temperature difference, counterflow, °R
$\dot{m}$	Mass flow rate, lb/s
n_{11}	Number parallel circuits
P_r	Prandtl number
$\dot{Q}$	Heat rate, Btu/s
r_B	Bulk radius, volume of ceramic per unit surface of the ceramic
Re	Reynold's number, $\rho\bar{V}d_h/\mu$
T	Absolute temperature, °R
(UA)'	Thermal conductance per unit tube length, Btu/hr-ft-°F
$\bar{V}$	Average velocity, ft/s
δ	Checker wall half thickness, ft; small increment
ϵ	Void fraction of checker

η	Fin efficiency, average surface temperature divided by root temperature
θ	Time interval, hrs
λ	Dimensionless stove height
μ	Absolute viscosity, lb/ft-s
ρ	Density, lb/ft^3
τ	Deminsionless stove period
ϕ	Heat exchanger effectiveness

Subscripts

a	Air
A	Argon
i	Inside
o	Outside
p	Products of combustion
s	Solid or refractory; symmetrical cycle for stoves
t	Tube

See Figure A 10.1.1 for system station numerical definitions.

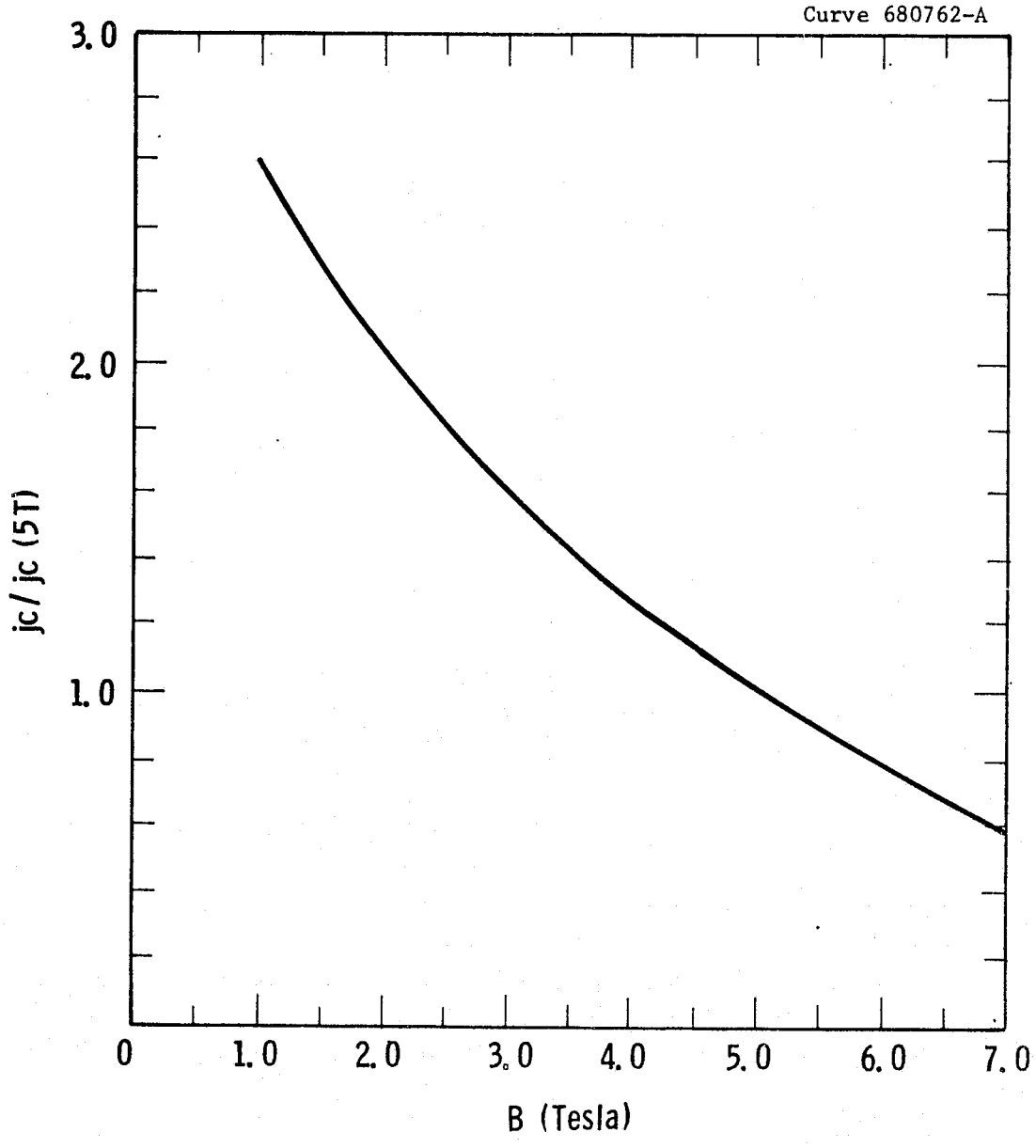

Fig. A 10.2.1 —Normalized J_c-H curve for NbTi superconductors

Appendix A 10.2

SUPERCONDUCTING MAGNET DESIGN FOR CLOSED-CYCLE PLASMA MHD GENERATORS

In Appendix A 9.9, the groundwork was laid for performing the analysis of the magnet design for both the open- and closed-cycle plasma MHD generators. The major difference between the open-cycle plasma and closed-cycle plasma MHD generator superconducting magnet designs is the magnetic field distribution. In the closed-cycle plasma MHD generator the peak field required is at the inlet and is tapered linearly to the exit of the duct.

The environment of a MHD magnet system does not require the selection of sophisticated superconductors primarily because there are no ac or transient magnetic fields present. Furthermore, the magnetic field distributions cannot accommodate graded winding designs because of the conical dipolar configurations. Since the peak magnetic field seen by the MHD duct for the closed-cycle concept is 5 T, and the estimated peak field at the superconducting windings (in the end turns at the entrance of the duct) is less than 6.3 T, filamentary niobium-titanium (Nb-Ti) conductors have been selected for the base case design.

The most important part of the conductor design is selecting a winding current density such that the winding will not quench during conventional operation. Illustrated in Figure A 10.2.1 is a normalized plot of the critical current density for niobium-titanium wires as a function of the peak field on the wire [where $j_{c(5\ T)} \approx 2\ GA/m^2$]. The operating current of the magnet system was arbitrarily set at 5000 A. A conductor with filaments of 100 μm or less must be twisted approximately 1 twist/ 2.54 cm (1 in) to inhibit the possibility of flux jump instability in the wire when the magnet is being either charged or discharged. A winding packing factor of 0.7 was established as sufficient spacing to accommodate

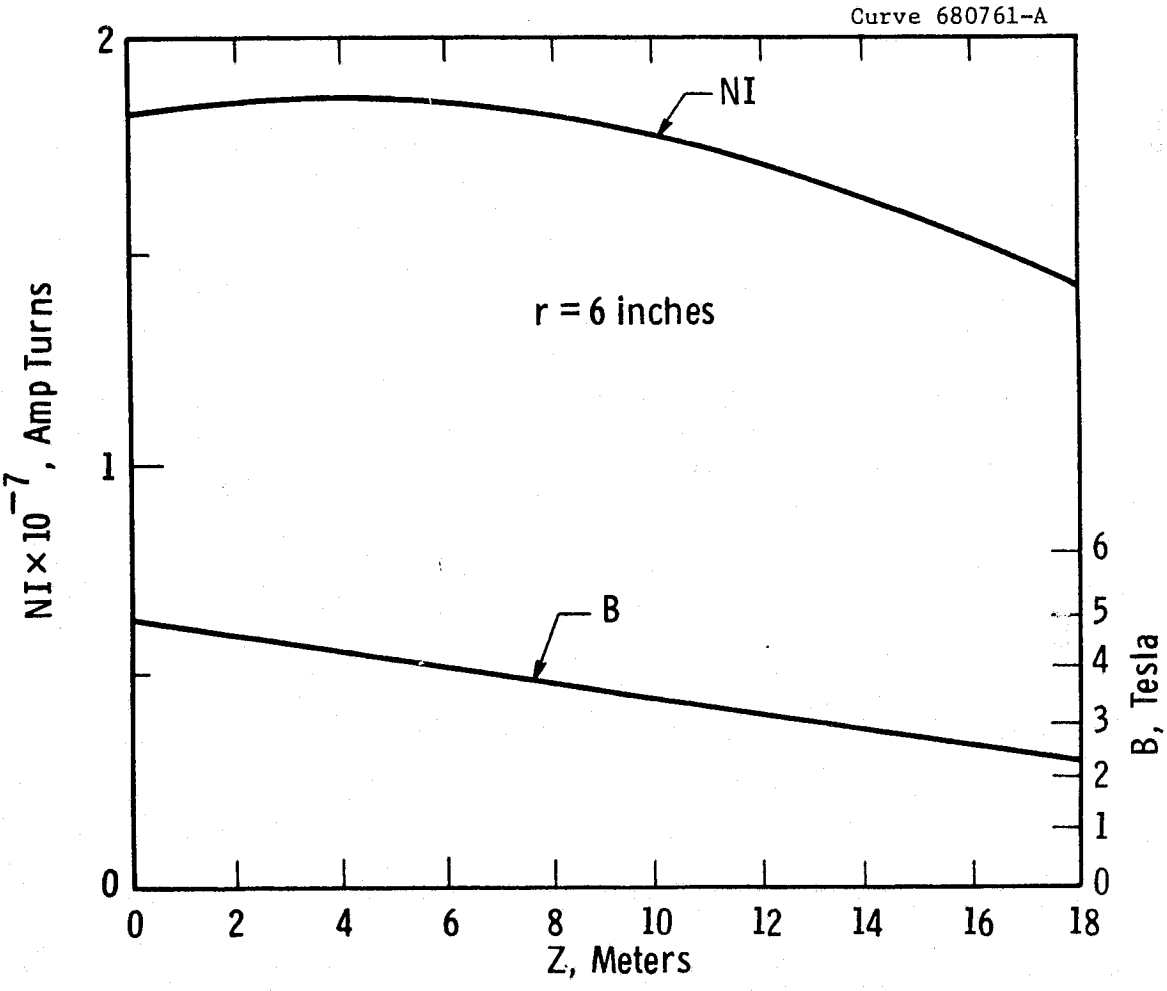

Fig. A 10.2.2—Winding current and magnetic field as a function of distance down the duct axis for the closed cycle, inert gas MHD generator Base Case design

liquid helium cooling ducts, headers, and the necessary distributed support structure within the winding. To ensure stable operation a 3:1 copper to superconductor ratio was selected, not enough copper to cryostabilize the winding but probably enough to dynamically stabilize the winding. Although the MHD magnet is a dc device, provisions for operational margin must be provided. If one has temperature excursions of between 0.1 to 0.2°K (0.18 to 0.36°F) from the nominal 4.2°K (-452.13°F) in the windings, an operational current density equal to 0.5 j_c at 4.2°K (-452.13°F) affords a reasonable compromise between high current density and thermal margin and was selected as the design point for the peak field region in the winding.

The base case electrical design for the closed-cycle generator was calculated for a 5 T field and a winding current density of $\lambda J = 1.64 \times 10^8$ A/m^2. Table A 10.2.1 presents the Reference case design parameters for the closed-cycle generator. The winding current and magnetic field are given in Figure A 10.2.2 as a function of distance down the generator axis. For this design, the magneto motive force (MMF) required is 1.853×10^7 A-turns.

Heat transfer analysis was performed, and a summary of the results are presented in Table A 10.2.2. The refrigeration systems for the closed-cycle plasma MHD design are comparable with the refrigeration system requirements for the 600 MVA open-cycle plasma MHS system. A 26.9 m^3 (950 ft^3), 9,072 Mg (10 ton), 140 W helium refrigerator and a 4.81 m^3 (170 ft^3), 3.402 Mg (3.75 ton), 12 kW nitrogen refrigerator are required. The installed cost of the above refrigerators is approximately $300,000.

The overall cost of the magnet system for open- and closed-cycle MHD generators was derived in Appendix A 9.9. A summary of the results obtained for the closed-cycle base case magnet design is illustrated in Table A 10.2.3. The cost per kVA for this design is $38/kVA. A detailed account of the cost breakdown for reference case, closed-cycle MHD magnet system is given in Table A 10.2.4. In the cost study performed

Table A 10.2.1 - Dipole Magnet Design for the Reference Case Closed-Cycle, Inert Gas MHD Generator

I	Z, m	L, m	D, m	d,m	NI A-turn	Mag. Ind (B),T	Z, m
1	0.000	1.354	2.291	.0995	0.18226+08	5.00	0.000
2	1.000	1.418	2.380	.0965	0.18365+08	4.85	1.000
3	2.000	1.483	2.469	.0935	0.18461+08	4.70	2.000
4	3.000	1.547	2.557	.0905	0.18515+08	4.55	3.000
5	4.000	1.611	2.646	.0875	0.18527+08	4.40	4.000
6	5.000	1.676	2.735	.0846	0.18496+08	4.25	5.000
7	6.000	1.740	2.824	.0816	0.18423+08	4.10	6.000
8	7.000	1.804	2.912	.0786	0.18307+08	3.95	7.000
9	8.000	1.869	3.001	.0756	0.18149+08	3.80	8.000
10	9.000	1.933	3.090	.0726	0.17949+08	3.65	9.000
11	10.000	1.997	3.179	.0696	0.17706+08	3.50	10.000
12	11.000	2.061	3.268	.0666	0.17421+08	3.35	11.000
13	12.000	2.126	3.356	.0637	0.17093+08	3.20	12.000
14	13.000	2.190	3.445	.0607	0.16723+08	3.05	13.000
15	14.000	2.254	3.534	.0577	0.16311+08	2.90	14.000
16	15.000	2.319	3.623	.0547	0.15856+08	2.75	15.000
17	16.000	2.383	3.712	.0517	0.15359+08	2.60	16.000
18	17.000	2.447	3.801	.0487	0.14819+08	2.45	17.000
19	18.000	2.512	3.889	.0458	0.14237+08	2.30	18.000

Table A 10.2.2 - Summary of Cooling Requirements for the Closed-Cycle Plasma MHD Design

Load	Heat Input, W	Mass Flow, lb/hr	Electrical Load kW
Helium Refrigerator			
Radiation	16.6	18.7	10.0
Electrical heads	75.0	84.0	135.0
Support structure	43.4	48.8	26.0
TOTALS	134.6	151.5	171.0
Nitrogen Refrigerator			
Helium refrigerator	648	25.8	5.2
Radiation	10365	412.5	82.9
Conduction	352	14.0	2.8
TOTALS	11365	452.3	90.9

Table A 10.2.3 - Summary of the Reference Case Closed-Cycle MHD Magnet Design

Nominal Duct Rating	600 MW
Inlet Cross-Sectional Area	1.833 m^2
Exit Cross-Sectional Area	6.302 m^2
Length of Duct	18 m
Field on Axis at Inlet	5T
Field on Axis at Exit	2.3T
Peak Ampere-Turns Required	1.853 x 10^7A-turns
Current per Turn	5000A
Average Winding Current Density	1.64 x 10^8A/m^2
Winding Packing Factor	0.7
Conductor Aspect Ratio	2:1
Fraction of Superconductor in Conductor	0.25
Inductance	122h
Stored Energy	1526 MJ
Number of Turns	3707
Conductor Operating Temperature	4.2°K
Liquid Helium Refrigerator Thermal Load	135 W
Liquid Helium Refrigerator Electrical Load	171 kW
Liquid Nitrogen Refrigerator Thermal Load	11.4 kW
Liquid Nitrogen Refrigerator Electrical Load	91 kW
Total Electrical Load	262 kW
Total Estimated Cost	$23,000,000
$/kVA	$38/kVA

Table A 10.2.4 - Cost Breakdown for the Reference Case Closed-Cycle MHD Magnet System

Superconductor (NbTi)	
Material cost ($25/lb @ 2 x 10^5 A/cm^2 @ 5 T)	$ 4,350,000
Volume, m^3	8.7 m^3
Weight (tons)	87
Fabrication cost ($16/lb)	$ 2,780,000
Total cost	$ 7,130,000
Structure (310 SS)	
Material cost ($1.60/lb)	$ 1,250,000
Volume	
Weight (tons)	390
Fabrication cost ($5.40/lb)	$ 4,210,000
Total cost	$ 5,460,000
Base Cost	$12,600,000
Engineering	$ 3,150,000
Construction	$ 3,150,000
Design allowance	$ 3,780,000
Total cost of magnet	$22,700,000
Refrigerator cost	$ 300,000
Total cost	$23,000,000 (± 25%)

on the open-cycle MHD magnet system the following parametric expression for the cost of the conductor was developed:

$$C = \frac{4.8\ B_{av}\ Z}{\mu_o\ \lambda J_{av}} \left(\frac{L_1 + L_2}{\sqrt{2}} + 2R \right) \qquad \text{(A 10.2.1)}$$

where C = cost of conductor system ($M)

B_{av} = average magnetic field (T)

Z = length of duct

μ_o = $4\pi \times 10^{-7}$ = permeability of free space

λJ_{av} = average winding current density (A/m^2)

L_1 = inlet duct width (m)

L_2 = exit duct width (m)

R = insulation thickness (m).

Appendix A 10.3

SIZE, WEIGHT, COSTS OF DC-TO-AC POWER-CONDITIONING SYSTEM FOR CLOSED-CYCLE MHD GENERATORS

The size, weight, and costs of dc-to-ac power conditioning systems to be used with MHD generators were analyzed. Since MHD generators are dc devices, their dc power has to be converted to ac to be compatible with the steam plant and for power transmission. The dc-to-ac converters can be either static-type, as solid state, or mechanical-type, as motor-generator sets. For the closed-cycle gas-type MHD generator in which the output voltage is 5 to 10 kV, and output currents of 2 to 5 kA are possible, a solid-state converter is plausible. The efficiency of such a system is on the order of 98 to 99%, which represents a very low power loss.

The proposed closed-cycle MHD generator duct and operation are similar to the open-cycle generator (Appendix A 9.11) except that the output power is 700 MW and the working fluid is argon or helium mixed with cesium seed. Either nonequilibrium or thermal ionization will be used. The procedures used to determine size, weight, and cost of the 700 MW dc-to-ac power conditioning system are the same as those for the open-cycle case. The segmented electrodes will be connected in series to attain a high-output voltage, and the electrode widths are selected to give the same current per electrode for a given series array of electrodes.

Figure A 10.3.1 shows the electrical characteristics of the MHD duct, in which the working fluid was argon and cesium, and nonequilibrium ionization case. This figure shows the terminal voltage, V, current density, J, effective Hall angle, θ, and effective electrode width, W_{el}, as a function of downstream distance. The electrode width is based on 5 kA

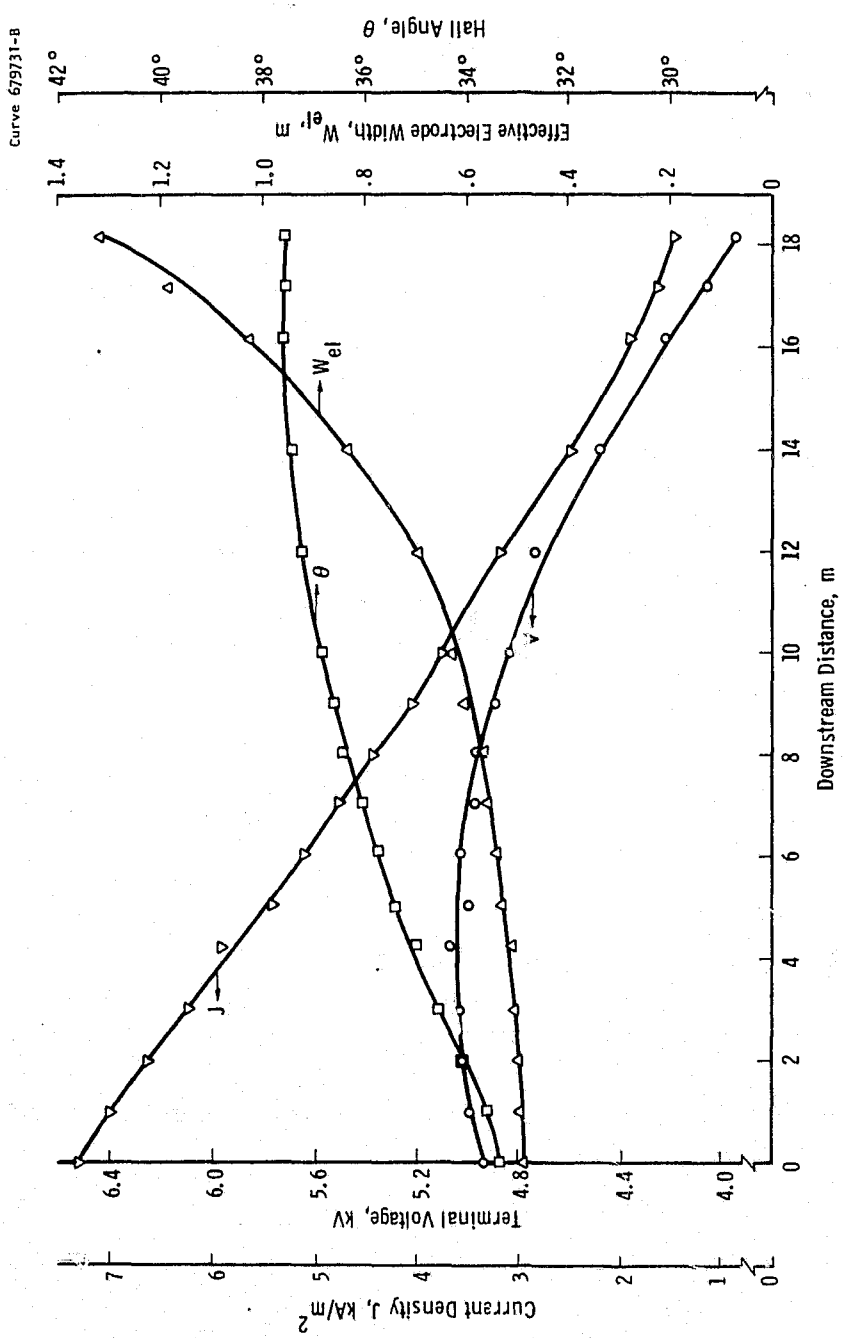

Fig. A 10.3.1 —Electrical characteristics of closed cycle MHD duct. Working fluid—argon + 0. 15% C_s.

per electrode. The information of Figure A 10.3.1 was used to lay out the various sets of series electrode arrays, as shown in Figure A 10.3.2. The figure shows an example of one array in which two pairs of electrodes are connected in series. A total of ten such arrays, however, and eight remaining pairs of electrodes will be needed to utilize the full output power of the duct. Each array or pair of electrodes constitutes a separate circuit to be fed to a dc-to-ac converter. Therefore, the circuits are:

- 10 to 10 kV/5 to 6 kA dc circuits, 50 to 60 MW each (2 pairs of electrodes in series)
- 8 to 5 kV/5 kA dc circuits, 25 MW (1 pair of electrodes).

The total output power of these circuits is approximately 700 MW. This layout is not the optimum design but is sufficient for calculating the size, weight, and cost of the power conditioning system.

In this example we have assumed a total of 10 x 2 + 8 = 28 pairs of electrodes. This array arrangement was assumed for the sake of obtaining dc voltages and currents suitable for feeding into the converter. For reasons of improving MHD generator performance under nonequilibrium ionization, the actual electrodes will be made of tungsten wire protruding slightly above the generator wall and extending into the stream. There will be 28 N pairs of such electrodes, and the integer N may be as high as 50 or 100. As mentioned before, this layout is probably not optimum; it was assumed for the purpose of estimating cost, weight, and size of the dc-to-ac conversion system only. Detailed electrode design is beyond the scope of this discussion.

A 10.3.1 Size, Weight, and Costs of 700 MWe Power-Conditioning System

A block diagram of the power conditioning system is shown in Figure A 10.3.3. Power from each of the eighteen dc circuits of the MHD generator is fed into a 12-pulse thyristor inverter bridge having the three-phase ac output which is fed into the primary of an inverter

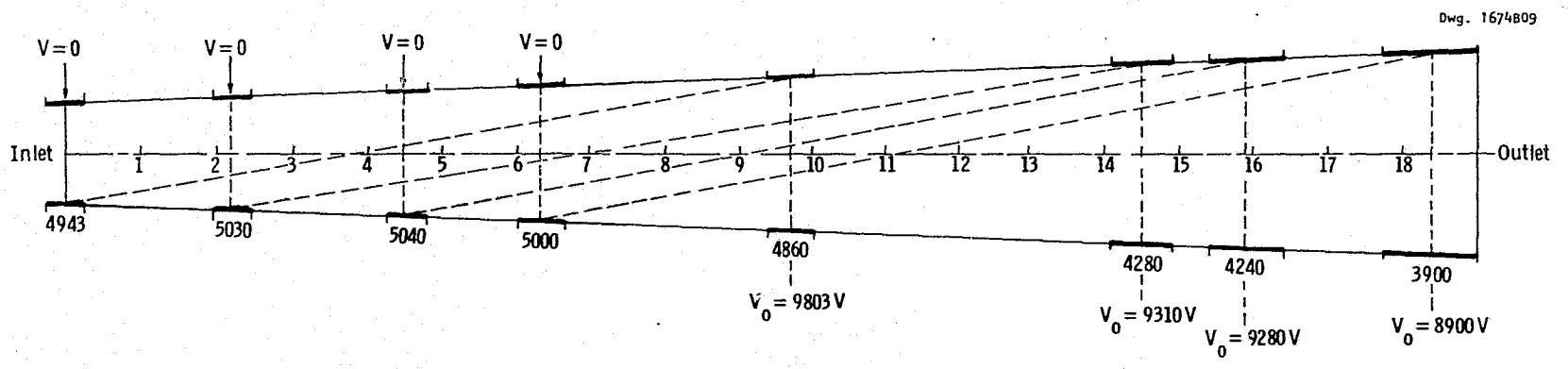

Fig. A 10.3.2—Layout of closed-cycle MHD duct electrode connections. Shown is possible placement of four sets of electrodes connected in series. The angle of connection of these electrodes equal to the arctan $(1-K)\beta/K$. The diagonal dash lines are equipotential lines.

Dwg. 16/4807

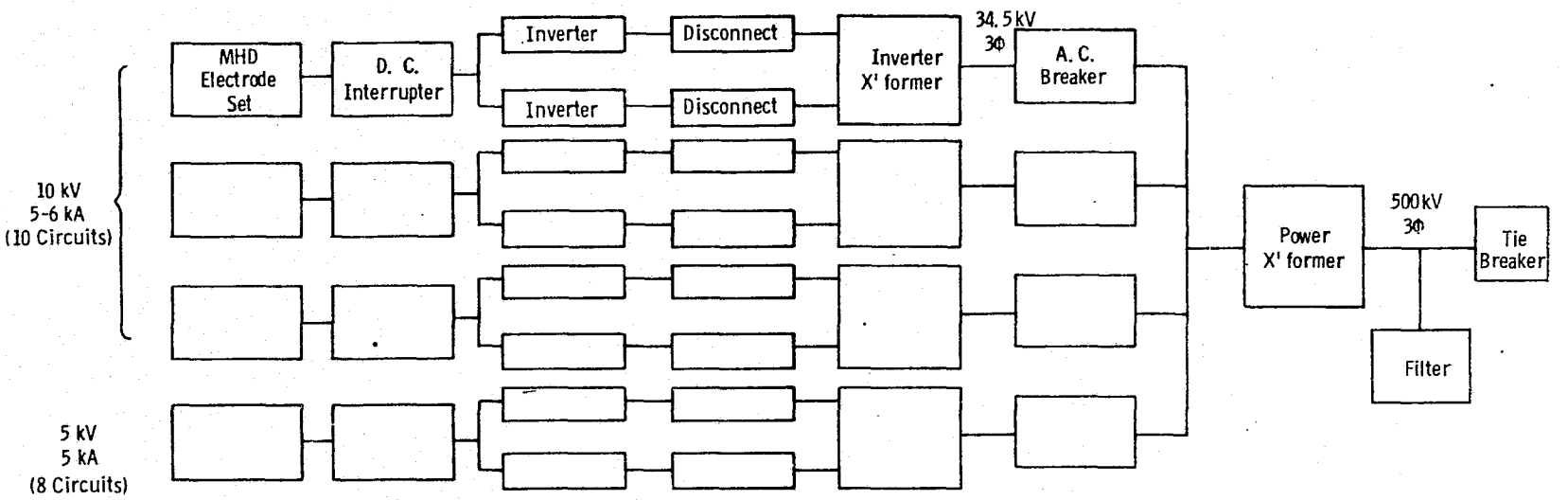

Fig. A 10.3.3– Block diagram of 700 MW d.c. to a.c. converter system for closed cycle MHD

transformer. The secondary winding of each inverter transformer is at 34.5 kV and is connected via an ac circuit breaker to the primary of a 34.5 kV/500 kV power transformer. The 500 kV secondary winding feeds power to the mains. A tunable filter is connected across the 500 kV line to filter out undesirable harmonics caused by the inverters. A dc interrupter is connected between the output of the MHD generator and the input of the inverters. Disconnect switches are placed in each leg between the output of the inverters and the primary of the inverter transformers. Details of the converter for each MHD circuit are shown schematically in Figure A 9.11.4 of Appendix A 9.11.

Table A 10.3.1 gives the volumes and weights of the components for each converter circuit and for the tunable filter across the mains to the input of the transmission line. These sizes and weights are based on the 26 MW system previously mentioned in Appendix A 9.11 and the scaling factor is the ratio of the megawatts raised to an exponent scaling power of 0.85. The transformer sizes and weights, however, were obtained from data supplied by the Westinghouse Transformer Division. The pad required to house the 700 MW power conditioning system is estimated to be 53.34 m (175 ft) long and 213.3 m (700 ft) wide. The overall weight of the components is 2693 Mg (2969 tons). See Figures A 10.3.4 and A 10.3.5 for layouts of a 50 MW circuit and the filter components; also Table A 10.3.2.

A 10.3.2 Cost of Power-Conditioning System

The cost of a 700 MW dc-to-ac power conditioning system for the closed-cycle MHD generator is based on the following cost per kilowatt for the dc and ac components according to the following schedule:

- Inverters (including dc filter reactor, interphase reactor, commutating circuits, inverter bridges, and cooling system) - $30/kW
- Inverter transformers - $7.2/kVA
- Tunable filter - $6/kVA

Table A 10.3.1 - Size and Weight of 700 MW System

A. 50 MW dc-ac Converter Circuit

	Item	Dimensions, ft	Weight, lb
1.	Inverter Set	9 H x 12 L x 6 W	9,700
2.	Inverter Cooling System	7 x 9 x 5	14,600
3.	Inverter Interphase Reactor	11 x 5.5 x 6.4	16,700
4.	DC Filter Reactor	20.6 H x 6.8 D	30,600
5.	Emergency Commutating Capacitors	6 x 9 x 6.6	27,700
6.	Emergency Commutating di/dt Reactor	3.4 x 5.3	3,400
7.	Emergency Commutating Reversing Reactor	4.3 x 3.7	1,500
8.	Inverter Transformers	28 x 15 x 16	180,000
9.	AC Circuit Breaker	11 x 5.1 x 13.4	9,620
		Total wt/circuit	293,820
		Total wt of 10 circuits	2,938,200

B. 25 MW dc-ac Converter Circuit

1.	Inverter Set	7 x 9 x 5	4,900
2.	Inverter Cooling System	5.7 x 7 x 4.2	7,300
3.	Inverter Interphase Reactor	9.1 x 4.5 x 5.2	9,300
4.	DC Filter Reactor	17 x 5.6	16,900
5.	Emergency Commutating Capacitors	4.7 x 7 x 5.2	13,800
6.	Emergency Commutating di/dt Reactor	2.8 x 4.4	1,900
7.	Emergency Commutating Reversing Reactor	3.5 x 3.1	900

Table A 10.3.1 (continued)

8.	Inverter Transformer	23 x 12 x 13	99,900
9.	AC Circuit Breaker	11 x 5.1 x 13.4	9,620
		Total wt/circuit	164,520
		Total wt of 8 Circuits	1,316,160
C.	700 MW Filter		
1.	Filter C, 11th Harmonic	19.5 x 45 x 9	323,100
2.	Filter L, 11th Harmonic	24 x 6.8	37,800
3.	Filter C, 13th Harmonic	19.5 x 32.5 x 9	226,100
4.	Filter L, 13th Harmonic	24 x 6.8	37,800
5.	Filter C, High Pass	19.5 x 22.5 x 9	121,100
6.	Filter L, High Pass	25.8 x 7.6	34,500
		Total filter wt	780,400
7.	Power Transformer	38.7 x 21.7 x 17.5	902,400
D.	Total System Weight		5,937,200

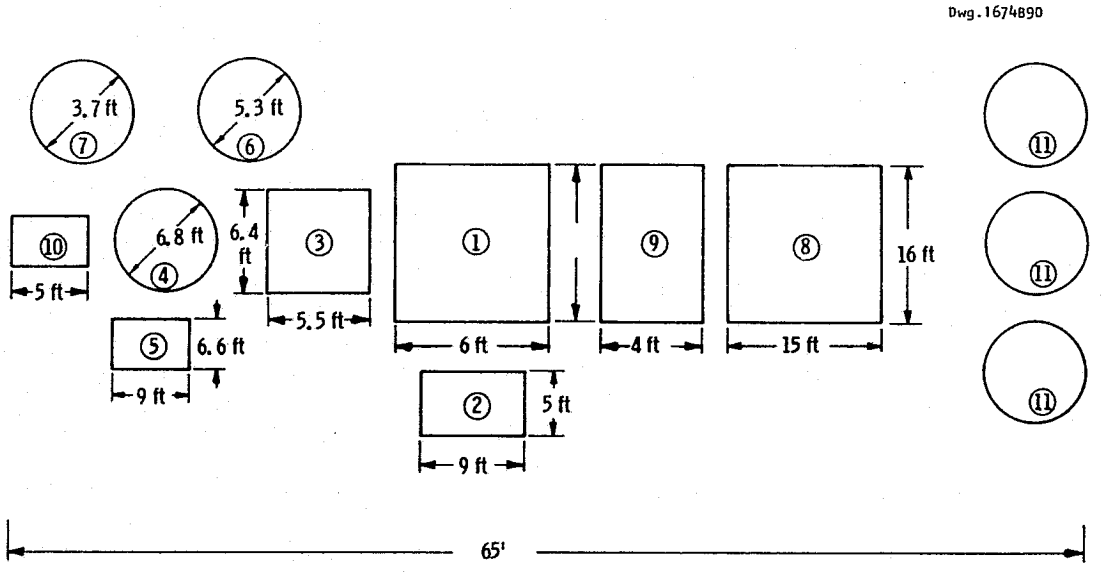

Fig. A 10.3.4 – 50 MW dc - ac converter circuit layout. See Table A 10.3.3 for component identification

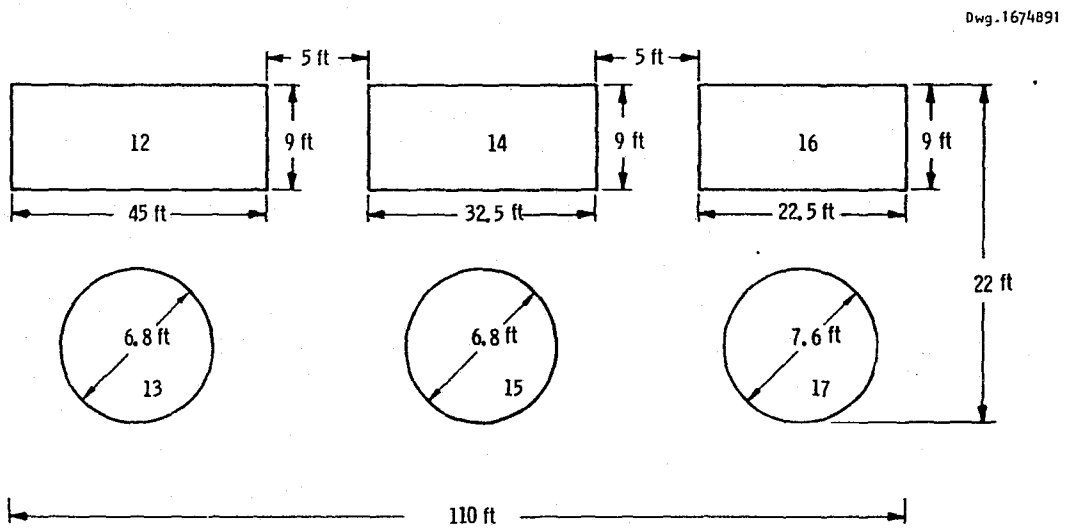

Fig. A 10.3.5—Layout of filter for 700 MW system. See Table A 10.3.3 for component identification

Table A 10.3.2 - Items Shown in Layout of Converter Circuits (Figures A 10.3.4 and A 10.3.5)

Item No.	Item
1	Inverters
2	Inverter Cooling System
3	Inverter Interphase Reactor
4	DC Filter Reactor
5	Emergency Commutating Capacitors
6	Emergency Commutating di/dt Reactor
7	Emergency Commutating Reversing Reactor
8	Inverter Transformer
9	Disconnect Switch Array
10	DC Interrupter
11	Lightning Arresters
12	Filter C, 11th Harmonic
13	Filter L, 11th Harmonic
14	Filter C, 13th Harmonic
15	Filter L, 13th Harmonic
16	Filter C, High Pass
17	Filter L, High Pass

Table A 10.3.3 - Cost Breakdown of 700 MW System

A.	10 kV, 5 kA DC Circuit	
	1. Inverter Set (50 MW)	$1,560,000
	2. Inverter Transformer (50 MVA, 7 kV/34.5 kV)	379,500
	3. DC Interrupter (50 MW)	300,000
	4. AC Circuit Breaker (34.5 kV, 1000 A, 2500 MVA)	24,200
	Total Cost/Circuit	$2,263,700
	Total Cost of 10 Circuits	$22,637,000
B.	5 kV, 5 kA DC Circuit	
	1. Inverter Set (25 MW)	$ 782,000
	2. Inverter Transformer (25 MVA, 3.5 kV/34.5 kV)	262,500
	3. DC Interrupter (25 MW)	150,000
	4. AC Circuit Breaker (34.5 kV, 1000 A, 2500 MVA)	24,200
	Total Cost/Circuit	$1,218,700
	Total Cost of 8 Circuits	$9,749,600
C.	500 kV Power Transformers and Filter	
	1. 700 MVA, 34.5 kV/500 kV Power Transformer	$1,750,000
	2. Filter	1,500,000
	Total System Cost	$35,636,600
	Cost/kW	$50.9/kW

- DC interrupter - $6.0/kW
- Power transformer - $2.5/kVA.

Results of the cost calculations are given in Table A 10.3.3. The total cost of the 700 MW system is $35.6 million, which represents a cost of $51/kW. These costs are FOB which do not include delivery and installation. The Power System Planning group at Westinghouse was consulted with regard to the costing of this dc-to-ac power conversion system. They arrived at a cost range of $40 to 50/kW. The most probable cost of this power conversion system, therefore, may be $51/kW. This cost is lower than that estimated for the smaller 26 MW system, which was $58/kW.

A 10.3.3 Circuit Protection and Response to Transients

The proposed power conditioning system is protected against (1) short circuits in the MHD generator and in the power transmission line, (2) voltage spikes caused by instabilities in the MHD generator, and (3) voltage spikes caused by lightning strokes or switching surges. See Appendix A 9.11 for more details.

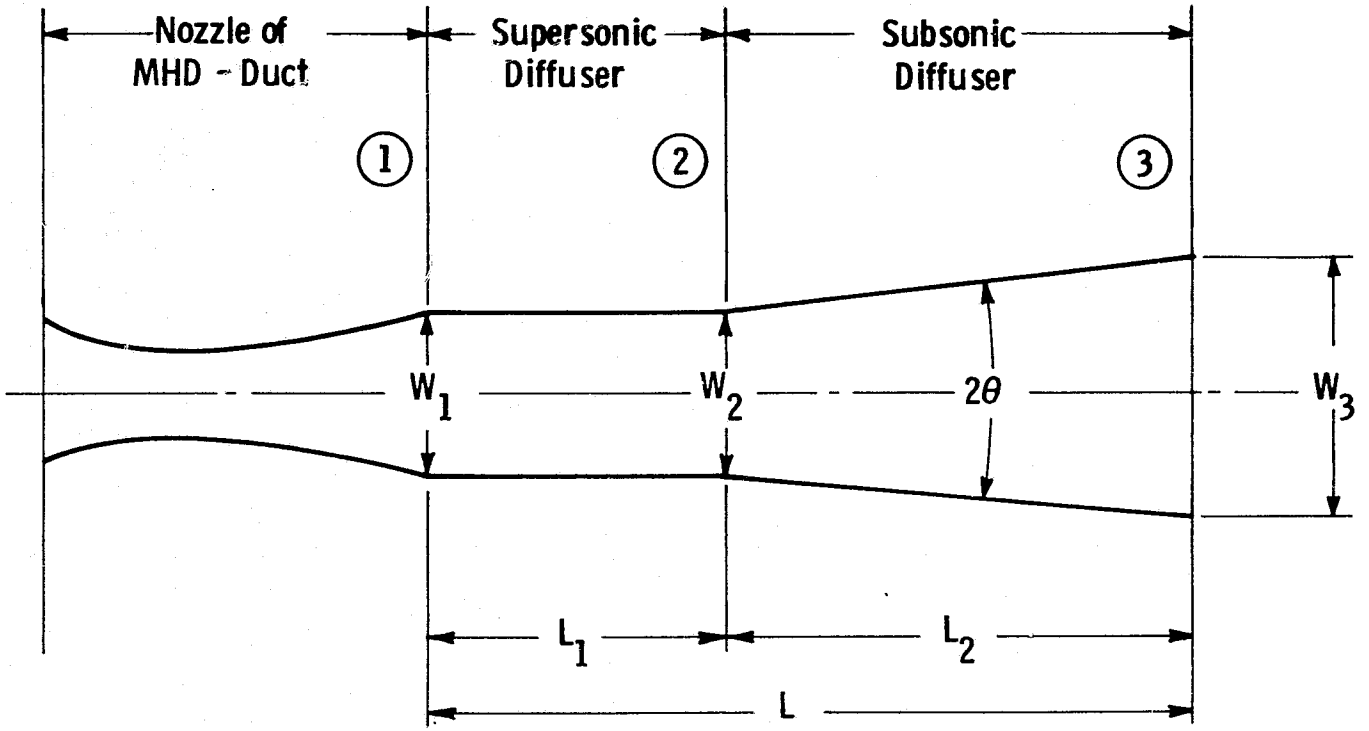

Fig. A 10.4.1 – Sketch of the diffuser geometry

Dwg. 6363A92

Appendix A 10.4

PERFORMANCE ESTIMATION OF DIFFUSERS

A 10.4.1 Introduction

In the study of closed-cycle MHD it is necessary to estimate the performance and the geometry of the diffuser which will decelerate the flow from a supersonic or high subsonic Mach number to low subsonic Mach number. The working medium is argon or helium with an isentropic exponent of $\gamma = 1.667$. Required are the efficiency or the static pressure rise and the corresponding diffuser length and area ratio.

The information reported here (Subsection A 10.4.2) is first used for the cycle analysis in a systematic study to evaluate the optimum operating conditions for the cycle. Then in Subsection A 10.4.3 we will present the final estimation of the diffuser geometry corresponding to these optimum operating conditions (base case conditions).

A 10.4.2 Diffuser Performance

The diffuser is divided into two parts, the supersonic* and the subsonic. This is schematically illustrated in Figure A 10.4.1. The flow leaves the MHD generator at a supersonic Mach number and enters the diffuser. The stations (or subscripts) 1, 2, and 3 correspond to the supersonic diffuser inlet, the subsonic diffuser inlet, and the exit, respectively. In the following we will discuss first the supersonic and then the subsonic diffuser.

---

*Here we will refer to the supersonic diffuser as the one which decelerates the supersonic flow to a high subsonic one. Then the subsonic diffuser, which has generally a divergent shape, will decelerate it further to a very low velocity.

A 10.4.2.1 Supersonic Diffuser

An experimental study of supersonic diffusers was reported by Neumann and Lustwerk (Reference 10.29). Air was used as the working medium. Both square and circular sections were tested and were found to behave similarly. The diffusion process is done by means of a so-called pseudoshock system (Reference 10.30) in a channel with approximately constant area. The static pressure ratio p_2/p_1 and the isentropic diffuser efficiency (η_{is}, defined later) are found to be very close to those yielded by a normal shock relation.

Although the medium used here is helium or argon, the fundamental behavior is expected to be the same. All the quantities such as p_2/p_1, η_{is}, exit Mach number, M_2, and static temperature ratio T_2/T_1, therefore, may be estimated from the normal shock relationships (see e.g., References 10.31 and 10.32) with $\gamma = 1.667$ in terms of M_1:

$$\frac{p_2}{p_1} = \left(\frac{2\gamma}{\gamma + 1}\right) M_1^2 - \frac{\gamma - 1}{\gamma + 1} \qquad \text{(A 10.4.1)}$$

$$\frac{T_2}{T_1} = \frac{\left(1 + \frac{\gamma - 1}{2} M_1^2\right)\left(\frac{2}{\gamma - 1} M_1^2 - 1\right)}{\frac{(\gamma + 1)^2}{2(\gamma - 1)} M_1^2} \qquad \text{(A 10.4.2)}$$

$$M_2^2 = \frac{M_1^2 + \frac{2}{\gamma - 1}}{\frac{2\gamma}{\gamma - 1} M_1^2 - 1} \qquad \text{(A 10.4.3)}$$

$$\eta_{is} = \frac{\frac{2}{\gamma - 1}\left[\left(\frac{p_2}{p_1}\right)^{\frac{\gamma - 1}{\gamma}} - 1\right]}{M_1^2 - M_2^2\left(\frac{T_2}{T_1}\right)} \qquad \text{(A 10.4.4)}$$

The definition of η_{is} is shown in Figure A 10.4.2. The derivation of Equation A 10.4.4 can be seen easily by applying the ideal gas relationships.

The length of this pseudoshock system is estimated from the figure on p 120 in Reference 10.30. The data reported there, however, are for pipes, and the length is nondimensionalized by the pipe diameter. To apply this figure to noncircular sections it is appropriate to use the hydraulic diameter to replace the pipe diameter.

Although it was found (Reference 10.33) that a variable geometry supersonic diffuser can perform better than the so-called fixed geometry diffusers reported in Reference 10.28, we do not have enough data from Reference 10.33 to cover the whole Mach number range of M_1. We have used Equations A 10.4.1 to A10.4.4, therefore, which are based on observations of Reference 10.38. Thus, the present estimation is somewhat conservative.

A 10.4.2.2 Subsonic Diffusers

For subsonic diffusers, it has been found that the straight wall channel diffusers* with aspect ratio ($= b_2/W_2$, where b = dimension perpendicular to W) equal to 1 and the conical diffusers are optimum (Reference 10.34). Performance maps can be found in Reference 10.35 for straight wall channel diffusers and in Reference 10.36 for conical diffusers. The performance depends primarily on the inlet Mach number M_2 and the inlet blockage B:

$$B = 1 - \frac{\text{actual mass flow rate}}{\text{ideal mass flow rate}} \qquad \text{(A 10.4.5)}$$

Note that B indicates how thick the inlet boundary layer is. For the present case the inlet flow can be assumed to be fully developed. Using a 1/7-power-law boundary layer velocity profile and neglecting the

*Note: defined as diffusers with linear wall and with constant double divergence angle 2θ and constant depth b.

Dwg. 6363A93

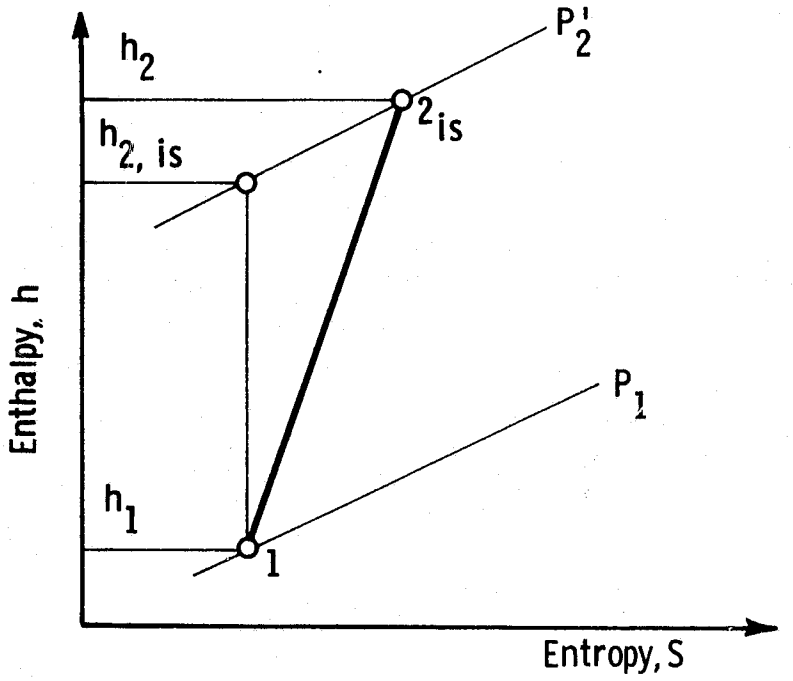

1 = Diffuser Inlet

2 = Diffuser Exit

2_{is} = Diffuser Exit for an isentropic process

$$\eta_{is} = \frac{h_{2,\,is} - h_1}{h_2 - h_1}$$

Fig. A 10.4.2– Definition of the isentropic diffuser efficiency, η_{is}

compressibility, we find that this corresponds approximately to an inlet blockage of 12%.

When the geometry is known, the achievable static pressure increase or the geometry for a required pressure rise can be obtained from References 10.35 and 10.36.

However, Reference 10.35 and 10.36 do not report the corresponding diffuser efficiency, although the total pressure p_{T_3} at the diffuser exit may be estimated by some boundary layer assumptions if the diffuser geometry is known. Nevertheless, for the whole diffusion process (supersonic and subsonic), it is justified to assume that the efficiency of the subsonic diffuser has not significant influence on the overall efficiency as the enthalpy increase in the supersonic part dominates. Therefore, in this estimation one can use the supersonic diffuser efficiency to represent the whole process. Since the static pressure ratio, however, is rather large in the subsonic part, it is recommended that References 10.35 and 10.36 be used to determine p_3/p_2.

A 10.4.3 Estimation of the Diffuser Geometry Corresponding to the Base Case Operating Conditions

The base case operating conditions found from the cycle study yield the following inlet and exit data for the diffuser:

Table A 10.4.1 - Diffuser Data Description

	Diffuser inlet	Diffuser exit
Static Pressure, kPa	94.0	236.9
Total Pressure, kPa	275.1	244.9
Mach Number	1.268	0.2

Referring to Figure A 10.4.1 again, we have to determine the diffuser widths at stations 1, 2, 3, W_1, W_2, W_3 as well as the lengths L_1 and L_2.

The diffuser is chosen to be a square section which behaves in a manner similar to that of conical diffusers. In this case the width of the square is equivalent to the diameter of the conical diffusers. We will consider the supersonic and subsonic diffuser separately.

A 10.4.3.1 Supersonic Diffuser

The supersonic flow is decelerated to subsonic velocities by means of a normal shock. In view of this relatively low supersonic Mach number, it is believed that the flow will not separate behind the shock (see Chang, Reference 10.37, p 231).

The flow at station 2 will have the following condition corresponding to a normal shock:

$$\text{static pressure } p_2 = 1.75\ p = 164.2 \text{ kPa}$$

$$\text{total pressure } p_{T_2} = 0.9875\ p_{T_1} = 272 \text{ kPa}$$

$$\text{Mach number } M_2 = 0.805$$

Based on the figure of Referece 10.30 p 120, the length L_1 is estimated to be four times the duct width W.

The supersonic part of the diffuser is assumed to have an approximately constant area; therefore, W_2 is equal to W_1.

A 10.4.3.2 Subsonic Diffuser

The inlet condition is identical to that of condition 2, with a blockage of 12%, as mentioned in Subsection A 10.4.2.

The Figure 67 of Reference 10.36 is used for this estimation. The following table shows what percentage of the design exit pressure p_3, (236.9 kPa) can be achieved using an optimum double divergence angle of $2\theta = 4$ degrees (Figure A 10.4.1). This angle follows from the performance

map in Figure 67 of Reference 10.36. The corresponding values of area ratio A_3/A_2, W_3/W_2, L/W are shown as well (Figure A 10.4.1):

Table A 10.4.2 - Subsonic Diffuser Data Description

L_2/W_1	p_3, kPa	$p_3/p_{3design}$ [%]	A_3/A_2	W_3/W_2	L/W_1
11.6	228.7	96.6	3.28	1.81	15.6
13.85	230.9	97.5	3.86	1.97	17.85
18.8	233.1	98.3	5.32	2.31	22.8
22.9	234.1	98.8	6.75	2.6	26.9

The values of $p_3/p_{3design}$ and A_3/A_2 are plotted vs L_2/W_1 in Figure A 10.4.3.

Due to the boundary layers the design value of p_3 cannot be achieved even by increasing the length. A small increase from L_2/W_1 = 11.6 to 13.85 results in 0.8% gain of $p_{3design}$ while a further 0.8% gain must be accompanied by increasing L/W_1 to 18.8. As a compromise between the length and the gain in pressure, we have selected L_2/W_1 = 13.85. The final dimensions, therefore, are (see Figure A 10.4.1):

$$W_1 = W_2 = 2.510 \text{ m}$$

$$W_3 = 4.935 \text{ m}$$

$$L_1 = 10.04 \text{ m}$$

$$L_2 = 34.76 \text{ m}$$

$$L = 44.8 \text{ m}$$

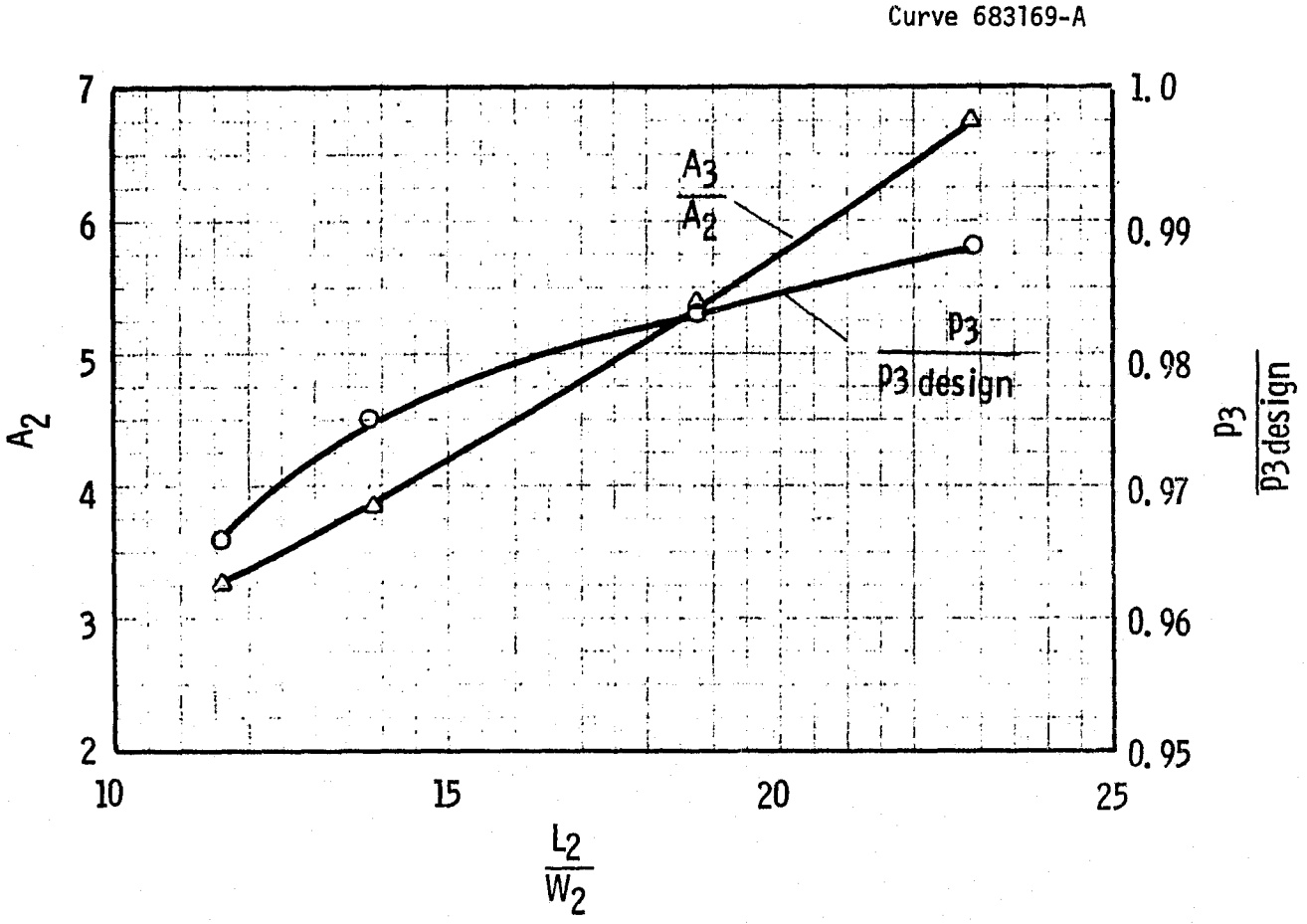

Fig. A 10.4.3—Area ratio A_3/A_2 and nondimensionalized exit static pressure $p_3/p_{3\,design}$ vs the nondimensionalized length for the subsonic diffuser

$2\theta = 4$ degrees.

square cross sections.

It is, of course, inconsistent that the exit pressure $p_3 = 230.9$ kPa is not equal to the design value. For the present purpose, we consider the difference to be negligible, while in the actual design it must, of course, be taken into account.

Dwg. 6370A39

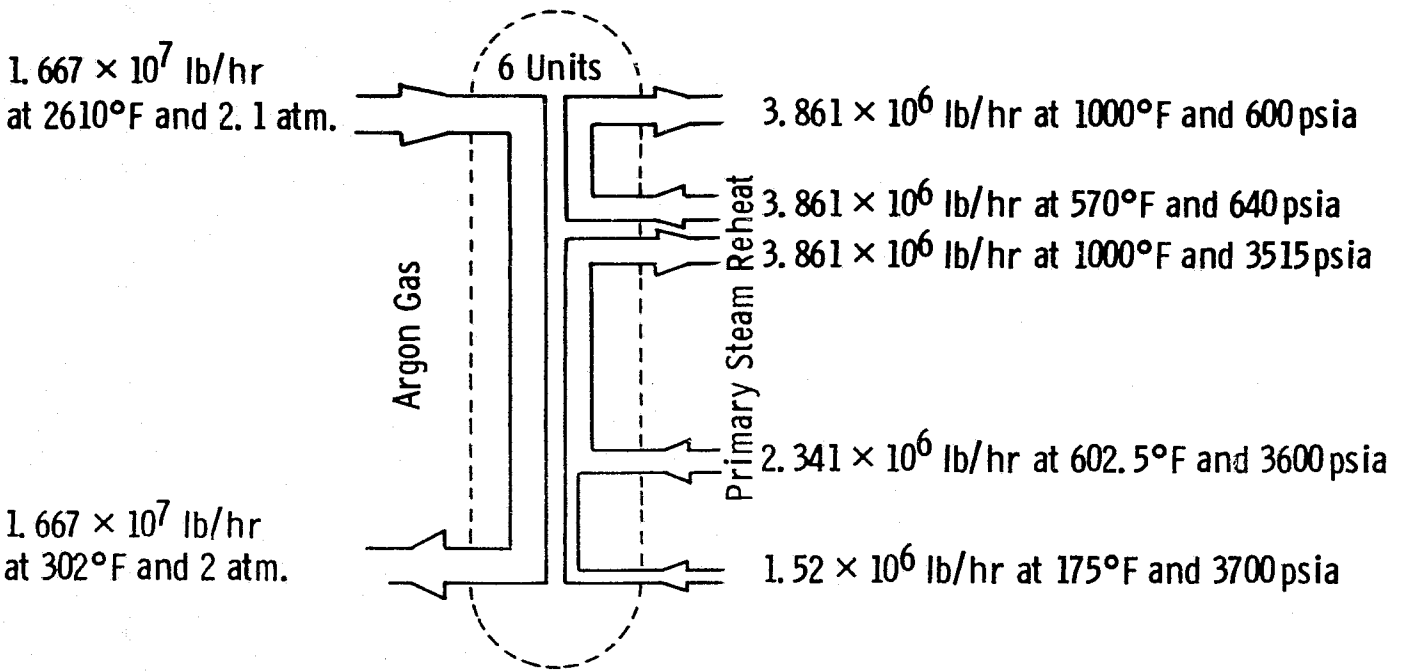

Fig. A 10.5.1—Steam generator flows

Appendix A 10.5

HEAT RECOVERY STEAM GENERATOR FOR CLOSED-CYCLE MHD SYSTEM

A 10.5.1 General Description and Duty of the Steam Generator Units

In the discussion which follows it will be shown that a bank of six steam generators is the most practical arrangement for handling the heat recovery duty.

The steam generator bank accepts 2100 kg/s (1.667×10^7 lb/hr) of argon from the MHD duct at 1705°K (2610°F) and 212.7 kPa (2.1 atm). This stream is cooled to 423°K (302°F) at 202.6 kPa (2 atm). The total heat transferred is, therefore, 1403 MWt (4.788×10^9 Btu/hr), in other words, 234 MWt (0.798×10^9 Btu/hr) per steam generator.

This heat is absorbed by a 191.5 kg/s (1.52×10^6 lb/hr) water stream which enters at 352.6°K (175°F) and 24.132 MPa (3500 psi) abs and a 295 kg/s (2.341×10^6 lb/hr) water stream which enters at 590°K (602.5°F) and 24.821 MPa (3600 psi) abs. These streams join and are raised to steam at 811°K (1000°F) at 24.235 MPa (3515 psi) abs. Additionally, steam is reheated from 572°K (570°F) at 4.413 MPa (640 psi) abs to 811°K (1000°F) at 4.137 MPa (600 psi) abs. The reheat flow is the full 486.4 kg/s (3.861×10^6 lb/hr). Figure A 10.5.1 illustrates this duty.

Although the argon pressure is a very modest 212.7 kPa (2.1 atm) at inlet, it must be contained in a pressure vessel since the inlet gas temperature is 1705°K (2610°F). This dictates that the gas should be insulated from the steel pressure vessel. A thin refractory metal liner should separate the gas from the insulation to prevent erosion and subsequent particle entrainment. This containment wall arrangement is illustrated by Figure A 10.5.2.

Table 10.5.1 - Variable Definitions for Equation A 10.5.1

Variable Name	Definition	Value
T_{g4}	Inlet Gas Temperature at Station 4	2610°F
T_{g3}	Gas Temperature at Station 3	2148°F
T_{g2}	Gas Temperature at Station 2	654°F
T_{g1}	Exhaust Gas Temperature at Station 1	302°F
T_{R4}	Exit Reheat Temperature at Station 4	1000°F
T_{R3}	Cold Reheat Temperature at Station 3	570°F
T_{S3}	Exit Superheat Temperature at Station 3	1000°F
T_{S2}	Second Steam Entering Water Temperature at Station 2	602.6°F
T_{S1}	First Stream Entering Water Temperature at Station 1	175°F
$\dot{m}_R$	Reheat Mass Flow	3.361×10^6 lb/h
$\dot{m}_{S2}$	Second Stream Waterflow	2.341×10^6 lb/h
$\dot{m}_{S1}$	First Stream Water Flow	1.52×10^6 lb/h
H_{R4}	Exit Reheat Enthalpy at Station 4	1515.6 Btu/lb
H_{R3}	Cold Reheat Enthalpy at Station 3	1265.7 Btu/lb
H_{S3}	Exit Superheat Enthalpy at Station 3	1421.7 Btu/lb
H_{S2}	Second Stream Entering Water Enthalpy at Station 2	611.9 Btu/lb
H_{S1}	First Stream Entering Water Enthalpy at Station 1	151.7 Btu/lb
Q	Overall Heat Load, MW	Btu/W

$$LMTD = \left\{ \frac{(T_{g4} - T_{R4}) - (T_{g3} - T_{R3})}{\ln \frac{(T_{g4} - T_{R4})}{(T_{g3} - T_{R3})}} \right\} \frac{\dot{m}_R (H_{R4} - H_{R3})}{Q} +$$

$$\left\{ \frac{(T_{g3} - T_{S3}) - (T_{g2} - T_{S2})}{\ln \frac{(T_{g3} - T_{S3})}{(T_{g2} - T_{S2})}} \right\} \frac{(\dot{m}_{S1} + \dot{m}_{S2})(H_{S3} - H_{S2})}{Q} +$$

$$\left\{ \frac{(T_{g2} - T_{S2}) - (T_{g1} - T_{S1})}{\ln \frac{(T_{g1} - T_{S2})}{(T_{g1} - T_{S1})}} \right\} \frac{\dot{m}_{S1} (H_{S2} - H_{S1})}{Q} . \qquad \text{(A 10.5.1)}$$

Table A 10.5.1 gives a definition and value for the variables appearing in Equation A 10.5.1).

For the base case considered, the value for mean temperature difference is 503.2°K (446.1°F).

In the equations which follow it is convenient to express the parameters of interest in terms of a few fundamental values which we are at liberty to select. These fundamental variables are:

- V_{max} - the maximum gas velocity between tubes
- d_o - the tube outside diameter
- N_{SG} - the number of steam generator modules used to carry the overall load.

A tube pitch diameter ratio, P_t/d_o, is first selected and then V_{max} chosen on the basis of the allowable overall pressure drop, ΔP. We shall see that this also fixes the number of tube rows, N_{row}, and the tube bank height, H. The number of modules, N_{SG}, is then selected to provide a sensible vessel diameter per module, D.

It is assumed that the argon gas passes through the staggered tube array in crossflow. The heat transfer correlation appropriate to this situation is:

$$h = 0.33 \frac{k}{d_o} \left(\frac{V_{max} \quad \rho \quad d_o}{\mu} \right)^{0.6} Pr^{0.33} \qquad \text{(A 10.5.2)}$$

This can most conveniently be expressed in the following form:

$$h, \text{ Btu/hr-ft}^2\text{-°F} = \left(\phi_1\right)\left(V_{max}^{0.6}\right)\left(d_o^{-0.4}\right) \qquad \text{(A 10.5.3)}$$

So that V_{max} might be expressed in ft/s units and d_o in inches, ϕ_1 must have the following form:

$$\phi_1 = \frac{(0.33)(12^{0.4})(k)(\rho^{0.6})(Pr^{0.33})(3600^{0.6})}{\mu^{0.6}} \left(\frac{in^{0.4}\ s^{0.6}\ Btu}{hr\text{-}ft^{2.6}\text{-°F}} \right) \qquad \text{(A 10.5.4)}$$

Values of thermal conductivity (k, Btu/hr-ft-°F), density (ρ, lb/ft^3) and viscosity (μ, lb/ft-hr) are evaluated at the arithmetic mean gas temperature. For the reference case considered, which has an average gas temperature of 1061°K (1450°F) at a pressure of 207.7 kPa (2.05 atm) ϕ_1 has a value of 1.335 in the units expressed in Equation A 10.5.4.

The pressure drop per row for flow over a staggered array of tubes is represented by the following equation:

$$\frac{\Delta p}{N_{row}} = \frac{4f\ \rho\ V_{max}^2}{2g \quad 144} \qquad \text{(A 10.5.5)}$$

where

$$f = \frac{0.507}{\left(\frac{V_{max}\ \rho\ d_o}{\mu}\right)^{0.15}} \qquad \text{(A 10.5.6)}$$

Equation A 10.5.5 can, therefore, be conveniently expressed as follows:

$$\frac{\Delta p}{N_{row}} = \phi_2 \cdot V_{max}^{1.85}\ d_o^{-0.15} \quad \text{(psi/row)} \qquad \text{(A 10.5.7)}$$

and so that V_{max} might be expressed in ft/s and d_o in in.

$$\phi_2 = \frac{(2)(0.507)(12^{0.15})}{(144)(3600^{0.15})(32.2)}\ \rho^{0.85}\ \mu^{0.15} \left(\frac{lb\ \ s^{1.85}}{in^{1.85}\ Pr^{1.85}}\right) \qquad \text{(A 10.5.8)}$$

For the reference case in question ϕ_2 takes on the value 5.946×10^{-6}, and the units are as shown in Equation A 10.5.8.

The required surface area for heat transfer per steam generator is given by Equation A 10.5.9:

$$A_s,\ ft^2 = \frac{Q}{(N_{SG})(MTD)(h)} \qquad \text{(A 10.5.9)}$$

Substituting Equation A 10.5.3 for h in Equation A 10.5.9, we obtain Equation A 10.5.10:

$$A_s,\ ft^2 = \frac{(Q)\ (V_{max}^{-0.6})\ (d_o^{0.4})}{(N_{SG})\ (MTD)\ (\phi_1)} \qquad \text{(A 10.5.10)}$$

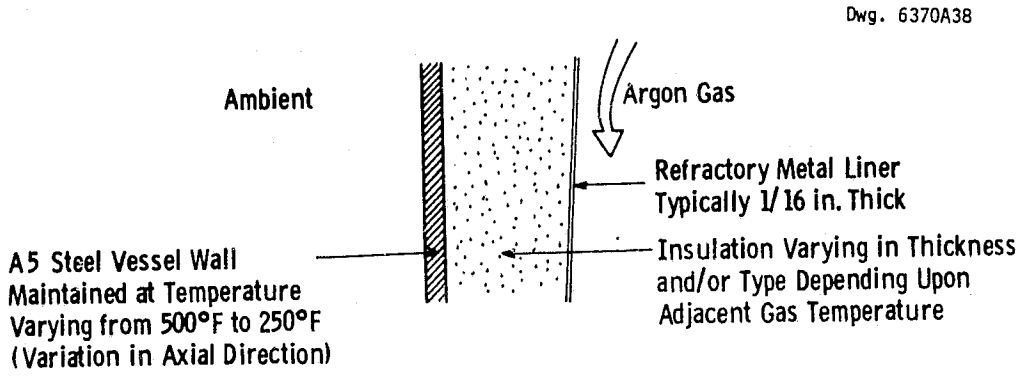

Figure A 10.5.2 - Containment Wall Arrangement.

A 10.5.2 Layout of Heat Transfer Surfaces and Temperature Approach Diagram

Due to the low exit gas temperature 423°K (302°F) it is necessary that the coolest water enter the steam generator at the level at which the gas is exhausted. It is advantageous that the water move upwards as it evaporates; indeed, it is essential that the water move in net upflow as it passes through the pseudocritical point. This requirement is discussed very fully in Appendix A 9.3. It is, therefore, required that the gas flow downward through the steam generator. The entire primary evaporator section can, therefore, be characterized as having gas flowing downward in crossflow over tube banks through which the water climbs in net upflow.

Likewise, the reheat section, which is located above the primary evaporator section, can be described as having gas flowing downward in crossflow over a tube bank through which the reheat steam flows in net upflow.

Figure A 10.5.3 illustrates the layout described above. Figure A 10.5.4 is the temperature approach diagram.

A 10.5.3 Method of Determining Sizes of Containment Vessel and Tube Banks from Heat Transfer and Pressure Drop Considerations

The method which is outlined below operates on the assumption that the resistance to heat transfer between the gas and the evaporating water is controlled by the heat transfer between the gas and the tube outside wall. An allowance is made for the contributions made by the tube wall and the inside tube wall to water resistances.

The method then takes the basic correlations for gas-side heat transfer and pressure drop and produces equations for the following parameters:

Outside Tube Surface Area,	A_s	(see Equations A 10.5.10 and A 10.5.31)
Flow Area,	$A_{f_{min}}$	(see Equations A 10.5.12 and A 10.5.32)
Vessel Diameter,	D	(see Equations A 10.5.17 and A 10.5.33)
Total Tube Length in One Tube Row,	L	(see Equations A 10.5.19 and A 10.5.34)
Number of Tube Rows,	N_{row}	(see Equations A 10.5.24 and A 10.5.35)
Overall Gas-Side Pressure Drop,	ΔP_g	(see Equations A 10.5.26 and A 10.5.36)
Height of Tube Banks	H	(see Equations A 10.5.30 and A 10.5.37)

The equation for outside tube surface area, for example, yields a total area for both primary steam and reheat combined. Later, this area is divided between the two sections on the basis of their relative load, heat transfer coefficient, and log mean temperature coefficient.

Firstly, an equation for a mean temperature difference between gas and water for the entire steam generator is required. Equation A 10.5.1, which follows, is a load-weighted average of the LMTD values pertaining to the part of the primary section which carries the first stream, the remainder of the primary section which carries the first and second stream, and the reheat section which carries the reheat stream.

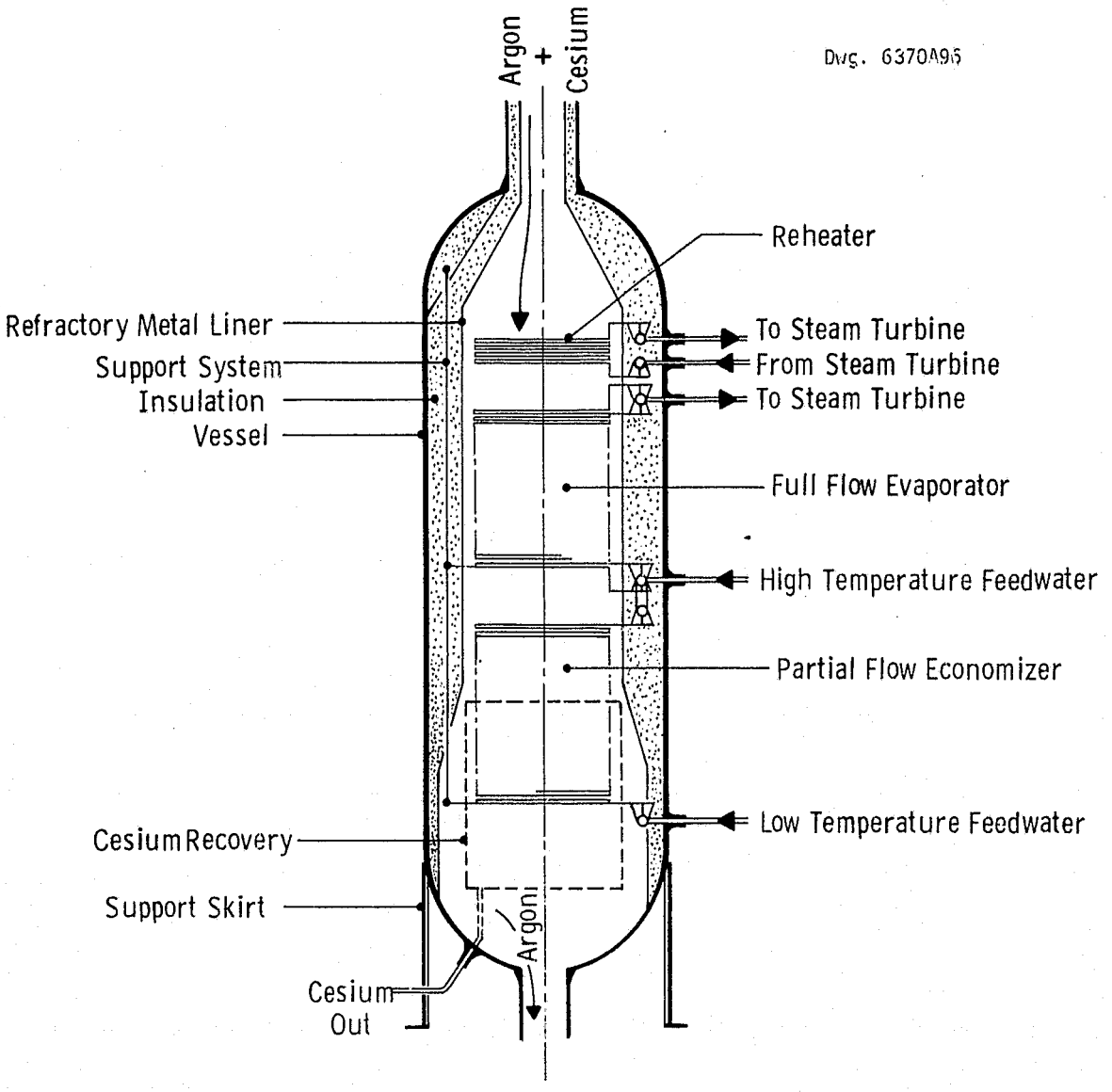

Fig. 10.5.3—Layout of heat recovery steam generator for closed-cycle MHD system

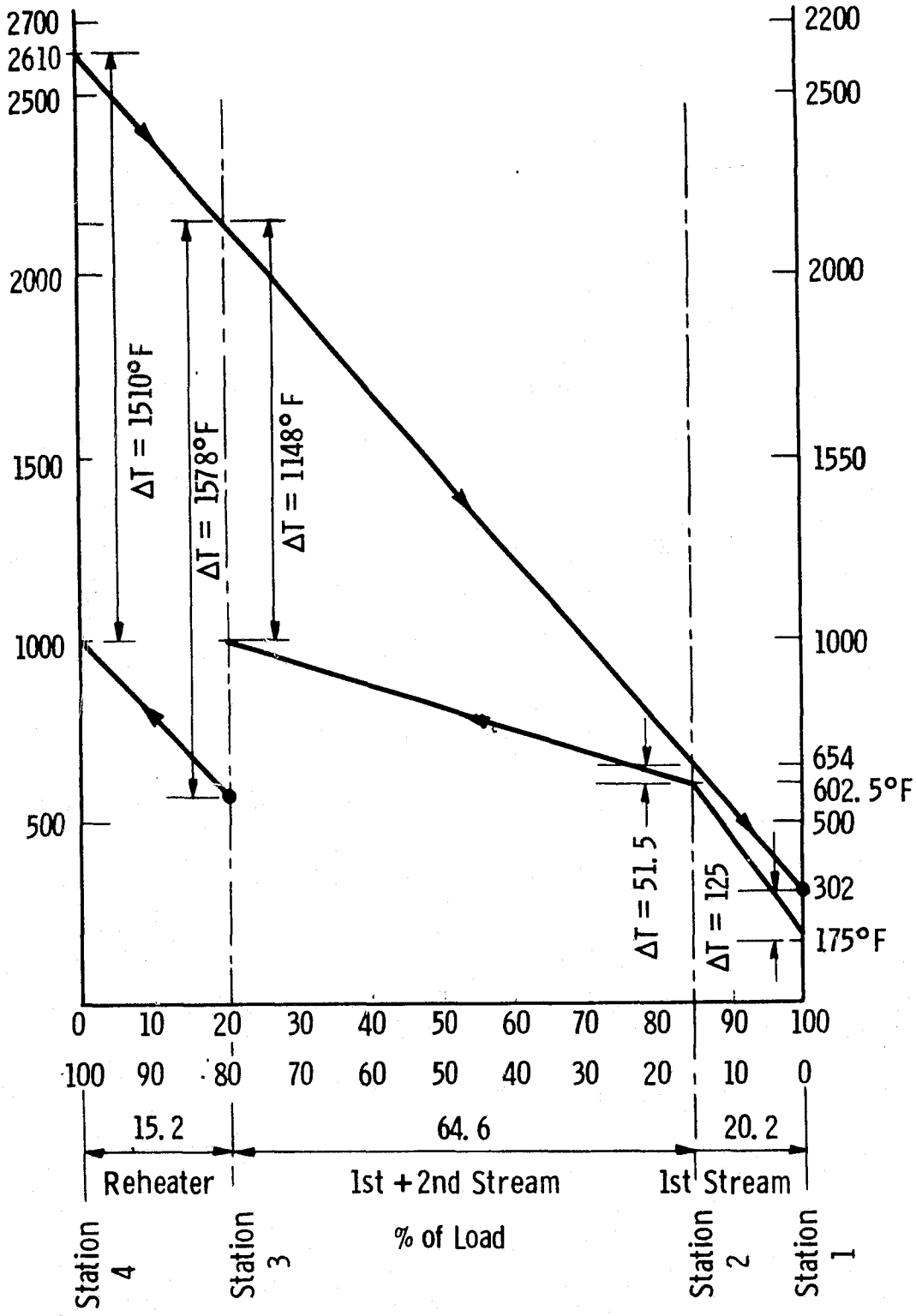

Fig. A 10.5.4—Temperature Approach Diagram

Equations A 10.5.11 and A 10.5.14, which follow, are fundamentally different ways of expressing the minimum area of flow per steam generator:

$$A_{f_{min}} = \eta \frac{\pi D^2}{4} \left(\frac{P_t - d_o}{P_t} \right) \qquad \text{(A 10.5.11)}$$

In Equation A 10.5.11, η is a factor which expresses the fraction of the available area within the shell diameter (D) which is utilized for the tube banks. The tube pitch (P_t) is in inches, as is d_o.

For a situation where the tube banks are housed in a refractory metal duct of square cross section, which itself is housed within a cylindrical pressure containment shell, η has a maximum value of $2/\pi$.

Consequently Equation A 10.5.11 can be restated as follows:

$$A_{f_{min}}, \text{ ft}^2 = \phi_3 D^2 \left(\frac{P_t - d_o}{P_t} \right) \qquad \text{(A 10.5.12)}$$

where

$$\phi_3 = \frac{\pi}{4} \times \frac{2}{\pi} = 0.5 \qquad \text{(A 10.5.13)}$$

The alternative way to express the minimum flow area is in terms of the mass flow rate of the gas, $\dot{m}_g$, and maximum velocity.

$$A_{f_{min}}, \text{ ft}^2 = \frac{\dot{m}_g}{(N_{SG})(V_{max})(\rho)(3600)} \qquad \text{(A 10.5.14)}$$

In Equation A 10.5.14, $\dot{m}_g$ is the total MHD duct gas mass flow rate in lb/hr; hence, the need for N_{SG} in the denominator to put the flow on a per module basis. The 3600 in the denominator is required because V_{max} is in units of ft/s.

Together, Equations A 10.5.12 and A 10.5.14 provide a means of expressing the inside shell diameter in terms of fundamental flow parameters.

$$\phi_3 \, D^2 \left(\frac{P_t - d_o}{P_t} \right) = \frac{\dot{m}_g}{(N_{SG})(V_{max})(\rho)(3600)} \qquad \text{(A 10.5.15)}$$

Letting

$$\phi_4, \frac{\text{lb s}}{\text{ft}^3\text{-hr}} = (\phi_3)(3600)(\rho) \qquad \text{(A 10.5.16)}$$

Equation A 10.5.15 can be conveniently rearranged as follows:

$$D = \left[\frac{m_g}{\phi_4} \left(\frac{P_t}{P_t - d_o} \right) \right]^{0.5} \left(N_{SG} \, V_{max} \right)^{-0.5} \qquad \text{(A 10.5.17)}$$

For the base case considered ϕ_4 has the value 100.8 s lb/ft^3-hr.

There exists yet another expression for the flow area which is fundamentally different from these presented heretofore and which when equated with Equation A 10.5.14 will yield an equation for the length of tube per tube row (L). This equation is:

$$A_f, \text{ ft}^2 = \frac{L \, (P_t - d_o)}{12} \qquad \text{(A 10.5.18)}$$

Equation A 10.5.18 is equivalent to saying that for every foot of tube length, L, there is a gap between tubes through which gas may flow, which is of width $(P_t - d_o)/12$ ft.

Equating A 10.5.18 with A 10.5.14 we obtain:

$$L = \left(\frac{\dot{m}_g}{(P - d_o)\ \phi_5\ N_{SG}\ V_{max}} \right) \qquad \text{(A 10.5.19)}$$

where

$$\phi_5 = \frac{(\rho)(3600)}{12} \ \frac{\text{lb-s}}{\text{hr-ft}^2\text{-in}} \qquad \text{(A 10.5.20)}$$

For the base case design ϕ_5 has to value 15.8 lb-s/hr-ft^2-in.

In order to formulate an equation for the number of tube rows required we evolve a second equation for the heat transfer surface area.

$$A_s = (\pi)\left(\frac{d_o}{12}\right)\ (L)\ (N_{row}) \qquad \text{(A 10.5.21)}$$

This is equated with a previous equation for A_s, namely Equation A 10.5.10. Hence:

$$\frac{(Q)(V_{max}^{-0.6})(d_o^{0.4})}{(N_{SG})\ (MTD)\ (\phi_1)} = (\ )\left(\frac{d_o}{12}\right)\ (L)\ (N_{row}) \qquad \text{(A 10.5.22)}$$

Now substituting Equation A 10.5.19 for L in Equation A 10.5.22 and expressing for N_{row} we obtain:

$$N_{row} = \frac{(12)(\phi_5)}{\pi\ \phi_1} \ \frac{Q\ (P_t - d_o)}{(LMTD)(\dot{m}_g)} \ (V_{max}^{0.4})(d_o^{-0.6}) \qquad \text{(A 10.5.23)}$$

$$N_{row} = \phi_6 \ \frac{(Q)\ (P/d_o - 1)}{(LMTD)(\dot{m}_g)} \ (V_{max}^{0.4})(d_o^{0.4}) \qquad \text{(A 10.5.24)}$$

In Equation A 10.5.24:

$$\phi_6 = \frac{12}{\pi}\frac{\phi_5}{\phi_1}\left(\frac{lb \quad s^{0.4} \ ^\circ F}{in^{0.4} \quad ft^{0.4} \quad Btu}\right) \qquad \text{(A 10.5.25)}$$

For the base case ϕ_6 has the value of 45.207 in the above units.

From Equation A 10.5.25 and A 10.5.7 we can obtain an equation for the overall pressure drop.

$$\Delta p = \phi_7 \left(\frac{Q\left(\frac{P_t}{d_o} - 1\right)}{(LMTD)(\dot{m}_g)}\right)(V_{max}^{2.25})\ (d_o^{0.25})\ lb/in^{0.2} \qquad \text{(A 10.5.26)}$$

In Equation A 10.5.26:

$$\phi_7 = \phi_2 = \phi_6\left(\frac{lb^2 \quad s^{2.25} \ ^\circ F}{Btu\ in^{2.25} \quad ft^{2.25}}\right) \qquad \text{(A 10.5.27)}$$

For the base case ϕ_7 has the value of 33.9 in the above units.

When the tubes are in an equilateral staggered array, the height of the tube bank is given by:

$$H = N_{rows}\frac{P_t}{12}\cos 30^\circ = N_{row}\left(\frac{0.867}{12}\right)P_t \qquad \text{(A 10.5.28)}$$

Substituting for N_{row} by Equation A 10.5.24 we obtain:

$$H = \frac{0.867}{12}\ \phi_6\ P_t\left(\frac{Q\left(\frac{P_t}{d_o} - 1\right)}{(LMTD)(\dot{m}_g)}\right)(V_{max}^{0.4})\ (d_o^{0.4}) \qquad \text{(A 10.5.29)}$$

TABLE A 10.5.2—PARAMETER EVALUATION

Parameter Equation	Q Btu/hr	LMTD, °F	$\dot{m}_g$ lb/hr	P_t/d_o	Equation V is in ft/s d_o is in inches P_t is in inches	d_o, in	$d_o^{0.4}$, in$^{0.4}$	$d_o^{0.25}$, in$^{0.25}$	V_{max}, ft/s	$V_{max}^{2.25}$, (ft/s)$^{2.25}$	$V_{max}^{0.6}$, (ft/s)$^{0.6}$	$V_{max}^{0.5}$, (ft/s)$^{0.5}$	$V_{max}^{0.4}$, (ft/s)$^{0.4}$	N_{SG}	$N_{SG}^{0.5}$	Parameter
	Fixed Parameter					Parameter Over Which We Excersise Choice										
$\Delta P, psi = (33.9)\ \frac{(Q)\left(\frac{P_t}{d_o}-1\right)}{(LMTD)\ (\dot{m})}\left(V_{max}^{2.25}\right)\left(d_o^{0.25}\right)$	4.79×10^9	446.1	1.667×10^7	2	$1.73\times10^{-4}\left(V_{max}^{2.25}\right)\left(d_o^{0.25}\right)$	2	1.32	1.189	40 50 60	4024 6648 10019						$\Delta P = 0.828$ psi $\Delta P = 1.367$ psi ⇐ Select 50 ft/s $\Delta P = 2.061$ psi Sines $\frac{\Delta P}{P} = 5\%$
$A_s, ft^2 = \frac{Q}{(1.335)\ (LMTD)}\left(V_{max}^{-0.6}\right)\left(d_o^{0.4}\right)\left(N_{SG}^{-1}\right)$					$9.462\times10^6\left(V_{max}^{-0.6}\right)\left(d_o^{0.4}\right)\left(N_{SG}^{-1}\right)$				50		10.46	7.07	4.78	2 4 6	1.414 2 2.45	$A_S = 3.426\times10^5$ ft^2/SG $A_S = 1.713\times10^5$ ft^2/SG $A_S = 1.142\times10^5$ ft^2/SG
$A_{fmin}, ft^2 = \left(\frac{\dot{m}_g}{201.6}\right)\left(V_{max}^{-1}\right)\left(N_{SG}^{-1}\right)$					$8.269\times10^4\left(V_{max}^{-1}\right)\left(N_{SG}^{-1}\right)$									2 4 6	1.414 2 2.45	$A_{fmin} = 827$ ft^2/SG $A_{fmin} = 413$ ft^2/SG $A_{fmin} = 276$ ft^2/SG
$D, ft = \left(\frac{\dot{m}_g}{100.8}\left(\frac{1}{\frac{d_o}{P_t}-1}\right)\right)^{-0.5}\left(V_{max}^{-0.5}\right)\left(N_{SG}^{-0.5}\right)$					$575\left(V_{max}^{-0.5}\right)\left(N_{SG}^{-0.5}\right)$									2 4 6	1.414 2 2.45	$D = 57.5$ ft $D = 40.68$ ft $D = 33.31$ ft ⇐ Use 6 SG's
$L, ft = \frac{\dot{m}_g}{15.8\ (P_t-d_o)}\left(V_{max}^{-1}\right)\left(N_{SG}^{-1}\right)$					$5.275\times10^5\left(V_{max}^{-1}\right)\left(N_{SG}^{-1}\right)$									2 4 6	1.414 2 2.45	$L = 5275$ ft/row $L = 2637$ ft/row $L = 1758$ ft/row
$N_{row} = (45.207)\ \frac{(Q)\ \frac{P_t}{d_o}-1}{(LMTD)\ (\dot{m}_g)}\ V_{max}^{0.4}\ d_o^{0.4}$					$29.12\left(V_{max}^{0.4}\right)\left(d_o^{0.4}\right)$											$N_{row} = 184$ rows
$H, ft = (2.45)\ \frac{(Q)\ (P_t)\left(\frac{P_t}{d_o}-1\right)}{(LMTD)\ (\dot{m}_g)}\left(V_{max}^{0.4}\right)\left(d_o^{0.4}\right)$					$2.104\left(V_{max}^{0.4}\right)\left(d_o^{0.4}\right)P_t$									$P_t = 4$ in		$H = 53.1$ ft

$$H = \phi_8 \left(\frac{P_t}{d_o}\right) \frac{(\frac{P_t}{d_o} - 1)(Q)}{(LMTD)(\dot{m}_g)} (V_{max}^{0.4})(d_o^{0.4}) \qquad \text{(A 10.5.30)}$$

In Equation A 10.5.30 ϕ_8 has the value 2.45 for the base case and the units are:

$$\frac{\text{lb s}^{0.4} \text{ °F ft}^{0.6}}{\text{in}^{1.4} \text{ Btu}} .$$

This value of H does not include any allowance for spacing between the various tube bank sections. Obviously it does not account for the height of the vessel heads, either. It is, therefore, a basis from which the overall vessel height can be determined.

Table A 10.5.2, which follows, shows how the key parameters were evaluated from the equations derived in this section.

A 10.5.4 Determination of Numbers of Tube Rows in Different Sections

The total number of tube rows in each of six steam generators was evaluated in Table A 10.5.2, i.e., $N_{row} = 184$. We must decide how this number should be distributed between the first evaporating section (carrying only stream 1), the second evaporating section (carrying stream 1 plus stream 2), and the reheat section.

Recall that the value of N_{row} was obtained using weighted mean values for the temperature difference between gas and tube and for the heat transfer coefficient. The relative actual value of the mean temperature difference and heat transfer coefficient for the three sections, along with the relative thermal loads, determine the fraction of the 184 tubes which is used in each section.

Let the first and second evaporator sections and the reheater be designated Section 1-2, Section 2-3, and Section 3-4, respectively. This is in line with the station points shown on Figure A 10.5.4.

Table A 10.5.3 - Comparison of Boiler Sections

	1-2 (1st Evaporator)	2-3 (2nd Evaporator)	3-4 (Reheat)
Load Fraction	0.152	0.646	0.202
Load Fraction Normalized to Section 2-3	$\frac{0.152}{0.646} = 0.235$	$\frac{0.646}{0.646} = 1$	$\frac{0.202}{0.646} = 0.313$
Average HTC over Section Btu/hr-ft^2-°F	11.9	14.0	15.4
HTC Normalized to Section 2-3	$\frac{11.9}{14.0} = 0.85$	$\frac{14.0}{14.0} = 1$	$\frac{15.4}{14.0} = 1.1$
LMTD °F	83.7	353.2	1322.4
LMTD Normalized to Section 2.3	$\frac{83.7}{353.2} = 0.237$	$\frac{353.2}{353.2} = 1$	$\frac{1322.4}{353.2} = 3.744$
$\left(\frac{\text{Load Fraction}}{\text{HTC x LMTD}}\right)$ Normalized to Section 2.3	$\frac{0.235}{0.85 \times 0.237} = 1.167$	$\frac{1}{1 \times 1}$	$\frac{0.313}{1.1 \times 3.744} = 0.076$

In short:

$$N_{row} = (\phi) \left[\text{Load Fraction}\right] \quad \left[\frac{1}{\text{HTC}}\right] \quad \left[\frac{1}{\text{LMTD}}\right] \qquad \text{(A 10.5.31)}$$

The second evaporator section carrying streams 1 and 2 (Section 2-3) is the largest section. Therefore, load fraction, heat transfer coefficient, and log mean temperature difference values for the other sections were normalized to Section 2-3. Table A 10.5.3 shows the ratio of number of tubes in a section to the number of tubes in Section 2-3.

Resulting from Table A 10.5.2 we may state:

$$N_{row} = 184 = (1.167 + 1 + 0.076) \quad (N_{row\ 2-3}), \qquad \text{(A 10.5.32)}$$

Therefore,

$$N_{row\ 2-3} = \frac{184}{2.243} = 82.1 \text{ say } 82 \qquad \text{(A 10.5.33)}$$

Also from Table A 10.5.3 we know

$$N_{row\ 1-2} = (1.167) \quad N_{row\ 2-3} = 1.167(82) = 95.7 \sim 96 \qquad \text{(A 10.5.34)}$$

Also,

$$N_{row\ 3-4} = (0.076) \quad N_{row\ 2-3} = (0.076)(82) = 6.23 \sim 8 \qquad \text{(A 10.5.35)}$$

Eight tubes are required for the reheater because this is the lowest integer number divisible by 2 above 6.23. Divisibility by 2 ensures that the inlet and exit headers are on the same side of the tube bank.

Table A 10.5.4 - Costing of Tube Banks

Section	Estimated Maximum Outside Tube Wall Temperature, °F	Material Selected	Stress Level, psi	Wall Thickness in	Cost/ft, $	Tube Length in Section, ft	Total Cost of Fabrication and Erection inc'l. Headers, $
1-2 Evaporator Carrying Stream 1	700	SA 213 T22	15000	0.25	4.05	96 x 1758 = 1.687×10^5	1.894×10^6
2-3 Evaporators Carrying Streams 1 & 2	1000 (50% of Bank) 1150 (50% of Bank)	304 SS 304 SS	13000 8000	0.25 0.375	10.50 15.80 } 13.15	82 x 1758 = 1.441×10^5	4.003×10^6
3-4 Reheater	1250	HA 188 or HS 25	13000	0.25	30.00	8 x 1758 = 0.1406×10^5	0.796×10^6

Note that the total number of tube rows has been increased to 186 because of the above considerations.

A 10.5.5 Costing Procedures

Firstly we shall deal with the cost of the tube banks. We shall later see that this is the dominant cost item, accounting for nearly 70% of the total cost. From exhaustive examination of the cost trends of several boiler tube banks, covering a wide range of size and differing materials, the following empirical cost equation emerged.

$$\text{Fabricated and Erected Tube Bank Cost Including Headers} = \text{Tube Length}\left[\overbrace{1.6(\text{Material Cost/ft}) + 13.2\,(0.273(\text{Material Cost/ft})^{0.3}\left(\frac{HTC}{50}\right)^{0.7}}^{\text{Header Contribution}}\right]$$

$$\text{Tube Nest Contribution}$$

(A 10.5.36)

In Equation A 10.5.36 HTC is the average heat transfer coefficient in units of Btu/hr-ft^2-°F pertaining to the tube bank in question. The tube length must be stated in feet.

Table A 10.5.4 illustrates how the tube bank costs are derived.

The selected pressure vessel material is carbon steel and since the internal insulation will limit its service temperature to 533°K (500°F), an allowable stress level of 94.46 MPa (13,700 psi) is appropriate. Strict adherence to Section 1 of the ASME code for fixed pressure vessels would require the shell to be of 1.27 cm (0.5 in) thickness and the heads to be 0.635 cm (0.25 in) thick when hemispherical and 0.952 cm (0.375 in)

Table A 10.5.5 - The Cost of Each One of Six Steam Generators Required for the Closed-Cycle MHD System Reference Case

Major Item (Subitem)	Subtotal $x10^{-6}$, $	Total $x10^{-6}$, $
Tube Banks and Headers		
(Section 1-2 of Evaporator)	1.894	
(Section 2-3 of Evaporator)	4.003	
(Section 3-4 Reheater)	0.796	
	6.693	6.693
Pressure Vessel with Ports and Manways, etc.		
(Vessel)	0.5394	
(Support Skirt)	0.1000	
(Internal Structure for Tube Bank Support)	0.3000	
	0.9394	0.9394
*Liquid Sodium Collection System (Niobium and Vanadium Drip Trays, Pipes and Manifolds)	1.77	1.77
*Trace Heating of Sodium Collection System	0.1	0.1
*Internal Monitoring Instrumentation (Thermocouples and Other Sensors)	0.1	0.1
Internal Vessel Insulation		
(Insulation)	0.24	
(Refractory Metal Liner)	0.26	
	0.5	0.5

Grand Total less Contingency	$10,102,000
15% Contingency	1,515,000
Grand Total for One SG	11,617,000
Grand Total for Six SG's	$69,702,000

thick when semielliptical. Since, however, the tube banks are to be supported from the upper head and the vessel body, a cylindrical shell of 1.587 cm (0.625 in) thickness and hemispherical vessel heads of 1.27 cm (0.5 in) thickness were employed.

Other important dimensions used in determining the weight, and hence the cost, of the pressure vessel were an inside diameter of 10.67 m (35 ft) and a cylindrical shell length between heads of 21.34 m (70 ft).

Using these dimensions, the weight of the carbon steel vessel is 122.3 Mg (134.85 tons). The following equation is then used to estimate the cost of such a vessel.

$$\text{Fabricated Cost of Pressure Vessel} = \Big[\text{Weight of Shell, lb}\Big]\Big[\Big(0.8,\ \$/\text{lb(Material)}\Big) + \Big(1.2,\ \$/\text{lb(Fabrication)}\Big)\Big] \qquad \text{(A 10.5.37)}$$

Using Equation A 10.5.37 we arrive at a cost of $539,400 per vessel. An additional cost of $100,000 per vessel is applied to account for the support skirt, and the cost of internal structures to support the tube banks is estimated to be $300,000 per vessel.

Table A 10.5.5 lists the major cost items for the steam generator in question. Items marked with an asterisk (*) have not been the subject of detailed cost analysis. The stated costs for these items represent our best estimates in the absence of detailed design work. It should be noted that the total cost of these items is thought to be less than 20% of the overall cost of the steam generator.

Dwg. 6352A16

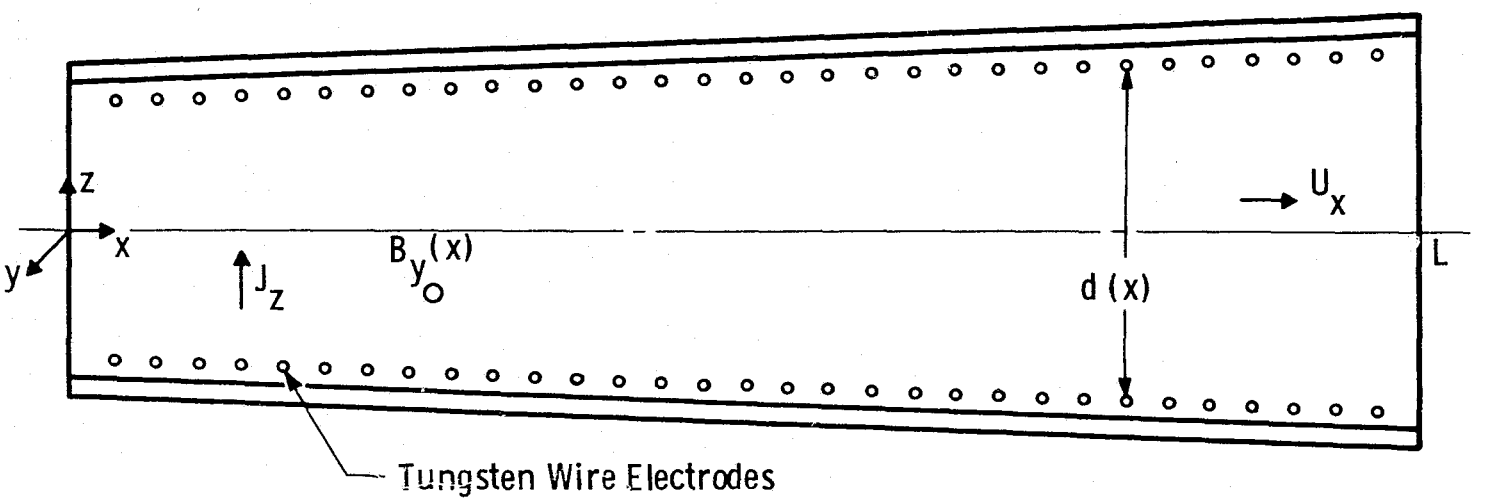

Fig. A 10.6.1—Schematic of MHD duct with wire electrodes. Distance, d (x), between electrodes is a function of x and magnetic flux density, $B_y(x)$, may also vary with x. J_z is current density and u_x is gas velocity

Appendix A 10.6

DESIGN OF CLOSED-CYCLE MHD GENERATOR AND SYSTEM

A 10.6.1 Introduction

Design equations for open-cycle MHD generator ducts and a computer program to solve these equations were developed by Westinghouse (Reference 10.38) in the early 1960s. These equations, however, and the computer program are not applicable to the closed-cycle analysis. Simple alterations of the open-cycle equations were not possible because the calculation of the electrical conductivity, enthalpy, and entropy are different since a noble gas is used as the working fluid. In addition, equations must be altered to include nonequilibrium ionization in which the electron temperature is higher than the temperature of the ions and neutral species. Consequently, a set of closed-cycle MHD duct design equations and a computer program to solve these equations have been developed by the Westinghouse Research Laboratories.

The purpose of this report is to describe the MHD duct design equations, the analysis of the closed-loop system with regard to temperature, pressure, velocity, entropy, enthalpy, at the various stations of the loop, and power output and efficiency of the overall cycle. The new computer program used to solve these equations and the use of the program are described. Hence, this report will serve as a reference for future designing of closed-loop MHD generator ducts and systems.

A 10.6.2 MHD Duct Physics

A 10.6.2.1 Duct Description

Figure A 10.6.1 is a sketch of the MHD duct. The wire electrodes are insulated from one another so that negligible Hall current

flows. Each electrode pair is assumed to be connected to an individual load electrically insulated from that of the other electrode pairs. The cross section of the duct is assumed to be square. For one-dimensional analysis, the gas properties, magnetic field, and current density are assumed to be uniform in the y and z directions but can vary in the x direction. End effects are neglected. The magnetic flux density, B, is in the y direction; and the gas velocity, u, is in the x direction.

The closed-cycle MHD systems analyzed can have working fluids of either helium or argon seeded with cesium. Other combinations of noble gases seeded with other alkali metals, however, could be used in this closed-cycle MHD duct analysis.

A 10.6.2.2 Basic MHD Equations

The basic quasi one-dimensional MHD equations are general for either the open-cycle or closed-cycle ducts. Given in differential steady-state form and including a friction factor, f, and a heat loss parameter, λ_2, the equations for momentum, energy, and mass conservation are:

$$\rho u \frac{du}{dx} + \frac{dp}{dx} = -jB \{1 + f/[\xi(1 - K)]\} \qquad \text{(A 10.6.1)}$$

$$\rho u \frac{d}{dx} (h + u^2/2) = -jBuK(1 + \lambda_2) \qquad \text{(A 10.6.2)}$$

$$\rho u A = \dot{m} \qquad \text{(A 10.6.3)}$$

where

$$\xi = 2\sigma r_h B^2/\rho u \qquad \text{(A 10.6.4)}$$

$$j = \sigma u B(1 - K) \qquad \text{(A 10.6.5)}$$

K is generator coefficient, r_h is the hydraulic radius of the generator duct, j is current density, ρ is gas density, A is the cross-sectional area of the duct, $\dot{m}$ is mass flow, p is gas pressure, h is enthalpy, and σ is electrical conductivity.

In the case of gas velocity varying through the duct, it is assumed that this variation is related to the gas pressure by

$$\frac{d}{dx}\left(\frac{u^2}{2}\right) = \frac{c}{\rho}\frac{dp}{dx} \qquad \text{(A 10.6.6)}$$

where c is a numerical constant referred to as the velocity coefficient. For example c = 0 for constant velocity design. The change in enthalpy of a noble gas is

$$dh = C_p dT \qquad \text{(A 10.6.7)}$$

where C_p is specific heat for constant pressure.

The calculation of electrical conductivity for thermal ionization is rather straightforward, but for nonequilibrium ionization, the calculation is more complex and is described in the following section.

A 10.6.2.3 Nonequilbrium Ionization

Electrical conductivity, σ, is related to the electron density, n_e, and the mobility, μ, of the gas by a general form of

$$\sigma = n_e e \mu \qquad \text{(A 10.6.8)}$$

Frost (Reference 10.39) has calculated this conductivity for alkali-seeded gases assuming local thermodynamic equilibrium. Both n_e and μ are a function of electron temperature which equals the gas temperature for thermal ionization. The electron density is calculated from

Saha (Reference 10.39) and the electron mobility is calculated from the momentum transfer collision cross sections of the electron-neutral and of the electron-ion interactions [see Frost (Reference 10.39)].

Various investigators (References 10.40 to 10.42) have shown that for MHD generators using alkali-seeded noble gases as working fluids, nonequilibrium ionization occurs, indicating that joule heating of the gas by the current causes the electron temperature to be higher than the gas temperature. To compute the electrical conductivity for this effect, the following equations are used. For nonequilibrium ionization MHD generators, the effective electrical conductivity rather than the scalar conductivity has to be used in the basic MHD equations. According to Zampaglione (Reference 10.5) the effective conductivity is:

$$\sigma_{eff} = \frac{\sigma[(\beta - \bar{\xi})^2 + \beta^2\xi^{-2}]}{\beta[\beta + \bar{\xi}(\beta^2 - 1)} \qquad \text{(A 10.6.9)}$$

where β is the Hall parameter and $\bar{\xi}$ is a plasma turbulence factor ranging from 0.5 to 1. The Hall parameter is:

$$\beta = \mu B \qquad \text{(A 10.6.10)}$$

As previously mentioned, the electron temperature, T_e, is needed in order to calculate σ. This is computed by the energy equation given by Brederlow and Witte (Reference 10.12) as:

$$\frac{j^2}{\sigma_{eff}} = \langle \dot{E}_{el} \rangle + \langle \dot{E}_r \rangle \qquad \text{(A 10.6.11)}$$

The left term is the joule heating which is equal to the elastic collision term $\langle \dot{E}_{el} \rangle$ plus the radiation term $\langle \dot{E}_r \rangle$. The elastic term is:

$$\langle \dot{E}_{el} \rangle = 3\delta k(T_e - T_g)\, n_e \sum_h \frac{m_e}{m_h} \nu_{eh} \qquad \text{(A 10.6.12)}$$

where δ is a loss factor, ν_{eh} is electron heavy particle collision frequency, m_e is electron mass, m_h is heavy particle mass, and k is Boltzmann constant. The radiation term $\langle \dot{E}_r \rangle$ is included in the loss factor. For example, if the joule heat energy is divided equally between the elastic collision energy and the radiation energy, δ is 2. Volkov (Reference 10.44) shows that for nonequilibrium ionization in helium-cesium and argon-cesium gases, δ is 1.2. When the current equation is substituted in Equation A 10.6.11, and Equations A 10.6.11 and A 10.6.12 are combined, the result is:

$$\sigma_{eff} u^2 \beta^2 (1 - K)^2 = 3\delta k n_e (T_e - T_g)\, m_e \sum_h \frac{\nu_{eh}}{m_h} \qquad \text{(A 10.6.13)}$$

Equation A 10.6.8 shows that the scalar conductivity is a function of the electron density and electron mobility. The electron mobility is:

$$\mu = \frac{e}{m_e \nu_2} \qquad \text{(A 10.6.14)}$$

where ν_2 is the collision frequency of electrons and neutrals and of the electrons and ions averaged over the electron energy distribution. This collision frequency is averaged differently from that of ν_{eh} as will be explained later on. To calculate n_e, Saha's equation is modified because $T_e > T_g$, and the effective ionization potential of the seed is lowered by the Debye cloud. The modified Saha's equation for n_e is:

$$\frac{[n_e]^2}{N_s^o} = K_1 = \frac{[n_e]^2}{\frac{F}{1+F}\left(\frac{p}{kT_g} - \frac{T_e}{T_g} n_e\right) - n_e} \qquad \text{(A 10.6.15)}$$

hence,

$$n_e = (K_1\bar{C})^{1/2}\left[\left(\frac{K_1\bar{\beta}^2}{4\bar{C}} + 1\right)^{1/2} - \left(\frac{K_1\bar{\beta}^2}{4\bar{C}}\right)^{1/2}\right] \qquad \text{(A 10.6.16)}$$

where

$$\bar{\beta} = \left(1 + \frac{T_e F}{T_g(1 + F)}\right) \qquad \text{(A 10.6.17)}$$

$$\bar{C} = \frac{Fp}{(1 + F)\ kT_g} \qquad \text{(A 10.6.18)}$$

$$K_1 = \frac{2Z_s^+}{Z_s^o}\frac{(2\pi m_e kT_e)^{3/2}}{h'^3}\exp[-e(V_o - \gamma^1)/kT_e] \qquad \text{(A 10.6.19)}$$

In these equations, F is mole fraction of seed, p is total gas pressure, N_s^o is the seed neutral density, Z_s^+ is the electronic partition function of the seed ion, Z_s^o is that of the seed neutrals, h' is Plank's constant, V_o is the ionization potential, and γ^1 is the lowering of the ionization potential by the Debye cloud. This is calculated from the following equations.

$$\gamma^1 = \frac{Z\ e^2}{4\pi\varepsilon_o\rho_d} \qquad \text{(energy)} \qquad \text{(A 10.6.20)}$$

For electrons and single-ionized species, the Debye radius, ρ_d is:

$$\rho_d = \sqrt{\frac{\varepsilon_o kT_e}{2e^2 n_e}}\ . \qquad \text{(A 10.6.21)}$$

Z is charge of the atom seen by the valence electron (Z = 1 for atoms, 2 for + ions, 3 for ++ ions, etc.) and ε_o is the permittivity of free space.

The collision frequencies ν_{eh} and ν_2 were obtained from momentum transfer cross section data for electrons scattered by neutrals in helium (Reference 10.45), argon (Reference 10.46), and cesium (Reference 10.48). Cross sections for electrons scattered by ions were also included. For the collision term in Equation A 10.6.13, each collision frequency is computed from the averaged cross section for that species. For a buffer gas and seed mixture, therefore, the $\Sigma\, \nu_{eh}/m_h$ is:

$$\nu_1^1 = \sum \nu_{eh}/m_h = \frac{4}{3}\left[\frac{8kT_e}{\pi m_e}\right]^{1/2}\left\{\frac{N_B}{m_B}\hat{Q}_{e-B} + \frac{N_s^o}{m_s}\hat{Q}_{e-s} + \frac{N_s^+}{m_s}\hat{Q}_{e-ion}\right\} \qquad \text{(A 10.6.22)}$$

where $\hat{Q}$ is averaged cross sections, the indices B, S, and ion indicate buffer gas, seed, and ions; and o and + indicate the neutrals and ions.

$$\hat{Q}_{e-ion} = \frac{\pi}{2}\left[\frac{e^2}{4\pi\varepsilon_o kT_e}\right]\ln\Lambda \qquad \text{(A 10.6.23)}$$

where

$$\Lambda = \frac{3}{2(\pi n_e)^{1/2}}\left(\frac{4\pi\varepsilon_o kT_e}{e^2}\right)^{3/2} \qquad \text{(A 10.6.24)}$$

Devoto (Reference 10.48) gives $Q_{e-\beta}$ as a function of electron temperature for helium and argon. Q_{e-s} for cesium was averaged over the electron density from cross section versus electron energy data given by Nighan (Reference 10.47).

Since the electron mobility depends as the reciprocal of the total collision frequency, it is not possible to combine separately averaged collision frequencies as in Equation A 10.6.22 for ν_1. The velocity-dependent total electron momentum transfer collision frequency must be obtained by adding up the contributions due to electron collisions with each species as a function of velocity,

$$\nu_T(v) = v[N_e Q_{e-B}(v) + N_s^{o} Q_{e-s}(v) + N_s^{+} Q_{e-ion}(v)] \qquad \text{(A 10.6.25)}$$

where v is the relative velocity between the electron and the heavy particle. This must then be averaged over the Maxwelliam electron velocity distribution F (v) by the integral:

$$\frac{1}{\nu_2} = \frac{4\pi}{3} \int_0^{\infty} F(v) \frac{d}{dv} \left(\frac{v^3}{\nu_T} \right) dv \qquad \text{(A 10.6.26)}$$

in order to evaluate the collision frequency average needed for mobility or conductivity, ν_2.

The unknowns are T_e, N_e, β, μ, σ, σ_{eff}, ν_1, ν_2; and there are eight independent equations, so there are enough equations to solve for the variables for a given set of gas conditions. Since these equations are transcendental or nonlinear, a digital computer must be employed to solve for the different variables.

A numerical integration of Equation A 10.6.26 using the appropriate cross-section data was made to evaluate ν_2 for helium and argon plus 0.2% cesium at various degrees of ionization, α.

$$\alpha = \frac{N_e}{(N_B + N_{cs})} \qquad \text{(A 10.6.27)}$$

where N_B is the density of helium or argon. For helium + 0.2% cesium:

$$\nu_2 = [3.10 \times (8085\ \alpha - 0.2268)^{1/1.4}]\ 10^{-14}\ N_{He} \quad \text{(A 10.6.28)}$$

if $8085\ \alpha - 0.2264 > 0$.

$$\nu_2 = (3.10)(10^{-14})\ N_{He}$$

if $(8085\ \alpha - 0.2264) < 0$.

For argon + 0.2% cesium:

$$\nu_2 = [0.533 + 0.641 \times (10^4\ \alpha)^{0.72}] \times 10^{-14}\ N_{Ar} \quad \text{(A 10.6.29)}$$

Here N_{He} and N_{Ar} are in units of m^{-3}. Equations A 10.6.28 and A 10.6.29 are sufficiently accurate for 101.3 to 1013.2 kPa (1 to 10 atm) of buffer gas and seeding of 0.15 to 0.25% cesium. Outside these pressures and seeding percentages, the accuracy is moderately reduced.

A 10.6.2.4 Electrode Voltage Drop

Significant electrode voltage drop has been measured by Zauderer and Tate (Reference 10.49) and others (Reference 10.40) in their nonequilibrium MHD shock-tube experiments. This voltage drop is caused (1) by anode and cathode sheaths and (2) by the cool boundary layer of gas near the electrode surfaces. Zauderer and Tate (Reference 10.49) have measured voltage losses on the order of 150 V in the presence of a magnetic field of 1.7 T and 80 V with a field of 1.2 T. For our analysis the electrode voltage drop is assumed to be independent of generator loading and magnetic field. This loss is important in small generators but can become insignificant for large generators because the Faraday voltage is at least an order of magnitude greater than the electrode loss. Subsequently, the electrode voltage drop can be included in the generator coefficient, K.

The generator coefficient with the electrode voltage drop, E_{el}, can be expressed in terms of the original coefficient by:

$$K' = K + \delta K \qquad \text{(A 10.6.30)}$$

where

$$\delta K = \frac{E_{el}}{uBd} \qquad \text{(A 10.6.31)}$$

and d is the duct height or distance between the opposite electrodes. Using the modified coefficient, K', the momentum and current equations for the duct are changed, but the energy equation remains the same. These equations are:

$$\text{Momentum } \rho u \frac{du}{dx} + \frac{dp}{dx} = -jB\left[1 + \frac{1}{\xi(1 - K')}\right] \qquad \text{(A 10.6.32)}$$

$$\text{Energy } \quad \rho u \frac{d}{dx}\left[h + \frac{u^2}{2}\right] = -jBuK(1 + \lambda_2) \qquad \text{(A 10.6.33)}$$

$$\text{Current } \quad j = \sigma uB(1 - K') \qquad \text{(A 10.6.34)}$$

Since the current equation is changed, the nonequilibrium ionization joule heating term is altered. Equation A 10.6.31, therefore, becomes:

$$\sigma_{eff} u^2 B^2 (1 - K')^2 = 3\delta k n_e (T_e - T_g) m_e \sum_h \frac{\nu_{eh}}{m_h} \qquad \text{(A 10.6.35)}$$

A 10.6.2.5 Limitation in Nonequilibrium Ionization MHD Generators

Current cutoff has been observed in MHD generators with nonequilibrium ionization by Zauderer, Tate, and Marston (Reference 10.13)

when the interaction parameter, S, becomes large. The interaction parameter is a measure of the ratio of the electrical to the kinetic gas energies of the duct and is given by:

$$S = \frac{jBL}{\rho u^2} \qquad \text{(A 10.6.36)}$$

where L is length of the duct. Zauderer, Tate, and Marston have observed from shock-tube MHD experiments that when flush electrodes are used, current cutoff occurred for S = 0.45, but not when pin electrodes are used. This higher current cutoff threshold is due to the fact that pin electrodes are less sensitive to the shock wave boundary layer interactions.

In designing an MHD duct, one of the constraints is to choose the velocity, gas density, current density, magnetic field, and length of duct so that S does not exceed 0.5 or whatever numerical value is considered appropriate.

Another limitation is the Hall parameter which must not become too large. Equation A 10.6.9 shows that the effective conductivity is related to the scalar conductivity by the Hall parameter. For very large β, $\sigma_{eff}/\sigma = \frac{1}{\beta\bar{\xi}}$, where $\bar{\xi}$ ranges from 0.5 to 1.0. Figure A 10.6.2 is a plot of σ_{eff}/σ and β_{eff} as a function of β for $\bar{\xi} = 0.5$ and $\bar{\xi} = 1.0$. Note that for $\beta = 8$, σ_{eff}/σ is 0.2. Consequently, the power density is drastically reduced. Since the electron mobility increases downstream of the duct because of the decrease of gas density, the magnet must be designed so that the magnetic field decreases accordingly with the downstream distance of the duct so that β does not become too large downstream. If β becomes too high, the Hall voltage will be very high and insulation between electrodes may become a serious problem.

A 10.6.2.6 Thermal Ionization

For thermal ionization the electron temperature is the same as the gas temperature. We simply set $T_e = T_g$ and calculate n_e, μ, and σ as

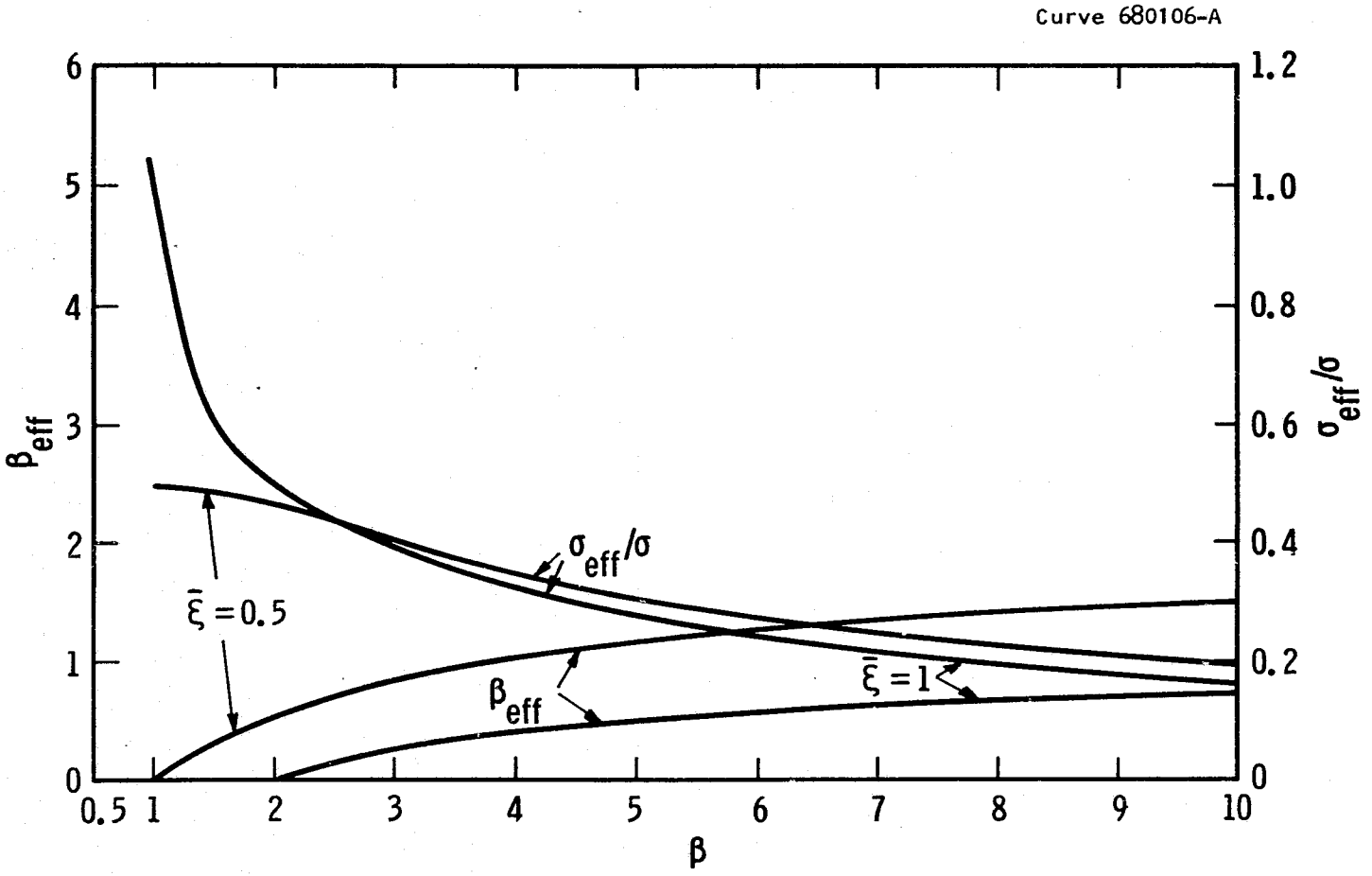

Fig. A 10.6.2—Effective Hall parameter, β_{eff}, and ratio of effective to scalar electrical conductivities, σ_{eff}/σ as a function of Hall parameter, β, for plasma turbulence factors, $\bar{\xi}$, of 0.5 and 1.0

in the nonequilibrium case. The effective conductivity σ_{eff} is here the same as σ. This is equivalent to setting $\vec{\xi} = 0$ in Equation A 10.6.9. We also neglect the electrode voltage drop in the thermal ionization case.

A 10.6.3 Closed-Cycle MHD

A 10.6.3.1 System Description

The closed-cycle MHD system configuration can be separated into three subsystems. These three subsystems are the fossil fuel/combustion gas open loop, the MHD closed loop, and the bottoming steam plant. The system is depicted schematically in Figure A 10.6.3. For our study, only the MHD loop is considered. Both the fossil fuel/combustion gas loop and bottoming steam plant can be characterized by their respective thermal efficiencies, η_{HS} and η_{BOT}. The thermal efficiency of the heat source is defined as:

$$\eta_{HS} = \frac{\text{useful heat received by MHD cycle}}{\text{energy input from fuel and air}} \qquad \text{(A 10.6.37)}$$

For the steam bottoming plant the thermal efficiency is defined as:

$$\eta_{BOT} = \frac{\text{net work out from bottoming plant}}{\text{useful heat received by bottoming plant}} \qquad \text{(A 10.6.38)}$$

A 10.6.3.1.1 MHD Closed Loop

The components in a basic MHD closed-cycle consists of a compressor, heat source, nozzle, MHD generator, diffuser, heat sink, and seed condenser. The working fluid is either the noble gas argon or helium, seeded with cesium to provide adequate conductivity. The seed is entrained in the gas upstream from the MHD channel in the vicinity of the nozzle. A preionizer is usually required for a nonequilibrium MHD generator. The seed is removed before entering the compressor and reinjected into the nozzle.

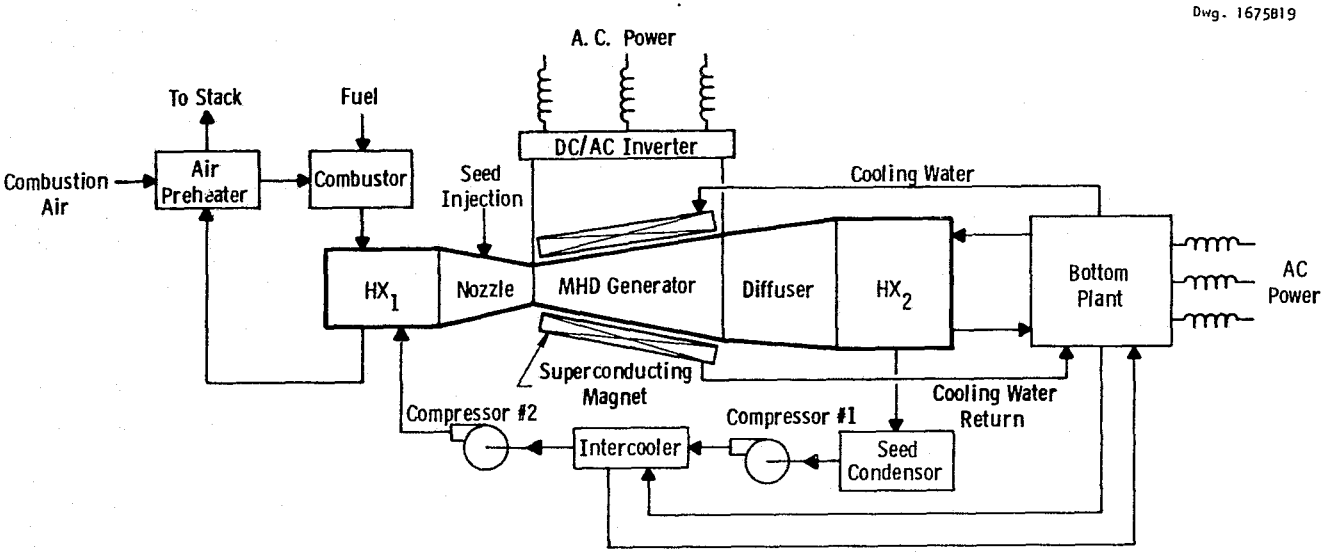

Fig. A 10.6.3—Schematic of MHD closed cycle system

The thermodynamic efficiency of the closed loop can be increased by intercooling, the heat removed from the intercooler being utilized in the bottoming plant. The number of stages of intercooling (NSI) depends on the overall pressure rise required to make up the pressure losses in the closed cycle, the marginal increase in thermodynamic efficiency obtained per stage of intercooling, and the increased cost of intercooling. Our base case cycle includes one stage of intercooling (NSI=1) and two compressors. Figure A 10.6.4 depicts the closed loop studied. The optimum of one stage of intercooling and two compressors can be easily demonstrated.

A 10.6.3.1.2 Steam Bottoming Plant

A numerical value for the thermal efficiency of the steam bottoming plant is needed to perform the analysis. A value of η_{BOT} equal to 0.450 is a reasonable estimate. This value is higher than conventional steam plant efficiencies because there are no combustion losses, no stack losses, and no draft fan losses. Tsu, Young, and Way (Reference 10.38) have reported results for an MHD open cycle which, after some data manipulation, yield a value of 0.459 for η_{BOT}. Booth (Reference 10.50) in an investigation of MHD cycle thermodynamics used a value of 0.458 for η_{BOT}. A more exact value for η_{BOT} can be computed only after working fluids, state points, and flow rates are specified for the interfaces between the MHD closed loop and the steam bottoming plant. Interfacing between these two systems occurs principally in HX_2, but also with the intercoolers, if any, and cooling water for the MHD generator and dc/ac inverter.

A 10.6.3.1.3 Heat Source

The closed-cycle MHD system has an external heat source. It is not necessary in the present analysis to know any of the details of this fossil fuel/combustion loop. An overall plant efficiency can be calculated by multiplying the efficiency of the fossil fuel/combustion loop into the cycle efficiency of the MHD loop, that is:

$$\eta_{plant} = \eta_{HS}\, \eta_{MHD\ cycle} \qquad \text{(A 10.6.39)}$$

Dwg. 6367A64

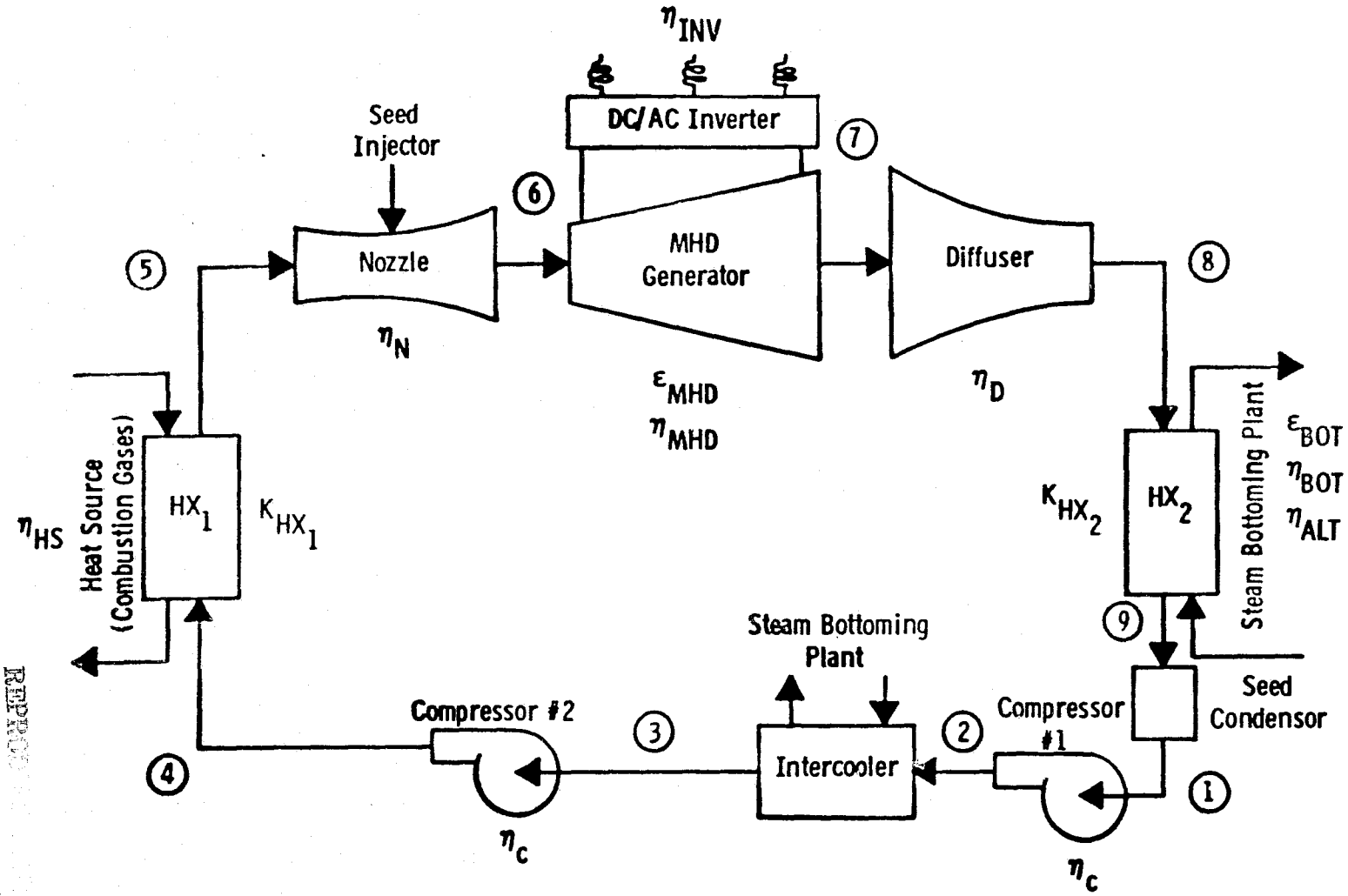

Fig. A 10.6.4—Schematic of MHD closed-cycle

A 10.6.3.2 Closed-Cycle MHD Components

A 10.6.3.2.1 MHD Generator

The MHD/generator equations have been described in detail in the section on MHD duct physics. Two parameters which characterize an MHD generator are the isentropic efficiency, η_{MHD}, and the enthalpy extraction ratio, ε_{MHD}. The definition of the isentropic efficiency is:

$$\eta_{MHD} = \frac{[\Delta h_o]_{actual}}{[\Delta h_o]_{isentropic}} = \frac{[C_p \Delta T_o]_{actual}}{[C_p \Delta T_o]_{isentropic}} \qquad \text{(A 10.6.40)}$$

and is depicted in Figure A 10.6.5. The extraction ratio is defined as:

$$\varepsilon_{MHD} = \frac{[\Delta h_o]_{MHD\ generator}}{\text{Heat added to cycle}} \qquad \text{(A 10.6.41)}$$

Because we are solving the MHD one-dimensional differential equations for the generator proper, both η_{MHD} and ε_{MHD} are results of the analysis, not assumed inputs.

A 10.6.3.2.2 Diffuser

A diffuser is used to decelerate the flow exiting from the MHD generator. Pressure recovery in the diffuser should occur with a minimum of loss. The diffusion process is assumed adiabatic, with the most common definition of adiabatic diffuse efficiency assuming the velocity leaving the diffuser to be negligible. An expression for the efficiency of either a subsonic or supersonic diffuser is:

$$\eta_D = \frac{(\Delta h)_{isentropic}}{\frac{u^2}{2}} \qquad \text{(A 10.6.42)}$$

Pressure relationships in the ideal diffuser yield the following equation for a perfect gas:

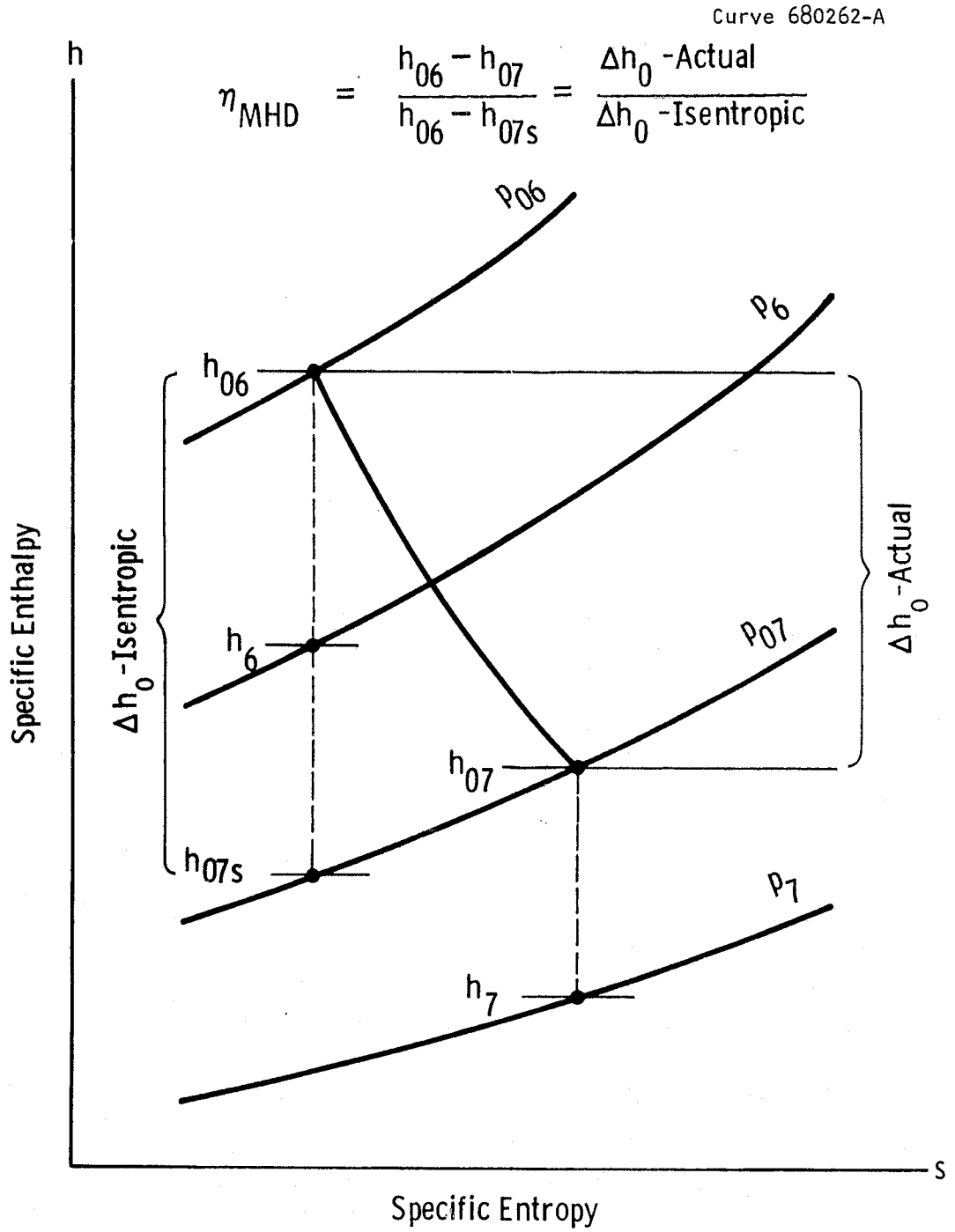

Fig. A 10.6.5—MHD generator isentropic efficiency

$$\eta_D = \frac{\left(\frac{p_{out}}{p_{in}}\right)^{\frac{\gamma-1}{\gamma}} - 1}{\frac{\gamma-1}{2} M_{in}^2} \qquad \text{(A 10.6.43)}$$

where $\gamma = C_p/C_v$ is the ratio of the specific heats at constant pressure to that at constant volume. Employing the isentropic relationship for p_o/p and substituting into Equation A 10.6.43 yields:

$$\eta_D = \frac{\left(1 + \frac{\gamma-1}{2} M_{in}^2\right)\left(\frac{p_{o_{out}}}{p_{o_{in}}}\right)^{\frac{\gamma-1}{\gamma}} - 1}{\frac{\gamma-1}{2} M_{in}^2} \qquad \text{(A 10.6.44)}$$

A 10.6.3.2.3 HX_2

Heat rejection for the MHD closed cycle occurs in the heat exchanger designated HX_2. While specific design details of HX_2 are not necessary, a pressure loss coefficient K_{HX_2} and an efficiency ε_{HX_2} of heat transfer to the steam bottoming plant is required. The pressure loss coefficient is given by:

$$K_{HX_2} = \frac{\Delta p}{p_{in}} \qquad \text{(A 10.6.45)}$$

Heat transfer efficiency to the steam plant is defined as:

$$\varepsilon_{BOT} = \frac{\text{Heat received by bottoming plant}}{\text{Heat rejected by MHD cycle}} \qquad \text{(A 10.6.46)}$$

A 10.6.3.2.4 Seed Condenser

It is assumed that all the seed condenses in the seed condenser with the condensation process being isobaric and isothermal. Thus, the only state property that changes in the process is the density.

A 10.6.3.2.5 Compressor-Intercooler System

The compression process is assumed adiabatic with an adiabatic compressor efficiency defined as:

$$\eta_c = \frac{[\Delta h_o]_{isentropic}}{[h_o]_{actual}} \qquad \text{(A 10.6.47)}$$

For an ideal gas this becomes:

$$\eta_c = \frac{T_{o_{in}} \left[\left(\frac{p_{o_{out}}}{p_{o_{in}}} \right)^{\frac{\gamma}{\gamma-1}} - 1 \right]}{T_{o_{out}} - T_{o_{in}}} \qquad \text{(A 10.6.48)}$$

Intercooling is an isobaric process with the outlet temperature from the intercooler taken equal to the inlet temperature to the compressor.

A 10.6.3.2.6 HX1

The MHD working fluid receives heat in the heat exchanger HX_1. The only characteristic of HX_1 required is the pressure loss coefficient K_{HX_1} where:

$$K_{HX_1} = \frac{\Delta p}{p_{in}} \qquad \text{(A 10.6.49)}$$

A 10.6.3.2.7 Nozzle

Either a subsonic converging or a supersonic converging-diverging nozzle is used to accelerate the flow to the velocity required by the MHD generator. The acceleration process is adiabatic with the adiabatic efficiency for the nozzle given by:

$$\eta_N = \frac{\left[\frac{u^2}{2}\right]_{actual}}{\left[\frac{u^2}{2}\right]_{isentropic}} = \frac{[h_o - h]_{actual}}{[h_o - h]_{isentropic}} \qquad \text{(A 10.6.50)}$$

A 10.6.3.3 MHD Closed-Cycle State Points

Given the state points at the exit of the MHD generator, the state points at the diffuser exit are when the values of M_8 and η_D are given:

$$p_8 = \left[\frac{\eta_D \frac{\gamma-1}{2} M_7^2 + 1}{1 + \frac{\gamma-1}{2} M_7^2}\right]^{\frac{\gamma}{\gamma-1}} \left[\frac{1 + \frac{\gamma-1}{2} M_7^2}{1 + \frac{\gamma-1}{2} M_8^2}\right] p_7 \qquad \text{(A 10.6.51)}$$

$$p_{o8} = p_8 \left[1 + \frac{\gamma-1}{2} M_8^2\right]^{\frac{\gamma}{\gamma-1}} \qquad \text{(A 10.6.52)}$$

$$T_{o8} = T_{o7} \qquad \text{(A 10.6.53)}$$

$$T_8 = \frac{T_{o8}}{\left[1 + \frac{\gamma-1}{2} M_8^2\right]} \qquad \text{(A 10.6.54)}$$

$$u_8 = M_8 (\gamma \bar{R} T_8)^{1/2} \qquad \text{(A 10.6.55)}$$

$$\rho_8 = \frac{p_8}{\bar{R} T_8} \qquad \text{(A 10.6.56)}$$

There is no heat transfer or work done in the diffusion process, that is:

$$Q_{7-8} = 0 \qquad \text{(A 10.6.57)}$$

$$W_{7-8} = 0 \qquad \text{(A 10.6.58)}$$

Knowing the state conditions at Point 8, the state conditions at Point 9 are, given the stagnation temperature T_{o9} ($T_{o9} = T_{o1}$) and M_9:

$$p_9 = (1 - K_{HX_2})\, p_8 \qquad \text{(A 10.6.59)}$$

$$p_{o9} = p_9 \left[1 + \frac{\gamma-1}{2} M_9^2\right]^{\frac{\gamma}{\gamma-1}} \qquad \text{(A 10.6.60)}$$

$$T_{o9} = T_{o1} \qquad \text{(A 10.6.61)}$$

$$T_9 = \frac{T_{o9}}{\left[1 + \frac{\gamma-1}{2} M_9^2\right]} \qquad \text{(A 10.6.62)}$$

$$u_9 = M_9(\gamma \bar{R} T_9)^{1/2} \qquad \text{(A 10.6.63)}$$

$$\rho_a = \frac{p_a}{\bar{R} T_9} \qquad \text{(A 10.6.64)}$$

No work is done during the process, but there is heat transfer from the MHD cycle to the bottoming plant.

$$Q_{8-9} = \dot{m} C_p (T_{o9} - T_{o8}) \qquad \text{(A 10.6.65)}$$

$$W_{8-9} = 0 \qquad \text{(A 10.6.66)}$$

The only change occurring in the seed condenser takes place in the density. Thus, given M_1:

$$p_1 = p_9 \qquad \text{(A 10.6.67)}$$

$$p_{o1} = p_1 \left[1 + \frac{\gamma-1}{2} M_1^2\right]^{\frac{\gamma}{\gamma-1}} \qquad \text{(A 10.6.68)}$$

$$T_{o1} = \text{Given} \qquad \text{(A 10.6.69)}$$

$$T_1 = \frac{T_{o1}}{\left[1 + \frac{\gamma-1}{2} M_1^2\right]} \qquad \text{(A 10.6.70)}$$

$$u_1 = M_1(\gamma R T_1)^{1/2} \qquad \text{(A.10.6.71)}$$

$$\rho_1 = \frac{p_1}{RT_1} \qquad \text{(A 10.6.72)}$$

where the gas constant R is that of the pure noble working gas as opposed to a weighted gas constant, $\bar{R}$, for the seed and noble gas. There is no heat transfer and no work done during the condensation process.

$$Q_{9-1} = 0 \qquad \text{(A 10.6.73)}$$

$$W_{9-1} = 0 \qquad \text{(A 10.6.74)}$$

At this point the pressure rise across the compressor-intercooler system is unknown. In fact, this is the information that permits closure of the cycle. To solve for the pressure ratio that will give compatibility to the complete cycle, we must now proceed from the MHD generator inlet backwards around the system. Conditions specified at this state point are M_6, p_6, and $\dot{m}$. The mass flow, $\dot{m}$, is constant throughout the loop. Now T_{o6} is known because the expansion process in the nozzle has been assumed adiabatic. Thus, T_{o6} equals T_{o5} where T_{o5} is a given value for the calculation. The remaining state conditions at Point 6 are:

$$p_6 = \text{Given} \tag{A 10.6.75}$$

$$p_{o6} = p_6 \left[1 + \frac{-1}{2} M_6^2\right]^{\frac{\gamma}{\gamma-1}} \tag{A 10.6.76}$$

$$T_{o6} = T_{o5} \tag{A 10.6.77}$$

$$T_6 = \frac{T_{o6}}{\left[1 + \frac{\gamma-1}{2} M_6^2\right]} \tag{A 10.6.78}$$

$$u_6 = M_6(\gamma \bar{R} T_6)^{1/2} \tag{A 10.6.79}$$

$$\rho_6 = \frac{p_6}{\bar{R} T_6} \tag{A 10.6.80}$$

State conditions at Point 5 given M_5 and T_{o5} are:

$$P_5 = \frac{P_6}{\left[1 - \frac{(\gamma-1)\, M_6^2 T_{o6}\left(1 + \frac{\gamma-1}{2} M_5^2\right)}{2\eta_N T_{o5}\left(1 + \frac{\gamma-1}{2} M_6^2\right)}\right]} \qquad \text{(A 10.6.81)}$$

$$P_{o5} = P_5 \left[1 + \frac{\gamma-1}{2} M_5^2\right]^{\frac{\gamma}{\gamma-1}} \qquad \text{(A 10.6.82)}$$

$$T_{o5} = \text{Given} \qquad \text{(A 10.6.83)}$$

$$u_5 = M_5 (\gamma R T_5)^{1/2} \qquad \text{(A 10.6.84)}$$

$$\rho_5 = \frac{P_5}{RT_5} \qquad \text{(A 10.6.85)}$$

There is no work done and no heat transfer in the expansion process in the nozzle.

$$Q_{5-6} = 0 \qquad \text{(A 10.6.86)}$$

$$W_{5-6} = 0 \qquad \text{(A 10.6.87)}$$

Going from state Point 4 to state Point 5, heat is added to the closed cycle. Given M_4, the state conditions at Point 4 are:

$$P_4 = \frac{P_5}{\left(1 - K_{HX_1}\right)} \qquad \text{(A 10.6.88)}$$

$$P_{o4} = P_4 \left[1 + \frac{\gamma-1}{2} M_4^2\right]^{\frac{\gamma}{\gamma-1}} \qquad \text{(A 10.6.89)}$$

This stagnation temperature depends on the pressure rise of the compressor-intercooler system. This expression for the stagnation temperature is given by:

$$T_{o4} = T_{o1}\left[1 + \frac{\left(\frac{p_{o4}}{p_{o1}}\right)^{\left(\frac{1}{NSI+1}\right)\left(\frac{\gamma-1}{\gamma}\right)} - 1}{\eta_c}\right] \qquad \text{(A 10.6.90)}$$

When NSI = 0 there is no intercooling and a single compressor. For NSI = 1 there is first a compression process, then intercooling, and finally a compression process. There is always one more compressor than there are stages of intercooling. The remaining state conditions are:

$$T_4 = \frac{T_{o4}}{\left[1 + \frac{\gamma-1}{2} M_4^2\right]} \qquad \text{(A 10.6.91)}$$

$$u_4 = M_4(\gamma R T_4)^{1/2} \qquad \text{(A 10.6.92)}$$

$$\rho_4 = \frac{p_4}{RT_4} \qquad \text{(A 10.6.93)}$$

The heat transfer and work done are:

$$Q_{4-5} = \dot{m} C_p (T_{o5} - T_{o4}) \qquad \text{(A 10.6.94)}$$

$$W_{4-5} = 0 \qquad \text{(A 10.6.95)}$$

Because the compression process is adiabatic, given M_3, the state conditions at Point 3 are:

$$P_{o3} = P_{o1}\left(\frac{P_{o4}}{P_{o1}}\right)^{\left(\frac{1}{NSI+1}\right)} \qquad \text{(A 10.6.96)}$$

$$p_3 = \frac{P_3}{\left[1 + \frac{\gamma-1}{2} M_3^2\right]^{\frac{\gamma}{\gamma-1}}} \qquad \text{(A 10.6.97)}$$

$$u_3 = M_3(\gamma R T_3)^{1/2} \qquad \text{(A 10.6.98)}$$

$$\rho_3 = \frac{P_3}{RT_3} \qquad \text{(A 10.6.99)}$$

Work done and heat transfer are:

$$Q_{3-4} = 0 \qquad \text{(A 10.6.100)}$$

$$W_{3-4} = \dot{m}C_p(T_{o3} - T_{o4}) \qquad \text{(A 10.6.101)}$$

Intercooling is an isobaric process, thus given M_2:

$$P_{o2} = P_{o3} \qquad \text{(A 10.6.102)}$$

$$p_2 = \frac{P_{o2}}{\left[1 + \frac{\gamma-1}{2} M_2^2\right]^{\frac{\gamma}{\gamma-1}}} \qquad \text{(A 10.6.103)}$$

$$T_{o2} = T_{o4} \qquad \text{(A 10.6.104)}$$

$$T_2 = \frac{T_{o2}}{\left[1 + \frac{\gamma-1}{2} M_2^2\right]} \qquad \text{(A 10.6.105)}$$

$$u_2 = M_2(\gamma R T_2)^{1/2} \qquad \text{(A 10.6.106)}$$

$$\rho_2 = \frac{P_2}{RT_2} \qquad \text{(A 10.6.107)}$$

Work done and heat transfer are:

$$Q_{2-3} = \dot{m}C_p(T_{o3} - T_{o2}) \qquad \text{(A 10.6.108)}$$

$$W_{2-3} = 0 \qquad \text{(A 10.6.109)}$$

The equations described in Sections A 10.2.2 through A 10.2.6 enable us to calculate the change of gas state throughout the MHD generator. The equations described in this section, Equations A 10.6.51 through A 10.6.109, enable us to calculate gas properties at all state points between the MHD generator exit and back to its inlet. In this way we have generated all the information needed to make a complete heat balance.

Now the MHD closed-cycle power out is:

$$P_{MHD} = \eta_{INV} W_{6-7} \qquad \text{(A 10.6.110)}$$

$$Q_{6-7} = \lambda_2 W_{6-7} \qquad \text{(A 10.6.111)}$$

Assuming the heat removed from the intercooler and heat losses from the MHD generator duct and the dc/ac inverter are recovered by the steam bottoming plant, we can calculate its net power output thus:

$$P_{\text{steam net}} = \left[\left[\left(\varepsilon_{BOT}\, Q_{8-9} + Q_{2-3} + Q_{6-7} + \left(1-\eta_{INV}\right) W_{6-7}\right) \eta_{BOT} - \left(NSI+1\right) W_{1-2}\right] \eta_{ALT} \right. \quad \text{(A 10.6.112)}$$

where η_{ALT} is the efficiency of the alternator in the bottoming plant.

Also:

$$P_{\text{steam total}} = \frac{P_{\text{steam net}}}{\eta_{ALT}} + (NSI+1)\, W_{1-2} \quad \text{(A 10.6.113)}$$

The cycle efficiency is:

$$\eta_{\text{MHD cycle}} = \frac{P_{\text{steam net}} + P_{MHD}}{Q_{4-5}} \quad \text{(A 10.6.114)}$$

A 10.6.4 Computer Program

The formulae presented in Subsections A 10.6.2 and A 10.6.3 of this report have been coded in FORTRAN for use on the Westinghouse Research Laboratories UNIVAC 1106 machine. This section describes the mechanics of the computer program, and lists the required input.

A 10.6.4.1 General Background

The computer program, presently called "BARNEY*VOSHALL," was written to analyze parametrically the proposed MHD closed-cycle model, as

shown in Figure A 10.6.4. When writing the program (see Subappendix AA 10.6.1 for the algorithm listing), an effort was made to generalize the code. That is, via input, the user has been given the flexibility of the following options:

1. Choose either helium or argon as the working fluid.
2. Choose any arbitrary seed gas at any fraction relative to the working fluid.
3. Choose either nonequilibrium or thermal equilibrium ionization gas model.
4. Choose any number of stages of intercooling.
5. Choose either a constant or variable gas velocity flow in the MHD generator.
6. Choose either a constant or variable magnetic flux density in the MHD generator.
7. Choose either a constant step size or variable step size integration procedure for solving the flow and energy derivatives describing the MHD generators.

In addition to these options the user may, via input, specify values of all parameters which will characterize the cycle.

A 10.6.4.2 Program Structure

Referring to Subappendix AA 10.6.1, the program consists of nine elements (MAIN, EULER, HAMMNG, EDERIV, OUTPUT, HFAIL, TEROOT, SIG, and QINTRP).

In general the algorithm listing of the above elements are well documented by comment cards. We will attempt here, however, to give more insight to the overall mechanics of the program.

A 10.6.4.2.1 MAIN

This element reads in all data, sets all the constants, and loops on two possible data input cycles. That is, there are cases and

subcases. The outer DO loop requires all input data to be resubmitted for each case, while the inner DO loop requires only the inlet conditions of Point 6 to be resubmitted for each subcase. In all, there are 23 read statements in the MAIN program. For the user's reference, all data read in are printed out, along with the printout of the final results for each case or subcase. Definitions of the required data input have been made part of the algorithm by use of comment cards.

For each case or subcase (after all required data have been read in, and all constants are set) the program calls on either a modified EULER (constant step size) integration subroutine, or a HAMMNG (variable step size) integration subroutine for determining the thermodynamic properties of the working fluid at Point 7. The above choice of integration is determined by the value assigned to the input data option "IDERIV". Then after successfully passing the criteria for terminating the integrations and having printed out the final results, control of the program is returned back to the main element which then reloops on the data input cycles and again calls on the integration routine.

A 10.6.4.2.2 EULER and HAMMNG

These elements are standard integration subroutines. Each employ predictor correction methods for stepping from one integration point to the other. EULER, however, is a constant-step size integration, and HAMMNG (which uses a Runge Kutta method for initializing) is a variable-step size integrator. Since these procedures have been described in References 10.51, 10.52, and 10.53; their intricate parts will not be described here. As written here both routines are in double precision. The HAMMNG routine has been slightly modified from that of the original code in that the absolute tolerances of the dependent variables were made to vary. This subroutine sets the absolute tolerances at 10^{-4}, 10^{-5}, and 10^{-2} respectively for pressure, kinetic energy per unit mass, and temperature. These values are further corrected by the factor of a single input data value "CABS" which is read in by the MAIN. Units of the above variables are in the MKS system as are all final results.

A 10.6.4.2.3 EDERIV, OUTPUT, and HFAIL

These three elements are utilized by the HAMMNG and EULER subroutines. In particular, HAMMNG calls on all three, but EULER calls only on the first two. The purposes of these elements follow:

The EDERIV element calculates the derivatives of each dependent variable. In addition EDERIV calls on two separate subroutines which determine the concurrent electron temperature (if the nonequilibrium ionization option is set) and electrical conductivity.

The OUTPUT element prints out all calculated results. The algorithm in the program is such that conditions at Points 6 and 7 will always be printed out (upon successful termination of integration). For purposes of MHD generator design, however, the OUTPUT element will print out (in addition to the above) the results of the integration calculations at specified (controlled via data input) successful integration points along the MHD generator. After successful termination of the integration the OUTPUT routine then prints out the thermodynamic and kinetic properties of the working fluid for all stations of the cycle. The OUTPUT element is used to test if either the EULER or HAMMNG routine should terminate and pass the program control back to the MAIN program. There are nine such tests as follow:

1. Interaction parameter test
   IF DSI $\geq$ TESTIP
2. K' test (see Equation A 10.6.3.1)
   IF 1-K' < 0
3. Total length test
   IF X > XL
4. Total power
   DSUMPE $\geq$ PGROSS
5. Mach number test at Point 7 if supersonic inlet conditions exist
   $M_7 \leq 1.05$

6. Length to local diameter test

   $X/D \geq$ TESTXD

7. Hall parameter test

   $\beta \geq$ TESTB

8. Test on gas temperature

   $T_g < 300$

9. Test on magnetic field

   $B < 0.$

On the printout sheets a flag will indicate which test or tests caused termination of the integration.

The HFAIL element is used by HAMMNG to terminate the execution of the program when a failure is detected in the relative and/or absolute tolerance requirements.

A 10.6.4.2.4 TEROOT

This element is a subroutine which determines the root (electron temperature) of a transcendental function generated in the subroutine called SIG. In this routine an iteration was introduced such that the upper bound placed on the electron temperature could be changed. In the routine the lower bound of the electron temperature was specifically taken as the gas temperature; hence, the value of the transcendental function at the onset is -1. To aid in making an initial guess of the electron temperature the upper bound of the electron is made some factor "TFAC" (see data input in main program) of the gas temperature. Using this value, the transcendental function is solved. If the function is negative, the upper bound is doubled until the function is positive or if a maximum doubling count (5) is exceeded at which point the execution will terminate.

A 10.6.4.2.5 SIG and QINTRP

The SIG element is a subroutine written to calculate the electrical conductivity of a seeded plasma. This routine calculates the chemical composition of the working fluid and seed and also provides the

transcendental electron temperature function utilized by the subroutine, TEROOT. In addition, the Hall parameter, BETA, is calculated in the SIG subroutine.

The SIG routine calls on the subroutine QINTRP which interpolates tables of energy-averaged electron momentum cross sections at a given electron temperature. The chemical composition calculation, as written in SIG, uses the electron number density previously calculated at the last successful integration point to determine the lowering of the ionization potential.

A 10.6.4.2.6 INPUT

The user defines his proposed model via input data cards: First, by stating the number of cases to be executed and, secondly, by supplying the data required by 22 additional read statements. These data calls are listed below in their proper sequence and in terms of the symbolic names used in the algorithm. All data calls are formated "Free Field," that is, each data value appears in its proper sequence but is not assigned to any particular set of columns on the data card. All data values on a given data card are to be separated by a comma. All data values are declared real, with the exception of those symbolic names which begin with the letters of I, J, K, L, M, or N.

READ STATEMENT No.	DATA
1	JCASE
2	ITITLE(I)
3	JOPTE
4	IGAS
5	RCP,RCV,RMWB,RMWS,FAC
6	RVO,RZI,RZO
7	REPS,RDEL
8	IQQ
9	Q1Q(I)
10	IQQQ
11	QCQ(I)
12	RSOO,SREFT,HOO,HREFT
13	RRB,COBBO
14	RRC,RRK,RRF,RRL2,EEL
15	PGROSS,TESTB,TESTXD,IFAC,TESTIP
16	IDERIV

```
17      XO,XL,HSTEP,PHSTEP
18      HSTEP,HMAX,HMIN,CREL,CABS,ICFACT
19      AMACH(1),AMACH(2),AMACH(3),AMACH(4),AMACH(5),
        AMACH(6),AMACH(8),AMACH(9)
20      TSTAG(1),TSTAG(5)
21      ETAD,ETAC,ETAN,HX1,HX2,ETACDC,ETASP,NSI,EHX2
22      NCASE
23      RPO,RMDOT
```

The definition and physical units of the above input data are given below (see also algorithm listing in Subappendix AA 10.6.1).

1. JCASE — Number of cases to be executed. For each case the following data are to be input.

2. ITITLE(I) — Title card, reads columns 1 through 72.

3. IOPTE — Option: If greater than zero, nonequilibrium conditions in the MHD generator are assumed; otherwise equilibrium prevails.

4. IGAS — Option: If IGAS = 18, argon is the inert buffer gas; if IGAS = 2, helium is the inert buffer gas.

5. RCP — Specific heat at constant pressure per universal gas constant of the inert buffer gas: C_p/R.

   RCV — Specific heat at constant volume per universal gas constant of the inert buffer gas: C_V/R.

   RMWB — Molecular weight of inert buffer gas (kg/kg mole).

   RMWS — Molecular weight of seed gas (kg/kg mole)

   FAC — Seed fraction: See Equation A 10.6.15.

6. RVO — Ionization potential V_o, see Equation A 10.6.19, electron volts.

	RZI	Electronic partitions function of ion fixed gas, see Equation A 10.6.19.
	RZO	Electron partition function of atom of seed gas, see Equation A 10.6.19.
7.	REPS	EPSILON: $\bar{\xi}$, see Equation A 10.6.9.
		DEL: δ, see Equation A 10.6.12.
8.	IQQ	Number of temperatures and corresponding energy averaged electron momentum transfer cross sections of the buffer gas to be read in for the Q1Q(I) array.
9.	Q1Q(I)	T and Q value array. Ordered as: T_1, Q_1, T_2, Q_2——T_N, Q_N (1, 2, 3, 4——IQQ -1, IQQ), T(°K) and Q(square Angstroms).
10.	IQQQ	Same as read in No. 8 but for the seed gas and QCQ(I) array.
11.	QCQ(I)	Same as read in No. 9 but for seed gas.
12.	RSOO	Reference Entropy of inert buffer gas at reference temperature SREFT, k cal/kg mole.
	SREFT	Reference temperature of above reference Entropy, °K.
	HOO	Reference Enthalpy of unit buffer gas at reference temperature HPEFT, k cal/kg mole.
	HREFT	Reference temperature of above reference Enthalpy, °K.
13.	RRB	Magnetic field B_o, T.
	COBBO	Magnetic field gradient coefficient, "b", such that $B = B_o (1 - bx)$, where x is distance along MHD generator.

14.	RRC	'c' parameter, see Equation A 10.6.6.
	RRK	'K' parameter, see Equations A 10.6.1, A 10.6.2, and A 10.6.5.
	RRF	'f' friction parameter, see Equation A 10.6.1.
	RRL2	Heat loss parameter, λ_2 in Equation A 10.6.2.
	EEL	Electrode loss parameter E_{el}, see Equation A 10.6.31, V.
15.	PGROSS	Gross electrical power of MHD generator, kW.
	TESTB	Termination test parameter for the Hall parameter.
	TESTXD	Termination test parameter for the MHD generator's length to diameter ratio.
	TFAC	Factor used to establish initial upper bound of electron temperature, T_e = TFAC* T_{gas}.
	TESTIP	Termination test parameter for the interaction parameter.
16.	IDERIV	Option: If greater than 0, HAMMNG integration subroutine will be used; otherwise, Euler integration subroutine will be used.
17.	XO	Initial position (length) of MHD generator where integration begins, m.
	XL	Termination test parameter for the maximum generator length, m.

HSTEP — Increments of length, m, at which the Euler routine will integrate the derivatives.

PHSTEP — Increments of length, m, at which printouts are desired, showing solutions of the integrals.

18. Note: This read statement is only called if IDERIV > 0.

HSTEP — Integration step size, m, at which Runge Kutta procedure in HAMMNG routine is initialized.

HMAX — Maximum step size, m, to be considered by HAMMNG integration routine.

HMIN — Minimum step size, m, to be considered by HAMMNG integration routine.

CREL — Relative error tolerance factor.

CABS — Absolute error tolerance factor.

IFACT — Factor in HAMMNG routine used to establish doubling criteria (Note: set to 100) of step size.

19. AMACH(1) — Mach number of gas flow at station 1.

AMACH(2) — Mach number of gas flow at station 2.

AMACH(3) — Mach number of gas flow at station 3.

AMACH(4) — Mach number of gas flow at station 4.

AMACH(5) — Mach number of gas flow at station 5.

AMACH(6) — Mach number of gas flow at station 6.

AMACH(7) — Mach number of gas flow at station 7.

AMACH(8) — Mach number of gas flow at station 8.

AMACH(9) — Mach number of gas flow at station 9.

20.	TSTAG(1)	Stagnation temperature of gas at station 1.
	TSTAG(5)	Stagnation temperature of gas at station 5.
21.	ETAD	Adiabatic diffuser efficiency.
	ETAC	Adiabatic compressor efficiency.
	ETAN	Adiabatic nozzle efficiency.
	HX1	Pressure loss coefficient for heat exchanger 1.
	HX2	Pressure loss coefficient for heat exchanger 2.
	ETACDC	dc to ac inverter efficiency.
	ETASP	Bottoming plant efficiency.
	NSI	Number of stages of intercooling.
	EHXZ	Fraction of heat received by bottoming plant from HX2.
22.	NCASE	Number of subcases to be executed with the above input but with the following changes.
23.	Note: For each NCASE input the following:	
	RPO	Pressure at Point 6, atm.
	RMDOT	Mass flow at Point 6, kg/s.

A 10.6.5 Nomenclature

A = cross section area of MHD duct, m^2

B = magnetic flux density, T

C_p = specific heat at constant pressure, joule/kg-°K

C_v = specific heat at constant volume, joule/kg-°K

E_{el} = electrode voltage drop, V

$\dot{E}_{el}$ = elastic collision energy rate, W

$\dot{E}_{r}$ = radiation energy rate, W

F = mole fraction of seed

$F(v)$ = electron velocity distribution

K = generator loading coefficient

K' = generator loading coefficient with electrode voltage losses

K_{HX_1} = pressure loss coefficient for heat exchanger number 1

K_{HX_2} = pressure loss coefficient for heat exchanger number 2

LTE = local thermal equilibrium

M = Mach number

N_a = gas density, m^{-3}

N_s = seed density, m^{-3}, superscript: i-ion, o-neutral

N_B = buffer gas density, m^{-3}

NSI = number of stages of intercooling

P = power, W

Q = heat transferred, W

Q_m = collision cross section, m^2 subscript: e-B-electron buffer gas, e-s-electron seed, e-ion-electron ion

R = gas constant for pure noble gas, J/kg-°K

$\bar{R}$ = weighted gas constant, J/kg-°K

S = interaction parameter

T = temperature, °K

T_e = electron temperature, °K

T_g = gas temperature, °K

T_o = stagnation temperature, °K

V_o = ionization potential of seed, V.

W = work done, W

Z = charge of the atom seen by the valence electron (Z = 1, 2, 3, etc.)

Z_s^o = electronic partition function of the seed neutral

Z_s^+ = electronic partition function of the seed ion

b = gradient of magnetic flux density along axis of MHD generator, m^{-1}

c = velocity coefficient

d = distance between electrodes, m

e = electronic charge, C

f = friction factor

h' = Plank's constant, J/s

h = enthalpy of the gas, J/kg

j = current density, A/m^2

k = Boltzmann constant, J/°K

M_k = mass, kg, subscript: k = B-buffer gas, e-electron, h-heavy particle, s-seed

$\dot{m}$ = mass flow, kg/s

n_e = electron density, m^{-3}

p = static gas pressure, Pa

p_o = stagnation gas pressure, Pa

r_h = hydraulic radius of MHD duct, m

u = gas velocity, m/s

ν = electron velocity, m/s

x, y, z = rectangular coordinates

β = Hall parameter

β_{eff} = effective Hall parameter

γ = ratio of C_p to C_v

δ = collision loss factor

ε_o = permittivity of free space

ε_{MHD} = enthalpy extraction ratio for MHD duct

ε_{BOT} = heat transfer efficiency of bottom plant steam generator

η = efficiency of MHD closed loop

η_c = adiabatic compressor efficiency

η_N = adiabatic nozzle efficiency

η_D = adiabatic diffuser efficiency

η_{MHD} = MHD generator isentropic efficiency

η_{BOT} = bottoming plant efficiency

η_{INV} = efficiency of dc/ac inverter

η_{ALT} = efficiency of alternator in bottom plant

λ_2 = heat loss parameter

μ = electron mobility, m^2/Vs

ν_{eh} = electron heavy particle collision frequency, s^{-1}

ν_1 = averaged of the sum of electron neutral and electron ion collision frequencies, s^{-1}

ν_2 = averaged collision frequency of electron neutral and electron ion collision frequencies, s^{-1}, used in mobility and Hall parameter calculations

$\bar{\xi}$ = plasma turbulence factor

ρ = gas density, kg/m^3

σ = electrical conductivity, $mho/m = \frac{1}{\Omega m}$

σ_{eff} = effective electrical conductivity, $mho/s = \frac{1}{\Omega m}$.

Subappendix AA 10.6.1

Program Listing

A listing of the MHD closed-cycle program, written in FORTRAN, appears on the following pages. This program was run on a UNIVAC 1106 computer system located at the Westinghouse Research Laboratories.

```
C*****       MAIN  PROGRAM
      IMPLICIT DOUBLE PRECISION  (D)
      COMMON/CONST/ D1,D2,DPS,DRBAR,DRHCUO,DPCON,DFM,DC,DTCON,DCP,DK,
     *  XTOL,YTOL,DHSTEP,DSSCON,EEL,D1MKP,TESTIP,DB30,COBBO,OPTE,
     1  IDERIV,DSICON,DMCON,PGROSS,DSUMPE,TESTB,TESTXD,DXEND,DPCOLD,
     2  D1PC,D1MK,DB,D1PL2,D4,DPO,DU20,DTO,DRHOO,DXO,DXOLD,DB2,IT,RMACHO
     3 ,DLTIME,DPRINT,DHO,GAM,DSOO,SREFT,TFAC
      COMMON/SIG1/ FACEV,GASKO,FAC,RVO,LOGSAC,QBO,PB,QBS,PS,CB1,CS1,
     1 CB2,CS2,CSIGO,CSIGE2,CSIGEI,CBETA,REPS,DCONT1,RFUNC,CLOW,CLDNE,
     2 RTE,BETA,XNB,XNA,XNE,XNU1,XNU2,XSIGO,XSIGEI,XSIGAD,XSIG,XSIGEF
      EXTERNAL    EDERIV,OUTPUT,HFAIL
      COMMON/SIG2/ DCONT2,RP,RT,RB,RMWB,RMWS,IGAS,CONEI,CONAQ
      COMMON/QQVAL/ QCQ(37)
      COMMON/QVALUE/ Q1Q(37)
      COMMON/STATIO/ TSTAT(9),TSTAG(9),AP(9),APS(9),ARHO(9),AVEL(9),
     1 AMACH(9),QQQ(9),WWW(9),XXX1,XXX2,XXX3,XXX4,XXX5,XXX6,XXX7,XXX8,
     2 ETAD,ETAC,ETAN,HX1,HX2,ETACDC,ETASP,NSI,
     3 CVGAM,CONDU2,RMDOT,CONDU3, RRBAR,BCP,EHX2,XXX9
      DIMENSION   DY(3),ITITLE(72)
C           JCASE       GRAND NUMBER OF CASES
      READ(5,5000) JCASE
      WRITE(6,2999) JCASE
 2999 FORMAT(1X,'TOTAL NUMBER OF CASES ',I4)
      DO 9999 LCASE=1,JCASE
      WRITE(6,3000)
C********     READ IN TITLE CARD ******** FIRST 72 COLUMNS **************
      READ(5,4000)(ITITLE(I),I=1,12)
      WRITE(6,4010)(ITITLE(I),I=1,12)
 4000 FORMAT(12A6)
 4010 FORMAT(1X,12A6)
C*    GAS  CONSTANT     JOULES/KILO MOLE - DEG K
      RO    = 8.31436E3
      RRR   = RO
C*    ONE ATM IN  MKS
      PO    = 1.01325E5
C*****       READ IN  GAS PARAMETERS
C            OPTE      OPTION    ** IF GT  0 TE>TG ELSE TE=TG
C
      READ(5,5000) OPTE
C
      WRITE(6,2998) OPTE
 2998 FORMAT (1X,'IONIZATION OPTION - EQUILIBRIUM IF.LE.0 OR NONEQUILIBR
     1IUM IF.GT.0    ',E8.1/)
C            IGAS      GAS TYPE  HELIUM IF 4, ARGON IF 18
C
      READ(5,5000) IGAS
C
      IF(IGAS.EQ.4)WRITE(6,4004)
 4004 FORMAT(1X,'BUFFER GAS IS HELIUM')
      IF(IGAS.EQ.18) WRITE(6,4018)
 4018 FORMAT(1X,'BUFFER GAS IS ARGON')
C            RCP       SPEFIC HEAT   CONSTANT  PRESSURE   PER R
C            RCV       SPEFIC HEAT   CONSTANT  VOLUME     PER R
C            RMWB      MOLECULAR  WEIGHT OF BUFFERGAS     (KG/KILO-MOLE)
C            RMWS      MOLECULAR  WEIGHT OF SEED GAS      (KG/KILO-MOLE)
C            FAC       FRACTION OF SEED
C
      READ(5,5000) RCP,RCV,RMWB,RMWS,FAC
      WRITE(6,4020) RCP,RCV,RMWB,RMWS,FAC
C
 4020 FORMAT (1X,'SPECIFIC HEAT AT CONSTANT PRESSURE / GAS CONSTANT    ',
     1E09.4,3X,'SPECIFIC HEAT AT CONSTANT VOLUME / GAS CONSTANT    ',E11.
     24/1X,'MOLECULAR WEIGHT OF BUFFER GAS (KG/KILO-MOLE)    ',E13.4,3X,'
     3MOLECULAR WEIGHT OF SEED (KG/KILO-MOLE)    ',E19.4/1X,'SEED FRACTIO
     4N    ',E45.4)
 5000 FORMAT( )
C            RMW       MOLECULAR  WEIGT OF MIXTURE    = RMWB+ FAC*RMWS
      RMW   =  RMWB  + FAC*RMWS
      DRBAR = RRR/RMW
      RRBAR=RRR/RMWB
      DCP   = RCP*RRR/RMW
      BCP=RCP*RRBAR
      GAM   = RCP
      VGAM  = RCP/RCV
C            RVO       IONIZATION POTENTIAL     ( EV )
```

```
C            RZI       PARTITION FUNCTION OF ION  FOR SEED
C            RZO       PARTITION FUNCTION OF NEUTRAL FOR SEED
C
      READ(5,5000) RVO,RZI,RZO
C
      WRITE(6,4025) RVO,RZI,RZO
 4025 FORMAT (1X,'IONIZATION POTENTIAL FOR SEED (EV)   ',E24.4/1X,'PARTI
     1TION FUNCTION OF ION FOR SEED   ',E24.4,3X,'PARTITION FUNCTION OF
     2NEUTRAL FOR SEED   ',E20.4/)
C            REPS      EPSILON  FOR SIGMA  CALCULATION
C            RDEL      DEL      FOR SIGMA  CALCULATION
C
      READ(5,5000)                          REPS,RDEL
C
      IF(OPTE.LE.0.) REPS=0.0
      WRITE(6,4030)                   REPS,RDEL
 4030 FORMAT (1X,'TURBULENCE FACTOR FOR NON-EQUILIBRIUM IONIZATION',42X,
     1F7.4/1X,'INCREMENT TO LOSS FACTOR FOR INELASTIC COLLISION AND RADI
     2ATION LOSSES (DELTA=1+INCREMENT)',01X,F7.4/)
C****     THE FOLLOWING READS ARE FOR BUFFER GAS
C            IQQ       NUMBER OF T,Q VALUES IN Q1Q ARRAY
C            Q1Q       T AND Q VALUE ARRAY  (DEG K, ANGS**2 UNITS )
C
      READ(5,5000) IQQ
      IQQ =IQQ +1
C
      READ(5,5000)(Q1Q(I),I=2,IQQ)
C
      Q1Q(1)=IQQ
      WRITE(6,4031)
 4031 FORMAT(1X,'AVERAGE BUFFER GAS XSECT FOLLOW')
      WRITE(6,4032)(Q1Q(I),I=1,IQQ)
 4032 FORMAT(1X,10E11.4)
C****     THE FOLLOWING READS ARE FOR SEED   GAS
C            IQQQ      NUMBER OF T,Q VALUES IN QCQ ARRAY
C            QCQ       T AND Q VALUE ARRAY  (DEG K, ANGS**2 UNITS )
C
      READ(5,5000) IQQQ
      IQQQ=IQQQ+1
C
      READ(5,5000)(QCQ(I),I=2,IQQQ)
C
      QCQ(1)=IQQQ
      WRITE(6,4033)
 4033 FORMAT(1X,'AVERAGE SEED   GAS XSECT FOLLOW')
      WRITE(6,4032)(QCQ(I),I=1,IQQQ)
C            RS00      ENTROPY CAL/MOLE DEG K AT TEMP SREFT
C            SREFT     REFERENCE TEMPERATURE
C            H00       ENTHALPY CAL/MOLE DEG K AT TEMP  HREFT
C            HREFT     REFERENCE  TEMPERATURE
C
      READ(5,5000)  RS00,SREFT,H00,HREFT
C
      WRITE (6,4040) SREFT,RS00,HREFT,H00
 4040 FORMAT (1X,'ENTROPY (CAL/MOLE.K) AT ',F8.2,' K ',15X,E11.4,3X,'ENT
     1HALPY (CAL/MOLE) AT ',F8.2,' K ',16X,E11.4/)
      DS00  = RS00*DRBAR/1.98717
      H00   = H00*DRBAR/1.98717
C*****       READ  IN  FIXED  PARAMETERS
C            RRB  = MAGNETIC FIELD STRENGTH
C            COBBO     COEFF FOR B=B0*(1.-COBBO*X)
C
      READ(5,5000) RRB,COBBO
C
      WRITE(6,4041) RRB,COBBO
 4041 FORMAT (1X,'MAGNETIC FIELD FLUX BO(1-B*X) WHERE BO = ',F6.2,' TESL
     1A AND B = ',F7.4,'/M'/)
C            RRC  = C  (CONSTANT)
C            RRK  = K
C            RRF  = F    FRICTION PARAMETER
C            RRL2 = HEAT LOSS PARAMETER LAM2
C            EEL  = ELECTRODE DROP
C
      READ(5,5000)      RRC,RRK,RRF,RRL2,EEL
C
      WRITE(6,4060)      RRC,RRK,RRF,RRL2,EEL
```

```
 4060 FORMAT (1X,'VELOCITY COEFFICIENT (C=RHO*VELOCITY*(D-VELOCITY/D-PRE
     1SSURE))',21X,F7.4/1X,'GENERATOR SEGMENT LOADING COEFFICIENT (K=IND
     2UCED VOLTAGE/OPEN CIRCUIT VOLTAGE)',04X,F7.4/1X,'FRICTION FACTOR',
     367X,F7.4/1X,'HEAT LOSS FACTOR (MHD HEAT LOSS / MHD POWER GENERATED
     4)',28X,F7.4/1X,'VOLTAGE DROP BETWEEN GAS AND ELECTRODE (VOLTS)',33
     5X,F7.1/)
C            PGROSS     GROSS POWER VALUE
C            TESTB      TEST PARAMETER FOR HALL TERM
C            TESTXD     TEST PARAMETER FOR X/D RATIO
C            TFAC       FACTOR FOR UPPER BOUND ON ELECTRON TEMP
C            TESTIP     TEST PARAMETER FOR THE INTERACTION PARAMETER
C
      READ(5,5000) PGROSS,TESTB,TESTXD,TFAC,TESTIP
C
      WRITE (6,4070) PGROSS,TESTB,TESTXD,TESTIP,TFAC
 4070 FORMAT (1X,'PARAMETER UPPER BOUND'/6X,'MHD GROSS POWER (W)',26X,E1
     11.4/6X,'HALL',41X,E11.4/6X'LENGTH / DIAMETER',28X,E11.4/6X,'INTERA
     2CTION',34X,E11.4/6X,'ELECTRON TEMPERATURE / GAS TEMPERATURE',E18.4
     3/)
C****    SET CONSTANTS
      ADEL=1.0+RDEL
      D1     = 1.0
      D2     = 2.0
      DPS    = 0.5
      DC     =RRC
      DK     =RRK
      D1PC   =  1.0 +RRC
      D1MK   =  1.0 -RRK
      DBBO=RRB
      DB     = RRB
      DB2    = RRB*RRB
      DPCON =   D1   /D1PC
      D1PL2 =   1.0 +RRL2
      DTCON =   DB2*DK      *D1PL2
      CONDU2=   VGAM*DRBAR
      CONDU3=VGAM*RRBAR
      DMCON =   1.0/SQRT(CONDU2)
C*****       SET   CONSTANTS   FOR   SIG   ROUTINE
      CLOW  =(((4.80294)**3)*2.0*SQRT(6.283/1.38047)/1.60209)*1.0E-13
      CONEI=SQRT(6.283*1.38047/9.1086)*(4.80294**4)*4.0E-8/
     *  (3.0*(1.38047**2))
      CONAQ   = SQRT(2.*1.38047/(3.1415*9.1086))*8.0E-16/3.0
      FACEV          =  (1.0/1.16052)*1.0E-4
      GASKO          =  (1.0/1.3804)*1.0E23
      A              =  2.0*RZI*2.412/RZO
      LOGSAC         = ALOG(A) + 21.0*ALOG(10.)
      CSIGO          =((1.60207)**2)/9.1086)*1.0E-7
      CSIGE2         = 1.550E13
      CSIGEI         = 1.913E4
      CBETA          = (1.60207/9.1086)*1.0E12
      OCONT1         =(3.*1.3804*ADEL*(5.4876E-4)     )*1.0E-23
C*****       SET   TOLERANCE FOR TROOT  ROUTINE
      XTOL           = 1.0E-4
      YTOL           = 1.0E-5
C*****       READ IN  HAMMING OR EULER  OPTION  IDERIV
C     IF     IDERIV  GT 0   HAMMING IS USED
C     IF     IDERIV  LE 0   EULER   IS USED
C
      READ(5,5000) IDERIV
C
      IF(IDERIV.GT.0) WRITE(6,4092)
 4092 FORMAT(1X,'HAMMING ROUTINE WILL BE USED FOR INTEGRATION')
      IF(IDERIV.LE.0) WRITE(6,4093)
 4093 FORMAT(1X,'  EULER ROUTINE WILL BE USED FOR INTEGRATION')
C*********  READ IN  THE  FOLLOWING   ************
C            XO             =  INITIAL POSITION
C            PHSTEP         =  LENGTH INCREMENTS FOR PRINT OUTS
C            HSTEP          =  LENGTH INCREMENTS FOR DERIVITIVE CALCULATION
C            XL             =  UPPER LENGTH LIMIT
C
      READ(5,5000)   XO,XL,HSTEP,PHSTEP
C
      WRITE(6,4094) XO,XL,HSTEP,PHSTEP
 4094 FORMAT (1X,'START ',F8.4,' M     STOP ',F8.4,' M     STEP SIZE ',F
     18.4,' M     PRINT EVERY ',F8.4,' M ')
      IF(IDERIV.LE.0) GO TO 40
```

```
      WRITE(6,3000)
 3000 FORMAT(1H1 )
      WRITE(6,4010)(TITLE(I),I=1,12)
C****** RESET MAGNETIC FIELD FOR THIS LOOPING
      DB=RRB
      DB2=DB*DB
      DTCON=DB2*DK*D1PL2
C*********  READ IN INITIAL CONDITIONS AT X= 0
C           RPO   PRESSURE
C           RTO   TEMPERATURE
C           RMACHO  MACH NUMBER
C           RMDOT   MASS FLOW
C
      READ(5,5000) RPO,RMDOT
      RTO    =TSTAT(6)
      RMACHO =AMACH(6)
      WRITE(6,4096) RPO,RTO,RMACHO,RMDOT
 4096 FORMAT(1X,'PO    ',E11.4,2X,'TO    ',E11.4,2X,'MACH  ',E11.4,2X,
     *  'MDOT  ',E11.4)
C
      RPO   = RPO*PO
C     FIND INITIAL DENSITY  FROM GAS LAW
      DRHOO =  RPO/(DRBAR*RTO)
C     FIND INITIAL VELOCITY  AND RHO*U  FROM SOUND VELOCITY EQ
      DU20 =     (RMACHO**2)*RTO*CONDU2/D2
      DUO     = DSQRT( D2*DU20)
      DRHOUO  = DRHOO*DUO
C     FIND  INITIAL ENTHALPY
      DHO  = DCP*(RTO-HREFT)+  HOO
C     FIND  INTIAL  D   (D4)
      D4    =DSQRT(RMDOT/DRHOUO)
C******** SET  SOME STATION VALUES
C         THE REMAINDER ARE SET IN OUTPUT ROUTINE
      ARHO(6) =DRHOO
      AVEL(6)= DUO
      AP(6)=RPO
      APS(6)=RPO*((TSTAG(6)/TSTAT(6))**GAM)
      AP(5)=RPO/((1.-CVGAM*(RMACHO**2)*(TSTAG(6)/TSTAG(5))*XXX5/
     *  (ETAN*XXX6))**GAM)
      APS(5) =  AP(5)*(XXX5**GAM)
      ARHO(5)=  AP(5)/(RRBAR*TSTAT(5))
      AP(4)  = AP(5)/(1.-HX1)
      APS(4) =AP(4)*(XXX4**GAM)
C**   SET  INTIAL  PRESS,TEMP,X  VALUES
      DPO   =RPO
      DTO   =RTO
      DFM   =RRF*D2*DRHOUO/(D4)
      DSICON     = DB2     /DRHOUO
      DSSCON =   DB2     *DK*RMDOT/DRHOUO
C     SET   IT  , AND  INTEGRAL DSUMPE
      IT    = 0
      DSUMPE       = 0.0
      DLTIME  =0.0
      DPOOLD=0.0
      DXO   = XO
      DXOLD = DXO
      DX    = DXO
      DPRINT= PHSTEP
      DHSTEP= HSTEP
      NEQA  = 3
      DXEND = XL
      DY(1) =     RPO
      DY(2) =     DU20
      DY(3) =     RTO
C****** FIND  NE FOR LOWERING OF IP(INITIAL VALUE)
      OLDNE=0.C
C*********  SET SIG2 COMMON
      RB=RRB
      RP=RPO
      RT=RTO
      D1MKP=D1MK-EEL/(DUO*RB*D4)
      DCONT2=(DUO*RB*D1MKP)**2
      A=RT
      B=TFAC*RT
      IF(OPTE.GT.0.)
     *CALL  TEROOT(A,B,XTOL,YTOL,IND)
```

```
C*****       READ PARAMETERS FOR HAMMING   ************
C            HSTEP          INITIAL TRIAL LENGTH INCREMENT FOR DERIVITIVE
C            HMAX           MAXIMUM  INCREMENT TO BE USED
C            HMIN           MINIMUM  INCREMENT TO BE USED
C            CREL           TOLERANCE FOR RELATIVE TEST
C            CABS           TOLERANCE FOR ABSOLUTE TEST
C            ICFACT         FACTOR USED FOR CRITERION OF DOUBLING HSTEP
C
      READ(5,5000)  HSTEP,HMAX,HMIN,CREL,CABS,ICFACT
C
      WRITE(6,4095) HSTEP,HMAX,HMIN,CREL,CABS,ICFACT
 4095 FORMAT(1X,'HSTEP ',E11.4,2X,'HMAX  ',E11.4,2X,'HMIN  ',E11.4,2X,
     *       'CREL  ',E11.4,2X,'CABS  ',E11.4,2X,'ICFACT',I8)
      DHSTEP       =    HSTEP
      DHMAX        =    HMAX
      DHMIN        =    HMIN
      DCREL        =    CREL
      DCABS        =    CABS
 40   CONTINUE
      CVGAM=(VGAM-1.)*0.5
C********     READ IN CLOSE CYCLE PARAMETERS
C            ETAD           EFFICIENCY FOR DIFFUSER
C            ETAC           EFFICIENCY FOR COMPRESSOR
C            ETAN           EFFICIENCY FOR NOZZEL
C            HX1            HEAT EXCHANGER EFF
C            HX2            HEAT EXCHANGER EFF
C            ETACDC         DC TO AC CONVERSION EFF
C            ETASP          EFFICIENCY FOR
C            NSI            NUMBER OF INTERCOOLER STAGES
C            EHX2           EFF
C            TSTAG( )       ARRAY FOR STAGNATION TEMP
C            TSTAT( )       ARRAY FOR STATIC TEMP
C            APS( )         ARRAY FOR STAGNATION  PRESSURE
C            AP( )          ARRAY FOR STATIC PRESSURE
C            ARHO( )        ARRAY FOR GAS DENSITIES
C            AVEL( )        ARRAY FOR GAS VELOCITIES
C            AMACH( )       ARRAY FOR MACH NUMBERS
      READ(5,5000) (AMACH(I),I=1,6),AMACH(8),AMACH(9)
      READ(5,5000) TSTAG(1),TSTAG(5)
      READ(5,5000) ETAD,ETAC,ETAN,HX1,HX2,ETACDC,ETASP,NSI,EHX2
      WRITE (6,6000) ETAC,ETAN,ETAD,ETACDC,ETASP,ETACDC,EHX2,HX1,HX2,NSI
 6000 FORMAT (1X,'EFFICIENCY OF COMPONENTS'/6X,'ADIABATIC COMPRESSOR',25
     1X,F8.4/6X,'ADIABATIC NOZZLE',29X,F8.4/6X,'ADIABATIC DIFFUSER',27X,
     2F8.4/6X,'DC TO AC INVERTER',28X,F8.4/6X,'BOTTOMING PLANT',30X,F8.4
     3/6X,'ALTERNATOR IN BOTTOMING PLANT',16X,F8.4/6X,'HEAT RECIEVED BY
     4BOTTOMING PLANT FROM HX2',04X,F8.4//1X,'PRESSURE LOSS COEFFICIENT,
     5 DELTA-P/P '/6X,'HX1',42X,F8.4/6X,'HX2',42X,F8.4//1X,'NUMBER OF ST
     6AGES OF INTERCOOLING',19X,I3/)
C********    SET FIXED VALUES
      XXX1    =    1. + CVGAM*(AMACH(1)**2)
      XXX2    =    1. + CVGAM*(AMACH(2)**2)
      XXX3    =    1. + CVGAM*(AMACH(3)**2)
      XXX4    =    1. + CVGAM*(AMACH(4)**2)
      XXX5    =    1. + CVGAM*(AMACH(5)**2)
      XXX6    =    1. + CVGAM*(AMACH(6)**2)
      XXX8    =    1. + CVGAM*(AMACH(8)**2)
      XXX9    =    1. + CVGAM*(AMACH(9)**2)
      TSTAG(6)  =TSTAG(5)
      TSTAG(3)  =TSTAG(1)
      TSTAG(9)  =TSTAG(1)
      TSTAT(9)=TSTAG(9)/XXX9
      TSTAT(6)=TSTAG(6)/XXX6
      TSTAT(5)=TSTAG(5)/XXX5
      TSTAT(3)=TSTAG(3)/XXX3
      TSTAT(1)=TSTAG(1)/XXX1
      AVEL(5)     =AMACH(5)*SQRT(CONDU3*TSTAT(5))
      AVEL(3)     =AMACH(3)*SQRT(CONDU3*TSTAT(3))
      AVEL(1)     =AMACH(1)*SQRT(CONDU3*TSTAT(1))
C
      READ(5,5000)  NCASE
C
      WRITE(6,4080) NCASE
 4080 FORMAT(1X,'NCASE ',I3)
C*****       NCASE LOOP          ************
      DO  9999  ICASE = 1,NCASE
C******** SKIP A PAGE *************
```

```
      K=1
      XTE=A
      CALL SIG(A,B,XTE,K)
      OLDNE=XNE+1.1
      IF(IDERIV.GT.0) GO TO 50
      CALL  EULER(NEQA,DX,DY,EDERIV,OUTPUT)
      GO TO 9999
   50 CONTINUE
      CALL  HAMMNG(NEQA,DX,DHSTEP,DHMAX,DHMIN,DCREL,DCABS,ICFACT,
     1  DY,EDERIV,OUTPUT,HFAIL)
 9999 CONTINUE
      END
      SUBROUTINE EULER(N,DT,DY0,F,O)
      IMPLICIT DOUBLE PRECISION (D)
      DIMENSION  DY0(1),DY1(7),DP(7),DDY1(7)
      LOGICAL RETN
      RETN = .FALSE.
      DOP5 =0.5D0
      DT1 =DT
      DO  10 I=1,N
   10 DY1(I)=DY0(I)
      CALL  F(DT1,DY1,DDY1)
   15 CALL O(DT,DY1,DDY1,RETN)
      IF(RETN) GO TO 35
      DHD2=DOP5*(DT-DT1)
      DO 20 I=1,N
      DS=DHD2*DDY1(I)
      DY =DY1(I)+DS
      DP(I)=DY
      DY1(I)=DY+DS
   20 CONTINUE
      CALL F(DT,DY1,DDY1)
      DO 30 I=1,N
   30 DY1(I)=DP(I)+DHD2*DDY1(I)
      DT1=DT
      CALL F(DT1,DY1,DDY1)
      GO TO 15
   35 RETURN
      END
```

```
      SUBROUTINE HAMMNG(K, X, H, HMAX, HMIN, CREL, CABS, ICFACT, YO,
     1 BOXA,BOXB,BOXD )
C HAMMING METHOD FOR SOLVING A SYSTEM OF FIRST ORDER ORDINARY
C          DIFFERENTIAL EQUATIONS                                        OOOOOOO
C          K           NUMBER OF EQUATIONS
C          X           INDEPENDENT VARIABLE CONTAINING ITS STARTING VALUE
C          H           VARIABLE CONTAINING STARTING VALUE OF STEP SIZE
C          HMAX        MAXIMUM ALLOWABLE STEP SIZE
C          HMIN        MINIMUM ALLOWABLE STEP SIZE
C          CREL        RELATIVE ERROR TOLERANCE
C          CABS        ABSOLUTE ERROR TOLERANCE
C          CFACT       FACTOR USED FOR THE CRITERION FOR DOUBLING  H
C          YO          ARRAY OF INITIAL VALUES OF DEPENDENT Y VARIABLES
C          BOXA        PROCEDURE FOR EVALUATING THE DERIVATIVES
C          BOXB        PROCEDURE FOR OUTPUT AFTER EACH SUCCESSFUL INTEGRATI
C          BOXD        PROCEDURE    FOR EXITING WHEN ERROR CRITERIA FAILS
      IMPLICIT LOGICAL(A-Z)
      DOUBLE PRECISION  X,H,HMAX,HMIN,CREL,CABS,YO(1)
      INTEGER  K,ICFACT
      DOUBLE PRECISION Y(7,9),DY(7,9),C(7),DC(7),YY(7),DYY(7),RK1(7),
     1                 RK2(7),RK3(7),DTABS(7)
      DOUBLE PRECISION  RTEST,ATEST,T,XTEMP,TT,TEST,CON1,CON2,CON3,TREL,
     1                  TABS,TDH,Y1,DY1,Y2,DY2,Y3,DY3
      INTEGER  IA,IB,I,IM1,J,L,LPI,LP1,LP2,LP3,LP4,I2M1
C
      IC    = .FALSE.
      RTEST = 15.*CREL
      ATEST = 15.*CABS
```

```
      DO 10 J=1,K
   10 Y(J,1) = YO(J)
      IF (HMAX.LT.0)  H = -ABS(H)
CXXXXXXX THE NEXT TWO STATEMENTS ADDED BY RWL  2/5/75
CXXXXXXX FOR OBTAINING INITIAL CONDITIONS
      CALL BOXA(X,YO,DYY)
      CALL BOXB(X,YO,DYY,IC)
C RUNGE-KUTTA FOURTH ORDER FOR STARTING INTEGRATION
      H = 2.*H
      IA = 2
      IB = 2
  100 DO 190 I=IA,IB                                                    CCCCCCC
      IM1 = I-1
      DO 110 J=1,K
  110 YY(J) = Y(J,IM1)
      CALL BOXA(X, YY, DYY)
      DO 120 J=1,K
      T = DYY(J)
      DY(J,IM1) = T
      T = T*H
      RK1(J) = T
      T = YY(J) + .5*T
      YY(J) = T
      Y(J,I) = T
  120 CONTINUE
      XTEMP = X+.5*H
      CALL BOXA(XTEMP, YY, DYY)
      DO 130 J=1,K
      T = DYY(J)
      DY(J,I) = T
      T = T*H
      RK2(J) = T
      T = Y(J,IM1) + .5*T
      YY(J) = T
      Y(J,I) = T
  130 CONTINUE
      CALL BOXA(XTEMP, YY, DYY)
      DO 140 J=1,K
      T = DYY(J)
      DY(J,I) = T
      T = T*H
      RK3(J) = T
      T = Y(J,IM1) + T
      YY(J) = T
      Y(J,I) = T
  140 CONTINUE
      X = X+H
      CALL BOXA(X, YY, DYY)
      DO 150 J=1,K
      Y(J,I) = Y(J,IM1)+.166666666666*(RK1(J)+2.*(RK2(J)+RK3(J)) +
     1    H*DYY(J))
  150 DY(J,I) = DYY(J)                                                  CCCCCCC
  190 CONTINUE                                                          CCCCCCC
  200 IF (.NOT.(IB.EQ.2)) GO TO 250
  210 DO 220 J=1,K
  220 C(J) = Y(J,2)
      X = X-H
      H = .5*H
      IF (ABS(H).GE.ABS(HMIN)) GO TO 240
      DO 230 J=1,K
      YY(J)= Y(J,1)
  230 DYY(J) = DY(J,1)
      CALL BOXD(X, YY, DYY)
      RETURN
  240 IB = 3
      GO TO 100
  250 IF (.NOT.(IB.EQ.3))  GO TO 300
      DO 260 J=1,K
      T = Y(J,3)
      TEST = ABS(C(J)-T)
      TT = ABS(T)*RTEST
      IF (.NOT.((TEST.GT.TT).AND.(TEST.GT.ATEST)))  GO TO 260
      X = X-H
      GO TO 210
  260 CONTINUE
      IA = 4
```

```
      IB = 4
      GO TO 100
  300 CONTINUE
      DO 310 J=1,K
  310 YY(J) = Y(J,4)
      CALL BOXA(X, YY, DYY)
      DO 320 J=1,K
  320 DY(J,4) = DYY(J)
C OUTPUT RUNGE-KUTTA RESULTS
      X = X - 4.*H
      DO 400 I=1,4
      X = X+H
      DO 330 J=1,K
      YY(J) = Y(J,I)
  330 DYY(J) = DY(J,I)
  400 CONTINUE
      CALL BOXB(X, YY, DYY, IC)
      IF (IC)      RETURN
C CONSTANTS AND TEST VARIABLES FOR HAMMING
      CON2 = 1./121.
      CON1 = 112.*CON2
      CON2 = 9.*CON2
      CON3 = 1./128.
      T = 1./CON2
      TREL = CREL*T
      TABS = CABS*T
      DTABS(1) =TABS*1.0E-4
      DTABS(2) =TABS*1.0E-5
      DTABS(3) =TABS*1.0E-2
      T = ICFACT
      IF (T.EQ.0.0) T = 100.
      TDH = TREL/T
      L = 1
      GO TO 510
C RESTORE Y AND DY
  410 DO 420 I=1,4
      LPI = L+I
      DO 420 J=1,K
      Y(J,I) = Y(J,LPI)
      DY(J,I) = DY(J,LPI)
  420 CONTINUE
      L = 1
C INTEGRATE
  510 X = X+H
      LP1 =  L+1
      LP2 =  L+2
      LP3 =  L+3
      LP4 =  L+4
      DO 520 I=1,K
      C(I) = Y(I,L)+1.33333333333*H*(2.*(DY(I,LP1)+DY(I,LP3)) -
     1    DY(I,LP2))
  520 CONTINUE
      CALL BOXA(X, C, DC)
      DO 600 I=1,K
      T = .125*(9.*Y(I,LP3) - Y(I,LP1) + 3.*H*(DC(I) + 2.*DY(I,LP3) -
     1    DY(I,LP2)))
      C(I) = C(I)-T
      Y(I,LP4) = T
      TT = TREL*ABS(T)
      TEST = ABS(C(I))
      TABS =DTABS(I)
      IF ((TEST.GT.TT).AND.(TEST.GT.TABS))  GO TO 710
  600 CONTINUE
  610 DO 620 I=1,K
      YY(I) = Y(I,LP4) + CON2*C(I)
  620 Y(I,LP4) = YY(I)
      CALL BOXA(X, YY, DYY)
      CALL BOXB(X, YY, DYY, IC)
      IF (IC)      RETURN
      DO 630 I=1,K
  630 DY(I,LP4) = DYY(I)
C CHECK FOR DOUBLING INTEGRATION STEP
      IF (ABS(2.*H).GT.ABS(HMAX))  GO TO 410
      DO 640 I=1,K
      TT = TDH*ABS(YY(I) )
      TEST = ABS(C(I))
```

```
      TABS =DTABS(I)
      IF ((TEST.GT.TT).AND.(TEST.GT.TABS))  GO TO 410
  640 CONTINUE
      IF (.NOT.L.EQ.3)  GO TO 700
      DO 650 I=1,4
      I2M1 = 2*I-1
      DO 650 J=1,K
      Y(J,I) = Y(J,I2M1)
      DY(J,I) = DY(J,I2M1)
  650 CONTINUE
      H = 2.*H
      L = 1
      GO TO 510
  700 L = LP1
      GO TO 510
C CHECK FOR HALVING STEP SIZE.  IF LESS THAN HMIN, TERMINATE
  710 IF (ABS(.5*H).GE.ABS(HMIN))  GO TO 730
      DO 720 I=1,K
      YY(I) = Y(I,LP3)
  720 DYY(I) = DY(I,LP3)
      X = X-H
      CALL BOXD(X, YY, DYY)
      RETURN
  730 DO 740 J=1,K
      Y1 = Y(J,LP1)
      Y2 = Y(J,LP2)
      Y3 = Y(J,LP3)
      DY1 = DY(J,LP1)
      DY2 = DY(J,LP2)
      DY3 = DY(J,LP3)
      Y(J,1) = CON3*(11.*Y3 + 72.*Y2 + 45.*Y1 - H*(3.*DY3 + 36.*DY2 -
     1     9.*DY1))
      Y(J,2) = Y2
      DY(J,2) = DY2
      Y(J,3) = CON3*(45.*Y3 + 72.*Y2 + 11.*Y1 + H*(-9.*DY3 + 36.*DY2 +
     1     3.*DY1))
      Y(J,4) = Y3
      DY(J,4) = DY3
  740 CONTINUE
      X = X-H
      H = H/2.
      L = 1
      T = X-3.*H
      TT = X-H
      DO 750 I=1,K
      C(I) = Y(I,1)
  750 YY(I) = Y(I,3)
      CALL BOXA(T, C, DC)
      CALL BOXA(TT, YY, DYY)
      DO 760 I=1,K
      DY(I,1) = DC(I)
  760 DY(I,3) = DYY(I)
      GO TO 510
C END HAMMNG
      END
```

```
      SUBROUTINE EDERIV(DX,DY,DDY)
C*****      THIS ROUTINE MAY BE USE EITHER BY HAMMING OR EULER ROTINES
C           DX     INDEPENDENT VARIABLE   DISTANCE (METERS)
C           DY( ) DEPENDENT   VARIABLES
C              1  DP    PRESSURE
C              2  DU2   KINETIC ENERGY PER MASS (U**2/2)
C              3  DT    TEMPERATURE  ( GAS  DEG KELVIN )
C           DDY( )   DERIVATIVES OF DEPENDENT  VARIABLES
      IMPLICIT DOUBLE PRECISION (D)
      DIMENSION  DY(1),DDY(1)
      COMMON/CONST/ D1,D2,DP5,DRBAR,DRHOU0,DPCON,DFM,DC,DTCON,DCP,DK,
     *  XTOL,YTOL,DHSTEP,DSSCON,EEL,D1MKP,TESTIP,DBB0,COBB0,OPTE,
     1  IDERIV,DSICON,DMCON,PGROSS,DSUMPE,TESTB,TESTXD,DXEND,DPOOLD,
     2  D1PC,D1MK,DB,D1PL2,D4,DP0,DU20,DT0,DRH00,DX0,DXOLD,DB2,IT,RMACHO
```

```
     3 ,DLTIME,DPRINT,DHO,GAM,DSOO,SREFT,TFAC
      COMMON/VAR/ DP,DU2,DU,DT,DRHO,DZ2,DZ3,SIGMA
      COMMON/SIG2/ DCONT2,RP,RT,RB,RMWB,RMWS,IGAS,CONEI,CONAQ
      DP    = DY(1)
      DU2   = DY(2)
      DU    = DSQRT(D2*DU2)
      DT    = DY(3)
C     FIND  GAS DENSITY  USING GAS LAW
      DRHO  = DP/(DRBAR*DT)
C     FIND  AREA  RATIO  USING CONTINUITY EQ
      DZ2   = DRHOUO/(DRHO*DU)
      DZ3   = DZ2*DSQRT(DZ2)
C     FIND  ELECTRON  TEMPERATURE
C     SET   SIG2  COMMON  FOR  SIG ROUTINE
      RB  = DB
      RT  = DT
      RP  = DP
      DCONT2  = (DU*DB*D1MKP)**2
C     SET  LOWER AND  UPPER BOUNDS  ON TE
      A  = DT
      B  = TFAC*DT
C     FIND  ELECTRON  TEMPERATURE
      IF(OPTE.GT.0.)
     *CALL  TEROOT(A,B,XTOL,YTOL,IND)
      K  = 1
      XTE = A
C     FIND  ELECTRICAL CONDUCTIVITY
      CALL  SIG(SIGMA,RFUNCK,XTE,     K)
C**** FIND  PRESSURE  GRADIENT
      DDY(1) = -DPCON*DU*(DZ3*SIGMA*DB2*D1MKP + DFM)/DZ3
C**** FIND  (U**2)/2   GRADIENT
      DDY(2) = DC*DDY(1)/DRHO
C**** FIND  TEMPERATURE GRADIENT
      DDY(3) = -(DTCON*DU*SIGMA*D1MKP/DRHO + DDY(2))/DCP
      RETURN
      END



      SUBROUTINE  OUTPUT(   DX,DY,DDY,RETN)
C**** THIS ROUTINE IS USED BY BOTH EULER AND HAMMING ROUTINES
      IMPLICIT DOUBLE PRECISION (D)
      DIMENSION DY(1),DDY(1)
      COMMON/CONST/ D1,D2,DPS,DRBAR,DRHOUO,DPCON,DFM,DC,DTCON,DCP,DK,
     *  XTOL,YTOL,DHSTEP,DSSCON,EEL,D1MKP,TESTIP,DBBO,COBBO,OPTE,
     1  IDERIV,DSICON,DMCON,PGROSS,DSUMPE,TESTB,TESTXD,DXEND,DPOOLD,
     2 D1PC,D1MK,DB,D1PL2,D4,DPO,DU2O,DTC,DRHOC,DXO,DXOLD,DB2,IT,RMACHO
     3 ,DLTIME,DPRINT,DHO,GAM,DSOO,SREFT,TFAC
      COMMON/VAR/ DP,DU2,DU,DT,DRHO,DZ2,DZ3,SIGMA
      COMMON/SIG1/ FACEV,GASKO,FAC,RVO,LOGSAC,QBO,PB,QBS,PS,CB1,CS1,
     1 CB2,CS2,CSIGO,CSIGE2,CSIGEI,CBETA,REPS,DCONTI,RFUNC,CLOW,OLDNE,
     2 RTE,BETA,XNB,XNA,XNE,XNU1,XNU2,XSIGO,XSIGEI,XSIGAD,XSIG,XSIGEF
      COMMON/STATIO/ TSTAT(9),TSTAG(9),AP(9),APS(9),ARHO(9),AVEL(9),
     1 AMACH(9),QQQ(9),WWW(9),XXX1,XXX2,XXX3,XXX4,XXX5,XXX6,XXX7,XXX8,
     2 ETAD,ETAC,ETAN,HX1,HX2,ETACDC,ETASP,NSI,
     3 CVGAM,CONDU2,RMDOT,CONDU3, RRBAR,BCP,EHX2,XXX9
      LOGICAL  RETN
      IT    = IT +1
C******** SET OLDNE TO PREVIOUS NE    **********
      OLDNE=XNE
C************  DETERMINE  LOCAL  CURRENT DENSITY  J
      DJ =  SIGMA*DU*DB*D1MKP
C************  INTEGRATE  GROSS ENERGY  (TRAPAZODIAL RULE)
      DELX  = DX-DXOLD
      DPONEW =DSSCON*SIGMA*DU2*DZ2*D1MKP
      DSUMPE = (DPONEW +DPOOLD)*DELX  +  DSUMPE
C     NOTE  0.5 FACTOR IS IN DU2
      DXOLD  = DX
      DPOOLD = DPONEW
C************  DETERMINE  LOCAL  INTERACTION PARAMATER
      DSI    =  SIGMA*DZ2*DSICON*DX*D1MKP
C************   DETERMINE  MACH  NUMBER
      RMACH =  DMCON*DU/DSQRT(DT)
      D     = D4*DSQRT(DZ2)
```

```
      AREA=D*D
      XOD    = DX/D
C******     TEST FOR STOPING INTEGRATION ******************************
C*****  INTERACTION PARAMETER TEST
      IF(.NOT.(DSI.GE.TESTIP)) GO TO 80
      RETN=.TRUE.
      WRITE(6,1998)
 1998 FORMAT(1X,'INTEGRATION TERMINATED DUE TO TEST ON INTERACTION PRA')
C****          1-K-E/(U*B*D)     TEST
 80     IF(.NOT.(D1MKP.LT.0.0)) GO TO 90
      RETN=.TRUE.
      WRITE(6,1999)
 1999 FORMAT(1X,'INTEGRATION TERMINATED DUE TO TEST ON D1MKP')
C*****         TOTAL LENGTH
 90   IF(.NOT.(DX.GT.DXEND)) GO TO 100
      RETN   =      .TRUE.
      WRITE(6,2001)
 2001 FORMAT(1X,'INTEGRATION TERMINATED DUE TO TEST ON TOTAL LENGTH')
C*****         TOTAL POWER
 100  IF(.NOT.(DSUMPE.GE.PGROSS)) GO TO 200
      RETN   =      .TRUE.
      WRITE(6,2002)
 2002 FORMAT(1X,'INTEGRATION TERMINATED DUE TO TEST ON TOTAL POWER')
C*****         MACH NUMBER
 200  IF(.NOT.(RMACH0.GT.1.0.AND.RMACH.LE.1.05)) GO TO 300
      RETN   =      .TRUE.
      WRITE(6,2003)
 2003 FORMAT(1X,'INTEGRATION TERMINATED DUE TO TEST ON MACH NUMBER')
C*****         LENGTH/DIAMETER RATIO
 300  IF(.NOT.(IT.GT.4.AND.XOD.GE.TESTXD)) GO TO 400
      RETN   =      .TRUE.
      WRITE(6,2004)
 2004 FORMAT(1X,'INTEGRATION TERMINATED DUE TO TEST ON L/D RATIO')
C*****         HALL PARAMETER
 400  IF(.NOT.(BETA.GE.TESTB)) GO TO 500
      RETN   =      .TRUE.
      WRITE(6,2005)
 2005 FORMAT(1X,'INTEGRATION TERMINATED DUE TO TEST ON HALL PARAMETER')
C*****         GAS TEMPERATURE
 500  IF(.NOT.(DT.LT.3.0D2)) GO TO 600
      RETN   =      .TRUE.
      WRITE(6,2006)
 2006 FORMAT(1X,'INTEGRATION TERMINATED DUE TO TEST ON GAS TEMP')
 600  CONTINUE
      IF(RETN)  IP =0
      IF(RETN) GO TO 25
C***** TEST FOR PRINT OUT (DEPENDENT ON USE OF HAMMING OR EULER )
      IP   = 0
      IF(IT.EQ.1) GO TO 25
      IF(IDERIV.GT.0.AND.IT.EQ.2) GO TO  25
      IF(DX.GE.(DLTIME+ DPRINT))  IP =1
      IF(IP.EQ.1) DLTIME = DLTIME + DPRINT
      IF(IP.EQ.1) GO TO 25
      GO TO 900
 25   CONTINUE
C*****  PRINT OUT RESULTS
C******* CALCULATE  ENTHALPY
      H   =  DH0 + DCP*(DT-DT0)
C******* CALCULATE  STAGNATION ENTHALPY
      HS =   H + DU2
C******* CALCULATE  STAGNATION TEMPERATURE BASED ON ISENTROPIC CHANGE
      TS =   DT  + DU2/DCP
C******* CALCULATE  STAGNATION PRESSURE  BASED  ON ISENTROPIC CHANGE
      PPS= DP*((TS/DT)**GAM)
C******* CALCULATE  ENTROPY
      S   = DS00  + DCP*DLOG(DT/SREFT) -DRBAR*DLOG(DP)
C******* CALCULATE STANATION DENSITY
      RHOS =PPS/(DRBAR*TS)
      RDY   =  DSQRT(DZZ)
      DM    =  D4*(RDY + 1.0)
      XPDMTD = (DX+DM)*DM
      RMU    = BETA/DB
      WRITE(6,1000)
      WRITE(6,1101)  DX,DELX,AREA,D1MKP,DB
      WRITE(6,1102)     DZ2,RDY,XOD,XPDMTD
      WRITE(6,1103)  DT,TS,RTE,RFUNC
```

```
      WRITE(6,1104)  IT,DP,PPS
      WRITE(6,1105)  DRHO,RHOS
      WRITE(6,1106)  H,HS,S,DSI
      WRITE(6,1107)  DU,DU2,RMACH,RMU,BETA
      WRITE(6,1108)  XSIGEF,XSIG,XNU1,XNU2,XSIGO
      WRITE(6,1109)  XNE,XNA,XNB,DJ,DSUMPE
      WRITE(6,1000)
 1000 FORMAT(1X,'*****************************************')
 1101 FORMAT(6X,'X ',E11.4, 1X,'AX     ',E11.4,6X,'A      ',E11.4,6X,
     *  '1-KP   ',E11.4,6X,'B      ',E11.4)
 1102 FORMAT(20X      ,'A/AO  ',E11.4,6X,'D/D4  ',E11.4,6X,'X/D    ',E11.4
     *,6X,'(X+DM)*DM',E11.4)
 1103 FORMAT(20X,'T      ',E11.4,6X,'TS     ',E11.4,6X,'TE     ',E11.4 ,
     *  29X,'FUNCTE',E11.4)
 1104 FORMAT(6X,I8,6X,'P      ',E11.4,6X,'PS     ',E11.4)
 1105 FORMAT(20X,'RHO    ',E11.4,6X,'RHOS   ',E11.4)
 1106 FORMAT(20X,'H      ',E11.4,6X,'HS     ',E11.4,6X,'S      ',E11.4,29X,
     1'INPRAM',E11.4 )
 1107 FORMAT(20X,'U      ',E11.4,6X,'U2     ',E11.4,6X,'MACH   ',E11.4,6X,
     1'MU     ',E11.4,6X,'MUB    ',E11.4)
 1108 FORMAT(20X,'SIGEFF',E11.4,6X,'SIG    ',E11.4,6X,'NU1    ',E11.4,6X,
     1'NU2    ',E11.4,6X,'LOWIP  ',E11.4)
 1109 FORMAT(20X,'NE     ',E11.4,6X,'NA     ',E11.4,6X,'NB     ',E11.4,6X,
     1'J      ',E11.4,6X,'POWER  ',E11.4)
 900  CONTINUE
      IF(.NOT.RETN) GO TO 9000
      TSTAG(7)=TS
      TSTAT(7)=DT
      AVEL(7)=DU
      AMACH(7)=RMACH
      AP(7)=DP
      APS(7)=PPS
      ARHO(7)=DRHO
      XXX7    =    1. + CVGAM*(AMACH(7)**2)
      XXX=(ETAD*CVGAM*(RMACH**2)+1.)/XXX8
      AP(8)=AP(7)*(XXX**GAM)
      APS(8)=AP(8)*(XXX8**GAM)
      TSTAG(8)=TSTAG(7)
      TSTAT(8)=TSTAG(8)/XXX8
      ARHO(8)=AP(8)/(DRBAR*TSTAT(8))
      AVEL(8)     =AMACH(8)*SQRT(CONDU2*TSTAT(8))
      AP(1)=(1.-HX2)*AP(8)
      APS(1)=AP(1)*XXX1
      APS(9)=APS(1)
      AP(9)=APS(9)/(XXX9**GAM)
      ARHO(9)=AP(9)/(DRBAR*TSTAT(9))
      AVEL(9)=AMACH(9)*SQRT(CONDU2*TSTAT(9))
      ARHO(1)=AP(1)/(RRBAR*TSTAT(1))
      XX=1./(1+NSI)
      XX2=1./GAM
      XXX=(APS(4)/APS(1))**XX
      TSTAG(2)=TSTAG(1)*(1.+(XXX**XX2-1.)/ETAC)
      TSTAT(2)=TSTAG(2)/XXX2
      APS(2)=APS(1)*XXX
      AP(2)=APS(2)/(XXX2**GAM)
      ARHO(2)=AP(2)/(RRBAR*TSTAT(2))
      AVEL(2)     =AMACH(2)*SQRT(CONDU3*TSTAT(2))
      APS(3)=APS(2)
      AP(3)=APS(3)/(XXX3**GAM)
      ARHO(3)=AP(3)/(RRBAR*TSTAT(3))
      TSTAG(4)=TSTAG(2)
      TSTAT(4)=TSTAG(4)/XXX4
      AVEL(4)     =AMACH(4)*SQRT(CONDU3*TSTAT(4))
      ARHO(4)=  AP(4)/(RRBAR*TSTAT(4))
      AVEL(6)     =AMACH(6)*SQRT(CONDU2*TSTAT(6))
C******** AT THIS POINT ALL STATION VALUES ARE SET
      XXX=(1.-(APS(7)/APS(6))**XX2)*TSTAG(6)
      ETAMHD=(TSTAG(6)-TSTAG(7))/XXX
      EMHD=(TSTAG(6)-TSTAG(7))/(TSTAG(5)-TSTAG(4))
C*** LOOSES
      WWW(1)=BCP*(TSTAG(1)-TSTAG(2))
      WWW(2)=0.
      WWW(3)=BCP*(TSTAG(3)-TSTAG(4))
      WWW(4)=0.
      WWW(5)=0.
      WWW(6)=DCP*(TSTAG(6)-TSTAG(7))/D1PL2
```

```
      WWW(7)=0.
      WWW(8)=0.
      WWW(9) = 0.
      QQQ(1) = 0.
      QQQ(2) =BCP*(TSTAG(3)-TSTAG(2))
      QQQ(3) = 0.
      QQQ(4) =BCP*(TSTAG(5)-TSTAG(4))
      QQQ(5) = 0.
      QQQ(6) = -WWW(6)*(D1PL2-1.0D0)
      QQQ(7) = 0.
      QQQ(8) =DCP*(TSTAG(9)-TSTAG(8))
      QQQ(9) = 0.
      GENMHD=ETACDC*WWW(6)
      STEAMP=ETACDC*(((1.-ETACDC)*WWW(6)-NSI*QQQ(2)-QQQ(8)*EHX2-QQQ(6))
     1 *ETASP*(1+NSI)*WWW(1))
      TOTALS=GENMHD+STEAMP
      EFFIC=TOTALS/QQQ(4)
      GENMHD=RMDOT*GENMHD
      STEAMP=RMDOT*STEAMP
      TOTALS=RMDOT*TOTALS
      WRITE(6,3000)
 3000 FORMAT(1X,/,1X,/,1X)
      WRITE(6,3010)
 3010 FORMAT(1X,'STATION',8X,'T',12X,'TS',11X,'P',12X,'PS',11X,'RHO',10X
     *  ,'U',12X,'M',12X,'Q',12X,'W')
      DO 800 I=1,9
      WWW(I)=WWW(I)*RMDOT
      QQQ(I)=QQQ(I)*RMDOT
      WRITE(6,3020)  I,TSTAT(I),TSTAG(I),AP(I),APS(I),ARHO(I),AVEL(I),
     *  AMACH(I),QQQ(I),WWW(I)
 3020 FORMAT(1X,I5,5X,9(E11.4,2X))
  800 CONTINUE
      WRITE(6,3000)
      WRITE(6,3030) GENMHD,STEAMP,TOTALS,EFFIC
 3030 FORMAT(1X,'MHD ',E11.4,5X,'STEAM PLANT',E11.4,5X,'TOTAL ',E11.4,
     *  5X,'EFFICIENCY',E11.4)
      WRITE(6,3040) ETAMHD,EMHD
 3040 FORMAT(1X,'ETA-MHD',E11.4,5X,'EFF-MHD',E11.4)
      GO TO 9999
 9000 CONTINUE
      IF(IDERIV.GT.0) GO TO 9999
      DX = DX * DHSTEP
 9999 CONTINUE
      DB=DBB0*(D1-C0BB0*DX)
      D82=DB*DB
      DTCON=DB2*DK*D1PL2
      DSICON=DB2/DRHOU0
      DSSCON=DB2*DK*RMDOT/DRHOU0
      D1MKP=D1MK-EEL/(DU*DB*D)
      IF(DB.LE.0.0D0) RETN=.TRUE.
      IF(DB.LE.0.0D0) WRITE(6,8888)
 8888 FORMAT(1X,'THIS CASE TERMINATED DUE TO TEST ON MAGNETIC FIELD')
      END



      SUBROUTINE HFAIL(DTIME,DY,DDY)
      IMPLICIT DOUBLE PRECISION (D)
      DIMENSION DY(1),DDY(1)
      RTIME=DTIME
      WRITE(6,2000)
 2000 FORMAT(6X,' FAILURE OCCURED IN HAMMING ROUTINE')
      WRITE(6,2500) RTIME
 2500 FORMAT(6X,'TIME AT FAILURE IS   ',E15.4)
      STOP
      RETURN
      END
```

```
      SUBROUTINE  TEROOT(A,B,XTOL,YTOL,IND)
      IND   = 0
      M=0
      K     = -1
      X1    = A
      X2    = B
      Y1    = -1.0
  100 CONTINUE
      CALL  SIG(R1,Y2,X2,   K)
      IF(Y2.GT.0.0) GO TO 120
      M=M+1
      IF(M.GT.8) STOP
      B=2.*B
      X2=B
      GO TO 100
  120 X3    = 0.0
      IF(X1*X2 .GT. 0.0) X3 = (X1+X2)*0.5
      CALL  SIG(R1,Y3,X3,   K)
  130 IF(ABS(Y3).LT.YTOL) GO TO 535
      IF(ABS(X2-X1).LT.XTOL) GO TO 531
  140 IF((Y3-Y1)*(Y2-Y3).LT.ABS(Y2-Y1)*YTOL) GO TO 210
  150 A1    =(X3-X2)/Y1
      A2    =(X1-X3)/Y2
      A3    =(X2-X1)/Y3
      X4    =(A1*X1 +A2*X2 + A3*X3)/(A1+A2+A3)
  160 CALL  SIG(R1,Y4,X4,   K)
  170 IF(ABS(Y4).LT.YTOL) GO TO 545
  180 IF(Y2*Y3.LT.0.)  GO TO 181
      X2    = X3
      Y2    = Y3
      GO TO 190
  181 X1    = X3
      Y1    = Y3
  190 IF(ABS(X2-X1).LT.XTOL)  GO TO 541
  200 X3    = X4
      Y3    = Y4
      GO  TO  140
  210 IF(Y2*Y3.LT.0.) GO TO 211
      X2    = X3
      Y2    = Y3
      GO  TO  120
  211 X1    = X3
      Y1    = Y3
      GO  TO  120
  531 IND   = 1
  535 A     = X3
      B     = Y3
      RETURN
  541 IND   = 1
  545 A     = X4
      B     = Y4
      RETURN
      END
```

```
      SUBROUTINE  SIG(SIGEF,RFUNCK,XTE,      K )
      IMPLICIT  DOUBLE  PRECISION (D)
      COMMON/SIG1/ FACEV,GASKO,FAC,RVO,LOGSAC,QBO,PB,QBS,PS,CB1,CS1,
     1 CB2,CS2,CSIGO,CSIGE2,CSIGEI,CBETA,REPS,DCONT1,RFUNC,CLOW,OLDNE,
     2 RTE,BETA,XNB,XNA,XNE,XNU1,XNU2,XSIGO,XSIGEI,XSIGAD,XSIG,XSIGEF
C*****   NOTE    THIS ROUTINE FINDS THE ELECTRICAL CONDUCTIVITY (K GT 0)
C        ALSO    THIS ROUTINE IS USE BY TEROOT  TO FIND
C        ELECTRON  TEMPERATURE  ( K LE 0 )
      COMMON/SIG2/ DCONT2,RP,RT,RB,RMWB,RMWS,IGAS,CONEI,CONAQ
      COMMON/QQVAL/ QCQ(37)
      COMMON/QVALUE/ QIQ(37)
      D1=1.0D0
      REV   = FACEV*XTE
      RNB   = GASKO*RP/RT
```

```
      RNC    = FAC*RNB/(1.C+FAC)
      R4NC   = 4.D*RNC
      RV1=RVO-CLOW*SQRT(OLDNE/XTE)
      DK1    = EXP(-RV1/REV + 1.5*ALOG(XTE) +LOGSAC)
      DK2    =     ((1.D +FAC*XTE/(RT*(1.C+FAC)))**2)*DK1
      DNE    = DSQRT(DK1*RNC)*(DSQRT(D1+DK2/R4NC) -DSQRT(DK2/R4NC) )
      RNE=DNE
      RNB    = (RNB-RNE*XTE/RT)/(1.D +FAC)
      RNA    = FAC*RNB
      RATIO=RNE/(RNB+RNA)
      CALL QINTRP(Q1Q,XTE,QQ)
      CALL QINTRP(QCQ,XTE,QQC)
      RNU1=CONAQ*SQRT(XTE)*(RNB*QQ/RMWB+(RNA-RNE)*QQC/RMWS)
     *    + RNE*CONEI*ALOG(1.55DE13*REV*SQRT(REV/RNE))/
     *    (XTE*SQRT(XTE)*RMWS)
      IF(IGAS.GT.4) GO TO 10
      R1=8085.C*RATIO-D.2264
      IF(R1.LT.D.) R1=D.D
      RNU2=(3.10*R1**D.71444)*(RNB*1.DE-14)
      GO TO 20
10    CONTINUE
      RNU2=(D.533+D.641*((RATIO*1.E4)**D.72))*(RNB*1.DE-14)
20    CONTINUE
      RSIG=CSIGO*RNE/RNU2
      RBETA = CBETA*RB/RNU2
      RFAC1 = ((RBETA-REPS)**2 +(RBETA*REPS)**2)/(RBETA*(RBETA +
     1  REPS*(RBETA**2 -1.D)))
      RSIGEF= RSIG*RFAC1
      DFUNCK=(DCONT1*RNE*RNU1*(XTE-RT))/(DCONT2*RSIGEF) -D1
      RFUNC = DFUNCK
      RFUNCK  = DFUNCK
      IF(K .LE.D)  GO TO  999
      SIGEF  = RSIGEF
      RTE    = XTE
      BETA   = RBETA
      XNB    = RNB
      XNA    = RNA-RNE,
      XNE    = RNE
      XNU1   = RNU1
      XNU2   = RNU2
      XSIGO  = RV1
      XSIG   = RSIG
      XSIGEF= RSIGEF
999   CONTINUE
      RETURN
      END
```

```
      SUBROUTINE QINTRP(Q,T,X)
      DIMENSION Q(1)
      M=(Q(1)+.1)
      M1=M-1
      L=-1
      DO 10 I=4,M1,2
10    IF(T.GE.Q(I-2).AND.T.LE.Q(I)) L=I
      IF(L.LT.D) STOP
      X=Q(L-1)+(Q(L+1)-Q(L-1))*(T-Q(L-2))/(Q(L)-Q(L-2))
      END
```

Subappendix AA 10.6.2

Sample Case

A sample case is presented to familiarize the reader with the actual execution of the MHD closed-cycle program. Data for this sample case is illustrative of data preparation for program execution. Typical program results for the sample data follow. All units are MKS. The MHD power out is 985.9 MW_e while the steam power out is 14.48 MW_e for a total output of 1000 MW_e. The efficiency of the MHD/steam combination is 56.96%. The MHD enthalpy extraction ratio is 0.7352 while the MHD isentropic efficiency is 0.6004.

```
DATA FOR SAMPLE CASE
1
REFERENCE CASE   SERIES 1
1.
18
2.5,1.5,39.948,132.905,0.0010
3.893,1.0,2.0
0.5 , 0.2
36
0.,0.735,500.,0.735,1000.,0.329,1500.,0.324,2000.,0.426,3000.,0.737
4000.,1.1,5000.,1.47,6000.,1.86,7000.,2.26,8000.,2.66,9000.,3.06
10000.,3.46,12000.,4.25,14000.,5.03,16000.,5.77,18000.,6.46,20000.,7.11
36
500.,1160.,1000.,1030.,1500.,793.,2000.,590.
2500.,450.,3000.,357.,3500.,296.,4000.,255.
4500.,228.,5000.,209.,5500.,195.,6000.,185.
6500.,177.,7000.,172.,7500.,167.,8000.,164.,10000.,154.,20000.,132.
36.9822,298.15,0.,298.15
4.0 , 0.02
0.200 , 0.750 , 0.008 , 0.050 , 100.
1.0E9 , 15.0 , 15.0 , 2.0 , 10.0
-1
0.000 , 25.000 , 0.010 , 100.0
0.0 , 0.0 , 0.0 , 0.0 , 0.0 , 1.10 , 0.20 , 0.0
423.0 , 2366.7
0.87,0.90,0.99,0.03,0.03,0.985,0.45,1,0.995
1
4.80 , 2030.0
```

REFERENCE CASE SERIES 1
IONIZATION OPTION - EQUILIBRIUM IF.LE.0 OR NONEQUILIBRIUM IF.GT.0 .1+01

BUFFER GAS IS ARGON

SPECIFIC HEAT AT CONSTANT PRESSURE / GAS CONSTANT	.2500+01	SPECIFIC HEAT AT CONSTANT VOLUME / GAS CONSTANT	.1500+01
MOLECULAR WEIGHT OF BUFFER GAS (KG/KILO-MOLE)	.3995+02	MOLECULAR WEIGHT OF SEED (KG/KILO-MOLE)	.1329+03
SEED FRACTION	.1000-02		
IONIZATION POTENTIAL FOR SEED (EV)	.3893+01		
PARTITION FUNCTION OF ION FOR SEED	.1000+01	PARTITION FUNCTION OF NEUTRAL FOR SEED	.2000+01

TURBULENCE FACTOR FOR NON-EQUILIBRIUM IONIZATION .5000
INCREMENT TO LOSS FACTOR FOR INELASTIC COLLISION AND RADIATION LOSSES (DELTA=1+INCREMENT) .2000

AVERAGE BUFFER GAS XSECT FOLLOW

.3700+02	.0000	.7350+00	.5000+03	.7350+00	.1000+04	.3290+00	.1500+04	.3240+00	.2000+04
.4260+00	.3000+04	.7370+00	.4000+04	.1100+01	.5000+04	.1470+01	.6000+04	.1860+01	.7000+04
.2260+01	.8000+04	.2660+01	.9000+04	.3000+01	.1000+05	.3460+01	.1200+05	.4250+01	.1400+05
.5030+01	.1600+05	.5770+01	.1800+05	.6460+01	.2000+05	.7110+01			

AVERAGE SEED GAS XSECT FOLLOW

.3700+02	.5000+03	.1160+04	.1000+04	.1030+04	.1500+04	.7930+03	.2000+04	.5900+03	.2500+04
.4500+03	.3000+04	.3570+03	.3500+04	.2980+03	.4000+04	.2550+03	.4500+04	.2280+03	.5000+04
.2090+03	.5500+04	.1950+03	.6000+04	.1850+03	.6500+04	.1770+03	.7000+04	.1720+03	.7500+04
.1670+03	.8000+04	.1640+03	.1000+05	.1540+03	.2000+05	.1320+03			

ENTROPY (CAL/MOLE.K) AT 298.15 K .3698+02 ENTHALPY (CAL/MOLE) AT 298.15 K .0000

MAGNETIC FIELD FLUX B0(1-B*X) WHERE B0 = 4.00 TESLA AND B = .0000/M

VELOCITY COEFFICIENT (C=RHO*VELOCITY*(D-VELOCITY/D-PRESSURE)) .2000
GENERATOR SEGMENT LOADING COEFFICIENT (K=INDUCED VOLTAGE/OPEN CIRCUIT VOLTAGE) .7500
FRICTION FACTOR .0080
HEAT LOSS FACTOR (MHD HEAT LOSS / MHD POWER GENERATED) .0500
VOLTAGE DROP BETWEEN GAS AND ELECTRODE (VOLTS) 100.0

PARAMETER UPPER BOUND

MHD GROSS POWER (W)	.1000+10
HALL	.1500+02
LENGTH / DIAMETER	.1500+02
INTERACTION	.1000+02
ELECTRON TEMPERATURE / GAS TEMPERATURE	.2000+01

EULER ROUTINE WILL BE USED FOR INTEGRATION
START .0000 M STOP 25.0000 M STEP SIZE .0100 M PRINT EVERY 100.0000 M

EFFICIENCY OF COMPONENTS

ADIABATIC COMPRESSOR	.9000
ADIABATIC NOZZLE	.9900
ADIABATIC DIFFUSER	.8700
DC TO AC INVERTER	.9850
BOTTOMING PLANT	.4500
ALTERNATOR IN BOTTOMING PLANT	.9850
HEAT RECIEVED BY BOTTOMING PLANT FROM HX2	.9950

PRESSURE LOSS COEFFICIENT, DELTA-P/P

HX1	.0300
HX2	.0300

NUMBER OF STAGES OF INTERCOOLING 1

NCASE 1

REFERENCE CASE SERIES 1

PO .4800+01 TO .1700+04 MACH .1100+01 MDOT .2035+04

X	.0000	AX	.0000	A	.1738+01	1-KP	.2274+00	B	.4000+01		
		A/AO	.1000+01	D/D4	.1000+01	X/D	.0000	(X+DM)+DM	.6954+01		
		T	.1686+04	TS	.2367+04	TE	.2457+04			FUNCTE	.1979-07
	1	P	.4964+06	PS	.1135+07						
		RHO	.1390+01	RHOS	.2311+01						
		M	.7200+06	MS	.1073+07	S	.2043+04			INPRAM	.0000
		U	.8400+03	U2	.7526+06	MACH	.1100+01	MU	.1272+01	MUB	.5087+01
		SIGEFF	.1428+02	SIG	.4629+02	NU1	.1748+10	NU2	.1383+12	LOWIP	.3884+01
		NE	.2271+21	NA	.2064+23	NB	.2087+26	J	.1091+05	POWER	.0000

INTEGRATION TERMINATED DUE TO TEST ON TOTAL POWER

X	.1253+02	AX	.1000-01	A	.1137+02	1-KP	.2354+00	B	.2998+01		
		A/AO	.6543+01	D/D4	.2558+01	X/D	.3715+01	(X+DM)+DM	.9078+02		
		T	.9216+03	TS	.1368+04	TE	.2627+04			FUNCTE	-.5886-05
	1254	P	.5012+05	PS	.1347+06						
		RHO	.2522+00	RHOS	.4743+00						
		M	.3333+06	MS	.5551+06	S	.2201+04			INPRAM	.3718+01
		U	.6800+02	U2	.2317+06	MACH	.1206+01	MU	.4642+01	MUB	.1392+02
		SIGEFF	.2504+02	SIG	.1692+03	NU1	.5309+09	NU2	.3789+11	LOWIP	.3884+01
		NE	.2261+21	NA	.3709+22	NB	.3935+25	J	.1203+05	POWER	.1001+10

STATION	T	TS	P	PS	RHO	U	M	Q	W
1	.4230+03	.4230+03	.1134+06	.1134+06	.1286+01	.0000	.0000	.0000	-.2969+09
2	.7041+03	.7041+03	.3660+06	.3660+06	.2498+01	.0000	.0000	-.2969+09	.0000
3	.4230+03	.4230+03	.3660+06	.3660+06	.4158+01	.0000	.0000	.0000	-.2969+09
4	.7041+03	.7041+03	.1182+07	.1182+07	.8064+01	.0000	.0000	.1756+10	.0000
5	.2367+04	.2367+04	.1146+07	.1146+07	.2327+01	.0000	.0000	.0000	.0000
6	.1686+04	.2367+04	.4864+06	.1135+07	.1390+01	.8400+03	.1100+01	-.5004+08	.1001+10
7	.9216+03	.1369+04	.5012+05	.1347+06	.2622+00	.6808+03	.1206+01	.0000	.0000
8	.1350+04	.1369+04	.1169+06	.1209+06	.4172+00	.1367+03	.2000+00	-.9953+09	.0000
9	.4230+03	.4230+03	.1134+06	.1134+06	.1292+01	.0000	.0000	.0000	.0000

MHD .9855+09 STEAM PLANT .1448+08 TOTAL .1000+10 EFFICIENCY .5896+00

ETA-MHD .7352+00 EFF-MHD .6004+00

@9RKPT PRINT$

Appendix A 10.7

Detailed Code of Accounts Listing for Point 2

Table A 10.7.1

CLOSED CYCLE MHD SYSTEM ACCOUNT LISTING
PARAMETRIC POINT NO. 2

ACCOUNT NO. & NAME.	UNIT	AMOUNT	MAT $/UNIT	INS $/UNIT	MAT COST.$	INS COST.$
SITE DEVELOPMENT						
1. 1 LAND COST	ACRE	231.0	1000.00	.00	231000.00	.00
1. 2 CLEARING LAND	ACRE	77.0	.00	600.00	.00	46195.38
1. 3 GRADING LAND	ACRE	231.0	.00	3000.00	.00	693000.00
1. 4 ACCESS RAILROAD	MILE	5.0	115000.00	110000.00	575000.00	550000.00
1. 5 LOOP RAILROAD TRACK	MILE	3.0	120000.00	70000.00	360000.00	210000.00
1. 6 SIDING R.R TRACK	MILE	.0	125000.00	80000.00	.00	.00
1. 7 OTHER SITE COSTS	ACRE	.0	.00	.00	477275.38	477275.38
PERCENT TOTAL DIRECT COST IN ACCOUNT 1 = .374				ACCOUNT TOTAL.$	1543275.37	1976470.75
EXCAVATION & PILING						
2. 1 COMMON EXCAVATION	YD3	268500.0	.00	3.00	.00	805500.00
2. 2 PILING	FT	716000.0	6.50	8.50	4654000.00	6086000.00
PERCENT TOTAL DIRECT COST IN ACCOUNT 2 = 1.192				ACCOUNT TOTAL.$	4654000.00	6891500.00
PLANT ISLAND CONCRETE						
3. 1 PLANT IS. CONCRETE	YD3	89500.0	70.00	80.00	6265000.00	7160000.00
3. 2 SPECIAL STRUCTURES	YD3	2340.0	.00	.00	.00	.00
PERCENT TOTAL DIRECT COST IN ACCOUNT 3 = 1.386				ACCOUNT TOTAL.$	6265000.00	7160000.00
HEAT REJECTION SYSTEM						
4. 1 COOLING TOWERS	EACH	12.0	.00	.00	1842000.00	918000.00
4. 2 CIRCULATING H2O SYS	EACH	1.0	.00	.00	785375.52	1053089.31
4. 3 SURFACE CONDENSER	FT2	295012.8	.00	.00	1457410.59	206508.96
PERCENT TOTAL DIRECT COST IN ACCOUNT 4 = .647				ACCOUNT TOTAL.$	4084786.09	2177598.25
STRUCTURAL FEATURES						
5. 1 STAT. STRUCTURAL ST.	TON	2650.0	650.00	175.00	1722500.00	463750.00
5. 2 SILOS & BUNKERS	TPH	.0	1800.00	750.00	.00	.00
5. 3 CHIMNEY	FT	400.0	.00	.00	435070.92	652606.38
5. 4 STRUCTURAL FEATURES	EACH	1.0	366000.00	231000.00	366000.00	231000.00
PERCENT TOTAL DIRECT COST IN ACCOUNT 5 = .462				ACCOUNT TOTAL.$	3123570.91	1347356.37
BUILDINGS						
6. 1 STATION BUILDINGS	FT3	4300000.0	.15	.16	588000.00	588000.00
6. 2 ADMINSTRATION	FT2	10000.0	16.00	14.00	160000.00	140000.00
6. 3 WAREHOUSE & SHOP	FT2	20000.0	12.00	8.00	240000.00	160000.00
PERCENT TOTAL DIRECT COST IN ACCOUNT 6 = .214				ACCOUNT TOTAL.$	1088000.00	989000.00
FUEL HANDLING & STORAGE						
7. 1 COAL HANDLING SYS	TPH	389.6	.00	.00	5467973.62	2351367.66
7. 2 DOLOMITE HAND. SYS	TPH	44.3	.00	.00	384952.38	219792.21
7. 3 FUEL OIL HAND. SYS	GAL	116000.0	.00	.00	22370.43	18100.14
PERCENT TOTAL DIRECT COST IN ACCOUNT 7 = .874				ACCOUNT TOTAL.$	5875296.37	2588259.97
FUEL PROCESSING						
8. 1 COAL DRYER & CRUSHER	TPH	.0	.00	.00	.00	.00
8. 2 CARBONIZERS	TPH	.0	.00	.00	.00	.00
8. 3 GASIFIERS	TPH	389.6	.00	.00	56501256.00	31781956.50
PERCENT TOTAL DIRECT COST IN ACCOUNT 8 = 9.116				ACCOUNT TOTAL.$	56501256.00	31781956.50

Table A 10.7.1 Continued

CLOSED CYCLE MHD SYSTEM ACCOUNT LISTING
PARAMETRIC POINT NO. 2

ACCOUNT NO. & NAME	UNIT	AMOUNT	MAT $/UNIT	INS $/UNIT	MAT COST,$	INS COST,$
FIRING SYSTEM						
9. 1		.0	.00	.00	.00	.00
PERCENT TOTAL DIRECT COST IN ACCOUNT 9 = .000 ACCOUNT TOTAL,$					.00	.00
VAPOR GENERATOR (FIRED)						
10. 1		.0	.00	.00	.00	.00
PERCENT TOTAL DIRECT COST IN ACCOUNT 10 = .000 ACCOUNT TOTAL,$					.00	.00
ENERGY CONVERTER						
11. 1 AIR PREHEATER	EA	1.0	7810000.00	5180000.00	7810000.00	5180000.00
11. 2 ARGON PREHEATER	EA	1.0	10575000.00	6651000.00	10575000.00	6651000.00
11. 3 REFRACTORY STOVES		1.0	392600000.00	19700000.00	392600000.00	19700000.00
11. 4 PIPING,VALVES,ETC		1.0	16909700000.00	5827000.00	16909700000.00	5823000.00
11. 5 HEADER & NOZZLE	EA	1.0	301193.00	301193.00	301193.00	301193.00
11. 6 MHD GENERATOR DUCT	EA	1.0	610335.00	716491.00	610335.00	716491.00
11. 7 SUPERCONDUCTING MAGNETS	EA	1.0	41300000.00	.00	41300000.00	.00
11. 8 DIFFUSSER	EA	1.0	200795.00	200795.00	200795.00	200795.00
11. 9 COMPRESSORS		1.0	7592000.00	.00	7592000.00	.00
11.10 INTERCOOLERS		1.0	1898000.00	.00	1898000.00	.00
11.11 COMPRESSED ARGON DISTRIB		1.0	200795.00	200795.00	200795.00	200795.00
11.12 CESIUM COLLECTOR/INJECT		1.0	100000.00	50000.00	100000.00	50000.00
11.13 A & CS INVENTORY		1.0	250000.00	.00	250000.00	.00
PERCENT TOTAL DIRECT COST IN ACCOUNT 11 =59.321 ACCOUNT TOTAL,$					67253104.00	38923264.00
COUPLING HEAT EXCHANGER						
12. 1 STEAM GENERATOR	EA	1.0	39037000.00	.00	39037000.00	.00
12. 2 COMP DRIVE TURBINE	EA	1.0	16022000.00	1104360.61	16022000.00	1104360.61
12. 3 STEAM TURB-GEN	EA	1.0	566000.00	103926.24	566000.00	103926.24
12. 4 FEED WATER HEATER STRING		1.0	275000.00	.00	275000.00	.00
PERCENT TOTAL DIRECT COST IN ACCOUNT 12 = 5.897 ACCOUNT TOTAL,$					55900000.00	1208286.84
HEAT RECOVERY HEAT EXCH.						
13. 1		.0	.00	.00	.00	.00
PERCENT TOTAL DIRECT COST IN ACCOUNT 13 = .000 ACCOUNT TOTAL,$					.00	.00
WATER TREATMENT						
14. 1 DEMINERALIZER	GPM	750.8	2000.00	560.00	1501174.67	420328.91
14. 2 CONDENSATE POLISHING	KWE	552200.0	1.25	.30	690249.98	165660.00
PERCENT TOTAL DIRECT COST IN ACCOUNT 14 = .287 ACCOUNT TOTAL,$					2191424.66	585988.91
POWER CONDITIONING						
15. 1 INVERTER SETS		1.0	30786000.00	3694320.00	30786000.00	3694320.00
15. 2 INVERTER TRANSFORMER		1.0	8303000.00	996360.00	8303000.00	996360.00
15. 3 DC INTERRUPTERS		1.0	5918000.00	710160.00	5918000.00	710160.00
15. 4 AC CIRCUIT BREAKERS		1.0	612000.00	73440.00	612000.00	73440.00
15. 5 POWER TRANSFORMERS		1.0	4578000.00	549360.00	4578000.00	549360.00
15. 6 STD TRANSFORMER		17355.6	.00	.00	549660.21	10993.20
PERCENT TOTAL DIRECT COST IN ACCOUNT 15 = 5.863 ACCOUNT TOTAL,$					50746660.00	6034633.19

Table A 10.7.1 Continued

CLOSED CYCLE MHD SYSTEM ACCOUNT LISTING
PARAMETRIC POINT NO. 2

ACCOUNT NO. & NAME,	UNIT	AMOUNT	MAT $/UNIT	INS $/UNIT	MAT COST,$	INS COST,$
AUXILIARY MECH EQUIPMENT						
16. 1 BOILER FEED PUMP &DR.	KWE	535554.4	1.67	.10	894375.88	53555.44
16. 2 OTHER PUMPS	KWE	581913.5	.88	.12	512083.91	69829.62
16. 3 MISC SERVICE SYS	KWE	969855.9	1.17	.73	1134731.39	707994.80
16. 4 AUXILIARY BOILER	PPH	3000000.0	4.00	.80	12000000.00	2400000.00
PERCENT TOTAL DIRECT COST IN ACCOUNT 16 =			.497	ACCOUNT TOTAL,$	2741191.19	1071379.84
PIPE & FITTINGS						
17. 1 CONVENTIONAL PIPING	TON	1975.0	3000.00	1800.00	5925000.00	3555000.00
17. 2 HIGT TEMP AIR PIPING	TON	.0	.00	.00	.00	.00
17. 3 LOW TEMP AIR PIPING	TON	.0	.00	.00	.00	.00
17. 4 RECIR PRODUCT PIPING	TON	.0	.00	.00	.00	.00
PERCENT TOTAL DIRECT COST IN ACCOUNT 17 =			.979	ACCOUNT TOTAL,$	5925000.00	3555000.00
AUXILIARY ELEC EQUIPMENT						
18. 1 MISC MOTERS,ETC		678899.1	1.40	.17	950458.77	115412.85
18. 2 SWITCHGEAR & MCC PAN	KWE	678899.1	1.95	.45	1323853.28	305504.61
18. 3 CONDUIT,CABLES,TRAYS	FT	5450000.0	1.32	1.36	7193999.94	7411999.94
18. 4 ISOLATED PHASE BUS	FT	250.0	510.00	450.00	127500.00	112500.00
18. 5 LIGHTING & COMMUN	KWE	969855.9	.35	.43	339449.56	417038.04
PERCENT TOTAL DIRECT COST IN ACCOUNT 18 =			1.899	ACCOUNT TOTAL,$	9935261.37	8362455.37
CONTROL, INSTRUMENTATION						
19. 1 COMPUTER	EACH	1.0	660000.00	15000.00	660000.00	15000.00
19. 2 OTHER CONTROLS	EACH	1.0	951000.00	571000.00	951000.00	571000.00
PERCENT TOTAL DIRECT COST IN ACCOUNT 19 =			.227	ACCOUNT TOTAL,$	1611000.00	586000.00
PROCESS WASTE SYSTEMS						
20. 1 BOTTOM ASH	TPH	.0	.00	.00	.00	.00
20. 2 DRY ASH	TPH	29.2	1829322.81	457330.70	1829322.81	457330.70
20. 3 WET SLURRY	TPH	44.3	1293194.58	323298.64	1233194.58	323298.64
20. 4 ONSITE DISPOSAL	ACRE	217.9	6698.33	9890.11	1459785.73	2155378.06
20. 5 SEED TREATMENT	EACH	.0	.00	.00	.00	.00
PERCENT TOTAL DIRECT COST IN ACCOUNT 20 =			.776	ACCOUNT TOTAL,$	4582303.06	2936007.41
STACK GAS CLEANING						
21. 1 PRECIPITATOR	EACH	.0	.00	.00	.00	.00
21. 2 SCRUBBER	KWE	.0	18.80	8.62	.00	.00
21. 3 MISC STEEL & DUCTS		.0	.00	.00	.00	.00
PERCENT TOTAL DIRECT COST IN ACCOUNT 21 =			.000	ACCOUNT TOTAL,$	.00	.00
TOTAL DIRECT COSTS,$					85047104.00	118074153.00

Table A 10.7.2 CLOSED CYCLE MHD SYSTEM COST OF ELECTRICITY,MILLS/KW.HR
PARAMETRIC POINT NO. 2

ACCOUNT	RATE, PERCENT	LABOR RATE, $/HR 6.00	8.50	10.60	15.00	21.50
TOTAL DIRECT COSTS,$	.0	917237528.	945085200.	968477256.	1017485168.	1089893120.
INDIRECT COST,$	51.0	34083555.	48287872.	60217817.	85213892.	122139911.
PROF & OWNER COSTS,$	8.0	7337900C2.	7560C6816.	77478180.	81389133.	87191449.
CONTINGENCY COST,$	11.0	100896127.	103959371.	106532497.	111923807.	119898242.
SUB TOTAL,$	.0	1125598192.	1172939248.	1212705744.	1296025968.	1419112704.
ESCALATION COST,$	6.5	334112896.	410589724.	424612420.	453785864.	496893012.
INTREST DURING CONST,$	10.0	502262116.	537786544.	541131064.	578310048.	633233560.
TOTAL CAPITALIZATION,$	.0	2021973200.	2120314512.	2178449216.	2328121856.	2549229248.
COST OF ELEC-CAPITAL	18.0	65.38204	68.13191	70.44181	75.28159	82.43126
COST OF ELEC-FUEL	.0	6.28651	6.28651	6.28651	6.28651	6.28651
COST OF ELEC-OP & MAIN	.0	.34533	.34533	.34533	.34533	.34533
TOTAL COST OF ELEC	.0	72.01388	74.76375	77.07365	81.91343	89.06310

ACCOUNT	RATE, PERCENT	CONTINGENCY, PERCENT -5.00	.00	11.00	5.00	20.00
TOTAL DIRECT COSTS,$	.0	968477256.	968477256.	968477256.	968477256.	968477256.
INDIRECT COST,$	51.0	60217817.	60217817.	60217817.	60217817.	60217817.
PROF & OWNER COSTS,$	8.0	77478180.	77478180.	77478180.	77478180.	77478180.
CONTINGENCY COST,$	20.0	-48423862.	0.	106532497.	48423862.	193695450.
SUB TOTAL,$	.0	1057749392.	1106173248.	1212705744.	1154597104.	1299868688.
ESCALATION COST,$	6.5	370356560.	387731516.	424612420.	404266472.	455131340.
INTREST DURING CONST,$	10.0	471986764.	493594356.	541131064.	515201952.	580024736.
TOTAL CAPITALIZATION,$	.0	1900092704.	1987079104.	2178449216.	2074065520.	2335024736.
COST OF ELEC-CAPITAL	18.0	61.44094	64.25371	70.44181	67.06643	75.50490
COST OF ELEC-FUEL	.0	6.28651	6.28651	6.28651	6.28651	6.28651
COST OF ELEC-OP & MAIN	.0	.34533	.34533	.34533	.34533	.34533
TOTAL COST OF ELEC	.0	68.07278	70.88555	77.07365	73.69832	82.13664

ACCOUNT	RATE, PERCENT	ESCALATION RATE, PERCENT 5.00	6.50	8.00	10.00	.00
TOTAL DIRECT COSTS,$	.0	968477256.	968477256.	968477256.	968477256.	968477256.
INDIRECT COST,$	51.0	60217817.	60217817.	60217817.	60217817.	60217817.
PROF & OWNER COSTS,$	8.0	77478180.	77478180.	77478180.	77478180.	77478180.
CONTINGENCY COST,$	11.0	106532497.	106532497.	106532497.	106532497.	106532497.
SUB TOTAL,$	.0	1212705744.	1212705744.	1212705744.	1212705744.	1212705744.
ESCALATION COST,$	.0	315274376.	424612420.	539753248.	704548816.	0.
INTREST DURING CONST,$	10.0	511168604.	541131064.	572634576.	617151224.	421615644.
TOTAL CAPITALIZATION,$	.0	2040148704.	2178449216.	2325108544.	2534405760.	1634321376.
COST OF ELEC-CAPITAL	18.0	65.96976	70.44181	75.18415	81.95193	52.84702
COST OF ELEC-FUEL	.0	6.28651	6.28651	6.28651	6.28651	6.28651
COST OF ELEC-OP & MAIN	.0	.34533	.34533	.34533	.34533	.34533
TOTAL COST OF ELEC	.0	72.60160	77.07365	81.81599	88.58377	59.47886

ACCOUNT	RATE, PERCENT	INT DURING CONST,PERCENT 6.00	8.00	10.00	12.50	15.00
TOTAL DIRECT COSTS,$	.0	968477256.	968477256.	968477256.	968477256.	968477256.
INDIRECT COST,$	51.0	60217817.	60217817.	60217817.	60217817.	60217817.
PROF & OWNER COSTS,$	8.0	77478180.	77478180.	77478180.	77478180.	77478180.
CONTINGENCY COST,$	11.0	106532497.	106532497.	106532497.	106532497.	106532497.
SUB TOTAL,$	.0	1212705744.	1212705744.	1212705744.	1212705744.	1212705744.
ESCALATION COST,$	6.5	424612420.	424612420.	424612420.	424612420.	424612420.
INTREST DURING CONST,$	15.0	307467132.	421243476.	541131064.	700042824.	869587368.
TOTAL CAPITALIZATION,$	.0	1944785280.	2058561632.	2178449216.	2337360960.	2506905504.
COST OF ELEC-CAPITAL	18.0	62.83611	65.56515	70.44181	75.58034	81.06269
COST OF ELEC-FUEL	.0	6.28651	6.28651	6.28651	6.28651	6.28651
COST OF ELEC-OP & MAIN	.0	.34533	.34533	.34533	.34533	.34533
TOTAL COST OF ELEC	.0	69.51795	72.19699	77.07365	82.21218	87.69453

Table A 10.7.2 Continued CLOSED CYCLE MHD SYSTEM COST OF ELECTRICITY, MILLS/KW.HR
PARAMETRIC POINT NO. 2

ACCOUNT	RATE, PERCENT	FIXED CHARGE RATE, PCT 10.00	14.40	18.00	21.60	25.00
TOTAL DIRECT COSTS,$	.0	968477256.	968477256.	968477256.	968477256.	968477256.
INDIRECT COST,$	51.0	60217817.	60217817.	60217817.	60217817.	60217817.
PROF & OWNER COSTS,$	8.0	77478180.	77478180.	77478180.	77478180.	77478180.
CONTINGENCY COST,$	11.0	106532497.	106532497.	106532497.	106532497.	106532497.
SUB TOTAL,$	.0	1212705744.	1212705744.	1212705744.	1212705744.	1212705744.
ESCALATION COST,$	6.5	424612420.	424612420.	424612420.	424612420.	424612420.
INTREST DURING CONST,$	10.0	541131064.	541131064.	541131064.	541131064.	541131064.
TOTAL CAPITALIZATION,$	.0	2178449216.	2178449216.	2178449216.	2178449216.	2178449216.
COST OF ELEC-CAPITAL	25.0	38.13424	56.35745	70.44181	84.53017	97.83585
COST OF ELEC-FUEL	.0	6.28651	5.28651	6.28651	6.28651	6.28651
COST OF ELEC-OP & MAIN	.0	.34533	.34533	.34533	.34533	.34533
TOTAL COST OF ELEC	.0	45.76618	62.98529	77.07365	91.16201	104.46769

ACCOUNT	RATE, PERCENT	FUEL COST, $/10**6 BTU .30	.85	1.50	2.50	1.02
TOTAL DIRECT COSTS,$	.0	968477256.	968477256.	968477256.	968477256.	968477256.
INDIRECT COST,$	51.0	60217817.	60217817.	60217817.	60217817.	60217817.
PROF & OWNER COSTS,$	8.0	77478180.	77478180.	77478180.	77478180.	77478180.
CONTINGENCY COST,$	11.0	106532497.	106532497.	106532497.	106532497.	106532497.
SUB TOTAL,$	.0	1212705744.	1212705744.	1212705744.	1212705744.	1212705744.
ESCALATION COST,$	6.5	424612420.	424612420.	424612420.	424612420.	424612420.
INTREST DURING CONST,$	10.0	541131064.	541131064.	541131064.	541131064.	541131064.
TOTAL CAPITALIZATION,$	.0	2178449216.	2178449216.	2178449216.	2178449216.	2178449216.
COST OF ELEC-CAPITAL	18.0	70.44181	70.44181	70.44181	70.44181	70.44181
COST OF ELEC-FUEL	.0	2.21877	6.28651	11.09384	18.48973	7.54381
COST OF ELEC-OP & MAIN	.0	.34533	.34533	.34533	.34533	.34533
TOTAL COST OF ELEC	.0	73.00591	77.07365	81.88098	89.27687	78.33095

ACCOUNT	RATE, PERCENT	CAPACITY FACTOR, PERCENT 12.00	45.00	50.00	65.00	80.00
TOTAL DIRECT COSTS,$	.0	968477256.	968477256.	968477256.	968477256.	968477256.
INDIRECT COST,$	51.0	60217817.	60217817.	60217817.	60217817.	60217817.
PROF & OWNER COSTS,$	8.0	77478180.	77478180.	77478180.	77478180.	77478180.
CONTINGENCY COST,$	11.0	106532497.	106532497.	106532497.	106532497.	106532497.
SUB TOTAL,$	.0	1212705744.	1212705744.	1212705744.	1212705744.	1212705744.
ESCALATION COST,$	6.5	424612420.	424612420.	424612420.	424612420.	424612420.
INTREST DURING CONST,$	10.0	541131064.	541131064.	541131064.	541131064.	541131064.
TOTAL CAPITALIZATION,$	.0	2178449216.	2178449216.	2178449216.	2178449216.	2178449216.
COST OF ELEC-CAPITAL	18.0	381.55980	101.74928	91.57435	70.44181	57.23397
COST OF ELEC-FUEL	.0	6.28651	5.28651	6.28651	6.28651	6.28651
COST OF ELEC-OP & MAIN	.0	.34534	.34533	.34533	.34533	.34533
TOTAL COST OF ELEC	.0	388.19165	109.38112	98.20619	77.07365	63.86581

Table A 10.7.3 CLOSED CYCLE MHD SYSTEM

ACCOUNT NO	AUX POWER, MWE	PERC PLANT POW	OPERATION COST	MAINTENANCE COST
4	6.69541	.68487	38.22156	10.72326
7	4.14085	.42356	236.75303	.00000
8	9.78184	1.00057	3.17873	.00000
14	.00000	.00000	59.45078	.00000
18	5.08520	.52016	.00000	.00000
20	6.42676	.65739	.00000	.00000
TOTALS	22.37572	2.28879	337.60410	10.72326

CLOSED CYCLE MHD SYSTEM BASE CASE INPUT

NOMINAL POWER, MWE	1000.0000	NET POWER, MWE	977.6243
NOM HEAT RATE, BTU/KW-HR	7230.4023	NET HEAT RATE, BTU/KW-HR	7395.8906
OFF DESIGN HEAT RATE	1.0187		
CONDENSER			
DESIGN PRESSURE, IN HG A	2.0000	NUMBER OF SHELLS	3.0000
NUMBER OF TUBES/SHELL	4350.0729	TUBE LENGTH, FT	77.4467
U, BTU/HR-FT2-F	591.4577	TERMINAL TEMP DIFF, F	5.0000
HEAT REJECTION			
DESIGN TEMP, F	51.4000	APPROACH, F	21.6744
RANGE, F	23.0000	OFF DESIGN TEMP, F	77.0000
OFF DESIGN PRES, IN HG A	2.9413	LP TURBINE BLADE LEN, IN	28.5000

1	1000.000	2	.593	3	.472	4	.000	5	8.000
6	14.200	7	2.000	8	686.000	9	3.000	10	2.000
11	1.000	12	538.000	13	2.000	14	4.000	15	1.000
16	2.000	17	231.000	18	3.000	19	5.000	20	3.000
21	.000	22	99500.000	23	2340.000	24	2530.000	25	400.000
26	4300000.000	27	10000.000	28	20000.000	29	110000.000	30	.600
31	1.000	32	1375.000	33	.000	34	.700	35	.700
36	5450000.000	37	250.000	38	1.000	39	1.000	40	966000.000
41	231000.000	42	660000.000	43	15000.000	44	951000.000	45	571000.000
46	1.000	47	.000	48	3.000	49	1.000	50	.000
51	.500	52	5.350						

1	1.000	2	1.000	3	1.000	4	1.000	5	1.000
6	1.000	7	1.000	8	1.000	9	1.000	10	1.000
11	1.000	12	1.000	13	1.000	14	1.000	15	5180000.000
16	10575000.000	17	5651000.000	18	332600000.000	19	19700000.000	20	159097000.000
21	5823000.000	22	301193.000	23	301193.000	24	610335.000	25	716481.000
26	41300000.000	27	.000	28	200795.000	29	200795.000	30	7592000.000
31	.000	32	1898000.000	33	.000	34	200795.000	35	200795.000
36	100000.000	37	50000.000	38	250000.000	39	.000	40	1.000
41	1.000	42	1.000	43	1.000	44	39037000.000	45	.000
46	16022000.000	47	.000	48	765000.000	49	.000	50	275000.000
51	.000	52	1.000	53	1.000	54	1.000	55	1.000
56	1.000	57	1.000	58	70786000.000	59	3694320.000	60	8303000.000
61	996360.000	62	5918000.000	63	710100.000	64	612000.000	65	73440.000
66	4578000.000	67	549360.000	68	300000.000	69	.000	70	.000
71	.000	72	.000	73	.000	74	.000	75	.000

*USGPO: 1976 — 660-301